SANDIA REPORT
SAND2008-6665
Unlimited Release
Printed April 2010

Assessment of Severe Accident Source Terms in Pressurized-Water Reactors with a 40% Mixed-Oxide and 60% Low-Enriched Uranium Core Using MELCOR 1.8.5

Scott G. Ashbaugh, Kenneth C. Wagner, Pamela Longmire, Randall O. Gauntt, Andrew S. Goldmann, and Dana A. Powers

Prepared by
Sandia National Laboratories
Albuquerque, New Mexico 87185 and Livermore, California 94550

Sandia National Laboratories is a multiprogram laboratory operated by Sandia Corporation, a wholly owned subsidiary of Lockheed Martin Company, for the U.S. Department of Energy's National Nuclear Security Administration under Contract DE-AC04-94AL85000.

Issued by Sandia National Laboratories, operated for the United States Department of Energy by Sandia Corporation.

Available to DOE and DOE contractors from
U.S. Department of Energy
Office of Scientific and Technical Information
P.O. Box 62
Oak Ridge, TN 37831

Telephone: (865) 576-8401
Facsimile: (865) 576-5728
E-Mail: reports@adonis.osti.gov
Online ordering: http://www.osti.gov/bridge

Available to the public from
U.S. Department of Commerce
National Technical Information Service
5285 Port Royal Rd.
Springfield, VA 22161

Telephone: (800) 553-6847
Facsimile: (703) 605-6900
E-Mail: orders@ntis.fedworld.gov
Online order: http://www.ntis.gov/help/ordermethods.asp?loc=7-4-0#online

SAND2008-6665
Unlimited Release
Printed April 2010

Assessment of Severe Accident Source Terms in Pressurized-Water Reactors with a 40% Mixed-Oxide and 60% Low-Enriched Uranium Core Using MELCOR 1.8.5

Scott G. Ashbaugh
Security Engineering Analysis, 4240

Kenneth C. Wagner, Pamela Longmire, and Randall O. Gauntt
Reactor Modeling and Analysis, 6762

Dana A. Powers
Advanced Nuclear Energy Program, 6770
Sandia National Laboratories
P.O. Box 5800
Albuquerque, New Mexico 87185-1116

Andrew S. Goldmann
Texas A&M University
College Station, Texas 77843

Abstract

As part of a Nuclear Regulatory Commission (NRC) research program to evaluate the impact of using mixed-oxide (MOX) fuel in commercial nuclear power plants, a study was undertaken to evaluate the impact of the usage of MOX fuel on the consequences of postulated severe accidents. A series of 23 severe accident calculations was performed using MELCOR 1.8.5 for a four-loop Westinghouse reactor with an ice condenser containment. The calculations covered five basic accident classes that were identified as the risk- and consequence-dominant accident sequences in plant-specific probabilistic risk assessments for the McGuire and Catawba nuclear plants, including station blackouts and loss-of-coolant accidents of various sizes, with both early and late containment failures.

Ultimately, the results of these MELCOR simulations will be used to provide a supplement to the NRC's alternative source term described in NUREG-1465. Source term magnitude and timing results are presented consistent with the NUREG-1465 format. For each of the severe accident release phases (coolant release, gap release, in-vessel release, ex-vessel release, and late in-vessel release), source term timing information (onset of release and duration) is presented. For all release phases except for the coolant release phase, magnitudes are presented for each of the NUREG-1465 radionuclide groups. MELCOR results showed variation of noble metal releases between those typical of ruthenium (Ru) and those typical of molybdenum (Mo); therefore, results for the noble metals were presented for Ru and Mo separately. The collection of the source term results can be used as the basis to develop a representative source term (across all accident types) that will be the MOX supplement to NUREG-1465.

TABLE OF CONTENTS

LIST OF FIGURES

LIST OF TABLES

ABBREVIATIONS

AFW	Auxiliary Feedwater
Ag	silver
ANS	American Nuclear Society
Ba	barium
BOC	beginning of cycle
CAV	MELCOR Cavity Package
Cd	cadmium
CDF	core damage frequency
Ce	cerium
CF	MELCOR Control Function Package
COR	MELCOR Core Package
Cs	cesium
CV	control volume
CVH	MELCOR Control Volume Hydrodynamics Package
DCH	Direct Containment Heating
DEGB	double-ended guillotine break
DOE	Department of Energy
ECCS	emergency core cooling system
EOC	end of cycle
Eu	europium
FL	MELCOR Flow Path Package
FWST	reactor fuel water storage tank
HM	heavy metal
I	iodine
ISGTR	induced steam generator tube rupture
Kr	krypton
La	lanthanum
LEU	low-enriched uranium
LLOCA	large-break loss-of-coolant accident
LOCA	loss-of-coolant accident
MLOCA	medium-break loss-of-coolant accident
Mo	molybdenum
MOX	mixed-oxide
MTIHM	metric tons initial heavy metal
mtU	metric tons uranium
MWd	megawatt-day
MW_{th}	megawatt, thermal

NRC	Nuclear Regulatory Commission
ORNL	Oak Ridge National Laboratory
PRA	probabilistic risk assessment
PRT	pressurizer relief tank
Pu	plutonium
PuO_2	plutonium dioxide
PWR	pressurized-water reactor
RaF	Re-alignment Failure
RCP	reactor coolant pump
RCS	reactor coolant system
RN	MELCOR Radionuclide Package
Ru	ruthenium
Sb	antimony (stibium)
SBO	station blackout
SGTR	steam generator tube rupture
SLOCA	small-break loss-of-coolant accident
Sn	tin
SORV	stuck-open relief valve
Sr	strontium
SRV	safety-relief valve
STCP	Source Term Code Package
TAF	top of active fuel
Te	tellurium
U	uranium
UO_2	uranium dioxide
U.S.	United States
WG-Pu	weapons-grade plutonium
ZrO_2	zirconium dioxide

1.0 INTRODUCTION

As part of a United States (U.S.) Nuclear Regulatory Commission (NRC) research program to evaluate the impact of using mixed-oxide (MOX) fuel in commercial nuclear power plants, a study was undertaken to evaluate the impact of the usage of MOX fuel on the consequences of postulated severe accidents. Two nuclear power plants, McGuire and Catawba, have expressed their desire to burn MOX fuel in support of a U.S. Department of Energy (DOE) initiative to dispose of weapons-grade plutonium (WG-Pu) [1]. The plant-specific assessments of the severe accident risks for the McGuire [2] and Catawba [3] nuclear power plants were reviewed to determine the applicable types of severe accidents. Both the frequency-dominant and risk-dominant accident sequences were identified and selected for comparative MOX versus normal low-enriched uranium (LEU) severe accident simulations. The accident simulations were performed using Version 1.8.5 of the MELCOR severe accident analysis code [4].

Ultimately, the results of these MELCOR simulations will be used to provide a supplement to the NRC's alternative source term described in NUREG-1465 [5]. The NUREG-1465 Source Term considers both the timing and the chemical composition of the source term, and it divides releases from degrading reactor fuel into five phases:

- coolant activity release,
- gap release,
- in-vessel release,
- ex-vessel release, and
- late in-vessel release.

Using the accident source terms calculated for the frequency- and risk-dominant accident sequences for McGuire and Catawba, representative source terms will be defined that can be generally applied in regulatory applications for Westinghouse four-loop pressurized-water reactors (PWRs) burning MOX fuels. The range of applicability of these results will be limited by administrative constraints of core loading (i.e., the number of MOX vs. LEU fuel assemblies) and MOX assembly burnup, as described later in this report.

The remainder of this report describes the results of the MELCOR calculations that were performed to provide a basis for development of the MOX supplement to the NUREG-1465 Source Term. Section 2 provides a description of the MELCOR input model and the specific enhancements performed to simulate MOX fuel. Section 3 presents the rationale for selection of the specific transients that were selected for inclusion in this study. The results of MELCOR calculations for these scenarios are presented in Section 4. A summary and references are presented in Sections 5 and 6, respectively.

2.0 MELCOR MODEL DESCRIPTION

The McGuire and Catawba nuclear power plants have expressed their desire to burn MOX fuel in support of a DOE initiative to dispose of WG-Pu. Both plants have a large, four-loop Westinghouse reactor coolant system (RCS) with an ice condenser containment. Sandia National Laboratories has previously developed a MELCOR model for a four-loop Westinghouse plant with an ice condenser containment [6] based on the Sequoyah nuclear power plant. In a previous report for this project, the attributes of the Sequoyah nuclear power plant were compared to the McGuire and Catawba plants [7]. The results of that comparison showed relatively few differences in the key parameters affecting the transients to be performed in this study. Plant-specific modifications were made to accurately model the core power, the reactor fuel water storage water tank (FWST), the containment flooding behavior, and the potential for passive flow from the FWST to the reactor during a station blackout accident.

The MELCOR reactor vessel, RCS, and containment model nodalizations used in this study are briefly described in Sections 2.1, 2.2, and 2.3. Section 2.4 summarizes the results of calculations to estimate the differences between end-of-cycle (EOC) fission product inventories (and associated decay heat) for a normal LEU core load and the proposed 40% MOX core load. Section 2.5 summarizes a new MELCOR MOX fission product release model that is based on results from the French RT-2 experiment on MOX fission product release.

2.1 Reactor Core and Vessel Nodalization

The Westinghouse reactor core represented in the MELCOR model is shown in Figure 2-1. This figure shows both the MELCOR control volume hydrodynamics (CVH) nodalization and the MELCOR core (COR) cell nodalization. Control volumes (CVs) represent the fluid state throughout the core (using the MELCOR CVH package), and COR cells resolve the core solid regions spatially. Within the active core region, three COR cells in axial order are housed within a single fluid CV with a one-to-one radial correspondence used between CV and COR regions. Each CV is connected both radially and axially with adjacent CVs by flow paths (FLs), thereby allowing prediction of two-dimensional fluid flow (liquid or vapor) within the core region. The total core operating power before shutdown is assumed to be 3411 MW_{th}.

Figure 2-2 shows the balance of the CVH/FL nodalization for the reactor vessel. The lower head region is represented by a single large volume; however, a finer CVH nodalization is used in the regions above the core plate in order to resolve natural circulation patterns associated with hot leg counter-current flow phenomena. Flow paths are also indicated in the figure.

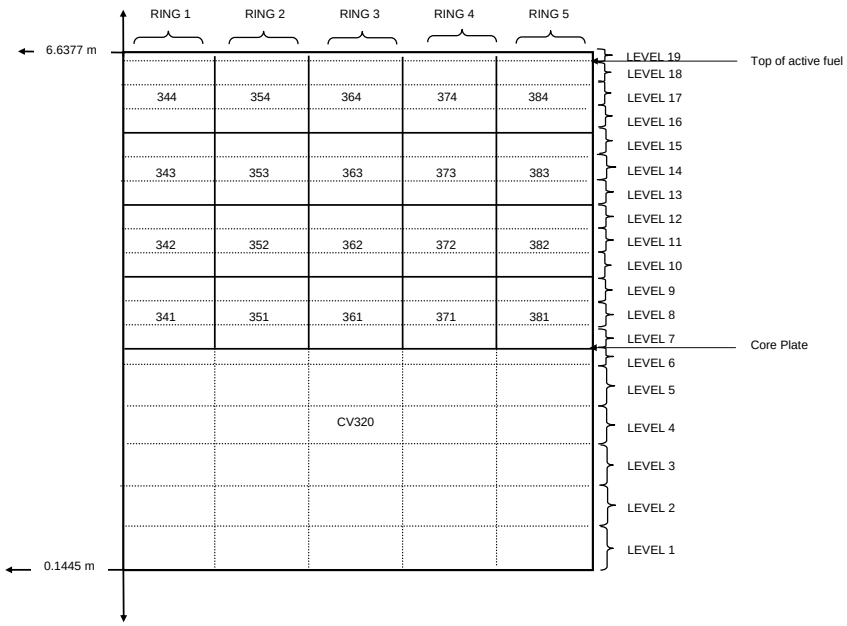

Figure 2-1. MELCOR COR/CVH Nodalization for Westinghouse Four-Loop PWR Core.

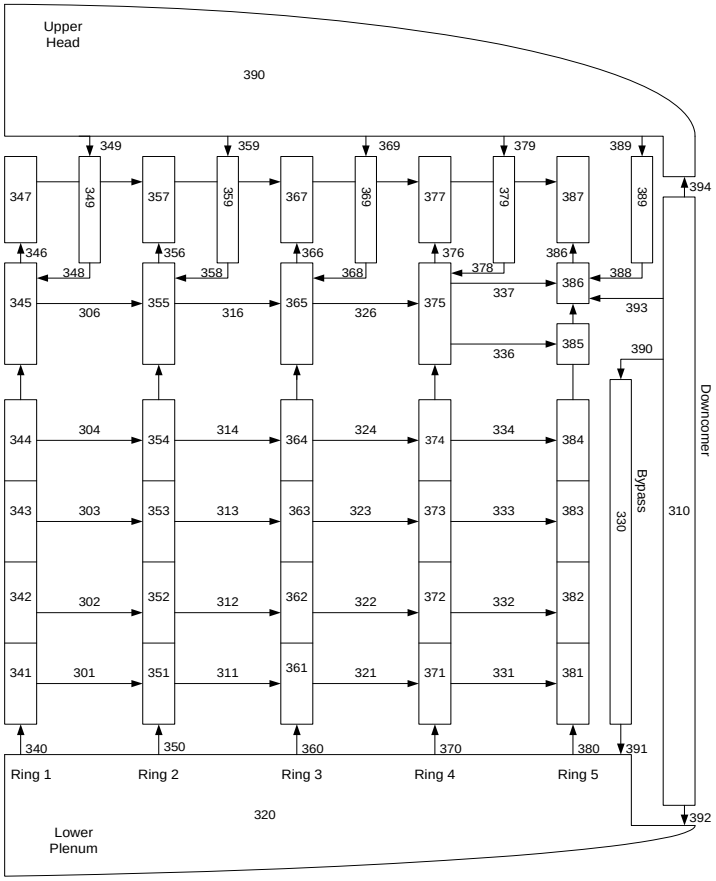

Figure 2-2. MELCOR CVH/FL Nodalization for Westinghouse Four-Loop PWR Vessel.

2.2 Reactor Coolant System Nodalization

The Westinghouse steam generators have an inverted U-tube design. When the secondary side of these steam generators is water-filled, heat rejection from the primary coolant system can be sustained during an accident with a loss of pumping power by full-loop natural circulation. Additionally, when the void fraction in the RCS hot legs and steam generator becomes large, vapor phase hot leg counter-current natural circulation patterns can form that have important heating effects on the hot leg, surge line, and steam generator tubes.

This MELCOR model uses a single RCS nodalization shown in Figure 2-3, capturing both of these important natural circulation phenomena that significantly affect the progression of high-pressure accidents. Details of those models are described elsewhere [6], but, in short, this is accomplished by splitting the RCS hot leg nodalizations into upper and lower halves that exhibit the correct flow resistances when the predominant coolant flow is either unidirectional or counter-current; the model is applicable for either liquid water or vapor flows. Transition from unidirectional liquid flow to counter-current vapor flow (motivated by vapor density differences within the steam generator tubes) is automatically handled by the model as the void fraction in the hot leg and steam generator becomes sufficiently large. When hot leg flows in the upper and lower halves are in opposing directions (counter-current), a pressure drop term representing the shear forces between the opposing flows is introduced using the MELCOR Quick-CF[1] pump feature. The shear forces vanish when the flows become unidirectional. Not shown in Figure 2-3 are the four cold leg accumulators.

Creep rupture models monitor the potential failure of the hot leg nozzles, the surge line, and the steam generator tubes as detailed in a previous report describing models for Westinghouse plants [6]. These models use the RCS pressure and the heat structure temperatures to estimate cumulative damage. When a creep rupture failure is predicted, a flow path is opened to allow for system depressurization at that location. In addition, a lower head creep rupture model is exercised to predict failure of the lower vessel head after hot core debris fails the lower core plate and relocates into the vessel lower plenum.

[1] CF = MELCOR Control Function.

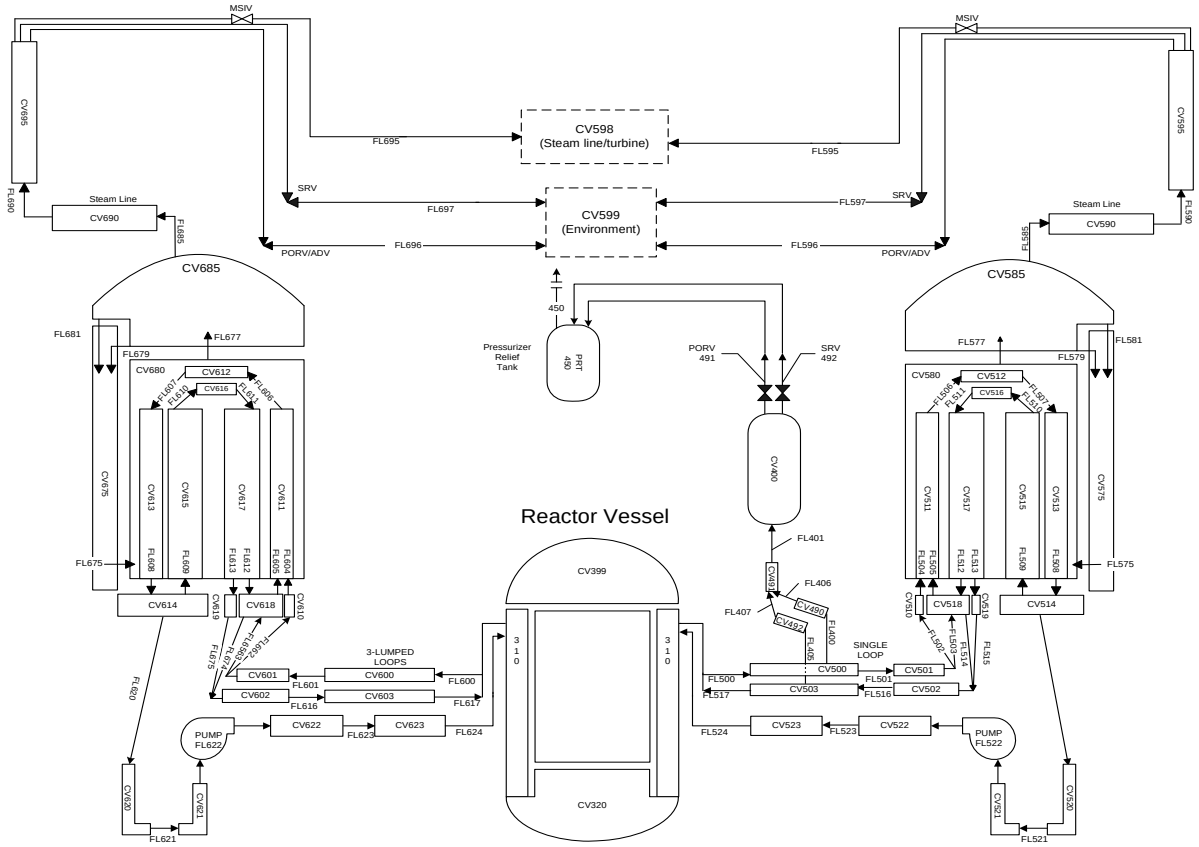

Figure 2-3. MELCOR CVH/FL Nodalization for Westinghouse Four-loop PWR RCS.

2.3 Containment Nodalization

The MELCOR containment model for the ice condenser containment is shown in Figure 2-4. The containment is divided into 12 separate volumes. A summary of the free volumes associated with the ice condenser containment is provided in Gauntt [6] (see Table 2-1). The RCS volumes are associated appropriately with the containment volumes so that pipe breaks or lifting relief valves vent into the correct containment locations. Containment rooms are connected with the flow paths indicated with respect to the constraints offered by walls and partitions, and liquid flow paths are defined with consideration given to fill elevations required for flooding in one room to spill over to other rooms. RCS pipe ruptures result in steam entering the bottom of the ice condenser volumes and exiting into the upper containment dome region.

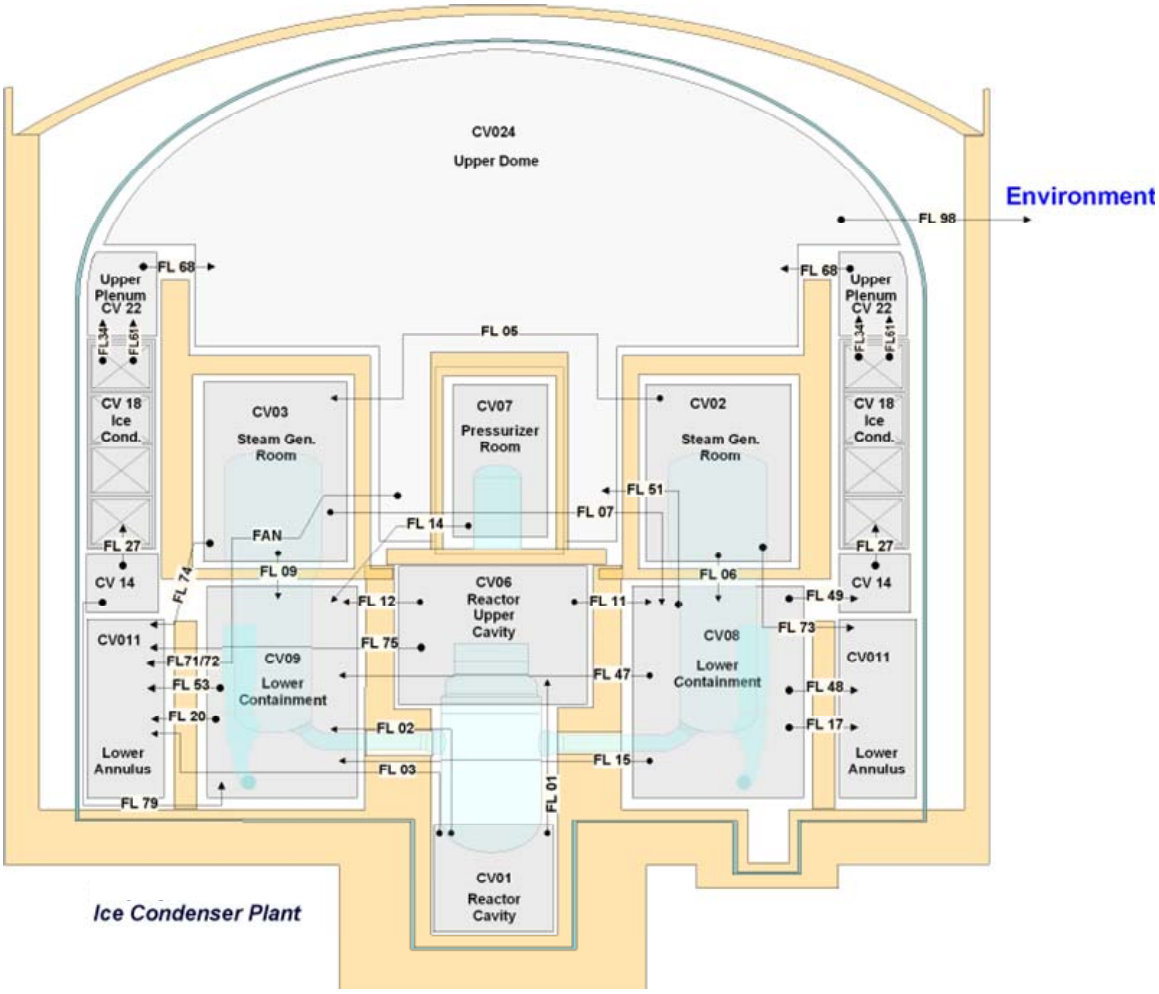

Figure 2-4. ELCOR CVH/FL Nodalization for the Ice Condenser Containment.

Table 2-1. Summary of Containment Control Volumes and Physical Volume.

CV Number	Description	Volume [m^3]
1	Cavity	396
2	Steam generator doghouse - single	362.5
3	Steam generator doghouse - triple	1,087.5
6	Reactor space	439
7	Pressurizer doghouse	135
8	Lower compartment – single	1,510
9	Lower compartment – triple	2,800
11	Lower annulus	2,556
14	Ice condenser lower plenum	685
18	Ice condenser baskets	2,440
22	Ice condenser upper plenum	1,330
24	Upper dome	18,626
	Total volume	32,367 (1,143,029 ft^3)

2.4 MOX and LEU Fission Product Inventories

Section 2.4 is divided into two subsections. Section 2.4.1 summarizes the attributes of the LEU and MOX fuel loadings, the fission product mass inventory, and the decay heat for each configuration as a function of time. Section 2.4.2 describes code and input modifications that were necessary to implement the new decay heat data into MELCOR.

2.4.1 Radionuclide Inventories

The Oak Ridge National Laboratory computer code ORIGEN2.2 [8] was used to determine the elemental composition of irradiated LEU and MOX PWR fuel assemblies, and these results were subsequently used to generate inventories for MELCOR radionuclide (RN) class input data.

Catawba Units 1 and 2 and McGuire Units 1 and 2 are Westinghouse PWRs licensed to produce 3411 MW_{th} thermal power. The reactor cores house 193 fuel assemblies of the 17 × 17 design, with 264 fuel pins per assembly. The current plan to dispose of WG-Pu places two administrative limits on the MOX/LEU cores that are important components of this analysis. First, the proposed core loading for any given cycle will limit the number of MOX assemblies to approximately 40% of the core (76 MOX assemblies). The second administrative limit imposed is that the specified assembly average MOX fuel burnup cannot exceed 45,000 megawatt-day (MWd)/metric tons initial heavy metal (MTIHM) [3].

The WG-Pu MOX fuel assemblies are based on the Framatome/COGEMA Fuels Advanced Mark-BW 17 × 17 fuel assembly. The ceramic plutonium dioxide (PuO_2)-and-uranium dioxide (UO_2) fuel pellets in WG-Pu MOX fuel contain between 2 to 5% fissile plutonium [3]. The isotopic composition vector of the WG-Pu MOX fuel is 93.6% ^{239}Pu, 5.9% ^{240}Pu, 0.4% ^{241}Pu, and 0.1% ^{242}Pu, and the UO_2 component has an enrichment of 0.25 wt-% ^{235}U.

Enrichments used in this analysis were 4.364 weight percent (wt-%) ^{239}Pu for the MOX fuel assemblies and 4.236 wt-% ^{235}U for the LEU assemblies. Listed in Table 2-2 are other parameter values used in the ORIGEN2.2 calculations.

Table 2-2. Reactor Operating Details and Fuel Assembly Data.

Parameter	Values [3]
Reactor design	Westinghouse PWR, four-loop cooling system
Thermal power	3411 MW(t)
Specific power level	38.7 kW/kg-HM
UO_2 feed assemblies (40% MOX)	48
MOX feed assemblies (40% MOX)	36
Fuel cycle duration	495 days [18 months]
Heavy Metal (HM) loading/assembly	463.3 kg/assembly
Weight of fuel if UO_2	220,213 lb [99,887.0 kg]
Cladding weight	56,841 lb (of Zircaloy-4) [25,782.7 kg]

Mission goals were taken into account when determining EOC values for which to calculate LEU and MOX PWR fuel assembly inventories. One mission goal is to achieve at least one cycle of reactor irradiation on all MOX fuel assemblies while achieving a burnup of at least 20,000 MWd/MTIHM. As stated earlier, the specified assembly average MOX fuel burnup limit is 45,000 MWd/MTIHM. Thus, in the ORIGEN2.2 model MOX fuel assemblies were irradiated for up to two cycles (average discharge burnup of 38,313 MWd/MTIHM). The criterion used for the LEU burnup is the current operational limit of 60,000 MWd/metric tons uranium (MTU). In the model, LEU fuel assemblies were irradiated for three cycles, attaining a maximum discharge burnup of 57,470 MWd/MTIHM. Table 2-3 lists EOC burnup values used in the ORIGEN2.2 calculations.

Table 2-3. Cycle Burnup Used in ORIGEN2.2 Calculations.

Fuel Cycle	Burnup (MWd/MTIHM)
1	19,157
2	38,313
3	57,470

Results of the ORIGEN2.2 calculations were grouped according to fuel type (i.e., LEU or MOX) for each irradiation cycle and further separated by mass, radioactivity, and thermal power. Reported were values at initial fuel charge, fuel discharge, and 1-, 2-, 12-, and 24-hr decay periods for each element.

A nominal 40% MOX, 60% LEU loading pattern for the Catawba and McGuire units is shown in Figure 2-5 [9]. There is a total of 193 fuel assemblies in the four-loop Westinghouse core. Of these assemblies, 117 are LEU and 76 are MOX. Table 2-4 lists the condition of the assemblies (i.e., fresh fuel, once-, twice, or three times burned) at the beginning of cycle (BOC) and EOC. Figure 2-6 represents the configuration for a typical LEU loading pattern [9]. Table 2-5 lists the condition for those assemblies. Since accident analyses typically assume EOC conditions, the MELCOR MOX and LEU core descriptions were assembled based on the EOC assembly conditions of Tables 2-4 and 2-5, respectively.

1					L-2	M-1	L-2	M-1	L-2	M-1	L-2				
2			L-2	L-1	M-0	L-0	M-0	L-0	M-0	L-0	M-0	L-1	L-2		
3		L-2	M-0	M-0	L-0	M-1	M-1	L-0	M-1	M-1	L-0	M-0	M-0	L-2	
4		L-1	M-0	L-1	L-1	M-1	L-0	L-1	L-0	M-1	L-1	L-1	M-0	L-1	
5	L-2	M-0	L-0	L-1	M-1	M-0	L-1	L-0	L-1	M-0	M-1	L-1	L-0	M-0	L-2
6	M-1	L-0	M-1	M-1	M-0	L-1	L-0	L-1	L-0	L-1	M-0	M-1	M-1	L-0	M-1
7	L-2	M-0	M-1	L-0	L-1	L-0	L-1	L-0	L-1	L-0	L-1	L-0	M-1	M-0	L-2
8	M-1	L-0	L-0	L-1	L-0	L-1	L-0	L-2	L-0	L-1	L-0	L-1	L-0	L-0	M-1
9	L-2	M-0	M-1	L-0	L-1	L-0	L-1	L-0	L-1	L-0	L-1	L-0	M-1	M-0	L-2
10	M-1	L-0	M-1	M-1	M-0	L-1	L-0	L-1	L-0	L-1	M-0	M-1	M-1	L-0	M-1
11	L-2	M-0	L-0	L-1	M-1	M-0	L-1	L-0	L-1	M-0	M-1	L-1	L-0	M-0	L-2
12		L-1	M-0	L-1	L-1	M-1	L-0	L-1	L-0	M-1	L-1	L-1	M-0	L-1	
13		L-2	M-0	M-0	L-0	M-1	M-1	L-0	M-1	M-1	L-0	M-0	M-0	L-2	
14			L-2	L-1	M-0	L-0	M-0	L-0	M-0	L-0	M-0	L-1	L-2		
15					L-2	M-1	L-2	M-1	L-2	M-1	L-2				
	O	N	M	L	K	J	I	H	G	F	E	D	C	B	A

Figure 2-5. Projected Loading Pattern for 40% MOX Core.

Table 2-4. Number of Assemblies in 40% MOX Core by Type and Condition.

Cycles Previously in Core	Beginning of Cycle		End of Cycle	
	LEU	MOX	LEU	MOX
Zero (feed)	48	36	-	-
One (once-burned)	44	40	48	36
Two (twice-burned)	25	-	44	40
Three (three times burned)	-	-	25	-

	O	N	M	L	K	J	I	H	G	F	E	D	C	B	A
1					L-2	L-1	L-2	L-1	L-2	L-1	L-2				
2			L-2	L-1	L-0	L-1	L-0	L-1	L-0	L-1	L-0	L-1	L-2		
3		L-2	L-1	L-0	L-1	L-0	L-1	L-0	L-1	L-0	L-1	L-0	L-1	L-2	
4		L-1	L-0	L-1	L-1	L-1	L-0	L-2	L-0	L-1	L-1	L-1	L-0	L-1	
5	L-2	L-0	L-1	L-1	L-1	L-0	L-1	L-0	L-1	L-0	L-1	L-1	L-1	L-0	L-2
6	L-0	L-1	L-0	L-1	L-0	L-2	L-0	L-2	L-0	L-2	L-0	L-1	L-0	L-1	L-0
7	L-2	L-0	L-1	L-0	L-1	L-0	L-1	L-0	L-1	L-0	L-1	L-0	L-1	L-0	L-2
8	L-0	L-1	L-0	L-2	L-0	L-2	L-0	L-2	L-0	L-2	L-0	L-2	L-0	L-1	L-0
9	L-2	L-0	L-1	L-0	L-1	L-0	L-1	L-0	L-1	L-0	L-1	L-0	L-1	L-0	L-2
10	L-0	L-1	L-0	L-1	L-0	L-2	L-0	L-2	L-0	L-2	L-0	L-1	L-0	L-1	L-0
11	L-2	L-0	L-1	L-1	L-1	L-0	L-1	L-0	L-1	L-0	L-1	L-1	L-1	L-0	L-2
12		L-1	L-0	L-1	L-1	L-1	L-0	L-2	L-0	L-1	L-1	L-1	L-0	L-1	
13		L-2	L-1	L-0	L-1	L-0	L-1	L-0	L-1	L-0	L-1	L-0	L-1	L-2	
14			L-2	L-1	L-0	L-1	L-0	L-1	L-0	L-1	L-0	L-1	L-2		
15					L-2	L-1	L-2	L-1	L-2	L-1	L-2				

Figure 2-6. Typical Loading Pattern for LEU Core.

Table 2-5. Number of Assemblies in LEU Core by Condition.

Cycles Previously in Core	Beginning of Cycle	End of Cycle
Zero (feed)	80	-
One (once-burned)	76	80
Two (twice-burned)	37	76
Three (three times burned)	-	37

The mass and power units of the ORIGEN results were grams of element per 1,000 kilograms of fuel and watts (generated by an element) per 1,000 kilograms of fuel, respectively. The ORIGEN results were specific to assembly type and condition, i.e., dependent upon whether the assembly was a MOX or LEU assembly and whether it was once-, twice; or three times burned. The mass and power units required by the MELCOR input are kilograms of element and watts per kilogram of element, respectively. The mass and power inputs by element to MELCOR are specified distinct for each assembly type, i.e., MOX or LEU, in order to properly characterize the different fission product release characteristics of the two fuels. Appropriate manipulations were performed to convert and collect the ORIGEN results into MELCOR input reflecting the fission product inventories and decay powers associated with the collective LEU and collective MOX assemblies of the core.

Mass and powers per unit mass were not input to MELCOR for every (or even most) of the elements in the ORIGEN results. Elements that were included were limited to those with meaningful decay powers. Accordingly, input to MELCOR were the masses and powers per unit mass for 37 ^{235}U-associated (LEU) elements and 37 Pu-associated (MOX) elements such that 99.9% of the total decay heat power reported for the 91 total elements in the ORIGEN results was captured.

The MOX and LEU element masses and powers per unit element mass formed from the ORIGEN results were input to MELCOR along with a specification for combining the individual elements into radionuclide classes. The 37 ORIGEN elements included in the MELCOR input are combined into MELCOR RN classes as shown in Table 2-6. While this table calls out only 37 elements and 13 classes, 74 elements and 26 classes were actually defined to account for LEU versus MOX associated radionuclides in order to distinguish, for example, cesium (Cs) resulting from MOX burnup versus Cs resulting from LEU burnup.

Table 2-6. Radionuclide Class Constitutive Elements.

Class #	Class Name	Representative Element	Constitutive Elements
1	Noble Gases	Xe	Kr, Xe
2	Alkali Metals	Cs	Cs, Rb
3	Alkaline Earths	Ba	Ba, Sr
4	Halogens	I	Br, I
5	Chalcogens	Te	Se, Te
6	Platinoids	Ru	Pd, Rh, Ru
7	Transition Metals	Mo	Mo, Nb, Tc
8	Tetravalents	Ce	Ce, Np, Pu, Zr
9	Trivalents	La	Cm, Eu, La, Nd, Pm, Pr, Sm, Y
10	Uranium	U	U
11	More Volatile Main Group Metals	Cd	As, Cd, Sb
12	Less Volatile Main Group Metals	Sn	Ag, Ge, In, Sn

Table 2-7 identifies the radionuclide class mass inventories input to MELCOR for the LEU and MOX cores. The masses in this table relate to core condition at reactor shutdown. Included in Table 2-7 for comparison purposes is the radionuclide mass inventory at shutdown per standard American Nuclear Society (ANS) calculation assuming a reactor operating at 3411 MW_{th} for 548 days.[2]

Table 2-7. Radionuclide Class Masses at Shutdown (kg).

Class #	Representative Element	Standard ANS Calculation	LEU Core	40% MOX Core		
				LEU Assemblies	MOX Assemblies	Total
1	Xe	3.421E+02	5.178E+02	3.187E+02	1.694E+02	4.882E+02
2	Cs	1.907E+02	2.910E+02	1.787E+02	1.009E+02	2.796E+02
3	Ba	1.501E+02	2.200E+02	1.352E+02	5.492E+01	1.901E+02
4	I	1.470E+01	2.346E+01	1.444E+01	1.137E+01	2.581E+01
5	Te	3.002E+01	4.865E+01	2.998E+01	2.050E+01	5.048E+01
6	Ru	2.111E+02	3.592E+02	2.221E+02	1.874E+02	4.095E+02
7	Mo	2.490E+02	3.728E+02	2.292E+02	1.208E+02	3.500E+02
8	Ce	4.393E+02	1.489E+03	9.134E+02	1.300E+03	2.213E+03
9	La	4.076E+02	6.996E+02	4.305E+02	2.105E+02	6.410E+02
10	U	8.458E+04	8.502E+04	5.151E+04	3.288E+04	8.439E+04
11	Cd	9.970E-01	1.491E+01	9.256E+00	8.470E+00	1.773E+01
12	Sn	5.662E+00	1.484E+01	9.166E+00	9.360E+00	1.853E+01
13	B	0.000E+00	0.000E+00	0.000E+00	0.000E+00	0.000E+00

[2] Note that with the exception of certain class combinations, MELCOR RN inventories are fixed in time. Also note that the oxygen identified in the ORIGEN results has not been included in the MELCOR RN class inventories. The oxygen bound up in the ceramic UO_2 and PuO_2 fuel is automatically included in the RN inventory, i.e., without specific user input.

Tables 2-8 through 2-12 identify the radionuclide class powers input to MELCOR for the LEU and MOX cores at shutdown, and at 1 hr, 2 hr, 12 hr, and 24 hr after shutdown, respectively.[3] Included in Table 2-8, again for comparison purposes, are the radionuclide class powers at shutdown per the standard ANS calculation.

Finally, Figure 2-7 shows the time history of fission product decay power for the LEU and MOX cores as well as the standard ANS calculation.

Table 2-8. Radionuclide Class Powers at Shutdown (Watts).

Class #	Representative Element	Standard ANS Calculation	LEU Core	40% MOX Core		
				LEU Assemblies	MOX Assemblies	Total
1	Xe	1.793E+07	1.432E+07	8.657E+06	4.148E+06	1.281E+07
2	Cs	3.287E+07	2.717E+07	1.644E+07	8.033E+06	2.447E+07
3	Ba	2.241E+07	1.957E+07	1.184E+07	6.157E+06	1.800E+07
4	I	2.502E+07	2.110E+07	1.278E+07	7.045E+06	1.982E+07
5	Te	1.038E+07	8.804E+06	5.332E+06	2.885E+06	8.217E+06
6	Ru	4.437E+06	5.216E+06	3.194E+06	3.186E+06	6.380E+06
7	Mo	3.436E+07	3.576E+07	2.176E+07	1.670E+07	3.846E+07
8	Ce	1.505E+07	1.685E+07	1.024E+07	6.069E+06	1.631E+07
9	La	4.254E+07	3.913E+07	2.372E+07	1.361E+07	3.732E+07
10	U	4.482E+06	5.126E+06	3.128E+06	1.751E+06	4.879E+06
11	Cd	7.992E+06	7.608E+06	4.615E+06	2.857E+06	7.472E+06
12	Sn	1.864E+06	2.965E+06	1.804E+06	1.255E+06	3.059E+06
13	B	0.000E+00	0.000E+00	0.000E+00	0.000E+00	0.000E+00
Totals		**2.193E+08**	**2.036E+08**	**1.235E+08**	**7.370E+07**	**1.972E+08**

[3] Note that the values in these tables are watts rather than watts per unit element mass as actually input to MELCOR.

Table 2-9. Radionuclide Class Powers 1 Hour After Shutdown (Watts).

Class #	Representative Element	LEU Core	40% MOX Core		
			LEU Assemblies	MOX Assemblies	Total
1	Xe	1.695E+06	1.024E+06	5.128E+05	1.537E+06
2	Cs	2.899E+06	1.758E+06	8.933E+05	2.652E+06
3	Ba	3.345E+06	2.024E+06	9.963E+05	3.020E+06
4	I	8.375E+06	5.081E+06	3.240E+06	8.321E+06
5	Te	1.860E+06	1.128E+06	7.045E+05	1.833E+06
6	Ru	1.813E+06	1.109E+06	1.125E+06	2.233E+06
7	Mo	3.707E+06	2.249E+06	1.423E+06	3.672E+06
8	Ce	7.125E+06	4.341E+06	2.449E+06	6.790E+06
9	La	1.215E+07	7.370E+06	4.202E+06	1.157E+07
10	U	1.032E+06	6.301E+05	3.081E+05	9.382E+05
11	Cd	8.321E+05	5.063E+05	3.898E+05	8.960E+05
12	Sn	2.341E+05	1.430E+05	1.256E+05	2.685E+05
13	B	0.000E+00	0.000E+00	0.000E+00	0.000E+00
Totals		**4.507E+07**	**2.736E+07**	**1.637E+07**	**4.373E+07**

Table 2-10. Radionuclide Class Powers 2 Hours After Shutdown (Watts).

Class #	Representative Element	LEU Core	40% MOX Core		
			LEU Assemblies	MOX Assemblies	Total
1	Xe	1.317E+06	7.959E+05	4.155E+05	1.211E+06
2	Cs	1.449E+06	8.804E+05	4.148E+05	1.295E+06
3	Ba	2.655E+06	1.606E+06	7.711E+05	2.377E+06
4	I	6.898E+06	4.185E+06	2.692E+06	6.877E+06
5	Te	1.033E+06	6.269E+05	4.094E+05	1.036E+06
6	Ru	1.667E+06	1.020E+06	1.035E+06	2.055E+06
7	Mo	3.096E+06	1.877E+06	1.132E+06	3.009E+06
8	Ce	7.016E+06	4.274E+06	2.410E+06	6.684E+06
9	La	1.024E+07	6.211E+06	3.528E+06	9.738E+06
10	U	3.306E+05	2.023E+05	6.185E+04	2.641E+05
11	Cd	4.933E+05	3.003E+05	2.393E+05	5.395E+05
12	Sn	1.802E+05	1.101E+05	9.934E+04	2.094E+05
13	B	0.000E+00	0.000E+00	0.000E+00	0.000E+00
Totals		**3.637E+07**	**2.209E+07**	**1.321E+07**	**3.530E+07**

Table 2-11. Radionuclide Class Powers 12 Hours After Shutdown (Watts).

Class #	Representative Element	LEU Core	40% MOX Core		
			LEU Assemblies	MOX Assemblies	Total
1	Xe	5.442E+05	3.298E+05	2.186E+05	5.484E+05
2	Cs	3.091E+05	1.910E+05	9.534E+04	2.864E+05
3	Ba	1.235E+06	7.470E+05	3.569E+05	1.104E+06
4	I	3.677E+06	2.232E+06	1.491E+06	3.723E+06
5	Te	3.967E+05	2.410E+05	1.746E+05	4.156E+05
6	Ru	1.179E+06	7.213E+05	7.452E+05	1.467E+06
7	Mo	2.457E+06	1.490E+06	8.867E+05	2.376E+06
8	Ce	6.093E+06	3.712E+06	2.090E+06	5.802E+06
9	La	6.330E+06	3.845E+06	2.231E+06	6.076E+06
10	U	1.790E+05	1.097E+05	1.070E+04	1.204E+05
11	Cd	1.302E+05	7.938E+04	6.623E+04	1.456E+05
12	Sn	7.860E+04	4.817E+04	4.689E+04	9.506E+04
13	B	0.000E+00	0.000E+00	0.000E+00	0.000E+00
Totals		**2.261E+07**	**1.375E+07**	**8.413E+06**	**2.216E+07**

Table 2-12. Radionuclide Class Powers 24 Hours After Shutdown (Watts).

Class #	Representative Element	LEU Core	40% MOX Core		
			LEU Assemblies	MOX Assemblies	Total
1	Xe	3.669E+05	2.225E+05	1.489E+05	3.714E+05
2	Cs	2.472E+05	1.536E+05	8.098E+04	2.346E+05
3	Ba	9.512E+05	5.758E+05	2.842E+05	8.600E+05
4	I	2.783E+06	1.690E+06	1.138E+06	2.828E+06
5	Te	3.290E+05	1.998E+05	1.439E+05	3.437E+05
6	Ru	1.040E+06	6.362E+05	6.593E+05	1.296E+06
7	Mo	1.938E+06	1.175E+06	6.965E+05	1.871E+06
8	Ce	5.236E+06	3.190E+06	1.792E+06	4.982E+06
9	La	5.433E+06	3.301E+06	1.952E+06	5.253E+06
10	U	1.698E+05	1.041E+05	1.017E+04	1.143E+05
11	Cd	7.497E+04	4.576E+04	3.890E+04	8.466E+04
12	Sn	5.758E+04	3.531E+04	3.452E+04	6.984E+04
13	B	0.000E+00	0.000E+00	0.000E+00	0.000E+00
Totals		**1.863E+07**	**1.133E+07**	**6.979E+06**	**1.831E+07**

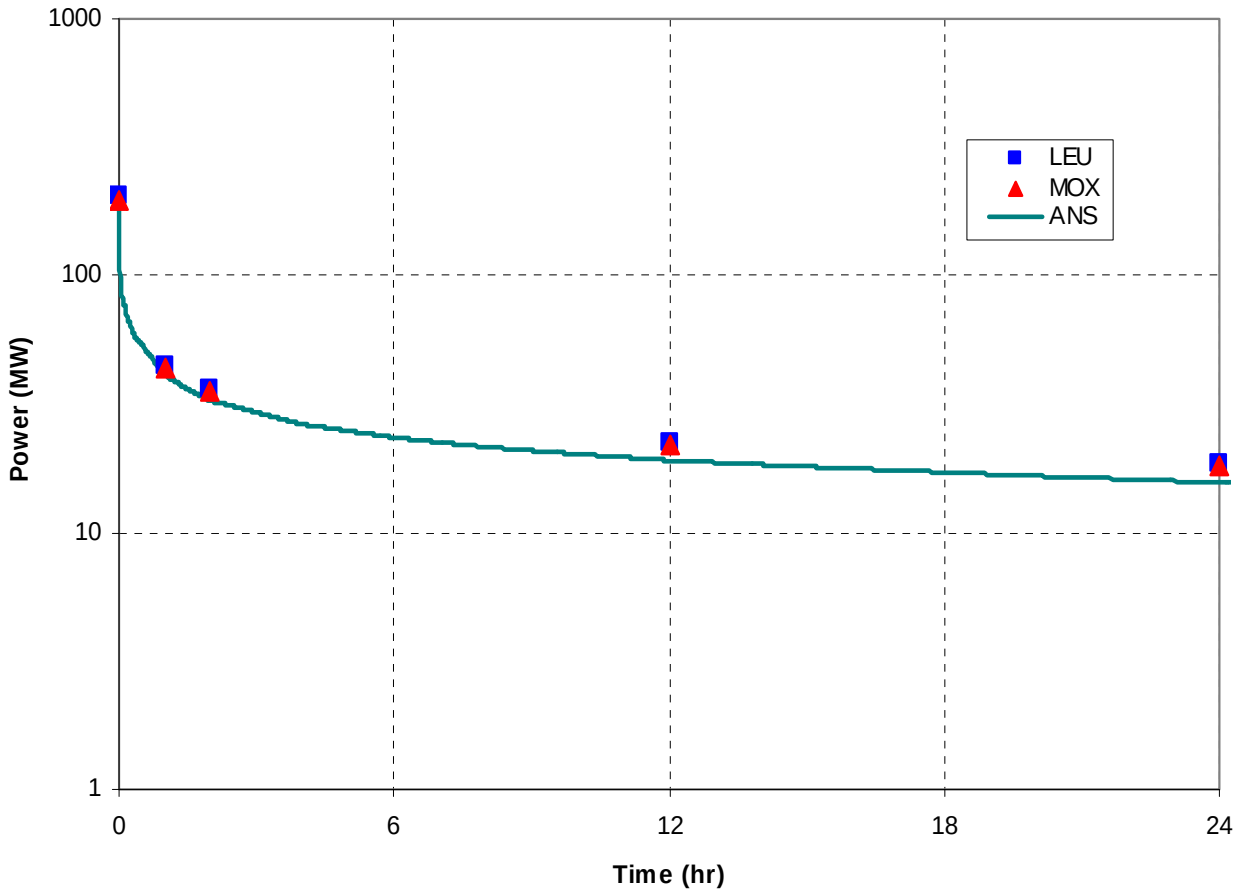

Figure 2-7. Fission Product Decay Power.

2.4.2 Modifications to Decay Power

The LEU- and MOX-core decay power histories derived from the ORIGEN2.2 calculations consist of only five points. When input to MELCOR, the logarithmic fit performed by the code between these points gave a somewhat poor approximation for the first hour after reactor shutdown (when compared to the standard ANS calculation). To better approximate the first few hours of decay power, intermediate points between the first three ORIGEN2.2 points were specified to MELCOR assuming the same nondimensional shape of the ANS calculation.

As can be seen in Figure 2-7, the decay power for the MOX core is slightly lower than that for the LEU core. This power difference affected the early thermal-hydraulic response, which led to differences in the late-phase accident response. Earlier scoping calculations renormalized the decay heat to eliminate these differences and the subsequent accident responses were more similar. However, all of the present calculations use the precise decay heat calculations as specified in Section 2.4.1.

2.5 MOX Fission Product Release Model

A new MOX fission product model was developed based upon an analysis of the available MOX fission product release experimental data. Section 2.5.1 shows the results from the VERCORS RT-2 test using MOX fuel. Section 2.5.2 describes the formulation of the MELCOR fission product release model. Finally, Section 2.5.3 describes the development of the release coefficients for MOX fuel.

2.5.1 VERCORS RT-2 Test

The VERCORS RT-2 test [10] was performed using MOX fuel from the Gravelines nuclear power plant in France having a burnup of approximately 47.3 MWd/tonne.[4] The objective of the VERCORS tests was to provide fission product release measurements for use in developing and validating models predicting such release under severe accident or off-normal conditions. The RT-2 test was analogous to the RT-1 test, which was performed using normal LEU fuel. Both tests were performed under similar conditions with a mixture of steam and hydrogen (0.5:25 mg/s of H_2:H_20) during fission product release up to temperatures nearing 2500K. Neither test RT-1 or RT-2 involved any re-irradiation of the test fuel samples before testing; thus no data were obtained on the release of iodine or other short-lived fission products. The test measurements focused on release of krypton (Kr), Cs, ruthenium (Ru), cerium (Ce), and europium (Eu), the latter three of which are generally considered to be of low volatility in comparison to Cs and iodine (I). RT-1 and RT-2 releases for these elements are shown in Table 2-13. The principal measurement in test RT-2 was for the time-temperature release of Cs, the results of which are shown in Figure 2-8. Total releases for other isotopes measured in tests RT-1 (LEU) and RT-2 (MOX) are summarized in Pontillon et al. [11].

Table 2-13. Comparison of Fission Product Release from VERCORS Tests RT-1 and RT-2.

Isotope	MELCOR Release Class	Fraction Released	
		RT-1 (LEU)	RT-2 (MOX)
^{106}Ru	Class 6 - Platinoids (Ru)	0.09	0.0535
^{110}Ag	Class 12 - Main Group, less volatile (Ag)	0.9	0.97
^{125}Sb	Class 11 - Main Group, more volatile (Cd)	0.96	0.77
^{134}Cs	Class 2 – Alkali Metals (Cs)	1.0	1.0
^{137}Cs	Class 2 – Alkali Metals (Cs)	1.0	1.0
^{144}Ce	Class 8 – Tetravalent (Ce)	0.03	0.02
^{154}Eu	Class 9 – Trivalents (La)	0.01	0.003
^{85}Kr	Class 1 – Noble Gases (Xe)	0.86	0.87

[4] A second MOX fission product release test was performed in the VERCORS program, test RT-7 [11]. This test was performed with release under pure reducing conditions. Since fission product release is expected to take place under conditions with both steam and hydrogen present, the RT-7 data is not considered to be as representative of in vessel release conditions overall, and for this reason is not considered this study.

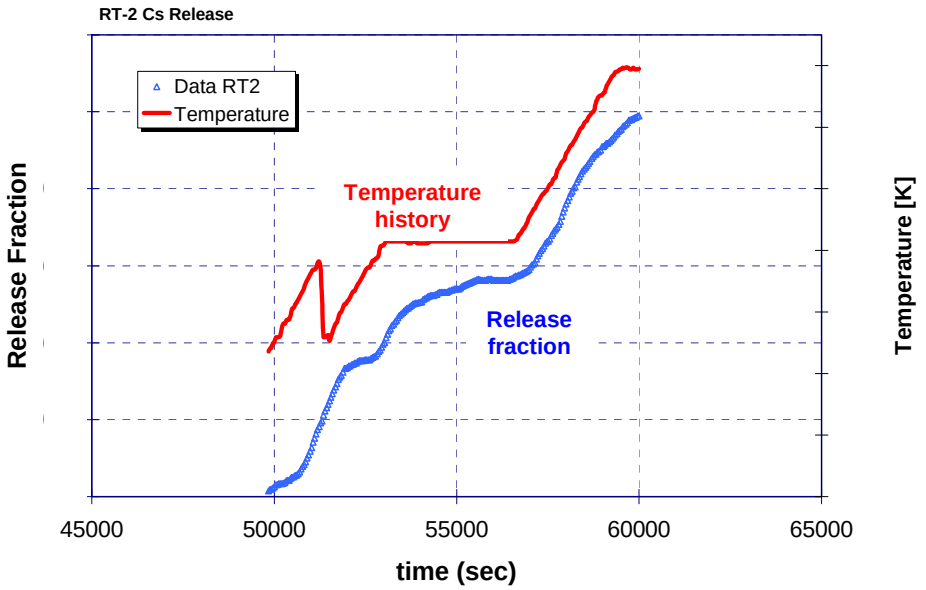

Figure 2-8. RT-2 Release of Cesium as a Function of Test Sample Temperature.[5]

2.5.2 Modeling of Fission Product Releases from LEU and MOX Fuel

The Booth diffusion model is one model available in MELCOR for calculating the release of fission products from overheating fuel; the Booth model is selected for this study because of its more mechanistic nature in comparison to the CORSOR fractional release rate models. In this treatment, the release of Cs is modeled to match the kinetics of the measured release for Cs, and other fission product releases are simply scaled to the Cs release to match those observed experimentally. The Booth release model is described briefly below.

In the Booth model, as implemented in MELCOR, the release of Cs from the fuel is treated as a diffusion process where Cs migrates through the fuel matrix to the surface of a fuel grain. From there, a mass transport limitation based on specie vapor pressure is considered before release to the local atmosphere. The effective diffusion coefficient for Cs in the fuel grain is given by

$$D = D_0 \exp\left(-Q/RT\right) \tag{1}$$

where R is the universal gas constant, T is the temperature, Q is an activation energy, and the pre-exponential factor D_o is a function of the fuel burnup. The Cs release fraction at time *t* is calculated from an approximate solution of the diffusion equation for fuel grains of spherical geometry [12],

$$f = 6\sqrt{\frac{D't}{\pi}} - 3D't \quad for\ D't < 1/\pi^2 \tag{2}$$

[5] The ordinate values and units are omitted from the graph because the data are considered proprietary.

$$f = 1 - \frac{6}{\pi^2}\exp\left(-\pi^2 D't\right) \quad for\ D't > 1/\pi^2 \tag{3}$$

where

$D't$ = Dt/a^2 (dimensionless), and
a = equivalent sphere radius for the fuel grain.

The parameters of the diffusion coefficient, D_o and Q, may be determined from experimental data by a fitting process described by Lorenz and Osborne [13]. In this process, Eqs. 4 and 5 are inverted to solve for the product Dt/a^2, as indicated below.

$$\frac{Dt}{a^2} = \frac{2}{\pi} - \frac{f}{3} - 2\sqrt{\frac{1}{\pi^2} - \frac{f}{3\pi}} \quad for\ f < 0.85 \tag{4}$$

$$\frac{Dt}{a^2} = \frac{-1}{\pi^2}\ln\left[\frac{\pi^2(1-f)}{6}\right] \quad for\ f > 0.85 \tag{5}$$

where f is the release fraction.

The parameters used to represent Cs diffusion release from MOX and LEU fuel are summarized in Table 2-14.

Table 2-14. Parameters for Diffusion Coefficient for MOX and LEU Fuel.

	D_o [m^2/s]	Q [J/kg-mole]
LEU Fuel (ORNL-Booth)	1×10^{-6}	3.814×10^5
MOX Fuel (MOX-Booth)	2×10^{-11}	1.664×10^5
Grain radius	6μm	6μm

2.5.3 MELCOR Analysis of RT-2 Experiment Using Fitted Booth Parameters

The Booth parameters for Cs release from MOX fuel determined from the RT-2 data are used in a MELCOR model of the RT-2 test to assess the predicted release against that observed experimentally. The results of the MELCOR release prediction for Cs in test RT-2 are shown in Figure 2-9. As seen in Figure 2-9, the kinetics of Cs release are well predicted by the MOX-Booth diffusion parameters, and that the low temperature release rate compared to that of LEU fuel (ORNL-Booth) is greater for the same assumed temperature history. Significant release of Cs is observed to begin at around 1700 K for MOX fuel, whereas a similar release rate in LEU fuel is not observed until temperatures exceed 2000 K. Figures 2-10 through 2-20 show release predictions for the other MELCOR release classes. Data from RT-2 measurements are shown compared to MELCOR predictions in Figures 2-10 through 2-15. Comparisons to FPT-1 measurements are shown in Figures 2-16 through 2-20 for the release classes where RT-2 measurements were not made.

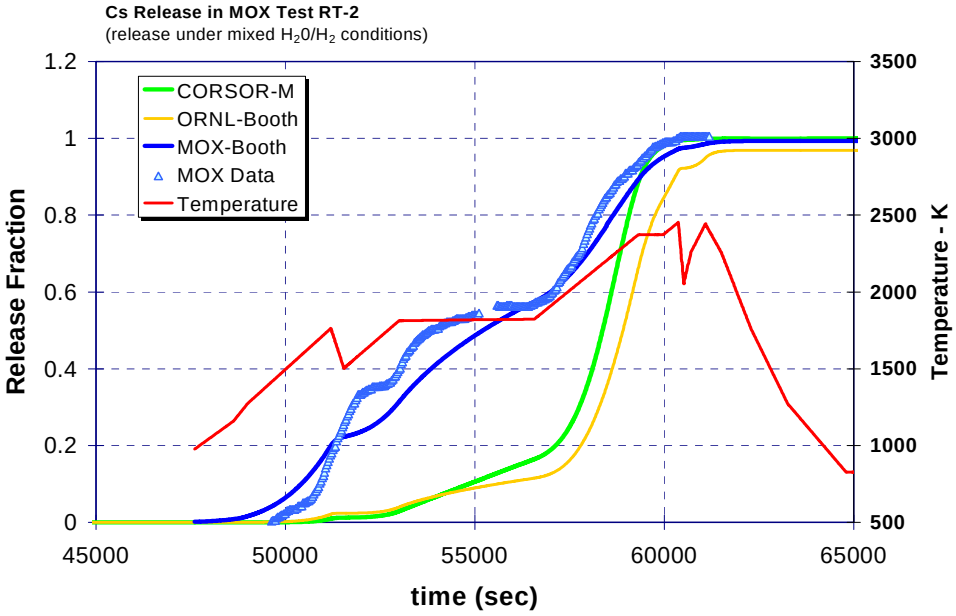

Figure 2-9. Comparison of the MELCOR-Predicted Release of Cs-Class for VERCORS Test RT-2 to the Experimental Measurement of Cs-137.[6]

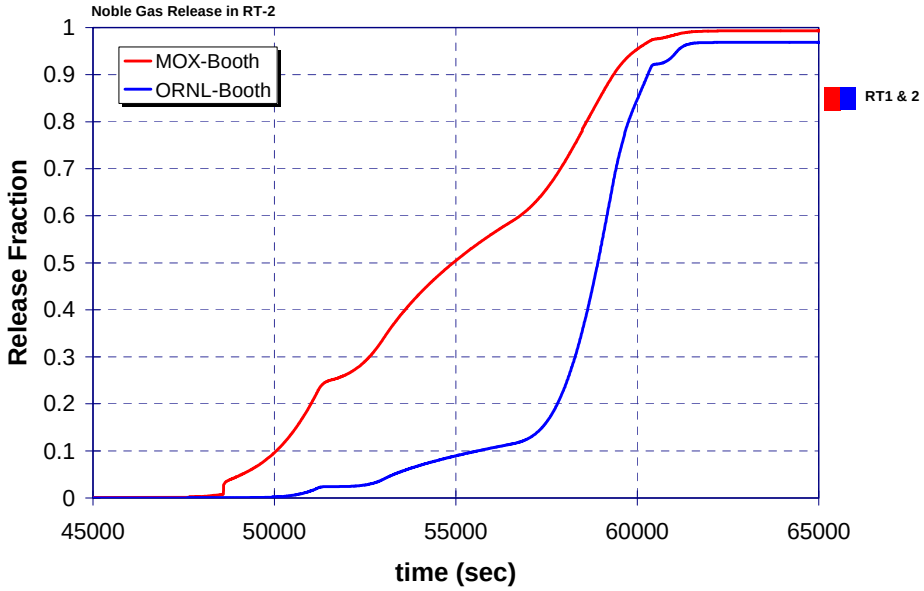

Figure 2-10. Comparison of the MELCOR-Predicted Release of the Noble Gases for VERCORS Test RT-2 to the Experimental Measurement of Kr-85 release.

[6] Also shown are MELCOR-predicted releases using the MELCOR default Cs release model (CORSOR-M) and the presently recommended ORNL-Booth release model for LEU fuel.

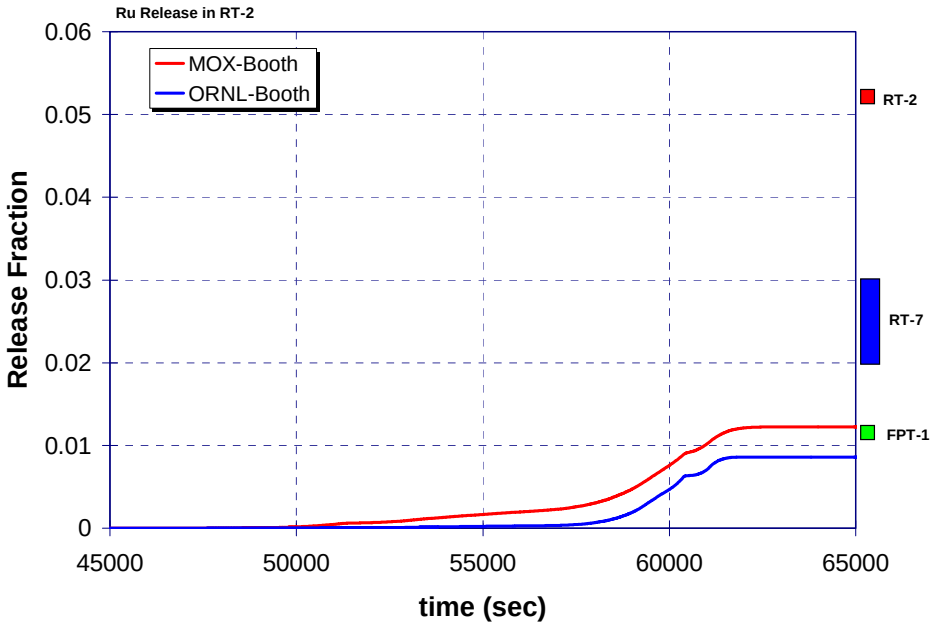

Figure 2-11. Comparison of the MELCOR-Predicted Release of Ruthenium from VERCORS Test RT-2 of the Experimental Measurement of Ru-106 Release.

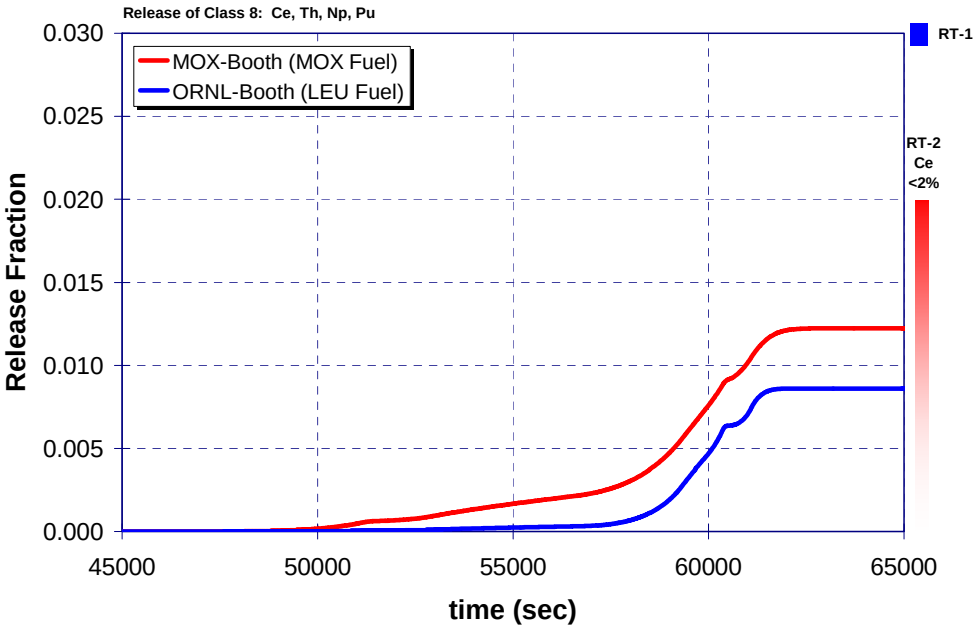

Figure 2-12. Comparison of the MELCOR-Predicted Release of Cerium Class from VERCORS Test RT-2 to the Experimental Measurement of Ce-144 Release.

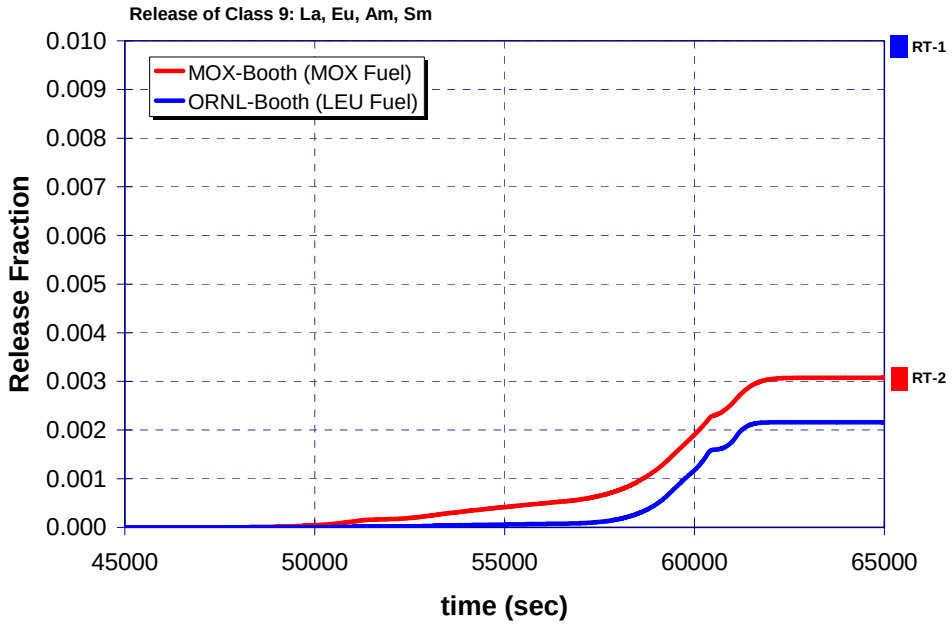

Figure 2-13. Comparison of the MELCOR-Predicted Release of Lanthanum for VERCORS Test RT-2 to the Experimental Measurement of Eu-154 Release.

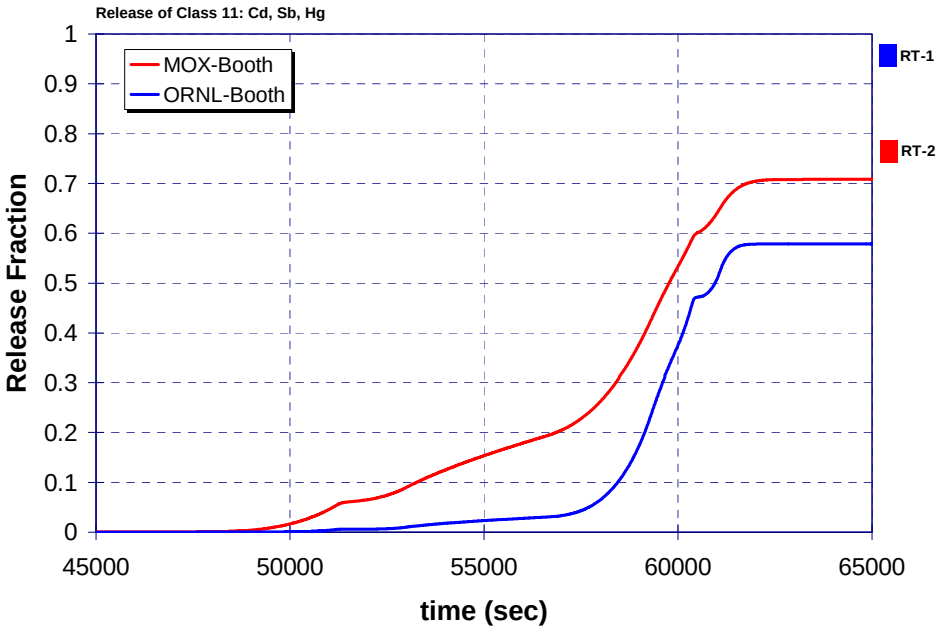

Figure 2-14. Comparison of the MELCOR-Predicted Release of Cadmium Class for VERCORS Test RT-2 Compared to the Experimental Measurement of Sb-125 Release.

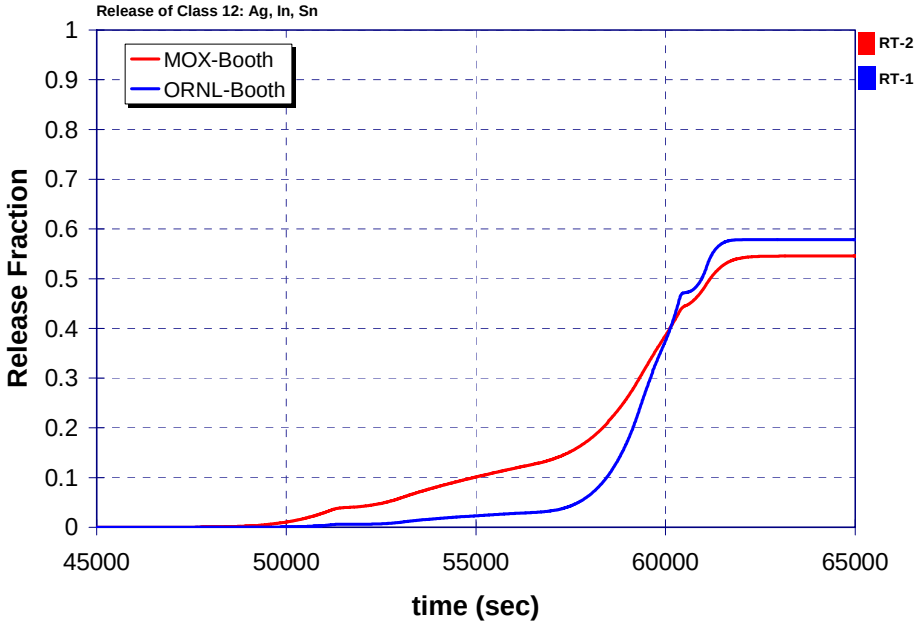

Figure 2-15. Comparison of MELCOR-Predicted Release of Silver Class from VERCORS Test RT-2 to the Experimental Measurement of Ag-110m Release.

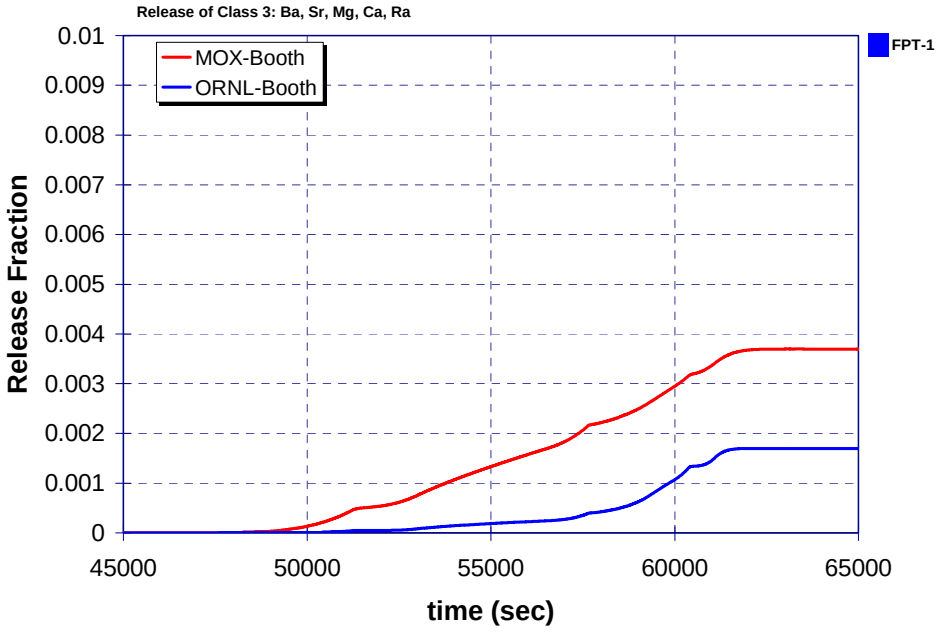

Figure 2-16. Comparison of the MELCOR-Predicted Release of Barium/Strontium Class from VERCORS Test RT-2 to the FPT-1 Measured Release.

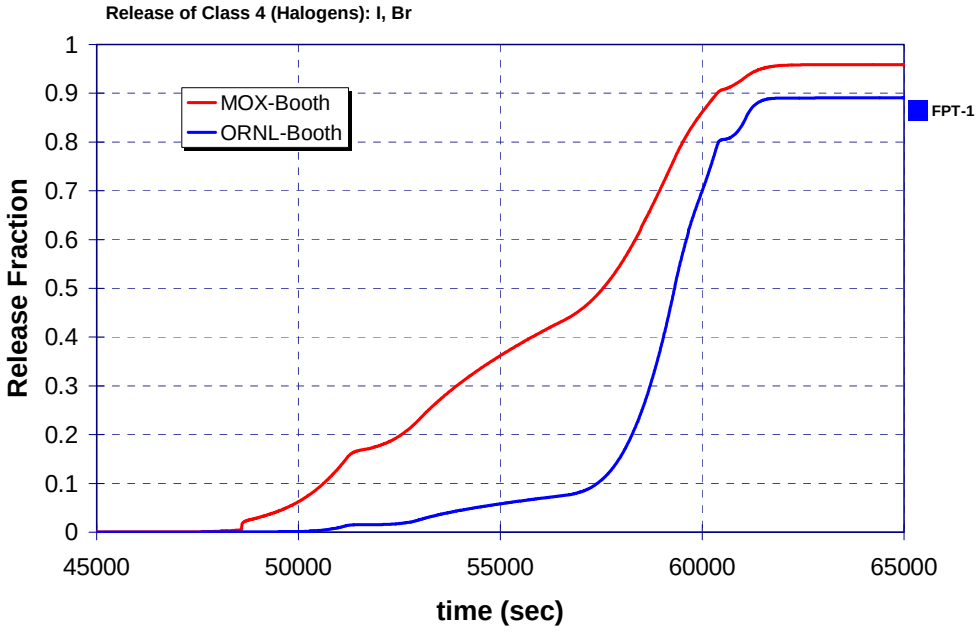

Figure 2-17. Comparison of the MELCOR-Predicted Release of Iodine-Class from VERCORS Test RT-2 to the FPT-1 Measured Release.

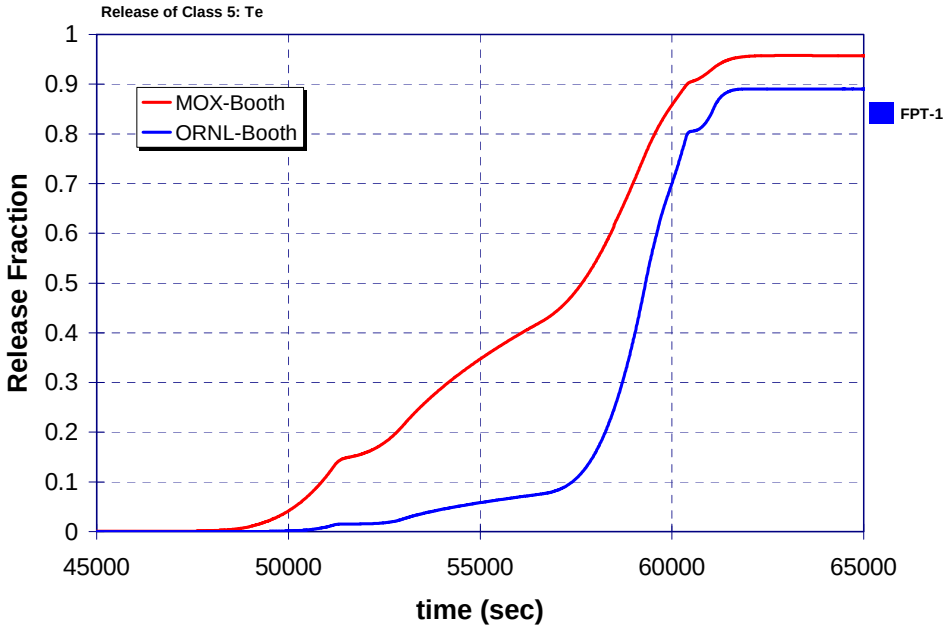

Figure 2-18. Comparison of the MELCOR-Predicted Release of Tellurium Class from VERCORS Test RT-2 for the FPT-1 Measured Release.

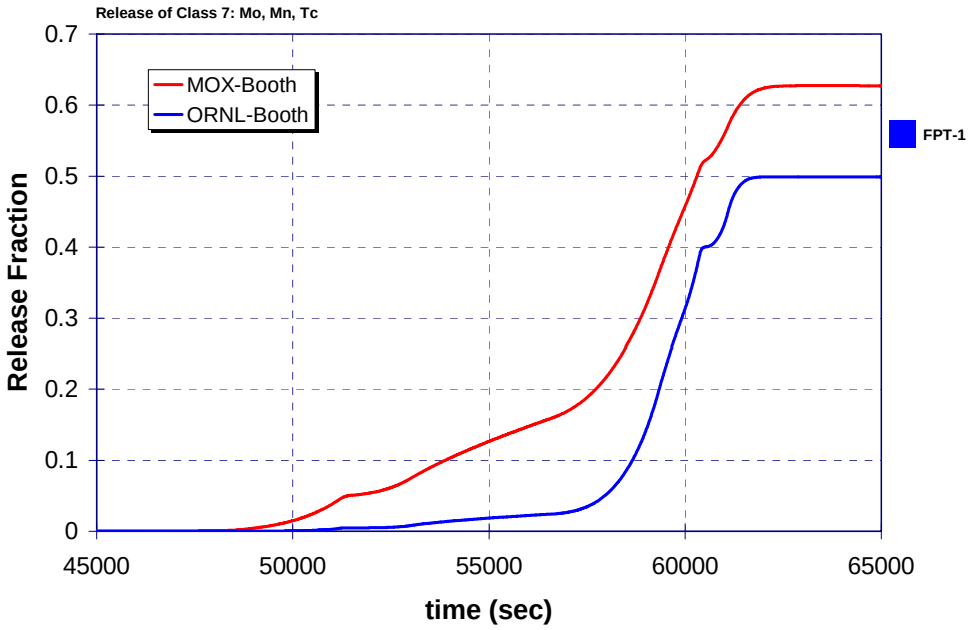

Figure 2-19. MELCOR-Predicted Release of Molybdenum Class from VERCORS Test RT-2 with the FPT-1 Measured Release Shown for Comparison.

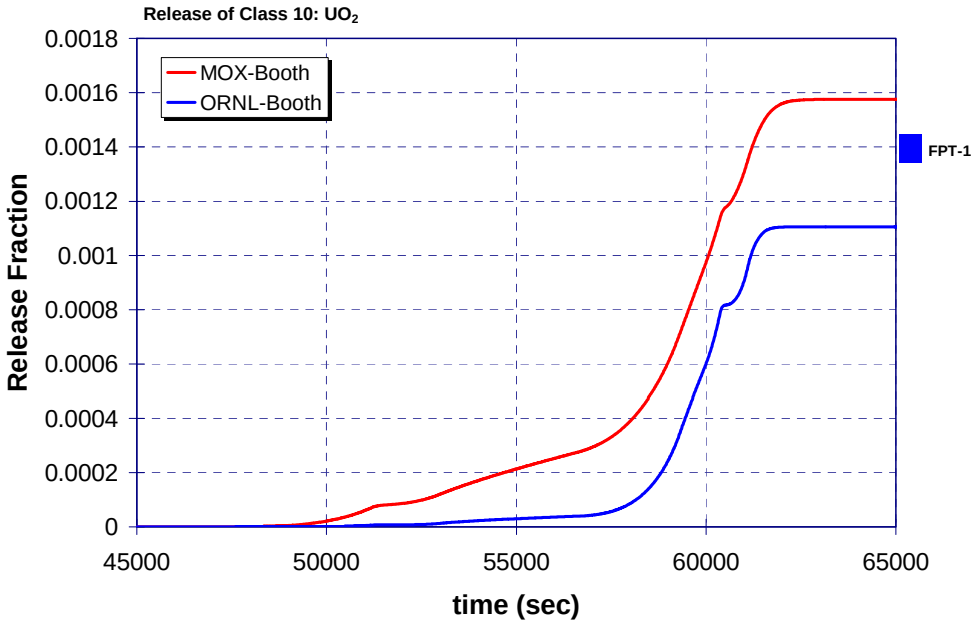

Figure 2-20. Comparison of the MELCOR-Predicted Release of Uranium Dioxide Class from VERCORS Test RT-2 with the FPT1-1 Measured Release.

3.0 DESCRIPTION OF SEVERE ACCIDENT CALCULATION MATRIX

To examine the impact of a 40% MOX core load on source term during a postulated severe accident, as compared to an LEU core load, a set of risk dominant MELCOR calculations was specified. Three accident initiators were selected along with two containment end-states. The accident initiators considered are:

1. Station blackout (SBO),
2. Small-break loss-of-coolant accident (SLOCA) with failure to realign the emergency core cooling system (ECCS), and
3. Large-break loss-of-coolant accident (LLOCA) with failure of the ECCS.

The containment end-states are:

1. Early failure (creep-rupture of the RCS is precluded and the vessel failure occurs from high pressure – CF is assumed to occur concurrently with vessel failure), and
2. Late failure (creep-rupture of the RCS is permitted – the containment fails late due to slow, over-pressurization from core-concrete interactions).

The rationale for selection of accident initiators and containment end-states is presented in Sections 3.1 and 3.2, respectively. Section 3.3 discusses a sensitivity case that was performed to address limitations on modeling of fuel material properties. Section 3.4 describes an additional sensitivity calculation intended to inform the interpretation of differences in results between LEU core and 40% MOX core calculations. Finally, Section 3.5 describes miscellaneous modeling issues for all of the calculations, including identification of some sensitivities that are intended to represent significant uncertainties identified in the plant probabilistic risk assessments (PRAs). The resulting MELCOR calculation matrix is presented in Table 3-1.

3.1 Accident Initiators

Considering the various accident initiators, SBOs account for 43% of the total core damage frequency (CDF) in Revision 2b of the Catawba PRA [14]. Loss-of-coolant accidents (LOCAs) account for 30% of the total. SLOCAs are larger contributors than LLOCAs, and failure to accomplish switchover of high pressure injection to recirculation mode is the dominant cause of core damage given an SLOCA. Most of the remaining CDF was attributed to transient events that caused plant shutdown, along with failures of emergency systems (e.g., ECCS). However, these events are equivalent to an SBO in terms of evaluating accident progression and source term. Therefore, transients were not addressed independently as part of this analysis. Steam generator tube rupture (SGTR) and induced SGTR (ISGTR) events were small contributors to CDF for these plants. Therefore, SGTRs were also not included in this analysis.[7] Contributions to CDF identified in the McGuire PRA are similar [2]. Cases 1A through 1G in Table 3-1 address the most likely SBOs and LOCAs identified in the plant-specific PRAs for a representative LEU core.[8] Cases 2A through 2G address the same accidents for the proposed 40% MOX core.

[7] Cases 1H and 2H were originally included in the calculation matrix as placeholders for SGTRs.

[8] Differences in containment end-states that differentiate some of these cases are discussed in Section 3.2.

Table 3-1. MELCOR Calculation Matrix for MOX Versus LEU Severe Accident Response.

Case	Core Loading[a]	Fuel Material Properties	Fission Product Release Parameters	Power	LOCA	ECCS	AFW[d]	Containment End-State
1A	LEU	LEU	LEU	SBO	none	no AC	3 hr	late
1B	LEU	LEU	LEU	SBO	none	no AC	3 hr	early
1D	LEU	LEU	LEU	AC/DC	1-in. cold leg	RaF[c]	on	late
1E	LEU	LEU	LEU	AC/DC	1-in. cold leg	RaF	on	early
1G	LEU	LEU	LEU	AC/DC	L[b] cold leg	fail	on	late
2A	MOX/LEU	LEU	Both	SBO	none	no AC	3 hr	late
2B	MOX/LEU	LEU	Both	SBO	none	no AC	3 hr	early
2D	MOX/LEU	LEU	Both	AC/DC	1-in. cold leg	RaF	on	late
2E	MOX/LEU	LEU	Both	AC/DC	1-in. cold leg	RaF	on	early
2G	MOX/LEU	LEU	Both	AC/DC	L cold leg	fail	on	late
2I	MOX/LEU	LEU	Both	AC/DC	6-in. cold leg	fail	on	late
2J	MOX/LEU	LEU	Both	AC/DC	6-in. hot leg	fail	on	late
2K	MOX/LEU	LEU	Both	AC/DC	10-in. cold leg	fail	on	late
2L	MOX/LEU	LEU	Both	AC/DC	10-in. hot leg	fail	on	late
2P	MOX/LEU	LEU	Both	SBO	none	no AC	fail	late
2Q	MOX/LEU	LEU	Both	AC/DC	2-in. cold leg	RaF	on	late
2R	MOX/LEU	LEU	Both	AC/DC	2-in. cold leg	fail	on	late
2S	MOX/LEU	LEU	Both	SBO	RCP[e]	no AC	fail	late
2T	MOX/LEU	LEU	Both	SBO	RCP/SORV[f]	no AC	3 hr	late
2U	MOX/LEU	LEU	Both	AC/DC	1-in. hot leg	fail	on	late
2V	MOX/LEU	LEU	Both	AC/DC	1-in. hot leg	RaF	on	late
3A	LEU	MOX	LEU	SBO	none	no AC	3 hr	late
4A	LEU	LEU	MOX	SBO	none	no AC	3 hr	late

[a] Core Loading ratio of MOX/LEU is 40% MOX, 60% LEU.
[b] L = large LOCA, defined as a guillotine rupture of RCS piping
[c] RaF = Re-alignment Failure
[d] AFW = Auxiliary Feedwater
[e] RCP = Reactor Coolant Pump (seal failure)
[f] SORV = Stuck-Open Relief Valve (on pressurizer)

3.2 Containment End-States

As expected, accidents involving containment failures account for most of the total population dose in the current Catawba PRA. Late containment failures account for 67% of the dose while early failures account for 23%. Accordingly, Table 3-1 includes SBO and SLOCA accidents where the containment fails early (before reactor vessel failure) and fails late (after vessel failure). Because severe accidents where the containment remains intact does not contribute to the population dose, these calculations were not included in this study.[9]

Previous NRC research [15] found that early containment failure is dominated by hydrogen combustion events (rather than by direct containment heating (DCH) events). The MELCOR calculations where early containment failure is desired preclude early creep-rupture failures of the RCS. Rather, the load for containment failure is the result of the blowdown at vessel failure and coincidental hydrogen burns.

[9] Cases 1C, 1F, 2C, and 2F were originally included in the calculation matrix as placeholders for SBOs with no containment failure.

Late containment failures in the MELCOR calculations are a result of the buildup of noncondensable gases generated by core-concrete interactions. Late containment failure is expected to occur in scenarios where the cavity is dry. The Catawba and McGuire PRAs report that a large amount of water is required before the lower cavity would be flooded. In particular, the inventory of the FWST, the RCS fluid, the accumulator water, and 80% of the ice mass must be accumulated before the lower containment water level would spill through the piping penetrations from the vessel through the reactor shield wall. In cases where very late containment failure is desired, it was assumed that the hatchway on the containment floor fails and the containment floor water floods the cavity.

Cases 1G and 2G in Table 3-1 are LLOCAs included for comparison to the historical NUREG-1465 Source Term [5]. No variations in the containment end-state were analyzed in Cases 1G and 2G.

3.3 Fuel Material Properties

Case 3A in Table 3-1 investigates the dependence of fuel material properties on accident progression. The material properties of LEU and MOX fuel, especially the melting points, differ somewhat and Case 3A is meant to exemplify the importance of the differences. Popov et al. [16] discusses the thermal-physical properties of plutonium fuels. The oxide forms of plutonium fuel have a melting temperature several hundred Kelvin below UO_2. However, characterization of debris thermo-physical properties is complicated because zircaloy and zirconium oxide (ZrO_2) mix with the Pu_xO_y fuel to form eutectic mixtures. For the purposes of this sensitivity study it was assumed that the melting temperature of the ZrO_2/Pu_xO_y mixture is 2400 K (i.e., 400 K less than the LEU model). The ZrO_2 shell failure was assumed to fail at the same temperature. The results of Case 3A are compared to those of Case 1A.

3.4 Fission Product Release Parameters

Case 4A is included in Table 3-1 to exemplify the differences in accident progression attributed specifically to the differences in the fission product release parameters of LEU and MOX fuel. This is done by applying the newly developed MOX fission product release model to *all* fuel assemblies in the 40% MOX core. The results of Case 4A would be compared to those of Case 1A. The fission product inventory and decay heat in the core is identical between these two calculations.

3.5 Miscellaneous Accident Modeling Points

In an SBO at Catawba, the turbine-driven auxiliary feedwater (AFW) pumps could be expected to deliver water to the steam generators for three hours [3]. A three-hour AFW operation period is included in the MELCOR SBO calculations, except for scenarios in which AFW was assumed to fail to operate, as specified in Table 3-1.

Following a LOCA that triggers containment sprays (e.g., the LLOCA), the sprays would operate for at least two but maybe for as many as ten hours before being shut down by the operators [5]. Sprays were allowed to operate for two hours in the LLOCA calculations.

The LOCAs described in the Catawba and McGuire risk assessments ranged from SLOCAs that were equivalent to a 1-in.-diameter break to LLOCAs that were the equivalent of a double-ended guillotine break (DEGB) of the cold leg pipe. The SLOCAs and LLOCAs simulated in Cases 1/2A through 1/2G were a 1-in. break and DEGB, respectively. All breaks were assumed to occur in the cold leg. To fully examine the range of possible LOCAs that were described in the risk assessments, a number of sensitivity calculations were performed. These included 2-in., 6-in,. and 10-in. breaks, covering both cold leg and hot leg failures. Some sequences were performed with failure of ECCS, and some were performed with failure to realign ECCS from injection mode to recirculation mode. These sensitivity calculations are included as Cases 2I, 2J, 2K, 2L, 2Q, 2R, 2U, and 2V. For these sensitivities, calculations were performed only for the 40% MOX core loading. It was assumed that there was enough information in the comparisons of Cases 1A-1G to 2A-2G to assess differences between LEU core and 40% MOX core severe accident source terms.

Three sensitivities were identified in the Catawba PRA as possible variations on the baseline SBO accident scenario. These variations included immediate failure of AFW, immediate failure of a reactor coolant pump (RCP) seal, and failure of a pressurizer safety valve to re-close (i.e., a stuck-open relief valve [SORV]). These sensitivities to the baseline SBO scenarios were examined in Cases 2P, 2S, and 2T, respectively. Again, calculations were only performed for the 40% MOX core loading for these sensitivities.

4.0 RESULTS

The results of the MELCOR calculations listed in Table 3-1 are described in the subsections below. However, the rationale for and description of the form of the source term results is provided first. As discussed previously, the results of these MELCOR simulations will be used to develop a MOX supplement to the NRC's alternative source term described in NUREG-1465 [5]. The NUREG-1465 source term considers both the timing and the chemical composition of the source term in a great deal more detail than past studies. Releases from the degrading reactor fuel are divided into five phases, as shown in Figure 4-1.

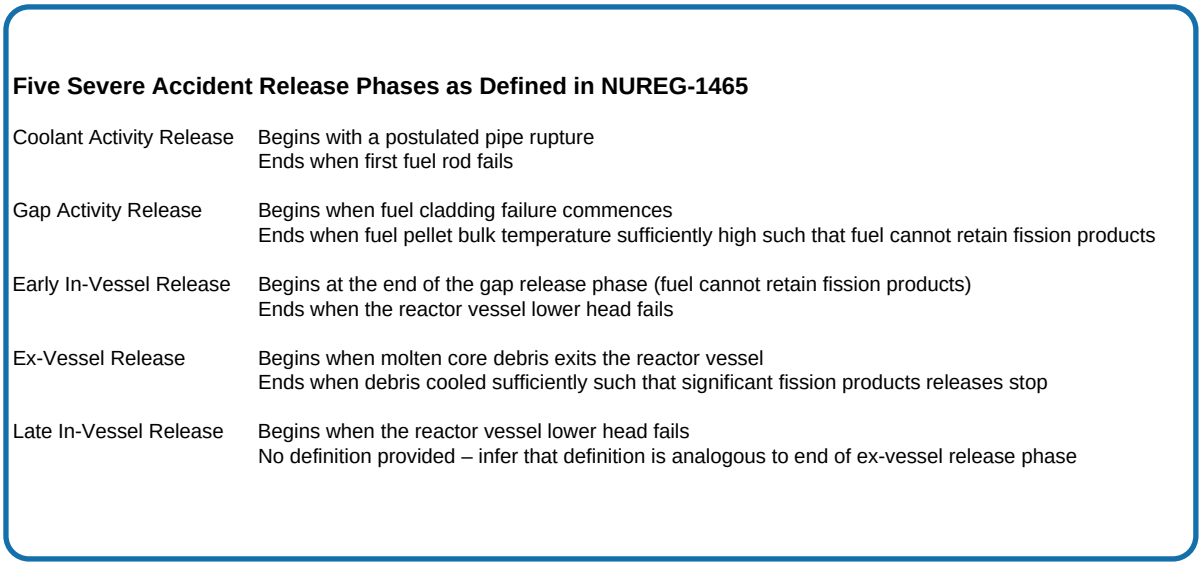

Figure 4-1. NUREG-1465 Severe Accident Release Phases.

Each of these phases has a specified duration and involves the release of specified fractions of the radionuclide inventory. The specifications themselves were derived from the results of many accident sequences for a variety of representative plants using the Source Term Code Package (STCP) and early versions of the MELCOR accident analysis code. The MELCOR calculations performed here were intended to provide a similar technical basis for development of the MOX supplement to the NUREG-1465 source term.

The coolant activity release is the expulsion of radioactive coolant into the containment that occurs early in an accident before fuel significantly overheats. MELCOR does not model activity of the coolant. Therefore, no mechanistic code information for the magnitude of the coolant release is directly available for use in the revised supplement. Therefore, the elemental composition of the release during the coolant release phase is not addressed, just as it is not addressed in the NUREG-1465 source term.

The gap release phase occurs once fuel is no longer covered by coolant and begins to overheat. It is expected that the zirconium alloy cladding on the fuel will expand and rupture venting radionuclides that have accumulated in the fuel-cladding gap and in the near-surface interstices of the fuel. If the accident cannot be arrested at this point, fuel continues to heat and

radionuclides diffuse from the fuel and vaporize. Heatup of the fuel may be augmented significantly by the exothermic reaction of steam with the zirconium alloy cladding. Eventually, residual metal cladding will melt and begin dissolving fuel. This dissolution will further affect radionuclide release.

Radionuclides vaporized from the fuel will pass out of the core region into cooler parts of the RCS. The vapors will condense and form aerosol particles. Both aerosol particles and vapors have opportunities to deposit on surfaces along this flow path. The NUREG-1465 source term specifies the net effect of release and successful passage of radionuclides through the RCS to the containment.

The ex-vessel accident release phase occurs when liquefied fuel and clad penetrates the reactor vessel and cascades into the reactor cavity. Processes contributing to the ex-vessel release include the pressurized expulsion of melt from the vessel and the subsequent interactions of the core debris with concrete. Pressurized expulsion of core debris from the reactor vessel can occur only if the vessel remains pressurized throughout the degradation process. At the time the NUREG-1465 source term was developed, it was thought that for many risk-important accidents, especially at PWRs, pressurization could be maintained throughout the degradation process. Releases associated with core debris interactions with concrete depend significantly on the amounts of metallic Zr still present in the core debris, and to a lesser extent on the nature of concrete used in the construction of the nuclear power plant.

Late in-vessel release occurs because substantial amounts of radioactive material released during the core degradation process are retained on surfaces within the RCS. The continued radioactive decay of these retained materials causes the surfaces to heat. Eventually, temperatures are sufficiently high that considerable vaporization of deposited radionuclides into the natural circulation of gases through the ruptured RCS can occur. The revaporization from surfaces is slow but occurs over a protracted period. It sustains the period over which there is substantial inventory of radioactive material suspended in the reactor containment atmosphere.

The calculated MELCOR parameters selected to determine the timing of each release phase described above for the accidents simulated are shown in Figure 4-2.

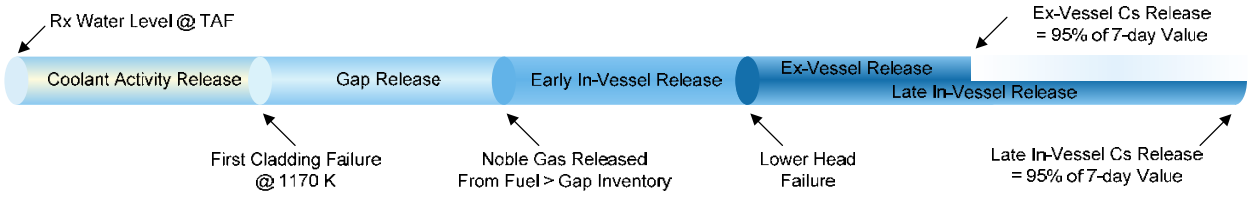

Figure 4-2. Release Phase Timing Definitions – Tie to Calculated MELCOR Results.

The NUREG-1465 source term groups radionuclides released during accidents into eight groups based on the similarities of chemistry. These groups are shown in Table 4-1, along with the MELCOR RN class that represents each group. Results of this study are presented in terms of the eight NUREG-1465 source term groups, with one exception. The in-vessel releases for Ru were found to be different enough from those of Mo, that it appeared inappropriate to group these elements together. Therefore, the noble metals are split into the "Ru Group" and the "Mo Group."

The fractional releases of the initial core inventories of these groups for accidents at PWRs are shown in Table 4-2. Note that the NUREG-1465 source term is expressed in terms of radionuclide release *to containment*, and not release to the environment. Thus, release magnitudes presented in this study are also presented as releases to containment. Graphical results will be presented in terms of radionuclide mass (kg) released to containment. This will provide a perspective on the differences between LEU results and MOX results in an absolute sense. Tabulated results will be presented in terms of "fraction of initial core inventory" for comparison to NUREG-1465 source term values.

Table 4-1. NUREG-1465 Radionuclide Groups.

NUREG-1465 Radionuclide Group	Title	MELCOR RN Class	Elements in Group
1	Noble Gases	1	Xe, Kr
2	Halogens	4 (I_2), 16 (CsI)	I, Br
3	Alkali Metals	2 (CsOH), 16 (CsI)	Cs, Rb
4	Tellurium Group	5	Te, Sb, Se
5	Barium, Strontium Group	3	Ba, Sr
6	Noble Metals	6 (Ru), 7 (Mo)	Ru, Rh, Pd, Mo, Tc, Co
7	Lanthanides	9	La, Zr, Nd, Eu, Nb, Pm, Pr, Sm, Y, Cm, Am
8	Cerium Group	8	Ce, Pu, Np

Table 4-2. NUREG-1465 Source Term to Containment for PWRs.

	Gap Release	In-vessel	Ex-vessel	Late In-vessel
Duration (hours)	0.5	1.3	2.0	10.0
Noble Gases	0.05	0.95	0	0
Halogens	0.05	0.35	0.25	0.1
Alkali Metals	0.05	0.25	0.35	0.1
Tellurium Group	0	0.05	0.25	0.005
Barium, Strontium	0	0.02	0.1	0
Noble Metals	0	0.0025	0.0025	0
Lanthanides	0	0.0002	0.005	0
Cerium Group	0	0.0005	0.005	0

Notes:
1. Values shown are fractions of initial core inventory.
2. See Table 4-1 for a listing of the elements in each group.
3. Gap release is 3% if long-term fuel cooling is maintained.

The MELCOR results are divided according to common characteristics of the various transients. Sections 4.1 through 4.3 present the various long-term SBO calculations that are summarized in Table 3-1. In Section 4.1, the results of four "baseline" long-term (i.e., includes 3 hr of AFW) SBO cases with late containment failure via overpressurization are presented and compared. The four cases are Cases 1A, 2A, 3A, and 4A. In Section 0, the results of two SBO calculations with early containment failure (i.e., Cases 1B and 2B) are presented and also compared to the fission product releases from Cases 1A and 2A. In Section 4.3, results are presented for MOX core SBO sensitivity calculations that demonstrate the effects of failure to initiate AFW, immediate failure of an RCP seal, and failure to reclose a pressurizer relief valve (i.e., an SORV). These calculations are compared to Case 2A.

The SLOCA cases are presented in Sections 4.4 through 4.6. Similar to the structure for the long-term SBOs, Section 4.4 has the late containment failure results, Section 4.5 has the early containment failure results, and Section 4.6 contains results for SLOCA sensitivities that examine the effects of slightly larger break sizes (2-in. instead of 1-in. diameter-equivalent), different break locations (hot leg instead of cold leg) and failure of ECCS (instead of failure to realign to recirculation mode).

Finally, Sections 4.7 and 4.8 contain the results of the LLOCA cases. Section 4.7 presents the results from LEU and MOX LLOCA calculations that represent the baseline LLOCA events presented in the Catawba and McGuire PRAs. Section 4.8 examines sensitivity of the MOX LLOCA results to smaller break sizes (6-in. and 10-in. transitional breaks instead of DEGB, sometimes termed medium-break LOCAs [MLOCAs]) and break location (hot leg instead of cold leg).

4.1 Long-Term SBO with Late Containment Failure

Long-term SBO simulations were performed with the MELCOR Westinghouse PWR ice condenser model (see Section 2.0) using contemporary best-estimate modeling practices for a long-term SBO (see Section 3.1). As described in Sections 3.1 through 3.4, four calculations (Cases 1A, 2A, 3A and 4A) were performed to examine the differences between an accident involving an LEU core versus a 40% MOX core, as well as modeling assumptions associated with MELCOR modeling of mixed LEU/MOX core loads. The specific differences between these four cases are identified in Table 3-1.

The accident sequence is initiated by a loss of offsite power and no ability to activate any safety systems (i.e., an SBO). The reactor is tripped at time "zero" after running at full power. Due to a loss of power to the RCP seal cooling system, a 21 gpm (per pump) leakage starts through the pump seals. There is emergency dc battery power available to drive the AFW system for 3 hr. However, once that system fails, the primary system begins to heat up and a severe accident ensues. A time line summarizing the major event timing for each of the four cases is provided in Table 4-3.

Table 4-3. Comparison of Key Event Timing for the Four Long-Term SBO Cases.

Case Core Baseline/Sensitivity Event	Case 1A LEU Baseline [hr]	Case 2A MOX/LEU Baseline [hr]	Case 3A LEU Fuel Properties [hr]	Case 4A LEU FP Release [hr]
Loss of ac power	0.0	0.0	0.0	0.0
Pump seals leak at 21 GPM	0.0	0.0	0.0	0.0
Loss of dc power	3.0	3.0	3.0	3.0
Steam generator secondary dry	5.9	5.9	5.9	5.9
PRT rupture disk fails	6.2	6.2	6.2	6.2
Vessel swollen water level at top of active fuel (TAF)	6.5	6.6	6.6	6.6
Start of fuel cladding failures	8.0	8.1	8.0	8.0
Containment design pressure	9.7	9.8	9.7	9.7
RCS Creep rupture failure	9.7	9.9	9.8	9.7
First hydrogen burn in containment	9.7	9.9	9.8	9.7
Accumulators empty	9.7	9.9	9.8	9.7
Start of core plate failures	11.3	11.6	10.3	10.9
Debris relocation to lower head	14.3	13.6	11.9	12.4
Vessel failure	17.9	16.7	15.7	15.7
Containment failure	70.2	68.7	66.7	73.3
Calculation terminated[10]	168.	162.	149.	168.

Figures 4-3 through 4-12 show comparisons of the MELCOR-calculated accident signatures for the four long-term SBOs with late containment failure. As shown in Table 3-1, Case 1A uses LEU fuel attributes, and Case 2A uses both LEU and MOX fuel attributes. The specific unique differences in the fuel attributes for the two cases include the fission product release characteristics and the fission product inventory. As discussed in Section 3.3, Case 3A has the same attributes as Case 1A but includes a lower melting temperature (i.e., consistent with MOX fuel) for the entire core.[11] As described in Section 3.4, Case 4A also has the same attributes as Case 1A but uses the fission product release characteristics of MOX fuel for the entire core.[12] Consequently, Cases 3A and 4A are sensitivity cases intended to isolate the importance of MOX melting temperature and MOX fission product release relative to the LEU fuel characteristics.

The RCS pressure response is shown in Figure 4-3. Initially, the pressure decreases as the heat removal from the steam generator exceeds the decay heat power. The RCS pressure drops until it reaches an equilibrium state with the secondary pressure (i.e., ~8 MPa). However, once the steam generators boil dry at ~5.9 hr (see Figure 4-4), the vessel water heats up to boiling and pressurizes the RCS. The RCS pressure rises until it reaches the pressurizer relief valve setpoint. The pressurizer relief valve opens and discharges steam into the pressurizer relief tank (PRT) in the containment. The pressurizer relief valve continues to cycle to relieve steam generated in the

[10] Cases 2A and 3A terminated early due to failures in the MELCOR Cavity (CAV) package at very low rates of core-concrete interaction.

[11] As discussed in Section 2.4, the proposed fuel configuration would be 40% MOX fuel and 60% LEU fuel. Case 3A assumes 100% of the fuel has a melting temperature consistent with MOX fuel.

[12] As discussed in Section 2.5, the proposed fuel configuration would be 40% MOX fuel and 60% LEU fuel. Case 4A assumes 100% of the fuel has the fission product release characteristics of MOX fuel.

core. The loss of inventory out the pressurizer relief valve drains the RCS and uncovers the core (see Figure 4-5). When the core starts to uncover at 6.5 to 6.6 hr, the fuel rod heatup begins (see Figure 4-6). As shown in Table 4-3, the fission product releases start between 8.0 to 8.1 hr.

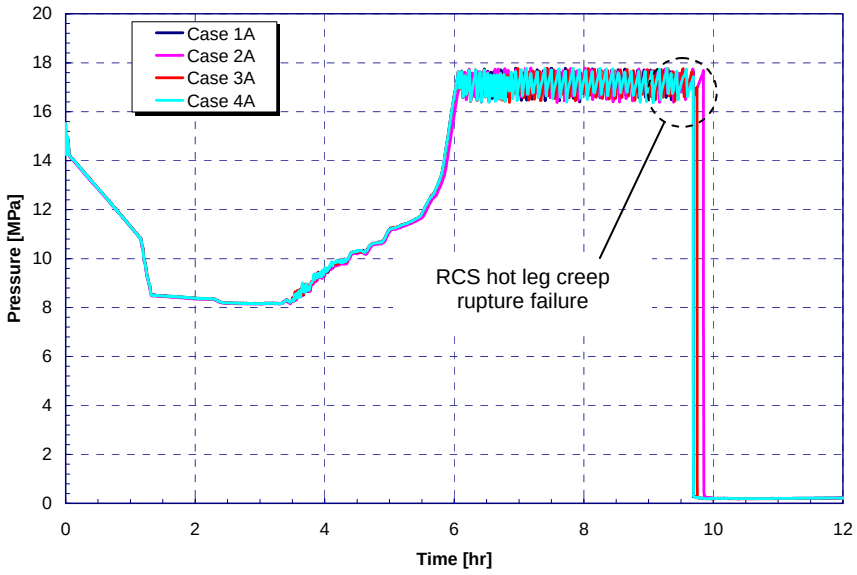

Figure 4-3. RCS Pressure Response for the Four Long-Term SBO Cases.

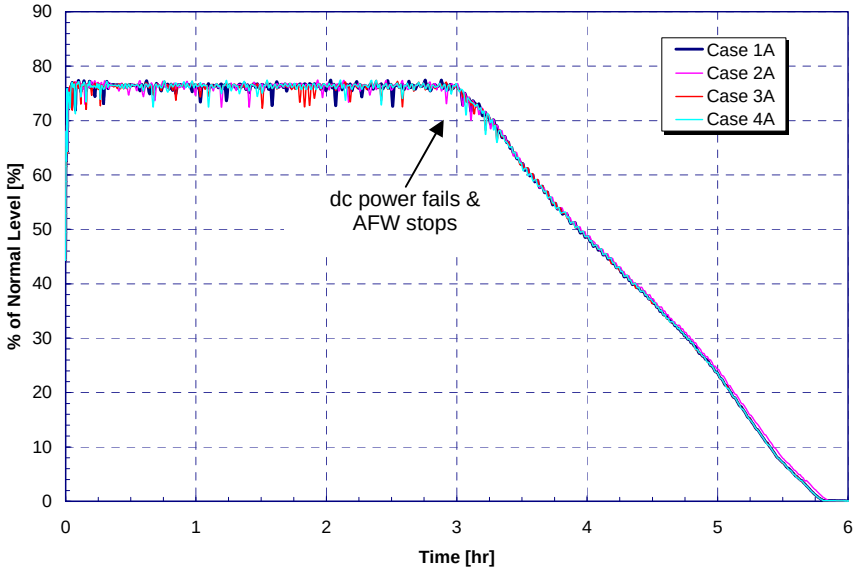

Figure 4-4. Steam Generator Water Level for the Four Long-Term SBO Cases.

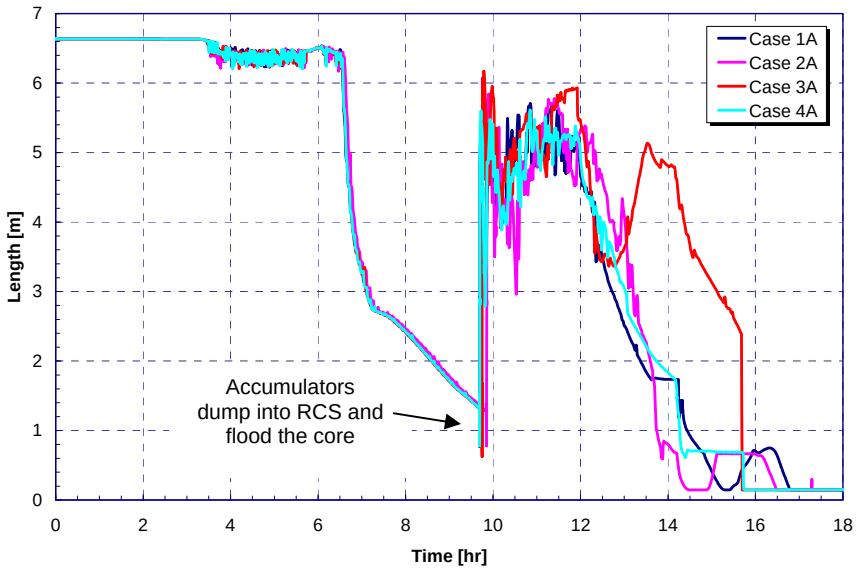

Figure 4-5. Vessel Swollen Water Level for the Four Long-Term SBO Cases.

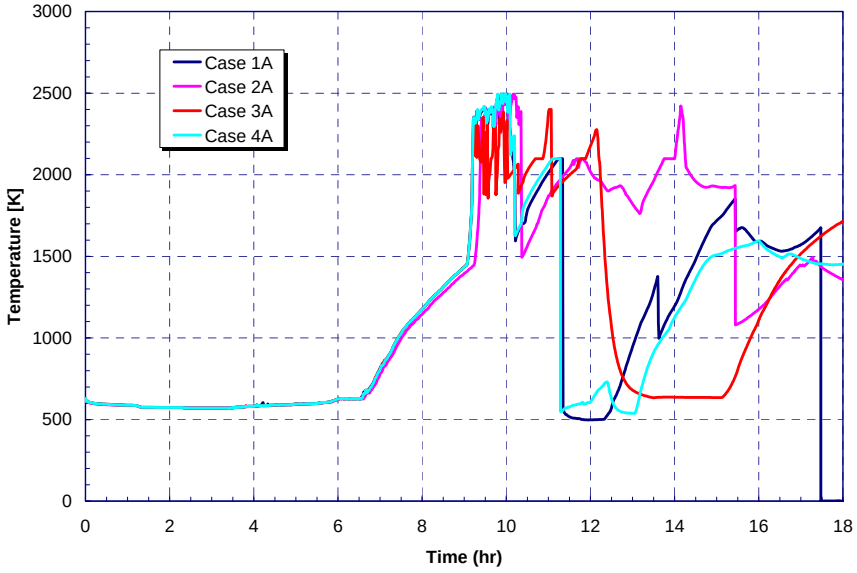

Figure 4-6. Peak Cladding Temperature for the Four Long-Term SBO Cases.

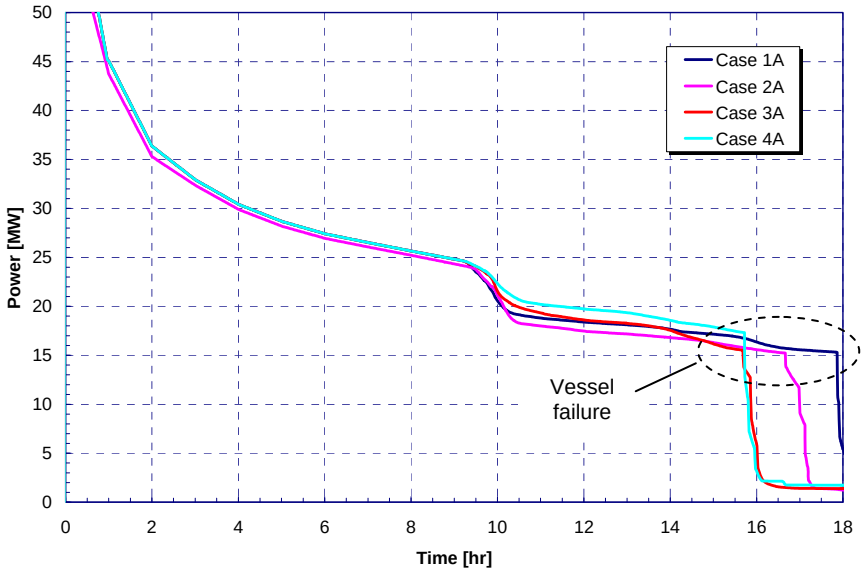

Figure 4-7. In-Vessel Decay Heat for the Four Long-Term SBO Cases.

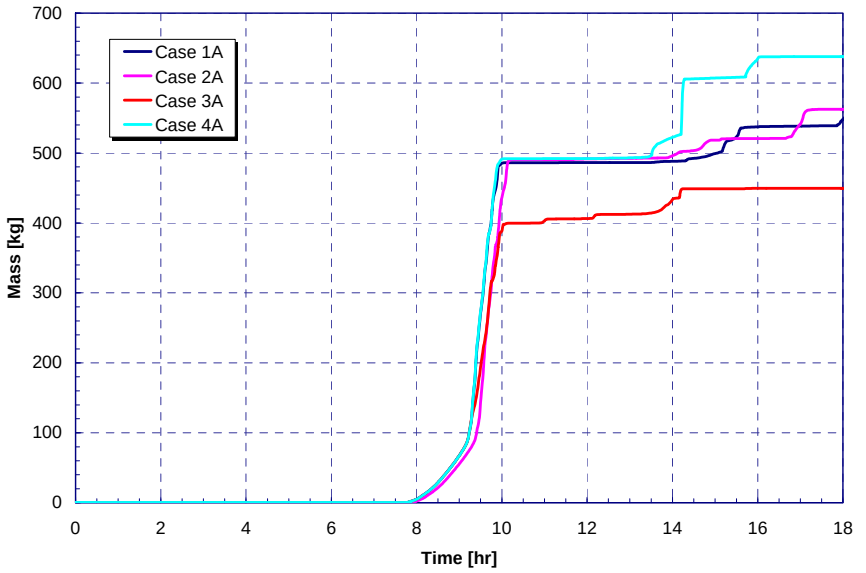

Figure 4-8. In-Vessel Hydrogen Production for the Four Long-Term SBO Cases.

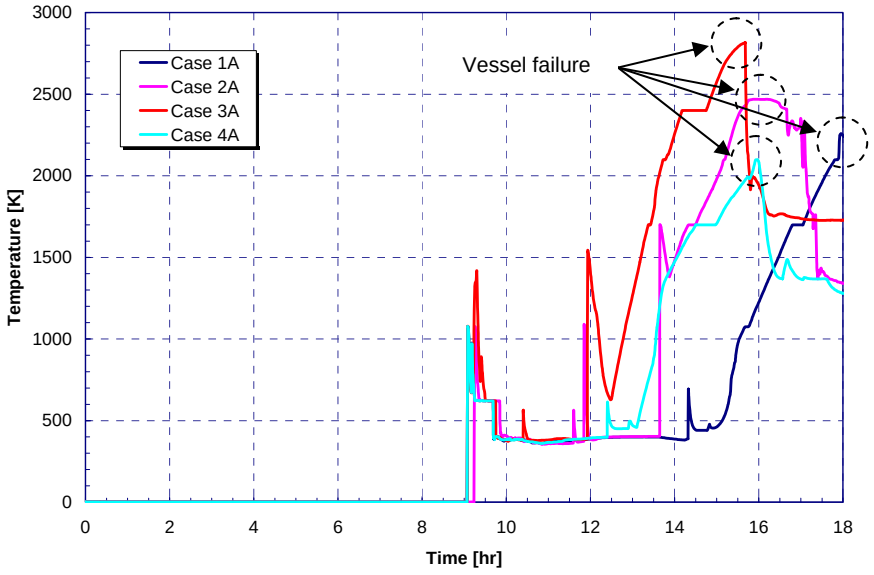

Figure 4-9. Lower Head Debris Temperature for the Four Long-Term SBO Cases.

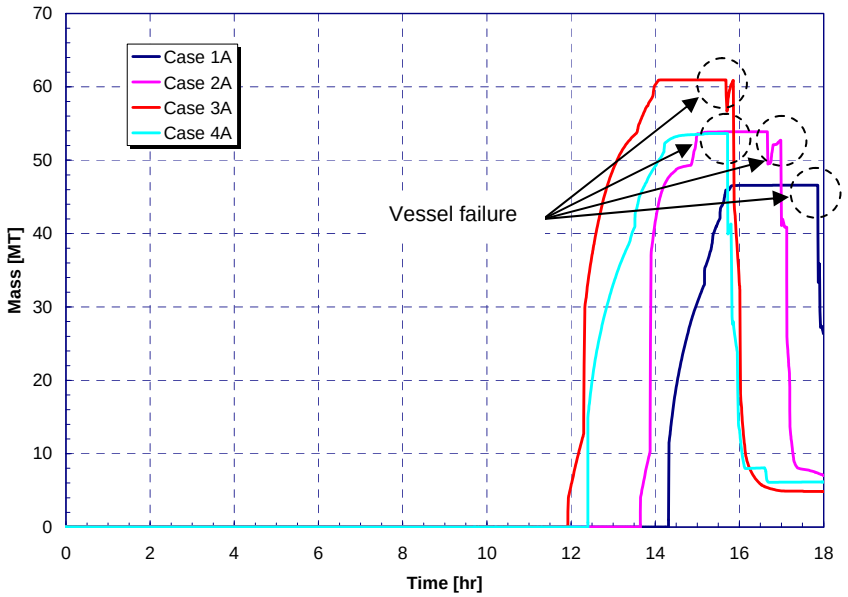

Figure 4-10. UO_2 Mass on the Vessel Lower Head for the Four Long-Term SBO Cases.

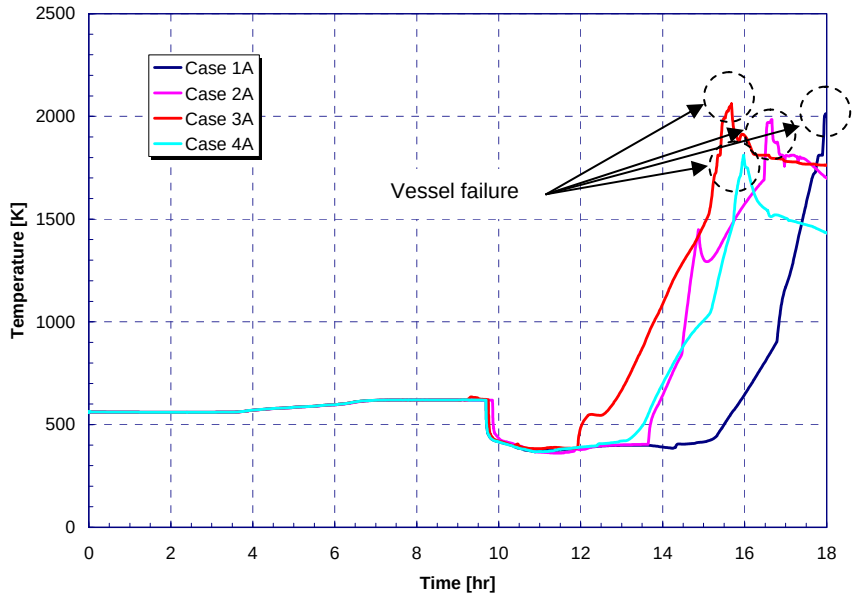

Figure 4-11. Lower Head Temperature for the Four Long-Term SBO Cases.

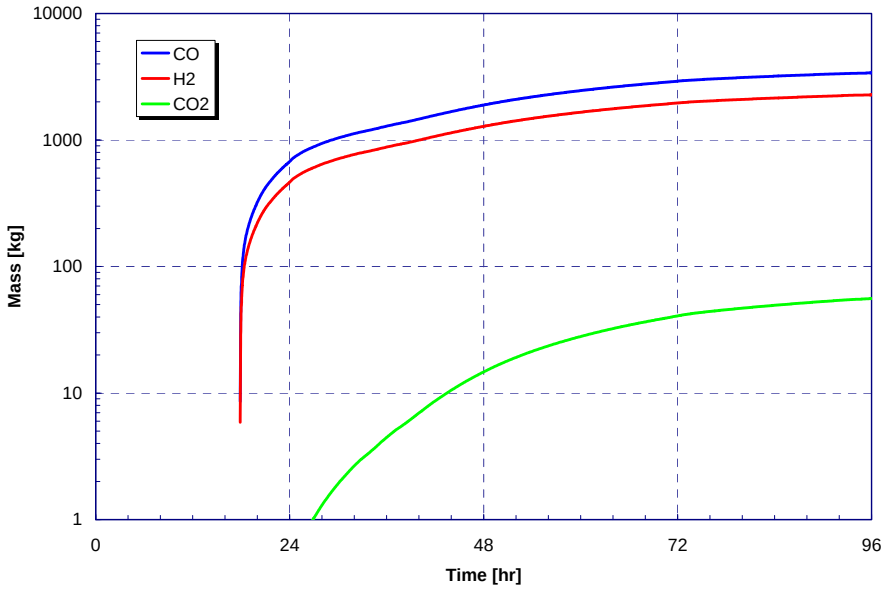

Figure 4-12. Non-Condensable Gas Production During Core-Concrete Interactions for Case 1A.

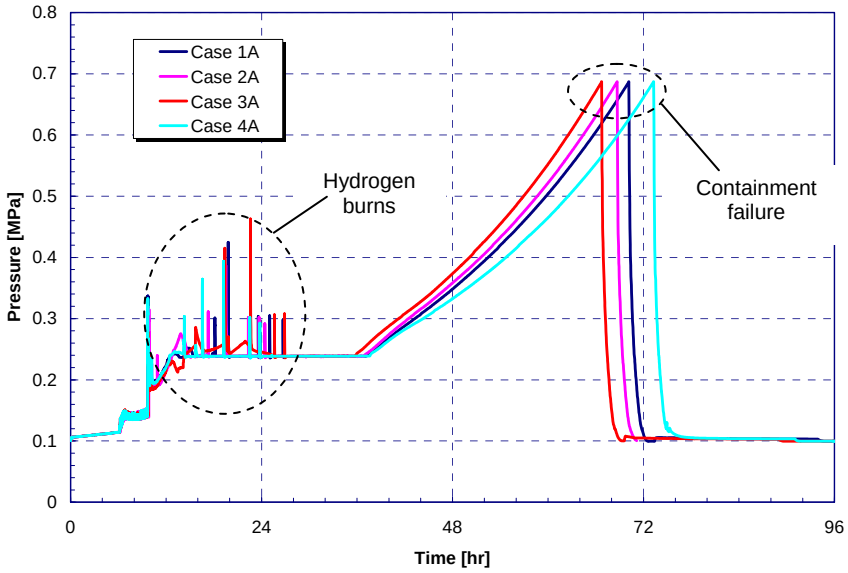

Figure 4-13. Containment Pressure for the Four Long-Term SBO Cases.

Accelerated steam-zirconium oxidation subsequently ensues, producing hydrogen in-vessel (Figure 4-8). The damaged cladding then relocates, and the fuel starts to collapse. The hot gases exiting the degrading core circulate into the primary system hot legs. During this time, molten Inconel relocates to the core support structures and drips through to the lower plenum. This can be seen in the lower head debris temperature spike at around 9 hr (Figure 4-9). This debris is quickly quenched by the water than remains in the lower plenum, and it does not have an impact on the remaining accident progression. Due to the combination of high pressure and temperature in the RCS, the hot leg nozzle adjacent to the vessel fails due to a thermomechanical creep rupture at 9.7 to 9.8 hr. The subsequent rapid depressurization (Figure 4-3) leads to an accumulator discharge, which refloods the core. The accumulator water does not arrive in time to quench the relocated core debris, and the fuel supporting structures (i.e., the core plate) begin failing between 10.3 and 11.6 hr. After the accumulator water boils away, the core heatup and degradation continues. Between 11.9 and 14.3 hr, the lower core plate fails and large-scale debris relocation into the lower plenum occurs (Figure 4-10). Lower head temperatures increase (Figure 4-11), and the vessel lower head fails between 15.7 and 17.9 hr.

After vessel failure, the fuel relocates from the vessel into the containment cavity where core-concrete interactions occur. The thermochemical interactions between the fuel debris and the concrete release noncondensable gases (e.g., see Figure 4-12 for response of Case 1A) that steadily pressurizes the containment to its failure point (see Figure 4-13). Following containment failure, the containment depressurizes and releases airborne fission products to the environment. The MELCOR ex-vessel fission product model considers both mechanical and thermochemical release mechanisms for the fission products within the ex-vessel debris bed. It is assumed that differences between the LEU and MOX fuel would not affect the physics of the

ex-vessel core-concrete interactions. Consequently, the ex-vessel LEU and MOX fission product releases are handled with the same model.

Before the start of the pressurizer relief valve cycling phase, the results for the four calculations are very similar. In general, the calculations with MOX fuel assemblies or MOX fission product release parameters show slightly faster accident progression than the LEU case. Case 3A, which has a lower fuel melting temperature, shows the most rapid accident progression. It also shows a reduced in-vessel hydrogen production, because the time period in which the core geometry remains intact for steam to cause cladding oxidation is reduced.

The fission product release results are shown in Figures 4-14 through 4-22, for the nine NUREG-1465 radionuclide groups. These figures summarize the total fission product mass released to containment. Durations of each of the NUREG-1465 release phases are presented in Table 4-4. In addition, the magnitudes of release to containment for each of the NUREG-1465 radionuclide groups are tabulated in Tables 4-5 through 4-8 for all release phases. In contrast to Figures 4-14 through 4-22, the results in the tables present the releases to containment as a fraction of the initial core inventory rather than absolute mass. This enables direct comparison with NUREG-1465 results.

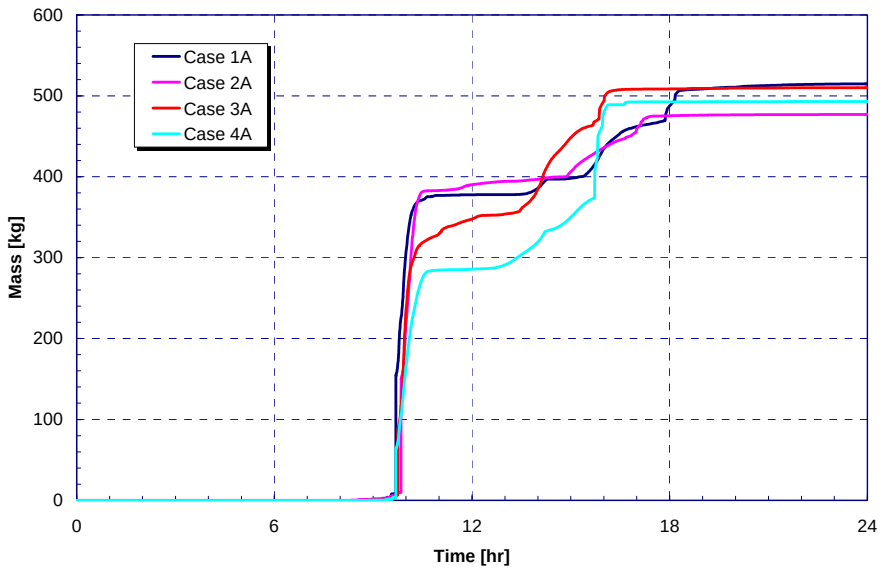

Figure 4-14. Noble Gas Release to the Containment for the Four Long-Term SBO Cases.

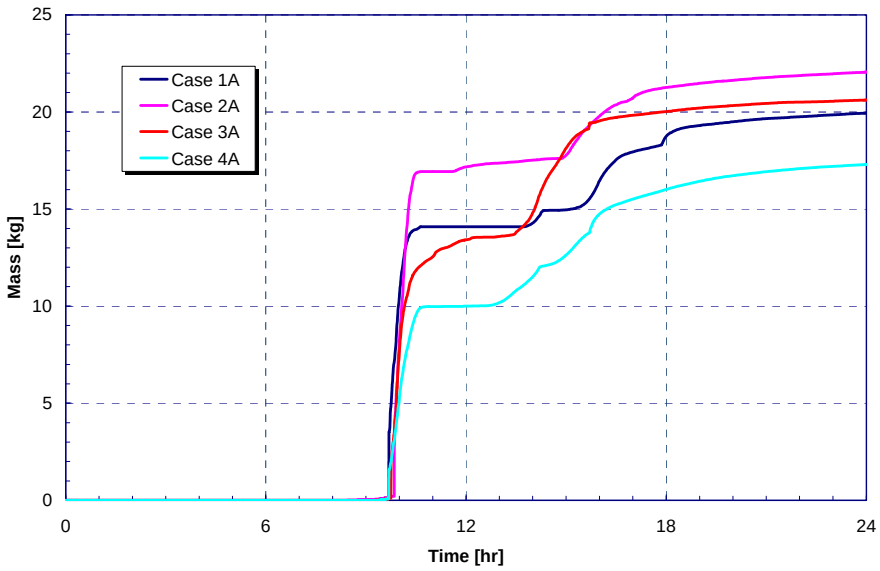

Figure 4-15. Halogen Release to the Containment for the Four Long-Term SBO Cases.

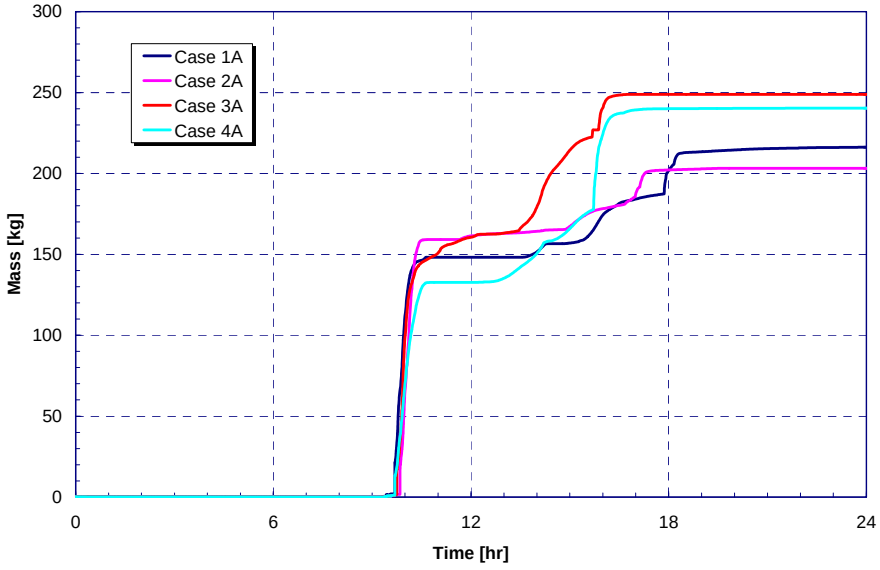

Figure 4-16. Alkali Metal Release to the Containment for the Four Long-Term SBO Cases.

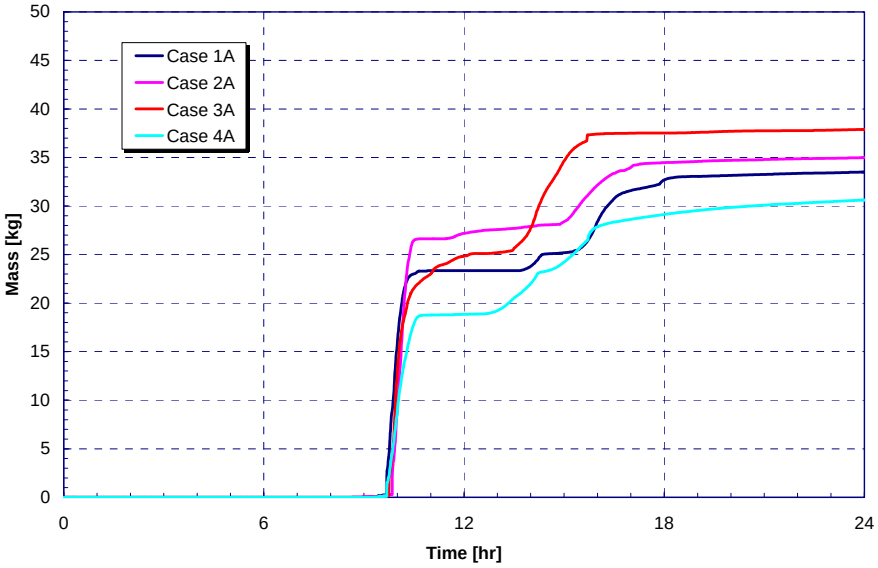

Figure 4-17. Tellurium Group Release to the Containment for the Four Long-Term SBO Cases.

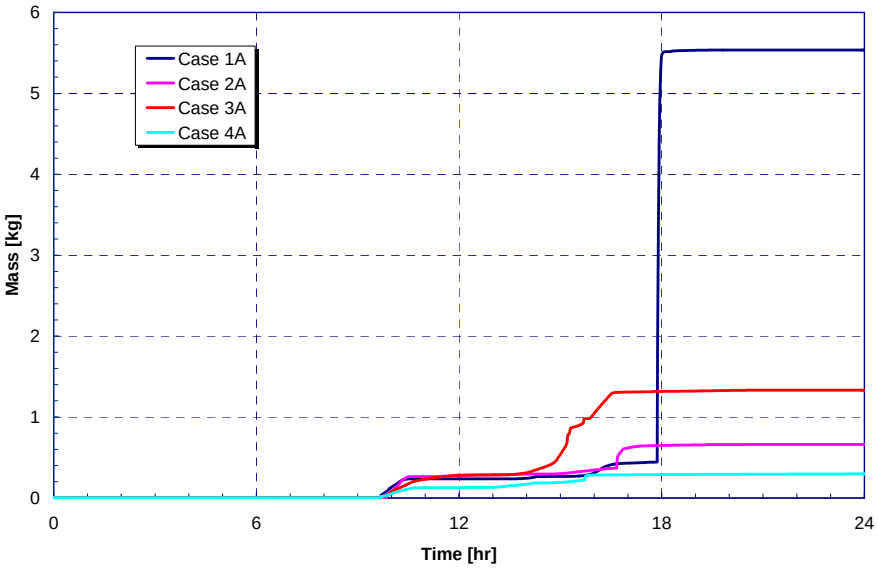

Figure 4-18. Barium, Strontium Group Release to the Containment for the Four Long-Term SBO Cases.

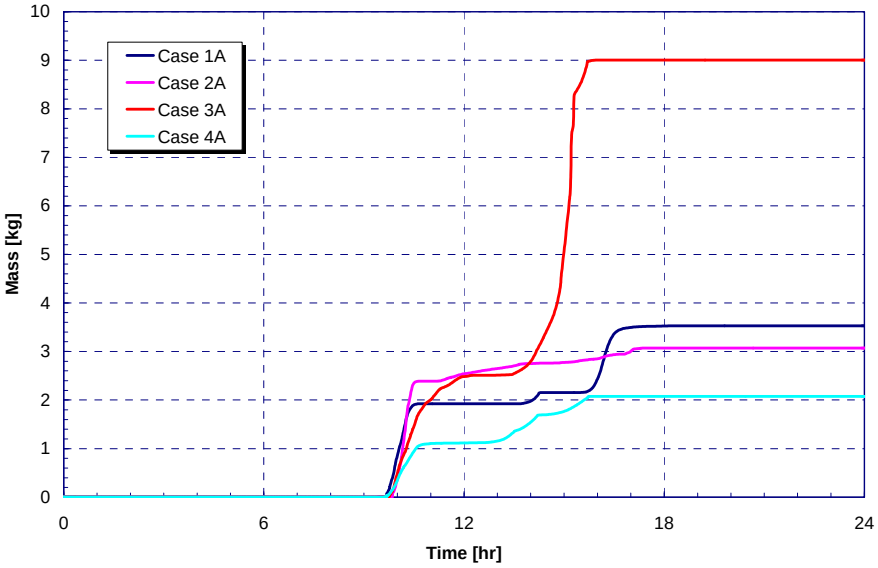

Figure 4-19. Noble Metal (Ru) Release to the Containment for the Four Long-Term SBO Cases.

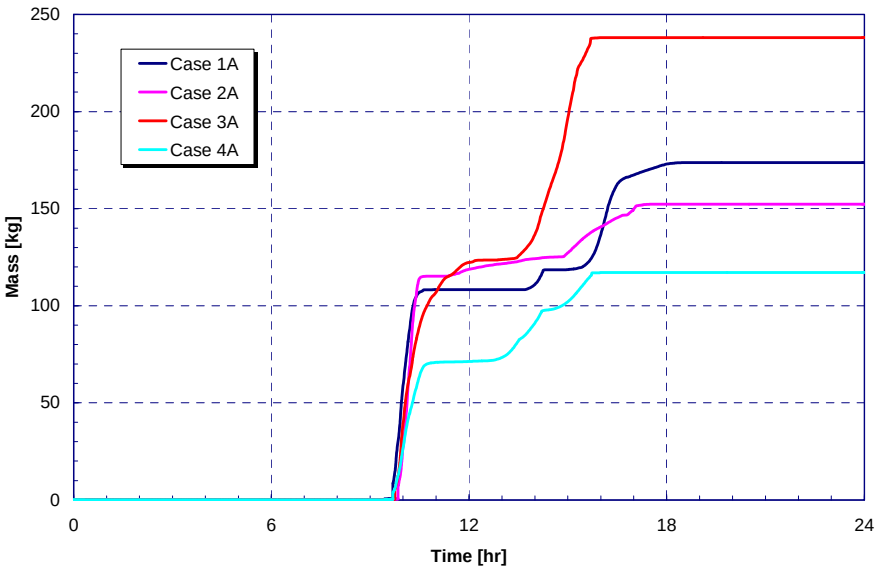

Figure 4-20. Noble Metal (Mo) Release to the Containment for the Four Long-Term SBO Cases.

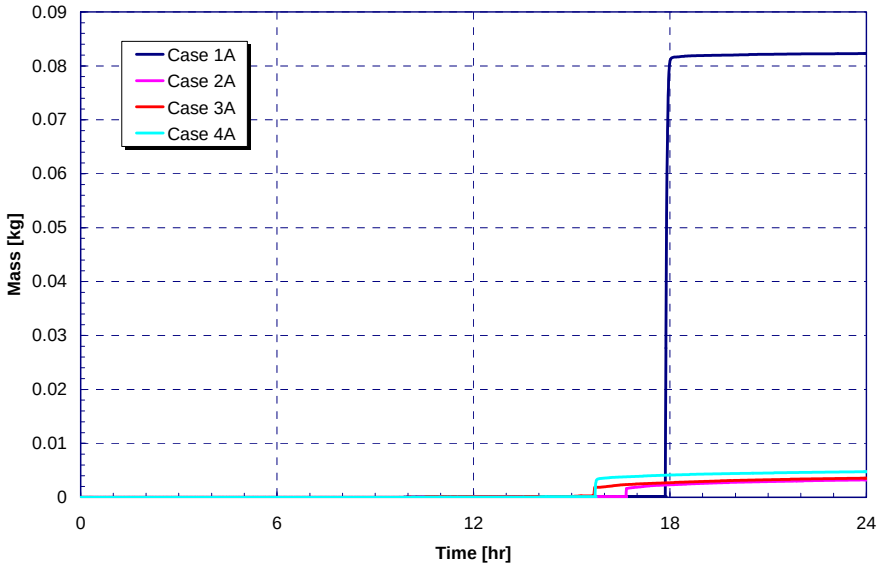

Figure 4-21. Lanthanide Release to the Containment for the Four Long-Term SBO Cases.

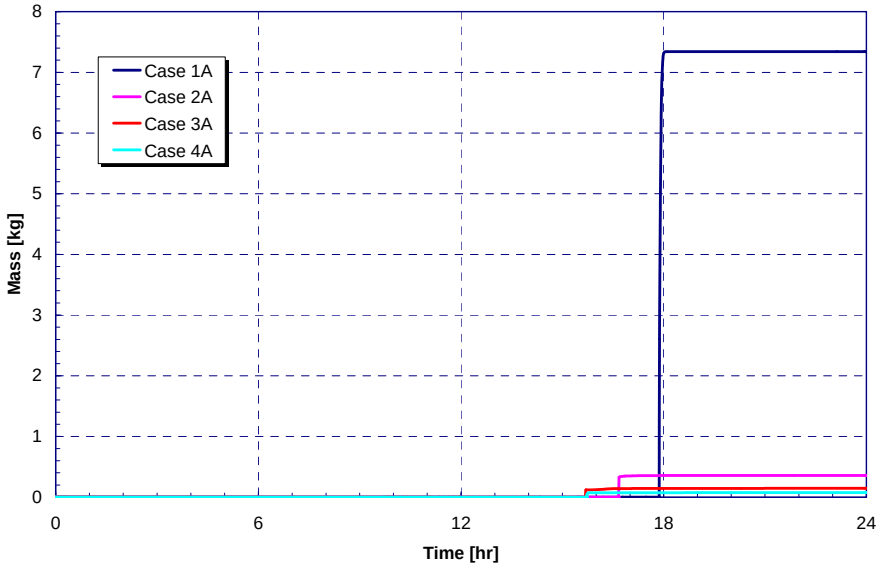

Figure 4-22. Cerium Group Release to the Containment for the Four Long-Term SBO Cases.

Table 4-4. Release Timing for Long-Term SBO with Late Containment Failure.

Timing (hr)	NUREG-1465	Case 1A	Case 2A	Case 3A	Case 4A
Onset of Release	~0	6.5	6.6	6.6	6.6
Coolant Release Duration		1.5	1.5	1.4	1.4
Gap Release Duration	0.5	0.6	0.7	0.6	0.6
In-Vessel Release Duration	1.3	9.2	7.9	7.1	7.1
Ex-Vessel Release Duration	2.0	6.6	85	81	86
Late I-Vessel Release Duration	10.0	0.6	91	0.2	0.3

Table 4-5. Gap Release Fractions for Long-Term SBO with Late Containment Failure.

	NUREG-1465	Case 1A	Case 2A	Case 3A	Case 4A
Noble Gases	0.05	1.2262E-02	1.2111E-02	1.5229E-02	1.3144E-02
Halogens	0.05	4.5848E-03	5.4231E-03	2.6952E-03	2.1616E-03
Alkali Metals	0.05	3.4017E-03	1.9500E-03	8.9329E-04	2.8096E-04
Te Group	0	4.9788E-03	2.6400E-03	6.9976E-03	6.4783E-03

Table 4-6. In-Vessel Release Fractions for Long-Term SBO with Late Containment Failure.

	NUREG-1465	Case 1A	Case 2A	Case 3A	Case 4A
Noble Gases	0.95	8.9411E-1	9.0820E-1	8.7978E-01	7.0892E-01
Halogens	0.35	7.6417E-1	7.8462E-1	7.6212E-01	6.0873E-01
Alkali Metals	0.25	6.4058E-1	6.4893E-1	4.2057E-03	1.0155E-03
Te Group	0.05	6.5686E-1	6.7000E-1	7.9643E-01	5.7506E-01
Ba, Sr Group	0.02	2.0000E-3	1.9474E-3	7.6507E-01	5.3523E-01
Ru Group	0.0025	9.7493E-3	7.0732E-3	2.5087E-02	5.7255E-03
Mo Group	0.0025	4.6113E-1	4.2000E-1	6.2991E-01	3.1050E-01
Lanthanides	0.0002	1.8571E-7	1.5133E-7	4.0780E-07	9.2837E-08
Ce Group	0.0005	1.8121E-7	1.4460E-7	4.0777E-07	9.3036E-08

Table 4-7. Ex-Vessel Release Fractions for Long-Term SBO with Late Containment Failure.

	NUREG-1465	Case 1A	Case 2A	Case 3A	Case 4A
Noble Gases	0	8.1925E-2	3.9130E-2	8.7652E-02	2.6248E-01
Halogens	0.25	6.7990E-2	5.8845E-2	8.6326E-02	2.5117E-01
Alkali Metals	0.35	1.0217E-1	7.2377E-2	2.0197E-03	5.9941E-04
Te Group	0.25	2.6451E-2	5.8582E-2	8.0507E-02	2.1602E-01
Ba, Sr Group	0.1	2.3524E-2	1.7224E-3	5.5009E-02	2.2704E-01
Ru Group	0.0025	2.0946E-9	4.333E-11	9.3796E-11	2.4884E-09
Mo Group	0.0025	2.318E-10	1.505E-08	3.7820E-09	5.3451E-08
Lanthanides	0.005	1.1916E-4	7.8937E-6	1.0038E-04	5.4092E-05
Ce Group	0.005	4.9592E-3	1.6611E-4	7.1881E-06	9.4133E-06

Table 4-8. Late In-Vessel Release Fractions for Long-Term SBO with Late Containment Failure.

	NUREG-1465	Case 1A	Case 2A	Case 3A	Case 4A
Noble Gases	0	5.8848E-3	2.5862E-2	5.1915E-05	1.3531E-06
Halogens	0.1	3.2290E-3	4.3894E-2	1.4474E-02	6.7170E-03
Alkali Metals	0.1	2.4069E-3	2.2330E-2	3.7284E-05	9.2335E-06
Te Group	0.005	3.3247E-3	6.3494E-2	1.2261E-02	6.5706E-03
Ba, Sr Group	0	1.3645E-9	1.0338E-4	1.4302E-02	5.8494E-03
Ru Group	0	1.7531E-5	3.4695E-4	3.0025E-04	5.1464E-05
Mo Group	0	3.4439E-3	2.6619E-2	7.2815E-03	3.1125E-03
Lanthanides	0	1.429E-13	2.028E-13	3.4902E-12	7.3831E-13
Ce Group	0	1.343E-13	5.016E-14	3.0800E-09	7.2862E-13

In general, fission product releases were similar between the LEU and 40% MOX cores (in terms of release fraction). As an illustration, the in-vessel releases for Case 1A is compared to Case 2A in Table 4-9. For the Noble Gas group and volatile fission products, the releases differ by less than 3%. Releases for the nonvolatile groups would be expected to show more variation, since the majority of releases for these groups occur ex-vessel (i.e., the in-vessel releases are relatively small). However, even in the case of the nonvolatile groups, the releases for the 40% MOX core are within a factor of two of those for the LEU core.

Table 4-9. Comparison of In-Vessel Release Fractions for LEU and 40% MOX Core, Long-Term SBO with Late Containment Failure.

	Case 1A	Case 2A	% Difference
Noble Gases	8.9411E-1	9.0820E-1	1.55
Halogens	7.6417E-1	7.8462E-1	2.61
Alkali Metals	6.4058E-1	6.4893E-1	1.29
Te Group	6.5686E-1	6.7000E-1	1.96
Ba, Sr Group	2.0000E-3	1.9474E-3	-2.70
Ru Group	9.7493E-3	7.0732E-3	-37.83
Mo Group	4.6113E-1	4.2000E-1	-9.79
Lanthanides	1.8571E-7	1.5133E-7	-22.72
Ce Group	1.8121E-7	1.4460E-7	-25.32

4.2 Long-Term SBO with Early Containment Failure

The early progression of events in Cases 1B and 2B are identical to Cases 1A and 2A, respectively (Table 4-10). However, unlike Cases 1A and 2A, a creep-rupture failure of the RCS piping is prevented. Consequently, the vessel fails at a higher pressure. While not modeled directly in the MELCOR calculation, it is assumed that an energetic pressurization (e.g., large burn, detonation, steam spike, and/or direct containment heating event) causes a simultaneous failure of the containment (see Section 3.2). Hence, as shown in Table 4-10, reactor vessel and containment failure occur simultaneously.

Table 4-10. Key Event Timing Comparison: SBOs with Early and Late Containment Failure.

Case Core Loading Containment Failure Event	Case 1A LEU Late [hr]	Case 1B LEU Early [hr]	Case 2A 40% MOX Late [hr]	Case 2B 40% MOX Early [hr]
Loss of ac power	0.0	0.0	0.0	0.0
Pump seals leak at 21 GPM	0.0	0.0	0.0	0.0
Loss of dc power	3.0	3.0	3.0	3.0
Steam generator secondary dry	5.9	5.9	5.9	5.9
PRT rupture disk fails	6.2	6.2	6.2	6.2
Vessel swollen water level at top of active fuel	6.5	6.5	6.6	6.6
Start of fuel cladding failures	8.0	8.0	8.1	8.1
Containment design pressure	9.7	11.1	9.8	11.5
RCS creep rupture failure	9.7	n/a	9.9	n/a
First hydrogen burn in containment	9.7	9.9	9.9	9.8
Accumulators empty	9.7	11.2	9.9	9.9
Start of core plate failures	11.3	10.1	11.6	10.2
Debris relocation to lower head	14.3	10.4	13.6	10.8
Vessel failure	17.9	11.1	16.7	11.5
Containment failure	70.2	11.1	68.7	11.5
Calculation terminated[13]	168.	110.	162.	99.

[13] Cases 1B, 2A, and 2B terminated early due to failures in the CAV at very low rates of core-concrete interaction.

Figures 4-23 through 4-27 compare key results of the calculated accident response for the SBO calculations with early containment failure to those with late containment failure (presented in Section 4.1). As described in Section 3.0, Cases 1A and 1B use LEU fuel attributes and Cases 2A and 2B use both LEU (60%) and MOX (40%) fuel attributes. The RCS pressure response is shown in Figure 4-23. The initial RCS pressure responses are identical between Cases 1A and 1B and Cases 2A and 2B, respectively. However, as described above, the early containment failure cases (i.e., Cases 1B and 2B) do not include RCS failures due to creep rupture before vessel failure. Consequently, Cases 1B and 2B remain at high pressure beyond the calculated RCS creep rupture time in Cases 1A and 2A (~10 hr) until just after 11 hr. At that time, hot debris on the vessel lower head causes a creep rupture failure of vessel lower head. The vessel failure in Cases 1A and 2A is later than Cases 1B and 2B due to the debris cooling effect when the accumulators discharge after the hot leg creep rupture failure (see effect on vessel water level in Figure 4-24). The accumulator discharge before vessel failure in Cases 1A and 2A interrupts the hydrogen production (see Figure 4-25) and retains the debris within the vessel longer (see Figure 4-26). Upon vessel failure, the containment fails in Cases 1B and 2B, respectively (see Figure 4-27). In contrast, the containment remains intact until approximately 70 hr in Cases 1A and 1B.

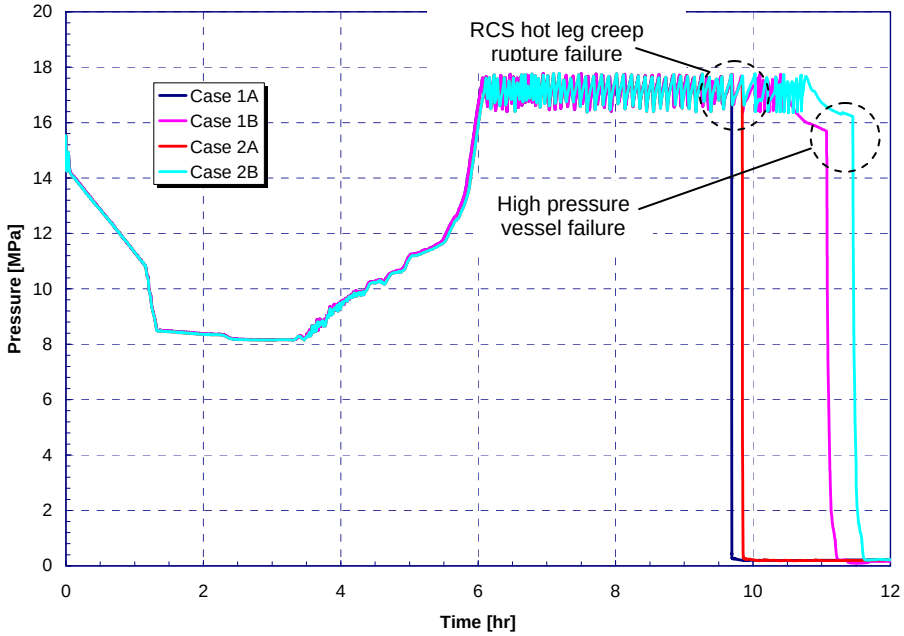

Figure 4-23. RCS Pressure for the Early/Late Containment Failure Long-Term SBO.

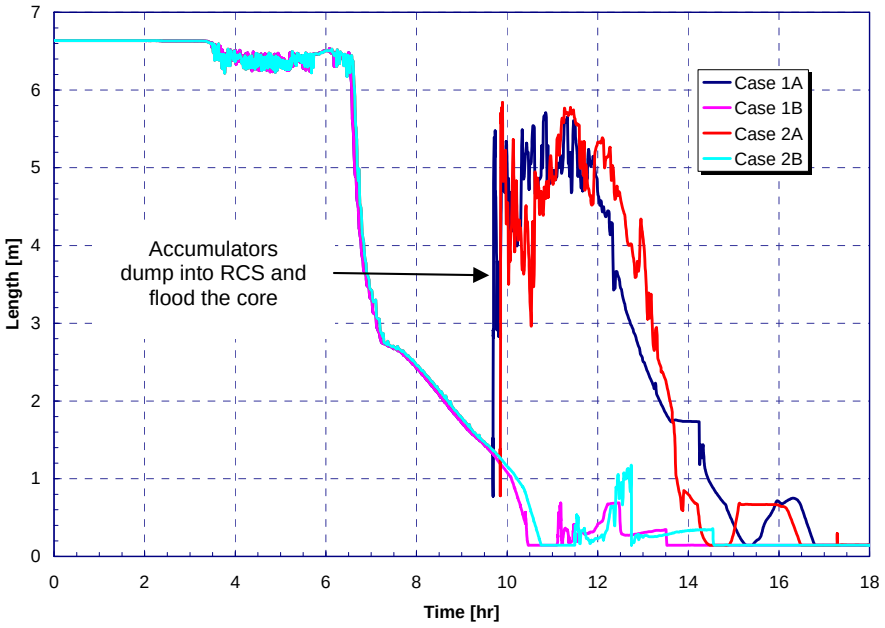

Figure 4-24. Vessel Swollen Water Level for Early/Late Containment Failure Long-Term SBO.

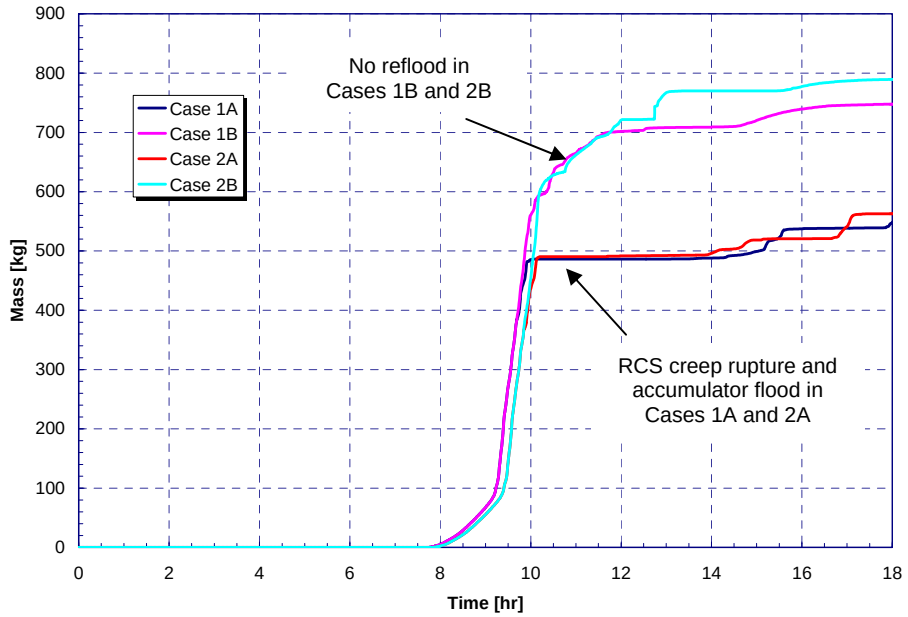

Figure 4-25. In-Vessel Hydrogen Production for Early/Late Containment Failure Long-Term SBO.

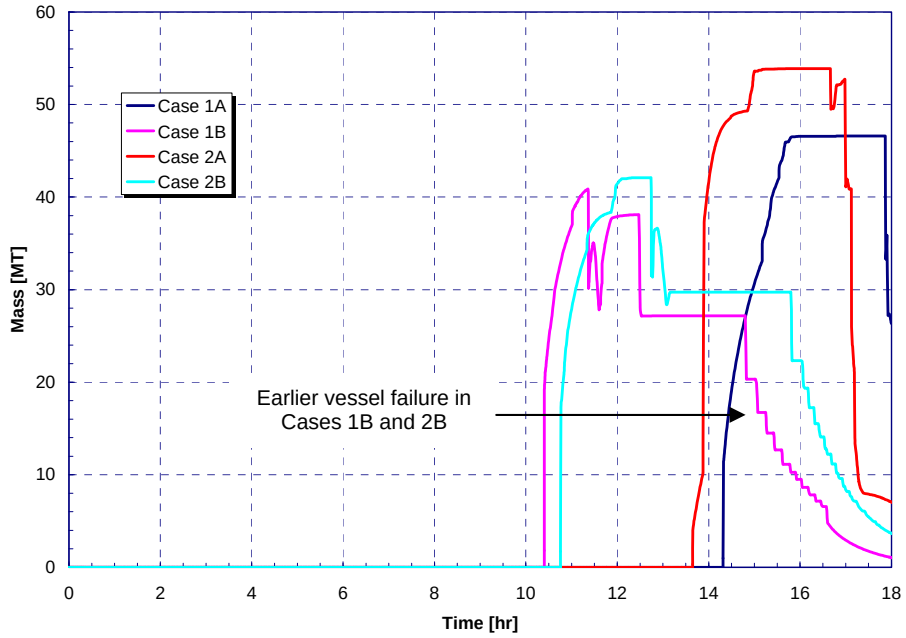

Figure 4-26. Uranium Dioxide Mass on the Vessel Lower Head for Early/Late Containment Failure Long-Term SBO.

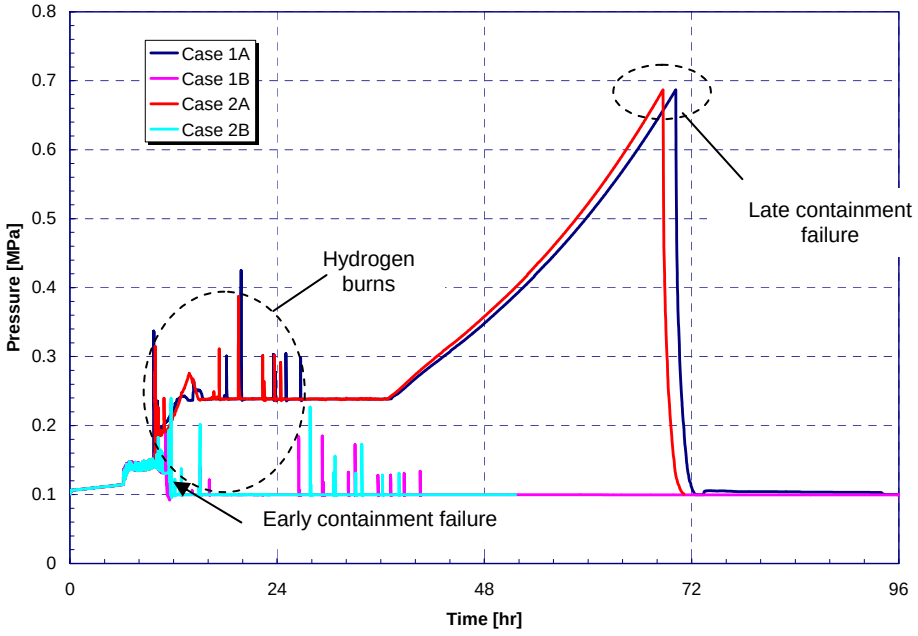

Figure 4-27. Containment Pressure Response for the Early/Late Containment Failure Long-Term SBO.

The fission product release results are shown in Figures 4-28 through 4-36, for the nine NUREG-1465 radionuclide groups. For illustrative purposes, the results from the early containment failure cases (1B and 2B) are compared to the late containment failure cases (1A and 2A). These figures summarize the total fission product mass released to containment. Durations of each of the NUREG-1465 release phases are presented in Table 4-11. In addition, the magnitudes of release to containment for each of the NUREG-1465 radionuclide groups are tabulated in Tables 4-12 through 4-15 for all release phases. In contrast to Figures 4-28 through 4-36, the results in the tables present the releases to containment as a fraction of the initial core inventory rather than absolute mass. This enables direct comparison with NUREG-1465 results. In addition, the tabulated values present only the results for the early containment failure cases (1B and 2B); the tabulated results for the late containment failure cases (1A and 2A) were included in Section 4.1.

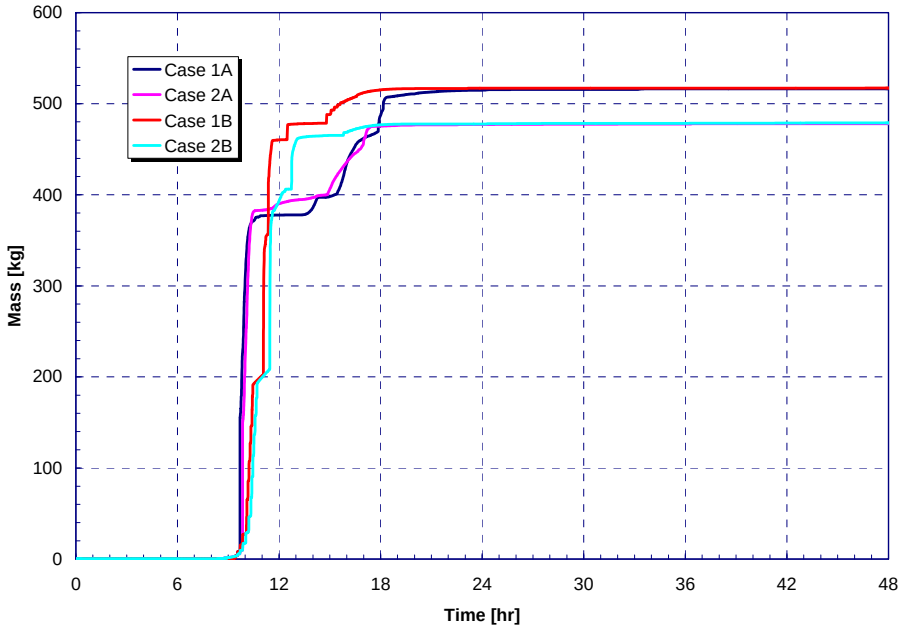

Figure 4-28. Noble Gas Release to Containment for Early/Late Containment Failure Long-Term SBO.

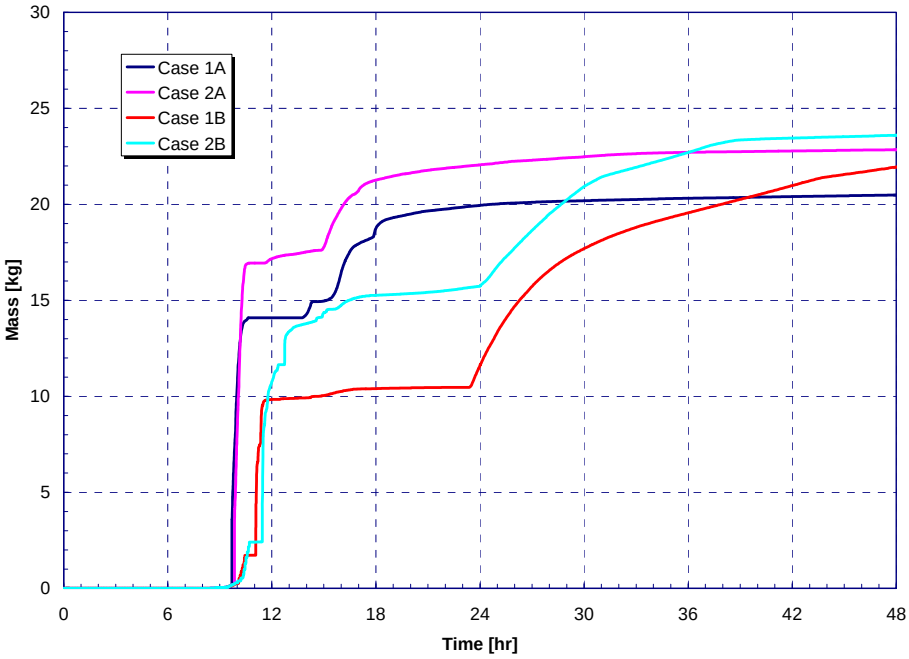

Figure 4-29. Halogen Release to Containment for Early/Late Containment Failure Long-Term SBO.

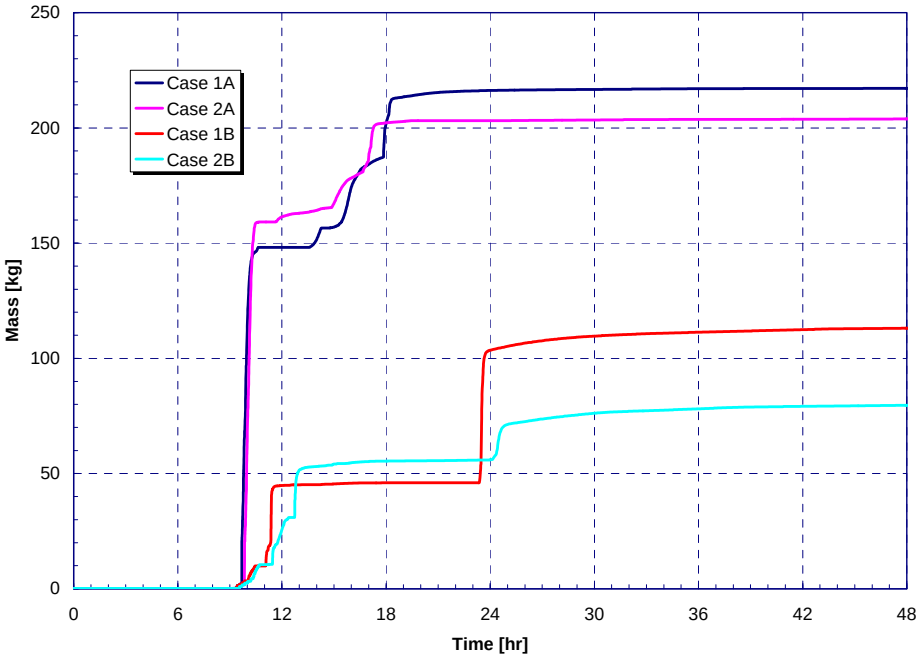

Figure 4-30. Alkali Metal Release to Containment for Early/Late Containment Failure Long-Term SBO.

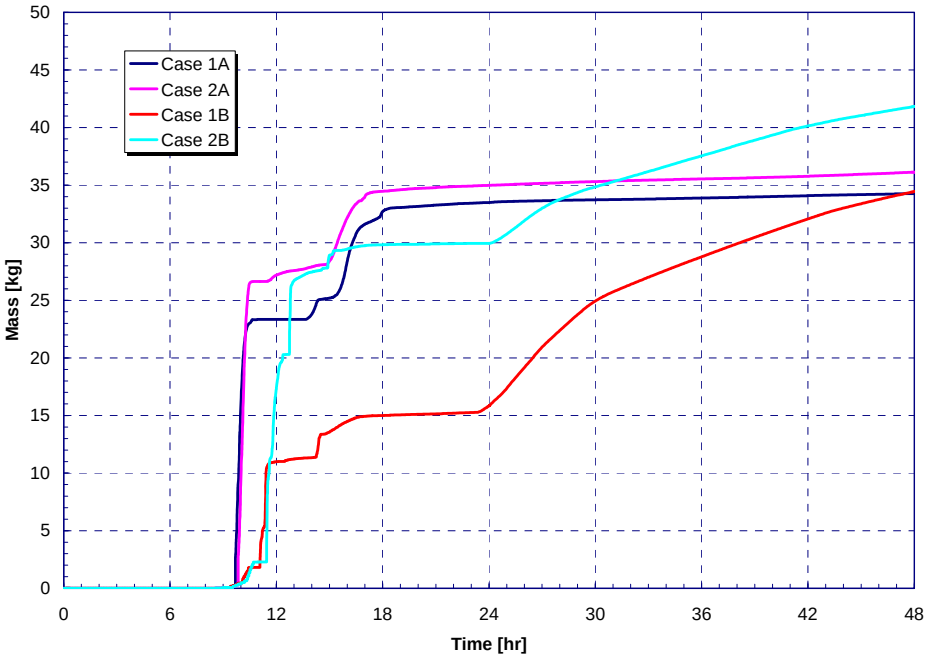

Figure 4-31. Tellurium Group Release to Containment for Early/Late Containment Failure Long-Term SBO.

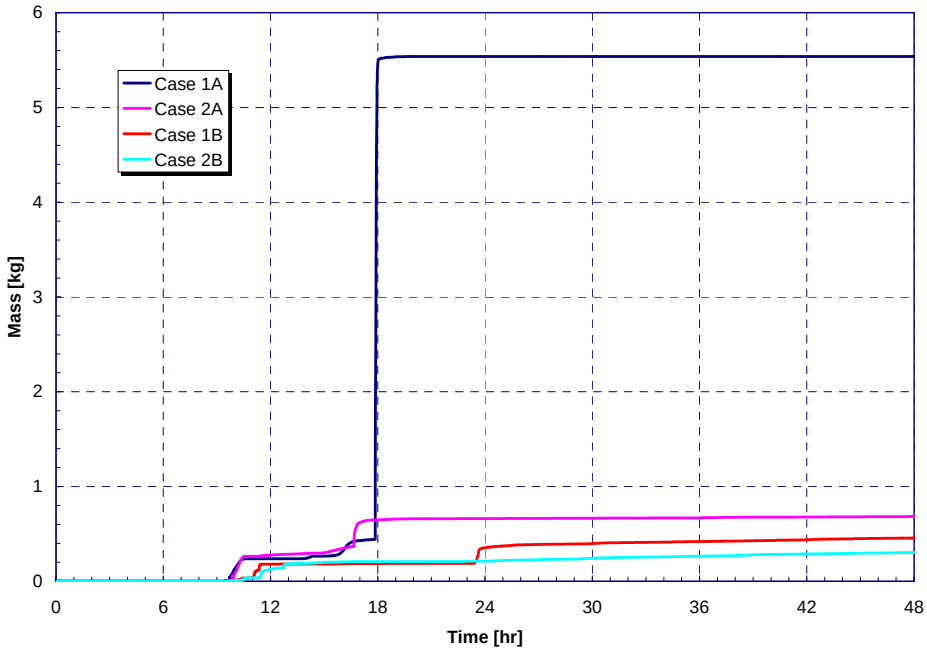

Figure 4-32. Barium, Strontium Group Release to Containment for Early/Late Containment Failure Long-Term SBO.

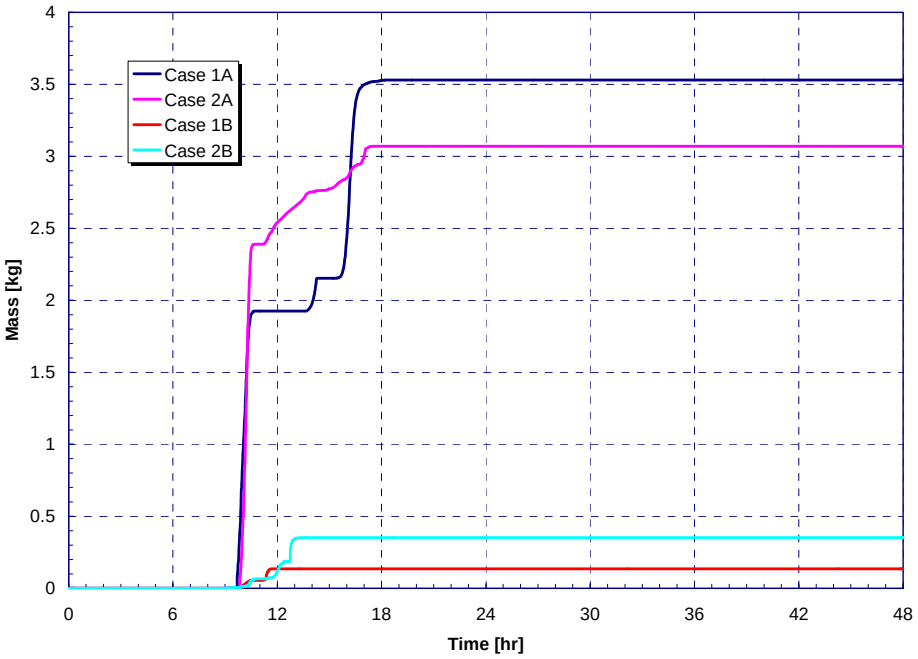

Figure 4-33. Noble Metal (Ru) Release to Containment for Early/Late Containment Failure Long-Term SBO.

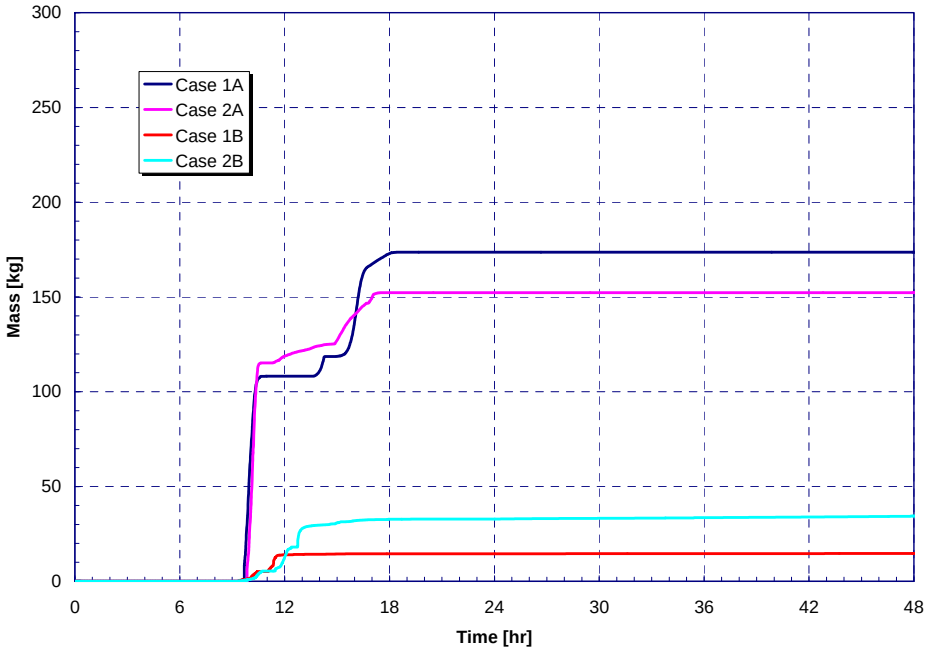

Figure 4-34. Noble Metal (Mo) Release to Containment for Early/Late Containment Failure Long-Term SBO.

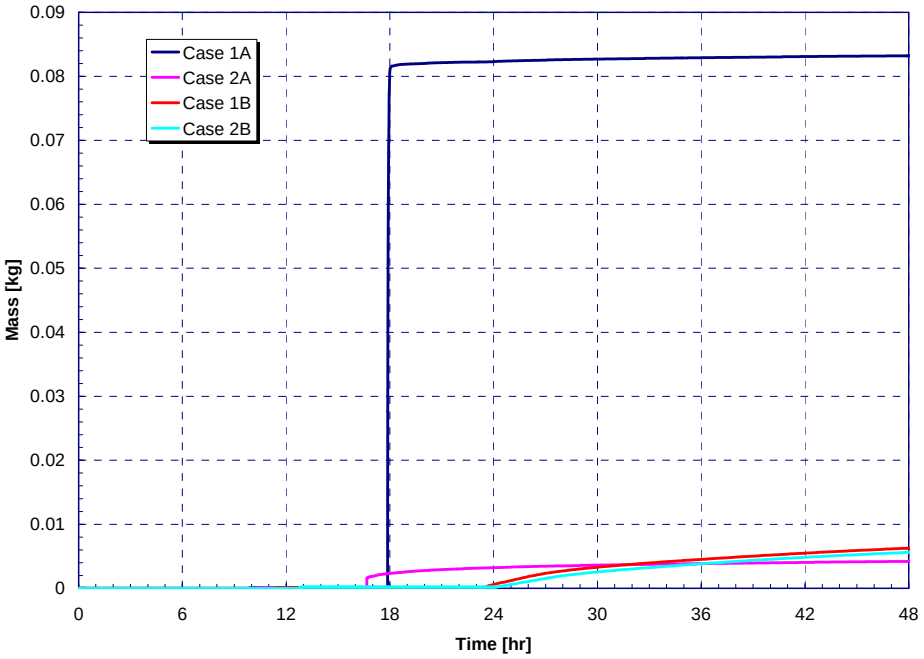

Figure 4-35. Lanthanide Release to Containment for Early/Late Containment Failure Long-Term SBO.

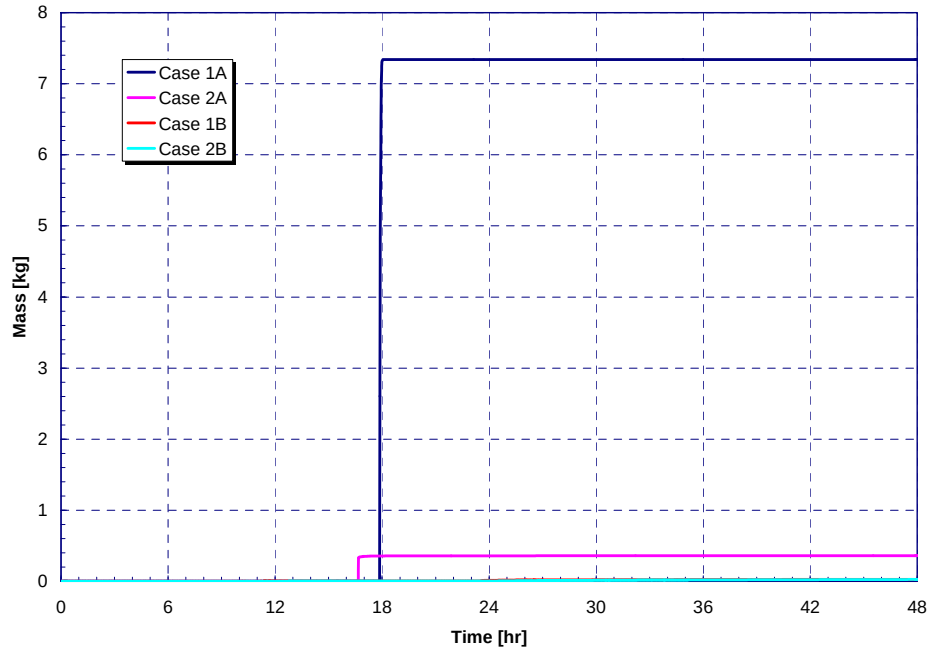

Figure 4-36. Cerium Group Release to Containment for Early/Late Containment Failure Long-Term SBO.

Table 4-11. Release Timing for Long-Term SBO with Early Containment Failure.

Timing (hr)	NUREG-1465	Case 1B	Case 2B
Onset of Release	~0	6.5	6.6
Coolant Release Duration		1.5	1.5
Gap Release Duration	0.5	0.6	0.7
In-Vessel Release Duration	1.3	2.4	2.7
Ex-Vessel Release Duration	2.0	17.2	16.8
Late I-Vessel Release Duration	10.0	18.3	25.3

Table 4-12. Gap Release Fractions for Long-Term SBO with Early Containment Failure.

	NUREG-1465	Case 1B	Case 2B
Noble Gases	0.05	1.2262E-02	1.2111E-02
Halogens	0.05	4.5848E-03	5.4231E-03
Alkali Metals	0.05	3.4017E-03	1.9500E-03
Te Group	0	4.9788E-03	2.6400E-03

Table 4-13. In-Vessel Release Fractions for Long-Term SBO with Early Containment Failure.

	NUREG-1465	Case 1B	Case 2B
Noble Gases	0.95	3.8594E-1	4.4078E-1
Halogens	0.35	6.8253E-2	8.8846E-2
Alkali Metals	0.25	3.0524E-2	3.6429E-2
Te Group	0.05	3.2980E-2	4.3600E-2
Ba, Sr Group	0.02	1.5909E-4	2.0000E-4
Ru Group	0.0025	1.5320E-4	1.6585E-4
Mo Group	0.0025	1.3941E-2	1.5714E-2
Lanthanides	0.0002	3.8571E-9	4.6802E-9
Ce Group	0.0005	3.7584E-9	4.4736E-9

Table 4-14. Ex-Vessel Release Fractions for Long-Term SBO with Early Containment Failure.

	NUREG-1465	Case 1B	Case 2B
Noble Gases	0	2.7965E-1	7.3003E-2
Halogens	0.25	2.1178E-1	8.5667E-2
Alkali Metals	0.35	2.7352E-1	1.0715E-1
Te Group	0.25	8.5661E-2	4.0369E-2
Ba, Sr Group	0.1	1.0853E-3	1.4321E-4
Ru Group	0.0025	1.449E-11	3.673E-11
Mo Group	0.0025	9.148E-12	3.369E-11
Lanthanides	0.005	3.3601E-6	3.3783E-6
Ce Group	0.005	1.2695E-5	5.5393E-6

Table 4-15. Late In-Vessel Release Fractions for Long-Term SBO with Early Containment Failure.

	NUREG-1465	Case 1B	Case 2B
Noble Gases	0	3.2215E-1	4.8091E-1
Halogens	0.1	3.8696E-1	6.8752E-1
Alkali Metals	0.1	6.3424E-2	1.3765E-1
Te Group	0.005	3.3364E-1	6.6507E-1
Ba, Sr Group	0	5.4893E-4	1.0124E-3
Ru Group	0	2.2636E-4	6.9462E-4
Mo Group	0	2.5306E-2	8.4576E-2
Lanthanides	0	7.5373E-9	3.1035E-8
Ce Group	0	5.6805E-8	2.9532E-8

4.3 Sensitivity of SBO Results to AFW Failure, RCP Seal Failure, and Pressurizer SORV (40% MOX Core)

Three calculations were performed to examine the sensitivity of the source term results to potential deviations from the baseline 40% MOX Core SBO (i.e., Case 2A) accident progression assumptions, as identified in the plant-specific PRAs. The first calculation, identified as Case 2P in Table 3-1, assumes failure to initiate AFW following main feedwater trip. The baseline case had assumed that AFW operated until dc power failure at 3 hr. Case 2S is identical to Case 2P, except that an RCP seal is assumed to fail immediately on loss of power in one of four loops. Finally, Case 2T is identical to the baseline case, except that the pressurizer safety-relief valve (SRV) is assumed to stick open on the 35th cycle. The timing of key events for the sensitivity cases are compared to the baseline case in Table 4-16.

Table 4-16. Key Event Timing Comparison: 40% MOX Core SBO Sensitivities.

Event	Case 2A [hr]	Case 2P [hr]	Case 2S [hr]	Case 2T [hr]
Loss of ac power	0.0	0.0	0.0	0.0
Pump seals leak at 21 GPM	0.0	0.0	0.0	0.0
Loss of dc power	3.0	0.0	0.0	3.0
Steam generator secondary dry	5.9	1.6	1.6	5.9
PRT rupture disk fails	6.2	1.8	2.0	6.2
Vessel swollen water level at TAF	6.6	2.4	2.3	6.6
Start of fuel cladding failures	8.1	3.3	3.2	8.1
Containment design pressure	9.8	4.8	4.8	10.3
SORV	n/a	n/a	n/a	9.0
RCS Creep rupture failure	9.9	4.8	4.8	n/a
First hydrogen burn in containment	9.9	4.8	4.8	9.3
Accumulators empty	9.9	4.8	4.8	10.3
Start of core plate failures	11.6	4.7	4.6	9.8
Debris relocation to lower head	13.6	8.7	9.7	11.8
Vessel failure	16.7	12.9	11.8	17.1
Containment failure	68.7	51.1	53.8	68.3
Calculation terminated[14]	162.	161.	168.	165.

[14] Case 2A and 2P terminated early due to failures in the CAV at very low rates of core-concrete interaction.

Failure to initiate AFW in Cases 2P and 2S accelerates accident progression due to loss of heat removal for the first 3 hr. This is evident in Figures 4-37 through 4-41, as the primary system heats and pressurizes to the SRV setpoint much more quickly in these two cases than in the baseline case. In both Cases 2P and 2S, this is followed by a more rapid loss of coolant, onset of cladding oxidation, core degradation and relocation, vessel failure, and containment pressurization. Note that the time of RCS creep-rupture is not affected by the small RCP seal leak in Case 2S. Other than a small difference in the initial pressure transient, these two cases are very similar in accident progression. Cases 2A and 2T are very similar, except that the SORV in Case 2T occurs approximately 1 hr before RCS creep-rupture occurs in Case 2A. There are some slight differences in accident progression behavior between the two cases, primarily due to the elevation difference of hole in the RCS. However, this does not result in major differences in results in the long term.

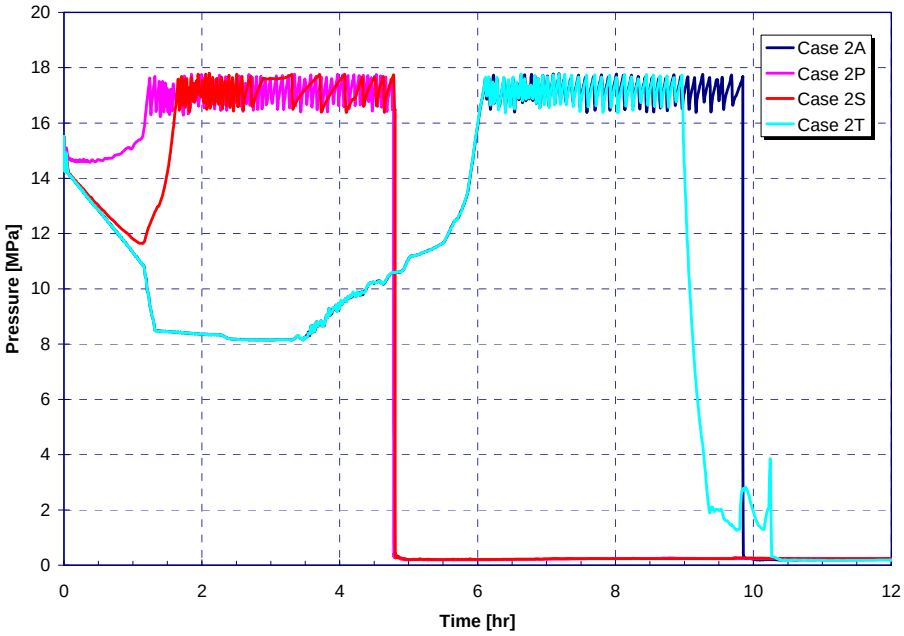

Figure 4-37. RCS Pressure for the Long-Term SBO Sensitivity Calculations.

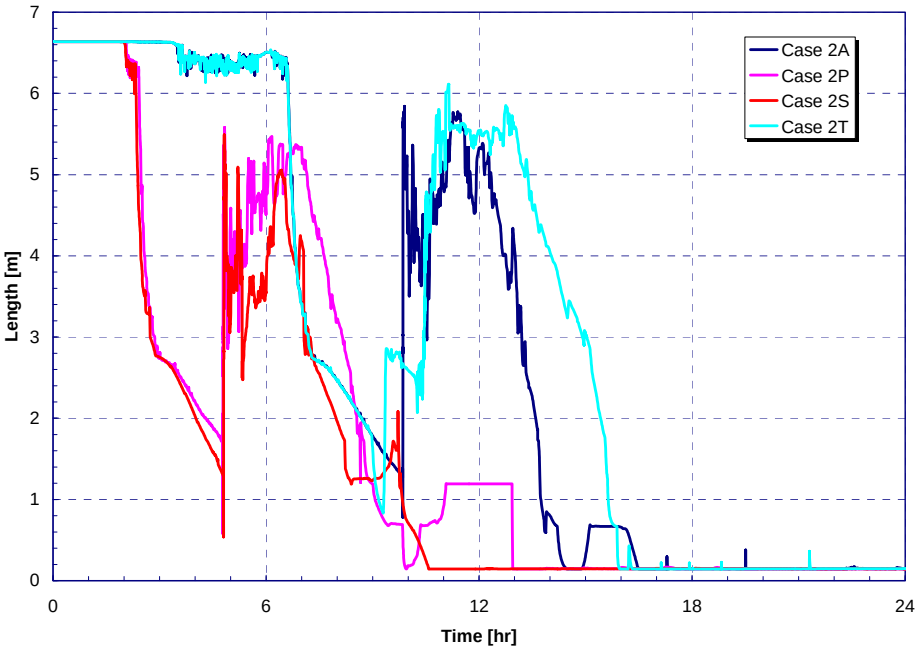

Figure 4-38. Vessel Swollen Water Level for the Long-Term SBO Sensitivity Calculations.

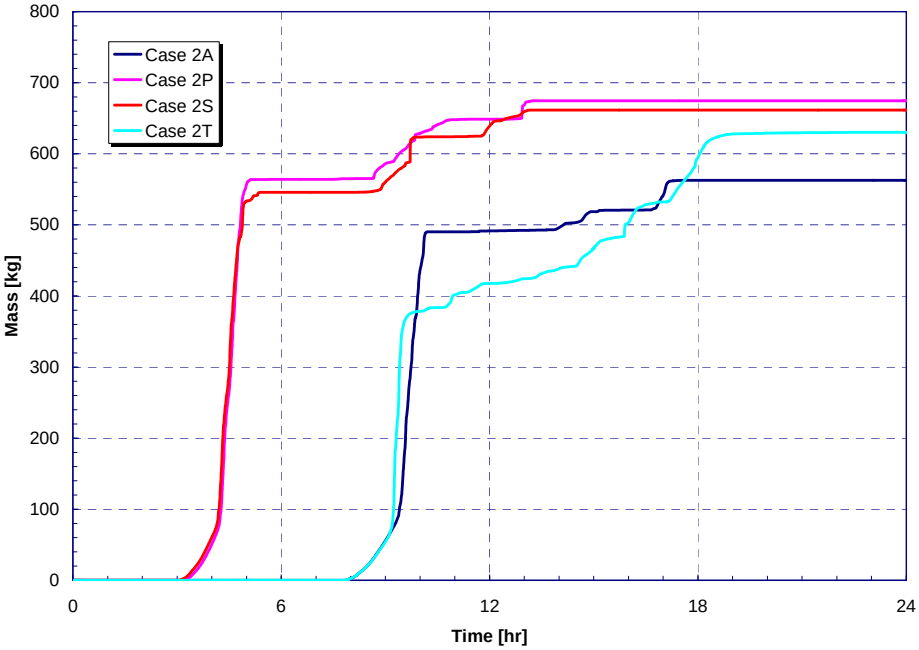

Figure 4-39. In-Vessel Hydrogen Production for the Long-Term SBO Sensitivity Calculations.

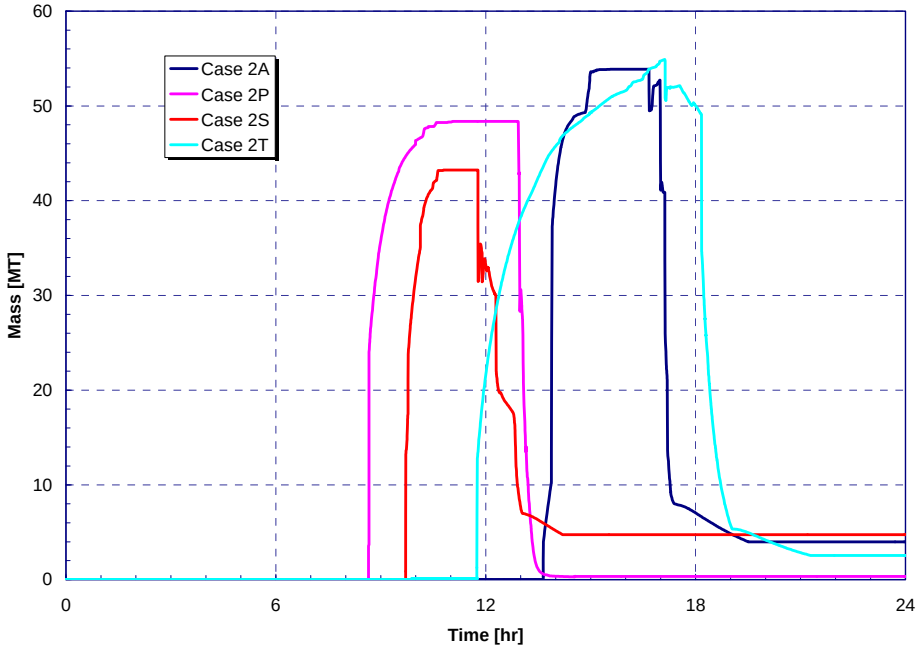

Figure 4-40. Uranium Dioxide Mass on the Vessel Lower Head for the Long-Term SBO Sensitivity Calculations.

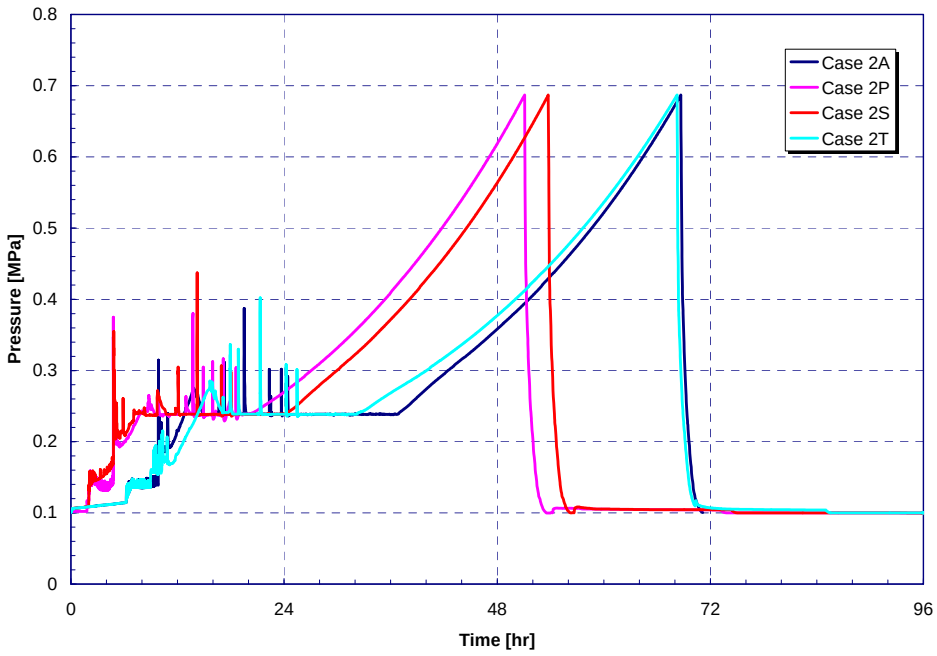

Figure 4-41. Containment Pressure Response for the Long-Term SBO Sensitivity Calculations.

The fission product release results for the sensitivity cases are compared to the 40% MOX SBO baseline case in Figures 4-42 through 4-50. These figures summarize the total fission product mass released to containment. Durations of each of the NUREG-1465 release phases are presented in Table 4-17. In addition, the magnitudes of release to containment for each of the NUREG-1465 radionuclide groups are tabulated in Tables 4-18 through 4-21 for all release phases. In contrast to Figures 4-42 through 4-50, the results in the tables present the releases to containment as a fraction of the initial core inventory rather than absolute mass. This enables direct comparison with NUREG-1465 results. In addition, the tabulated values present only the results for the three sensitivity cases (2P, 2S, and 2T); the tabulated results for the baseline case (2A) were included in Section 4.1.

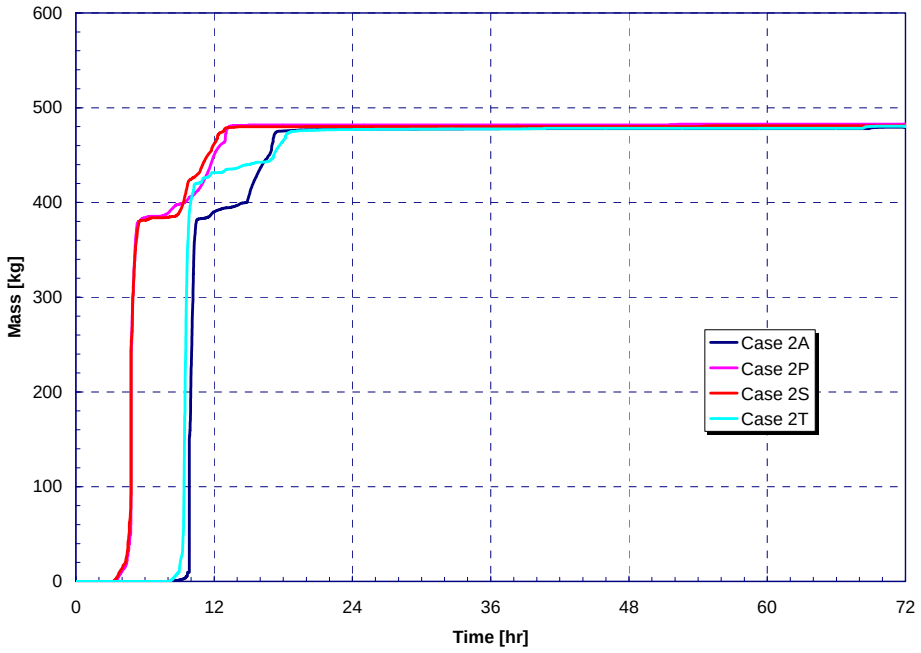

Figure 4-42. Noble Gas Release to Containment for Long-Term SBO Sensitivity Calculations.

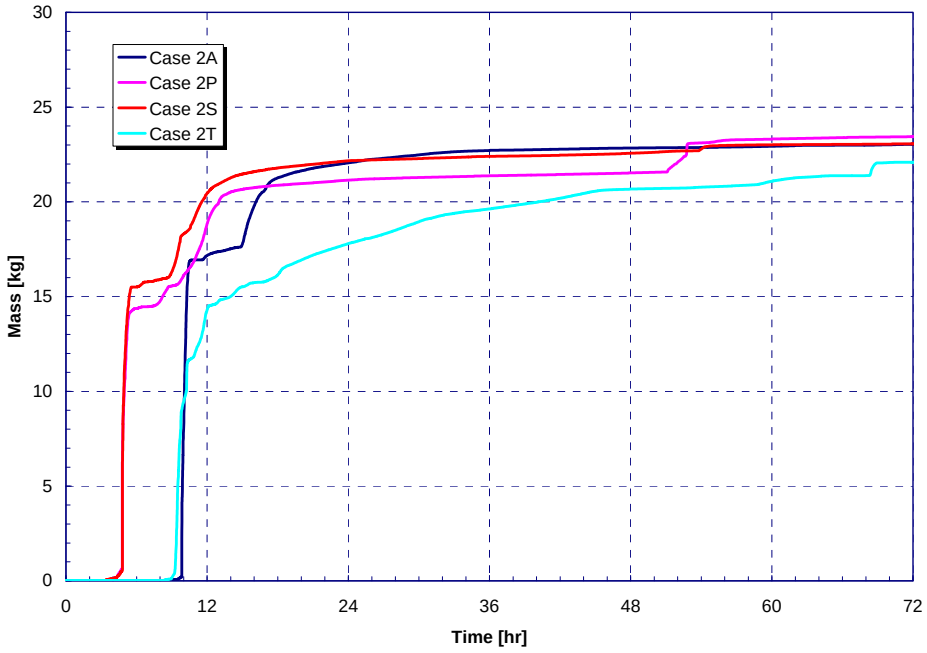

Figure 4-43. Halogen Release to Containment for Long-Term SBO Sensitivity Calculations.

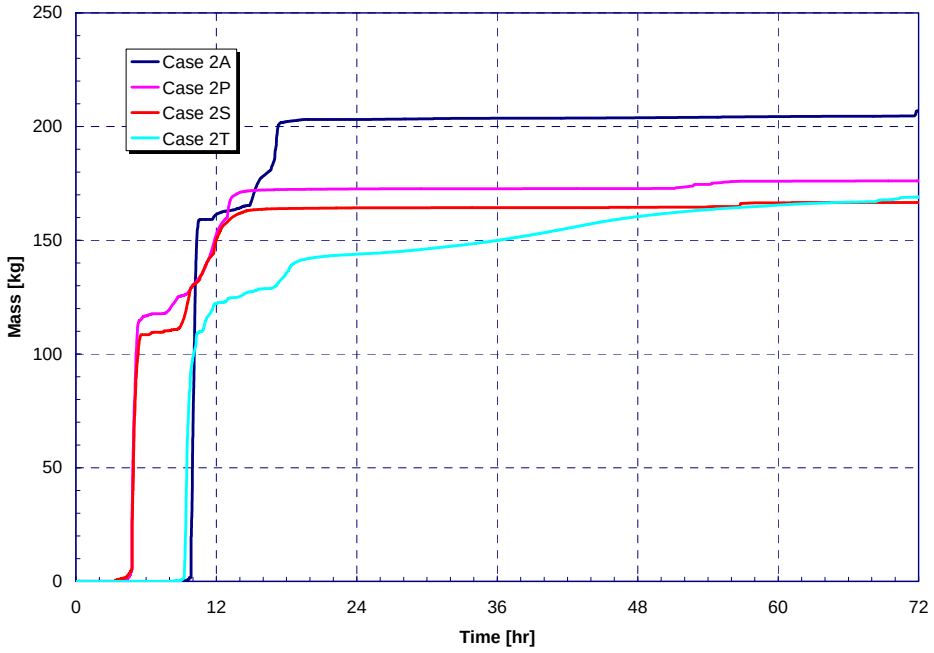

Figure 4-44. Alkali Metal Release to Containment for Long-Term SBO Sensitivity Calculations.

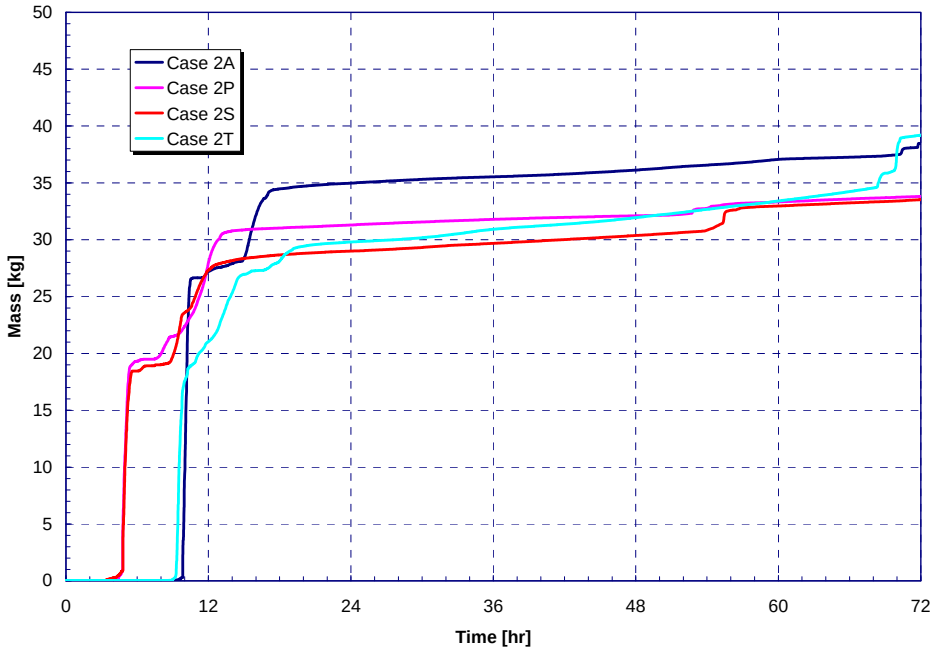

Figure 4-45. Tellurium Group Release to Containment for Long-Term SBO Sensitivity Calculations.

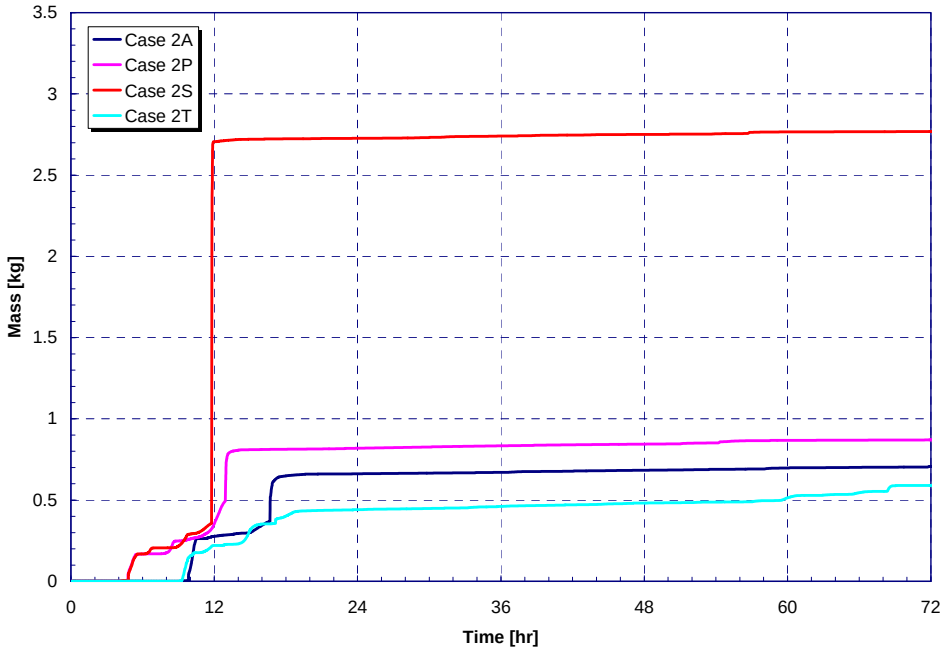

Figure 4-46. Barium, Strontium Group Release to Containment for Long-Term SBO Sensitivity Calculations.

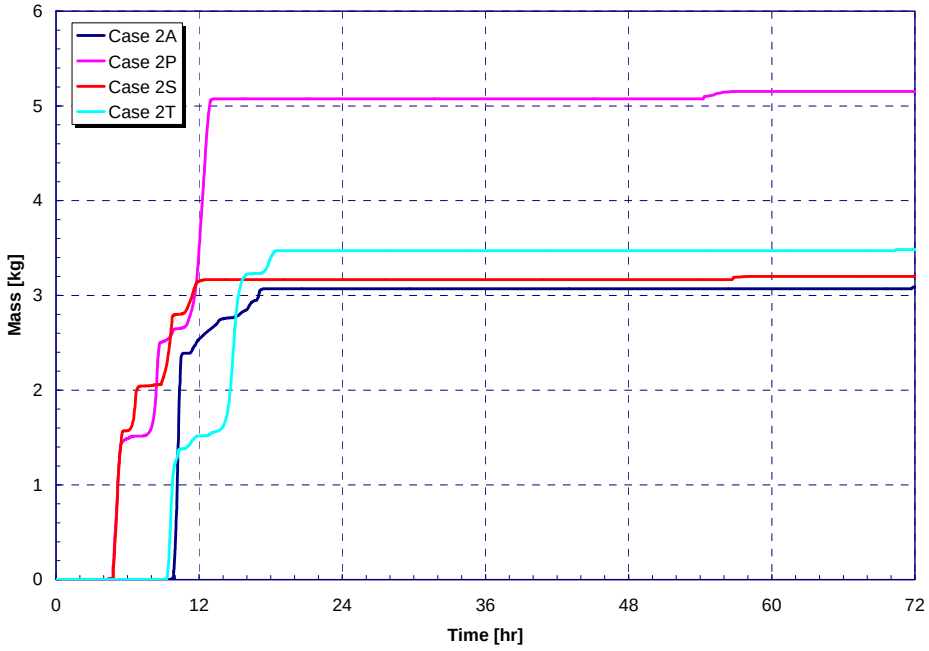

Figure 4-47. Noble Metal (Ru) Release to Containment for Long-Term SBO Sensitivity Calculations.

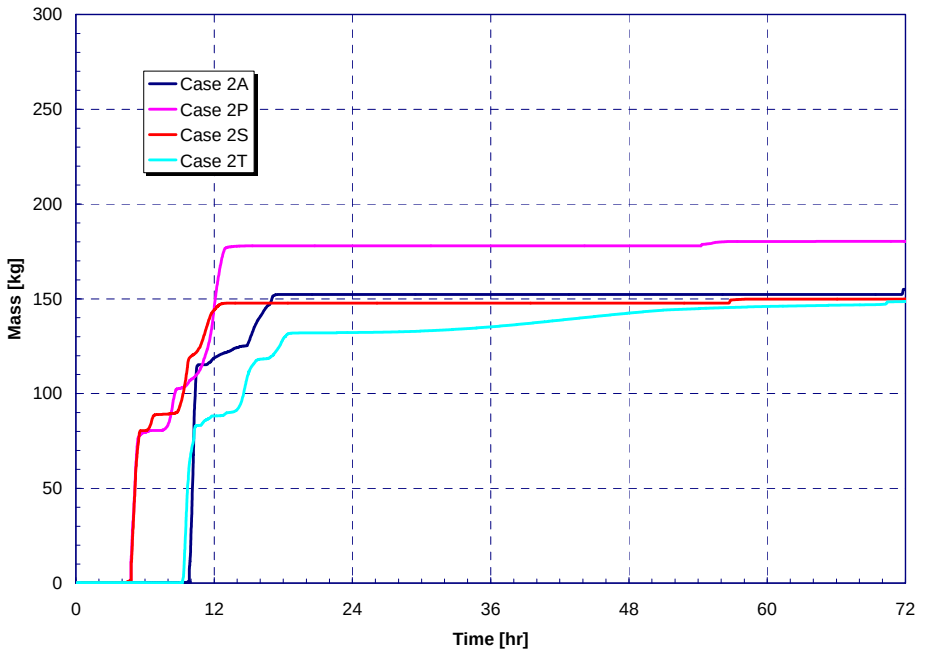

Figure 4-48. Noble Metal (Mo) Release to Containment for Long-Term SBO Sensitivity Calculations.

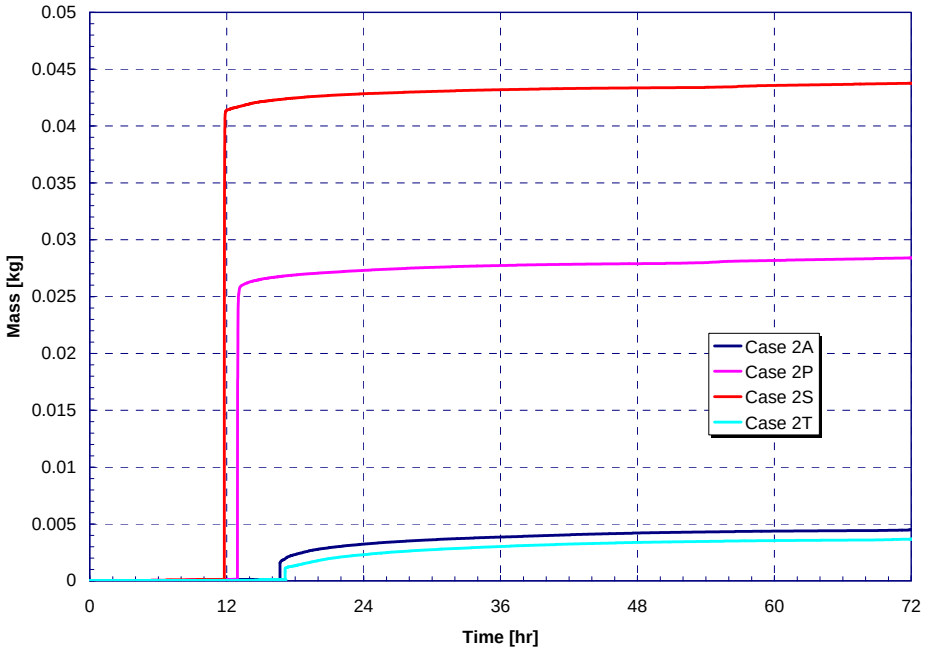

Figure 4-49. Lanthanide Release to Containment for Long-Term SBO Sensitivity Calculations.

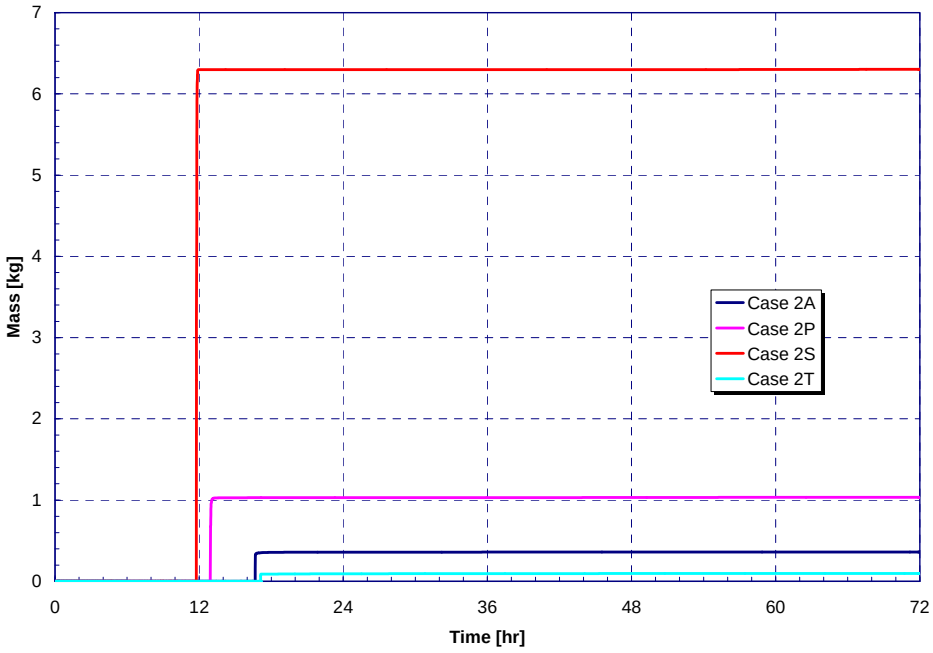

Figure 4-50. Cerium Group Release to Containment for Long-Term SBO Sensitivity Calculations.

Table 4-17. Release Timing for Long-Term SBO Sensitivity Cases.

Timing (hr)	NUREG-1465	Case 2P	Case 2S	Case 2T
Onset of Release	~0	2.4	2.3	6.6
Coolant Release Duration		0.9	0.9	1.5
Gap Release Duration	0.5	0.5	0.6	0.7
In-Vessel Release Duration	1.3	9.1	8.0	8.4
Ex-Vessel Release Duration	2.0	8.7	24.6	87.3
Late I-Vessel Release Duration	10.0	54.1	124.3	118.8

Table 4-18. Gap Release Fractions for Long-Term SBO Sensitivity Cases.

	NUREG-1465	Case 2P	Case 2S	Case 2T
Noble Gases	0.05	1.6214E-02	2.0838E-02	1.6758E-02
Halogens	0.05	3.4645E-03	4.0278E-03	3.5018E-03
Alkali Metals	0.05	6.8973E-04	3.7525E-03	9.9706E-04
Te Group	0	6.6604E-04	3.9471E-03	1.0479E-03

Table 4-19. In-Vessel Release Fractions for Long-Term SBO Sensitivity Cases.

	NUREG-1465	Case 2P	Case 2S	Case 2T
Noble Gases	0.95	9.3412E-1	9.1074E-1	8.9966E-1
Halogens	0.35	7.6128E-1	7.7297E-1	6.0545E-1
Alkali Metals	0.25	5.7060E-1	5.1116E-1	4.6321E-1
Te Group	0.05	6.0131E-1	5.3541E-1	5.4992E-1
Ba, Sr Group	0.02	2.5970E-3	1.8800E-3	1.8768E-3
Ru Group	0.0025	1.2309E-2	7.6366E-3	7.8806E-3
Mo Group	0.0025	5.0420E-1	4.0733E-1	3.4375E-1
Lanthanides	0.0002	2.3109E-7	1.6837E-7	1.4431E-7
Ce Group	0.0005	2.2069E-7	1.6092E-7	1.4260E-7

Table 4-20. Ex-Vessel Release Fractions for Long-Term SBO Sensitivity Cases.

	NUREG-1465	Case 2P	Case 2S	Case 2T
Noble Gases	0	3.4747E-2	3.7696E-2	2.7171E-2
Halogens	0.25	3.2927E-2	4.6742E-2	3.8505E-2
Alkali Metals	0.35	4.1672E-2	6.0875E-2	3.5126E-2
Te Group	0.25	1.9328E-2	3.1775E-2	5.0247E-2
Ba, Sr Group	0.1	1.6973E-3	1.2746E-2	4.9414E-4
Ru Group	0.0025	1.342E-08	1.448E-09	3.048E-10
Mo Group	0.0025	9.449E-10	1.294E-09	3.055E-08
Lanthanides	0.005	4.2619E-5	6.7982E-5	7.0169E-6
Ce Group	0.005	4.7057E-4	2.8622E-3	4.5174E-5

Table 4-21. Late In-Vessel Release Fractions for Long-Term SBO Sensitivity Cases.

	NUREG-1465	Case 2P	Case 2S	Case 2T
Noble Gases	0	3.9307E-3	1.6216E-2	4.3567E-2
Halogens	0.1	9.1594E-2	6.5507E-2	2.2671E-1
Alkali Metals	0.1	1.4831E-2	2.0431E-2	1.3258E-1
Te Group	0.005	2.9339E-2	1.9367E-1	2.6286E-1
Ba, Sr Group	0	6.9347E-5	2.0350E-4	8.1510E-4
Ru Group	0	2.5908E-4	1.6936E-4	6.1817E-4
Mo Group	0	1.0864E-2	2.2461E-2	9.9687E-2
Lanthanides	0	0.0000E+0	0.0000E+0	3.9018E-9
Ce Group	0	0.0000E+0	0.0000E+0	2.260E-13

4.4 SLOCA with Failure to Realign ECCS and Late Containment Failure

SLOCAs with failure to realign the ECCS are simulated with LEU and 40% MOX cores in Case 1D and 2D, respectively. This accident sequence begins with a 1-in. diameter-equivalent break in the pump suction portion of the cold leg. The ECCS initially works in injection mode. However, once the refueling water storage tank is drained, there is a failure to realign ECCS, and it fails to operate in recirculation mode. Timing of key events in the SLOCA accident progression is provided in Table 4-22.

Table 4-22. Key Event Timing for SLOCA with Late Containment Failure.

Event	Case 1D [hr]	Case 2D [hr]
SLOCA	0.0	0.0
Reactor trip	0.07	0.07
ECCS starts	0.07	0.07
Containment spray signal	0.11	0.13
FWST Empty	0.63	0.65
ECCS and containment sprays fail	0.63	0.65
RCS pumps fail on high void	0.86	0.88
Vessel swollen water level at TAF	2.7	3.0
Start of fuel cladding failures	4.0	4.1
Start of core plate failures	4.8	4.9
First hydrogen burn in containment	5.0	5.2
Containment design pressure	5.3	5.2
Debris relocation to lower head	5.7	6.0
Accumulators injection starts	6.5	6.4
Vessel failure	9.4	8.1
Accumulators empty	9.4	8.1
Containment failure	40.7	35.9
Calculation terminated[15]	168.	144.

[15] Case 2D terminated early due to failures in the CAV at very low rates of core-concrete interaction.

Figures 4-51 through 4-59 show comparisons of the calculated responses for the two baseline SLOCA simulations with late containment failure (see Table 3-1). The SLOCA is simulated as a 1-in. diameter-equivalent hole. As described in Section 3.0, Case 1D uses LEU fuel attributes and Case 2D uses both LEU and MOX fuel attributes. The specific unique differences in the fuel attributes for the two cases include the fission product release characteristics and the fission product inventory.

The RCS pressure response is shown in Figure 4-51. Upon formation of the SLOCA, the RCS pressure steadily decreases. The reactor trips on low pressurizer level at 0.07 hr and there is an immediate ECCS signal. The ECCS flow stabilizes the RCS pressure above 10 MPa. Slightly after the ECCS signal, a high containment pressure signal activates the containment sprays. With both systems taking suction from the FWST, it empties at approximately 0.6 hr. It is assumed that the ECCS and containment spray systems are not successfully realigned to recirculation mode using water from the containment sump. Consequently, no RCS injection or containment heat removal is available thereafter.

As shown in Figure 4-52, the vessel water drops below the top of the core at approximately 3 hr. By 6 hr the vessel is completely drained. The maximum intact fuel temperatures (i.e., rod geometry rather than debris bed) are shown in Figure 4-53. Cladding failures begin at approximately 4 hr (i.e., at cladding temperatures of 1173 K) and the maximum fuel temperatures reaches 2500 K by 4.3 hr. It should be noted that since the SLOCA depressurized the RCS (i.e., esp. after ECCS failure), the mechanical potential for creep-rupture failure of the RCS was diminished. In fact, no RCS creep-rupture failures were predicted in the SLOCA cases.

The relocation of debris materials into the lower plenum starts at approximately 6 hrs. Since there is still water in the lower plenum, there are fuel debris-coolant interactions that cool the debris and generate steam. Because of variations in the magnitude of the initial debris relocation into lower plenum (Figure 4-55), Case 2D had a slightly larger pressurization and initially provided more steam cooling (Figure 4-53). More debris continued to relocate into the lower plenum in Case 2D, leading to further rapid increase in oxidation and hydrogen generation. As the debris collects on the lower head, it is cooled by the remaining water in the lower plenum (Figure 4-56). After the water boils away (Figure 4-52), the debris heats up lower head of the vessel (Figure 4-57). Although the accumulators start injecting at approximately 6.5 hr (Figure 4-52), there is an insufficient cooling effect and the debris remains hot. At 9.4 hr and 8.1 hr (Figure 4-51) for Cases 1D and 2D, the vessel lower head fails due to creep rupture.

In general, the in-vessel responses for the two cases are similar. However, variations in debris relocation behavior, debris cooling, and vessel structural failures create cumulative changes to the late phase in-vessel accident progression. The debris relocation variations result in differences in the vessel failure timing, in-vessel fission product releases, and the in-vessel hydrogen production.

Similar to the in-vessel behavior, the ex-vessel behavior also showed late-phase differences. Figure 4-58 shows the containment pressure response. In particular, Case 2D pressurized to containment failure more quickly than Case 1D. From vessel failure to approximately 24 hr (especially between 18 and 24 hr), Case 1D pressurized at a slower rate than Case 2D. A comparison of the ex-vessel debris temperature (Figure 4-59) showed very similar behavior during this time period. However, more water spilled into the cavity from the containment pool in Case 2D to create a higher steam pressure load. The net result was a 5-hr delay in the containment failure in Case 1D. However, this difference is within an expected range of late-phase (i.e., after start of core degradation) phenomenological variations (e.g., see [6]).

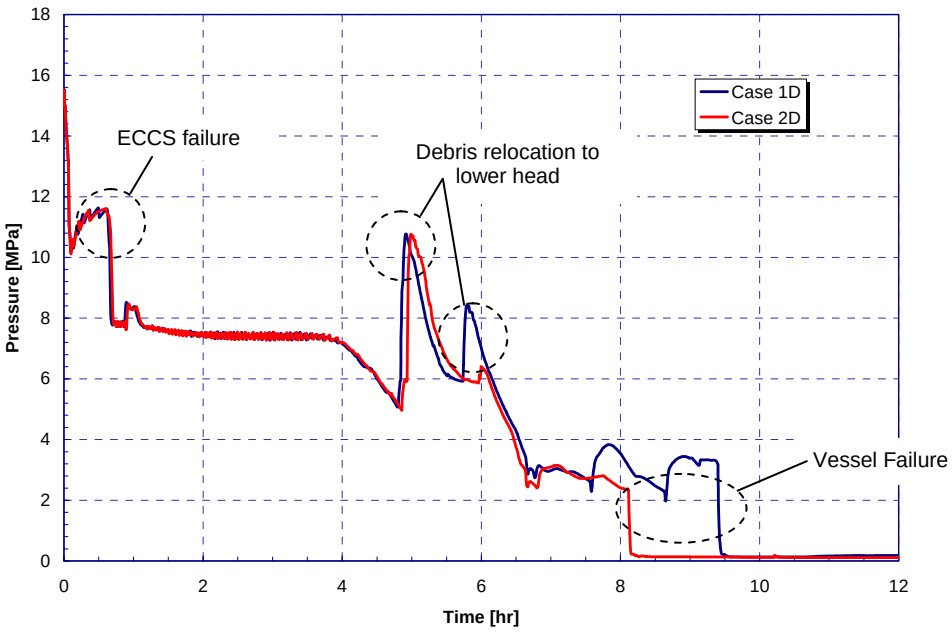

Figure 4-51. RCS Pressure Response for SLOCA with Late Containment Failure.

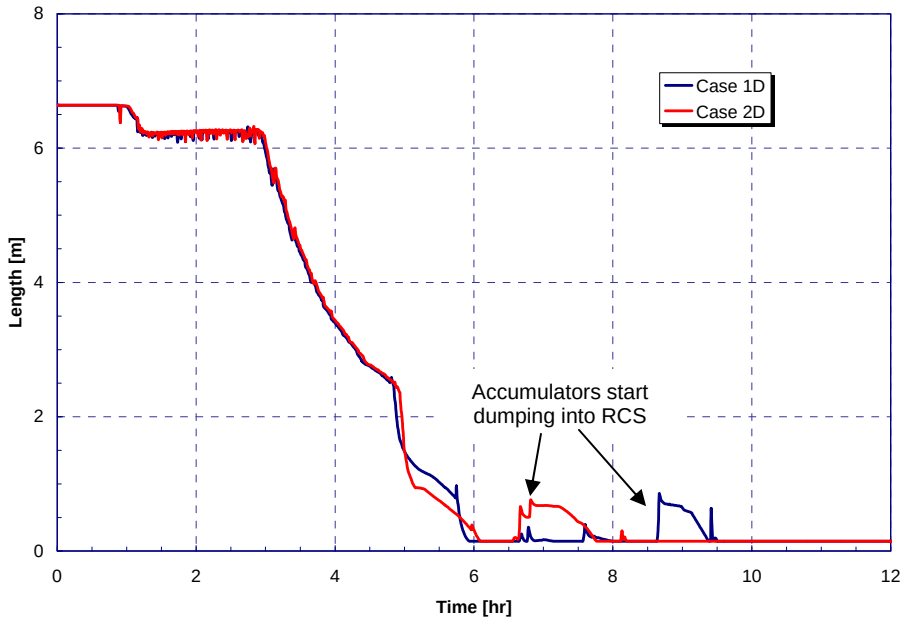

Figure 4-52. Vessel Level Response for SLOCA with Late Containment Failure.

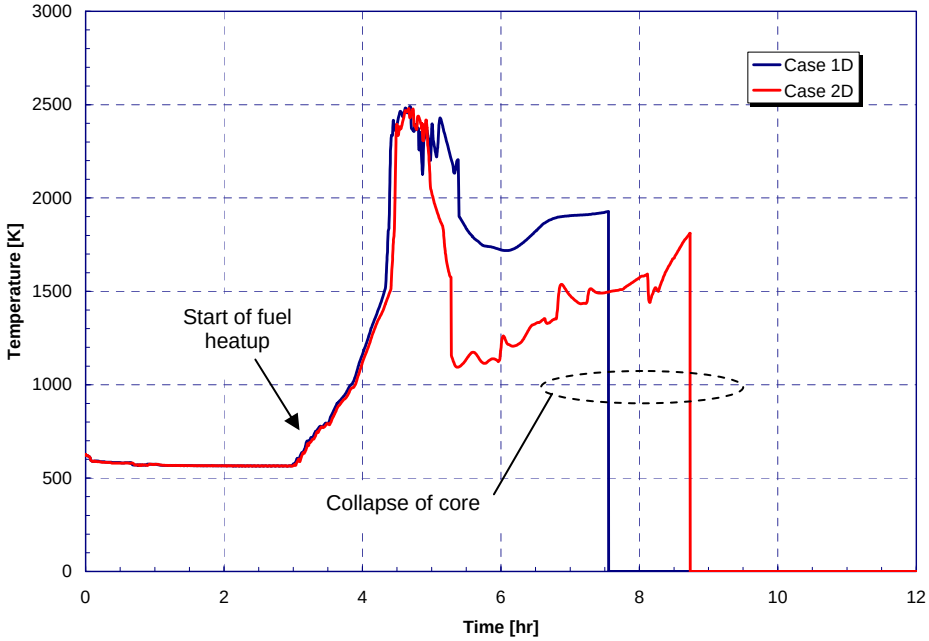

Figure 4-53. Peak Cladding Temperature Response for SLOCA with Late Containment Failure.

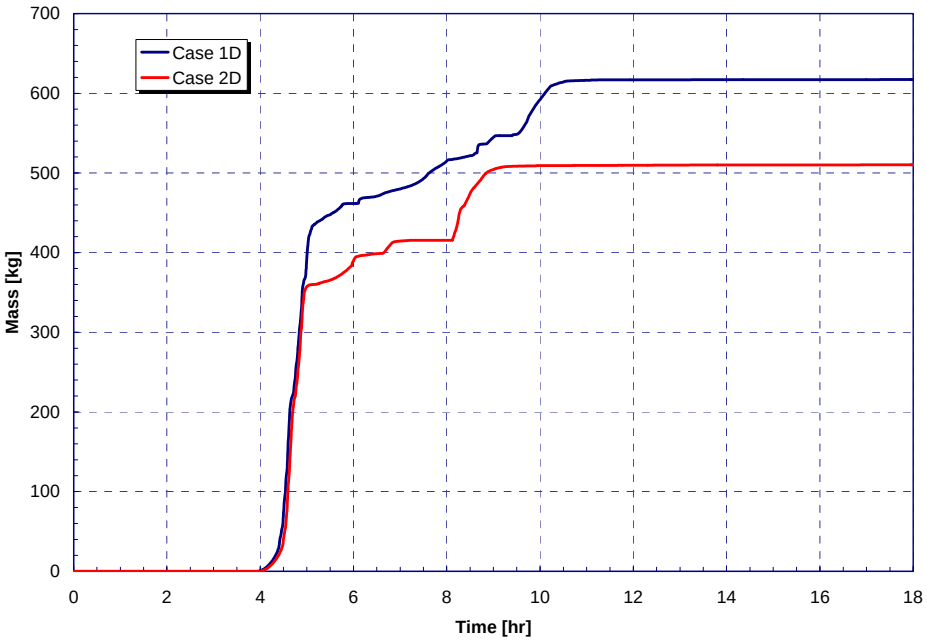

Figure 4-54. In-Vessel Hydrogen Production for SLOCA with Late Containment Failure.

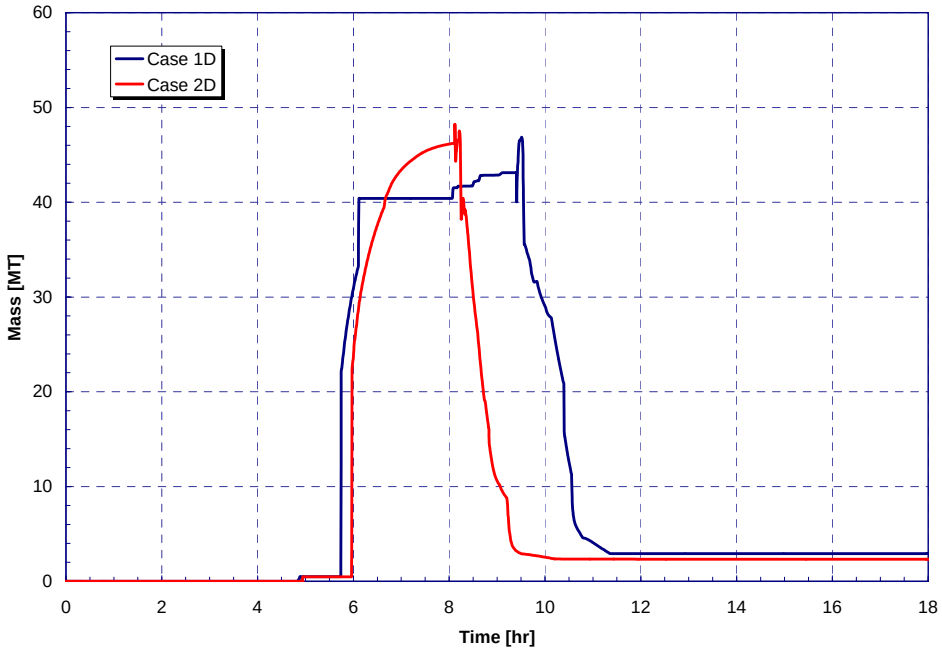

Figure 4-55. Uranium Dioxide Mass on the Vessel Lower Head for SLOCA with Late Containment Failure.

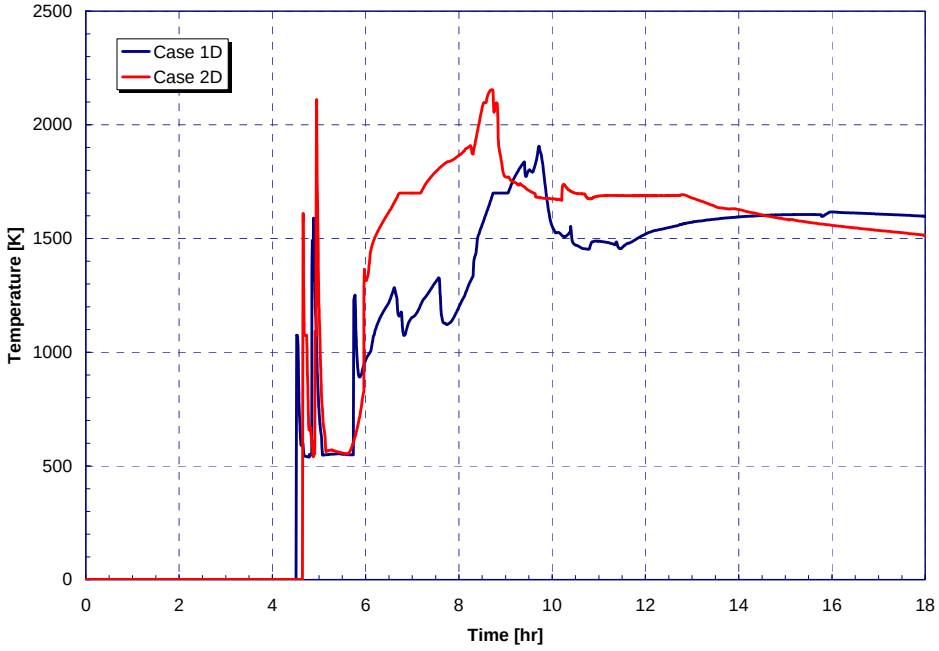

Figure 4-56. Lower Head Debris Temperature for SLOCA with Late Containment Failure.

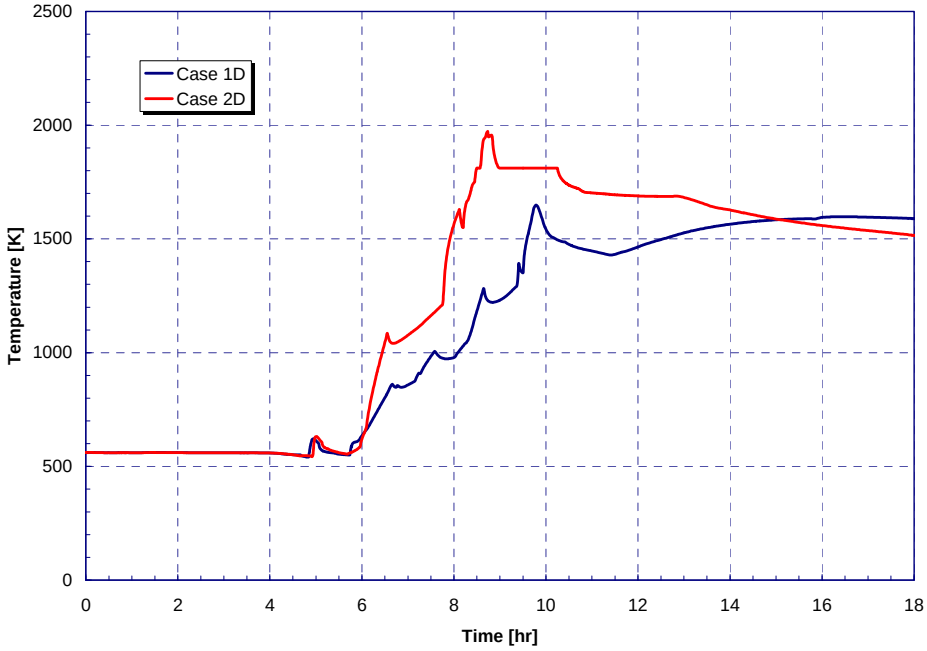

Figure 4-57. Lower Head Temperature Response for SLOCA with Late Containment Failure.

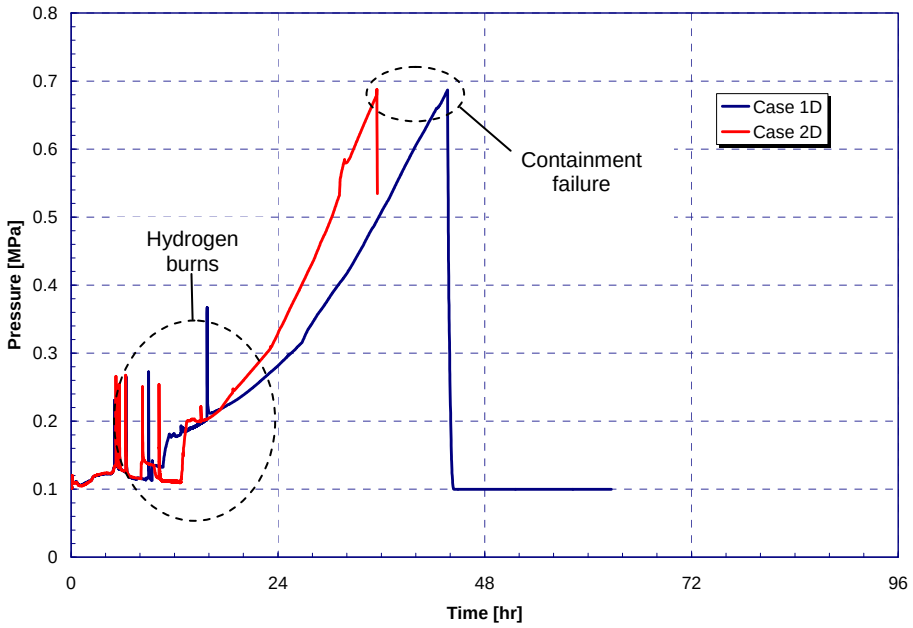

Figure 4-58. Containment Pressure Response for SLOCA with Late Containment Failure.

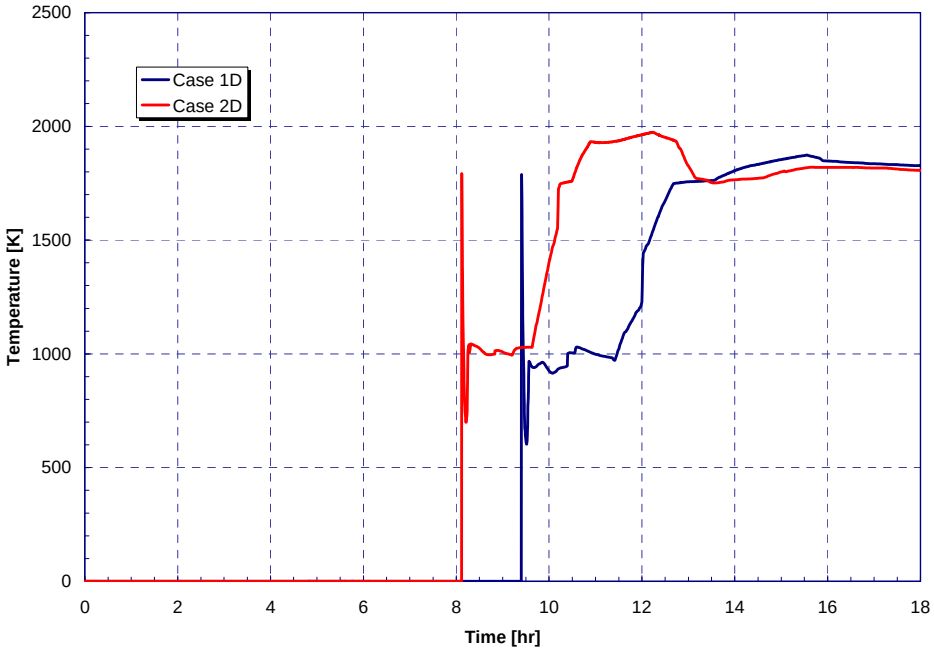

Figure 4-59. Ex-Vessel Debris Temperature Response for SLOCA with Late Containment Failure.

The fission product release results are shown in Figures 4-60 through 4-68, for the nine NUREG-1465 radionuclide groups. These figures summarize the total fission product mass released to containment. Durations of each of the NUREG-1465 release phases are presented in Table 4-23. In addition, the magnitudes of release to containment for each of the NUREG-1465 radionuclide groups are tabulated in Tables 4-24 through 4-27 for all release phases. In contrast to Figures 4-60 through 4-68, the results in the tables present the releases to containment as a fraction of the initial core inventory rather than absolute mass. This enables direct comparison with NUREG-1465 results.

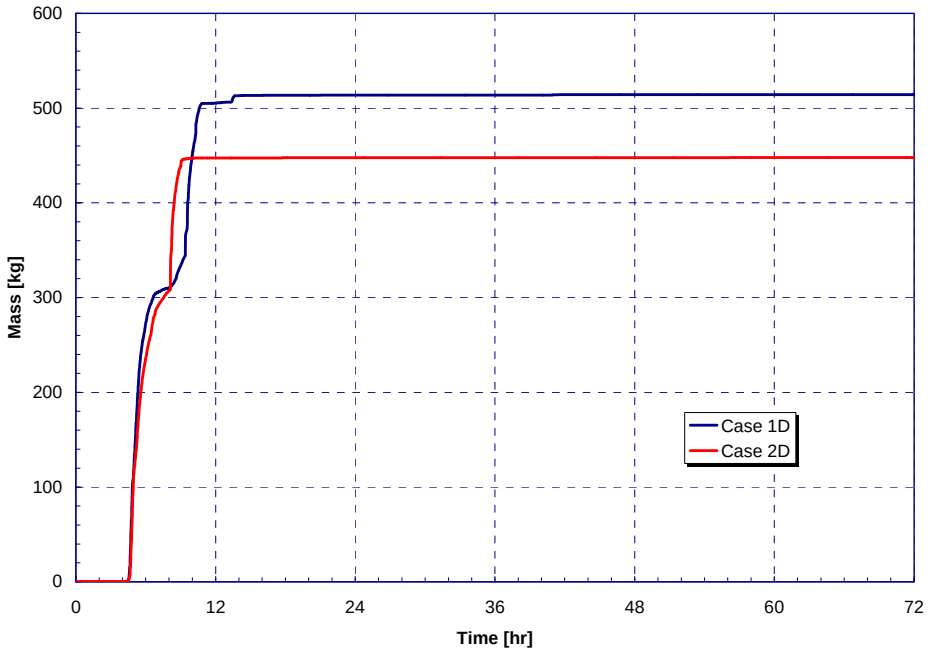

Figure 4-60. Noble Gas Release to Containment for SLOCA with Late Containment Failure.

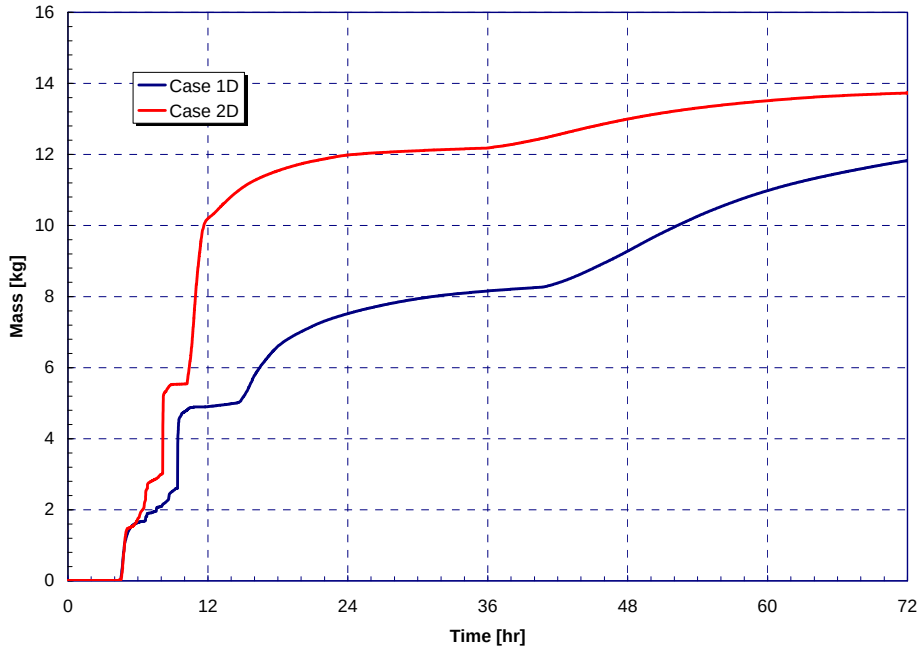

Figure 4-61. Halogen Release to Containment for SLOCA with Late Containment Failure.

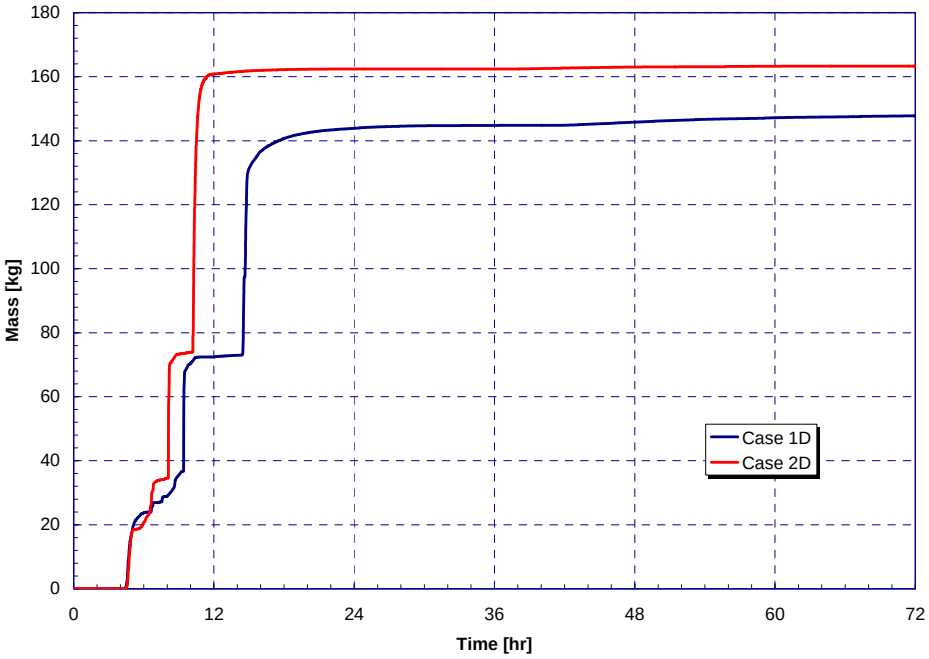

Figure 4-62. Alkali Metal Release to Containment for SLOCA with Late Containment Failure.

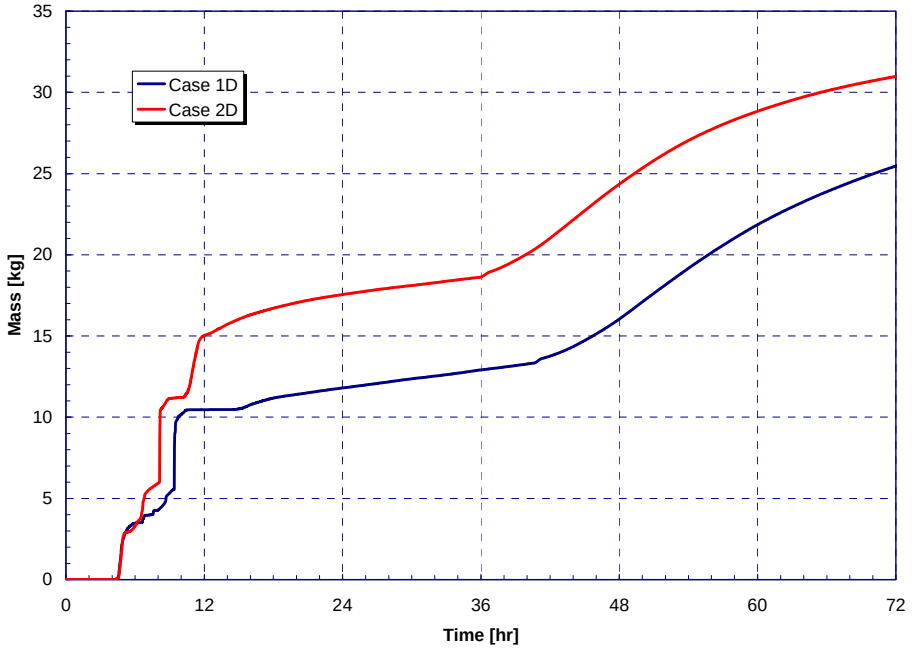

Figure 4-63. Tellurium Group Release to Containment for SLOCA with Late Containment Failure.

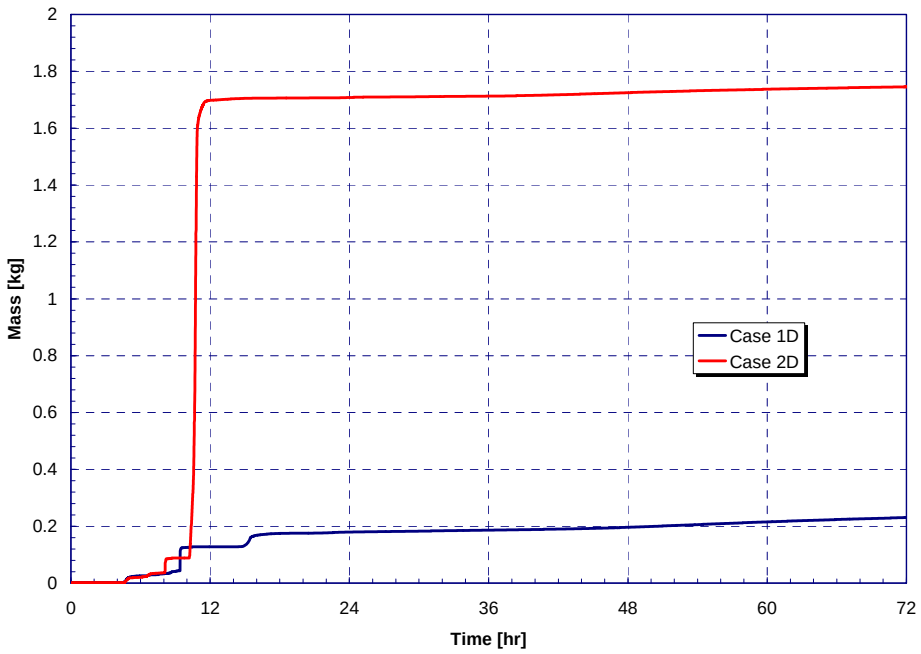

Figure 4-64. Barium, Strontium Group Release to Containment for SLOCA with Late Containment Failure.

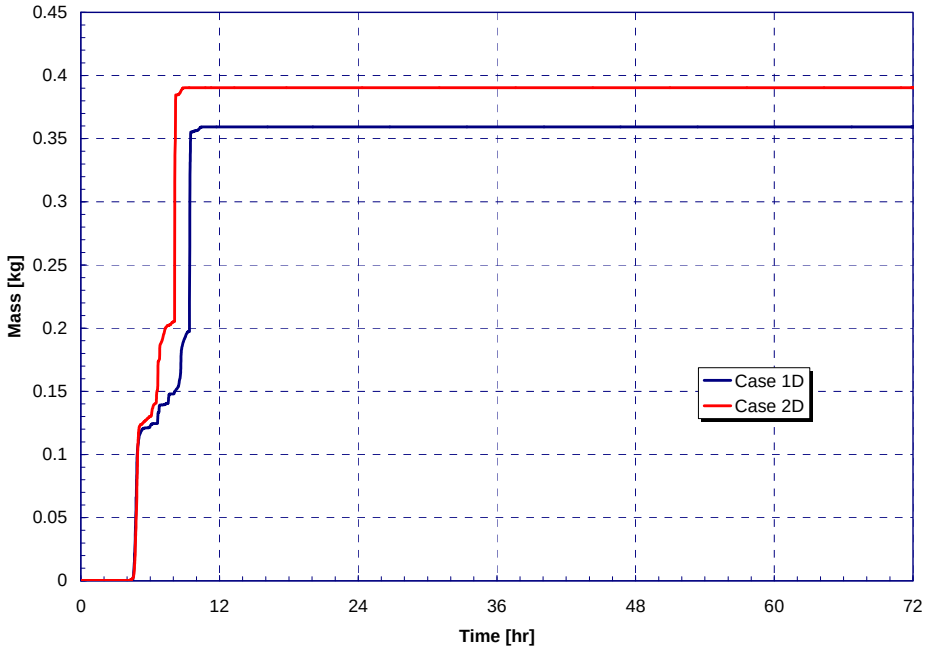

Figure 4-65. Noble Metal (Ru) Release to Containment for SLOCA with Late Containment Failure.

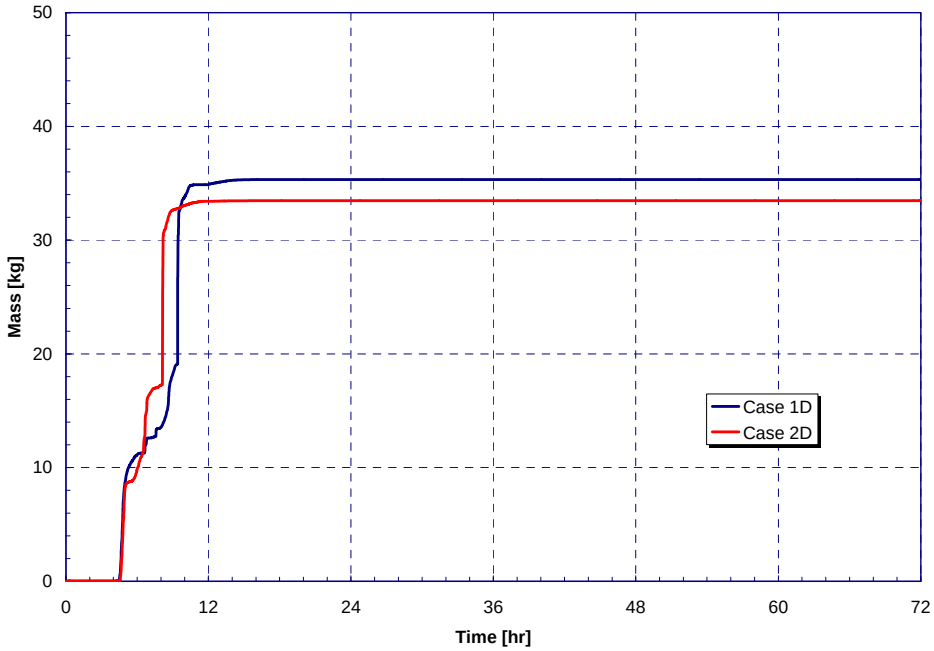

Figure 4-66. Noble Metal (Mo) Release to Containment for SLOCA with Late Containment Failure.

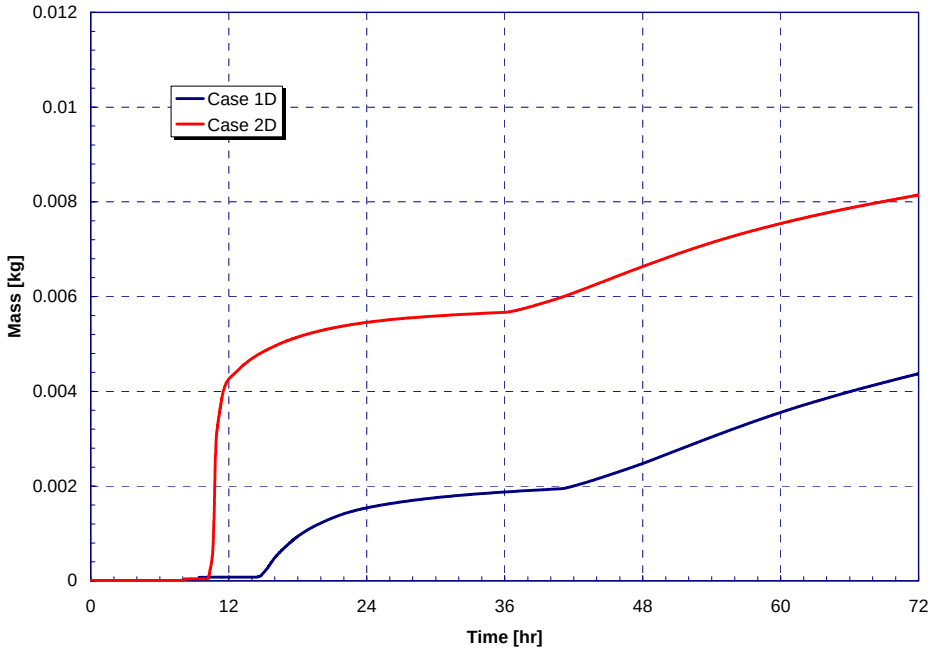

Figure 4-67. Lanthanide Release to Containment for SLOCA with Late Containment Failure.

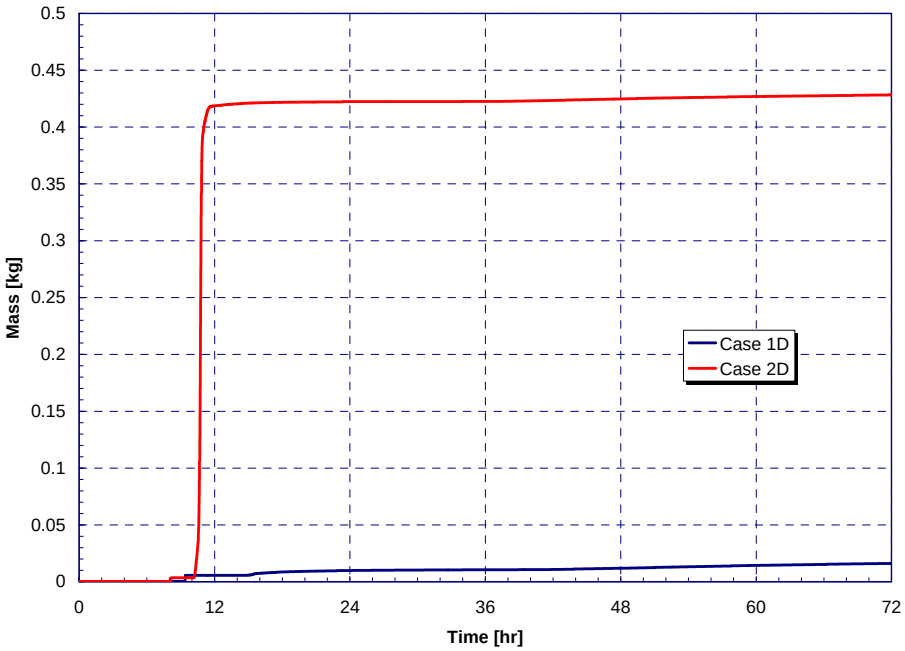

Figure 4-68. Cerium Group Release to Containment for SLOCA with Late Containment Failure.

Table 4-23. Release Timing for SLOCA with Late Containment Failure.

Timing (hr)	NUREG-1465	Case 1D	Case 2D
Onset of Release	~0	2.7	3.0
Coolant Release Duration		1.3	1.1
Gap Release Duration	0.5	0.4	0.5
In-Vessel Release Duration	1.3	5.0	3.6
Ex-Vessel Release Duration	2.0	38.2	3.2
Late I-Vessel Release Duration	10.0	0.9	0.5

Table 4-24. Gap Release Fractions for SLOCA with Late Containment Failure.

	NUREG-1465	Case 1D	Case 2D
Noble Gases	0.05	3.0108E-03	1.1906E-02
Halogens	0.05	1.5600E-03	7.7405E-03
Alkali Metals	0.05	2.1424E-03	5.0886E-03
Te Group	0	2.5722E-03	7.1874E-03

Table 4-25. In-Vessel Release Fractions for SLOCA with Late Containment Failure.

	NUREG-1465	Case 1D	Case 2D
Noble Gases	0.95	6.6191E-1	6.1998E-1
Halogens	0.35	1.0717E-1	1.1016E-1
Alkali Metals	0.25	1.2411E-1	1.1872E-1
Te Group	0.05	1.1072E-1	1.1480E-1
Ba, Sr Group	0.02	1.9545E-4	1.9474E-4
Ru Group	0.0025	5.5710E-4	5.1220E-4
Mo Group	0.0025	5.0938E-2	5.1429E-2
Lanthanides	0.0002	1.3714E-8	1.3261E-8
Ce Group	0.0005	1.3423E-8	1.4460E-8

Table 4-26. Ex-Vessel Release Fractions for SLOCA with Late Containment Failure.

	NUREG-1465	Case 1D	Case 2D
Noble Gases	0	2.7498E-1	2.4983E-1
Halogens	0.25	1.6887E-1	1.4720E-1
Alkali Metals	0.35	2.6649E-1	3.3477E-1
Te Group	0.25	9.4534E-2	5.7292E-2
Ba, Sr Group	0.1	5.2318E-4	8.4958E-3
Ru Group	0.0025	5.340E-12	2.294E-11
Mo Group	0.0025	1.595E-09	1.272E-11
Lanthanides	0.005	3.4900E-6	5.8528E-6
Ce Group	0.005	7.9901E-6	1.8673E-4

Table 4-27. Late In-Vessel Release Fractions for SLOCA with Late Containment Failure.

	NUREG-1465	Case 1D	Case 2D
Noble Gases	0	4.2756E-2	2.9003E-2
Halogens	0.1	9.0945E-2	9.3185E-2
Alkali Metals	0.1	1.0631E-1	1.0700E-1
Te Group	0.005	9.7179E-2	9.8135E-2
Ba, Sr Group	0	1.5079E-4	1.6050E-4
Ru Group	0	4.4749E-4	4.4506E-4
Mo Group	0	4.0958E-2	4.2390E-2
Lanthanides	0	1.0629E-8	1.1192E-8
Ce Group	0	9.7490E-9	1.1078E-8

4.5 SLOCA with Failure to Realign ECCS and Early Containment Failure

The early progression of events in Cases 1E and 2E (see Table 3-1) are identical to Cases 1D and 2D, respectively. Unlike Cases 1D and 2D, the containment is assumed to fail coincidently with vessel failure. While not modeled directly in the MELCOR calculation, it is assumed that an energetic pressurization (e.g., large burn, detonation, steam spike, or direct containment heating event) causes a simultaneous failure of the containment (see Section 3.2). Hence, as shown in Table 4-28, reactor vessel and containment failure occur simultaneously.

Table 4-28. Key Event Timing for SLOCA with Early Containment Failure.

Event	Case 1E [hr]	Case 2E [hr]
SLOCA	0.0	0.0
Reactor trip	0.07	0.07
ECCS starts	0.07	0.07
Containment spray signal	0.11	0.13
FWST Empty	0.63	0.65
ECCS and containment sprays fail	0.63	0.65
RCS pumps fail on high void	0.86	0.88
Vessel swollen water level at TAF	2.7	3.0
Start of fuel cladding failures	4.0	4.1
Start of core plate failures	4.8	4.9
First hydrogen burn in containment	5.0	5.2
Containment design pressure	5.3	5.2
Debris relocation to lower head	5.7	6.0
Accumulators injection starts	6.5	6.4
Vessel failure	9.4	8.1
Accumulators empty	9.4	8.1
Containment failure	9.4	8.1
Calculation terminated[16]	157.	130.

[16] Cases 1E and 2E terminated early due to failures in the CAV at very low rates of core-concrete interaction.

After vessel failure, the containment was assumed to fail in Cases 1E and 2E. As shown in Figure 4-69, the containment pressure in Cases 1E and 2E fell to near atmospheric conditions after vessel failure (~9.4 and 8.1 hr for Cases 1E and 2E, respectively). Both the early and late failure cases show pressure spikes from hydrogen burns following vessel failure.

Similar to Cases 1B and 2B, the most significant impact was an earlier and larger release of fission products. The fission product release results are shown in Figures 4-70 through 4-78 for the nine NUREG-1465 radionuclide groups. These figures summarize the total fission product mass released to containment. Durations of each of the NUREG-1465 release phases are presented in Table 4-29. In addition, the magnitudes of release to containment for each of the NUREG-1465 radionuclide groups are tabulated in Tables 4-30 through 4-33 for all release phases. In contrast to Figures 4-70 through 4-78, the results in the tables present the releases to containment as a fraction of the initial core inventory rather than absolute mass. This enables direct comparison with NUREG-1465 results.

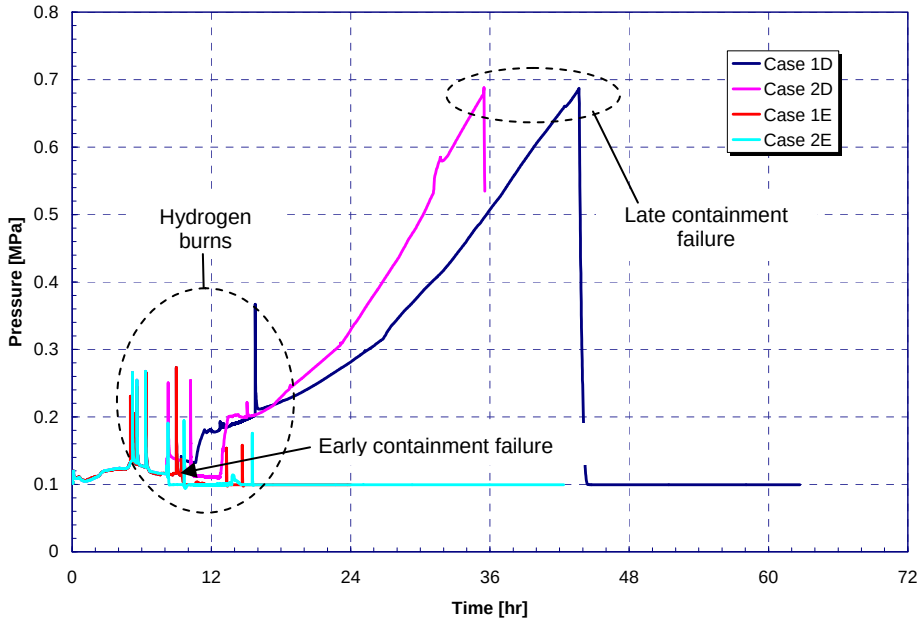

Figure 4-69. Comparison of the Containment Pressure Response for the Late and Early Containment Failure SLOCA Cases.

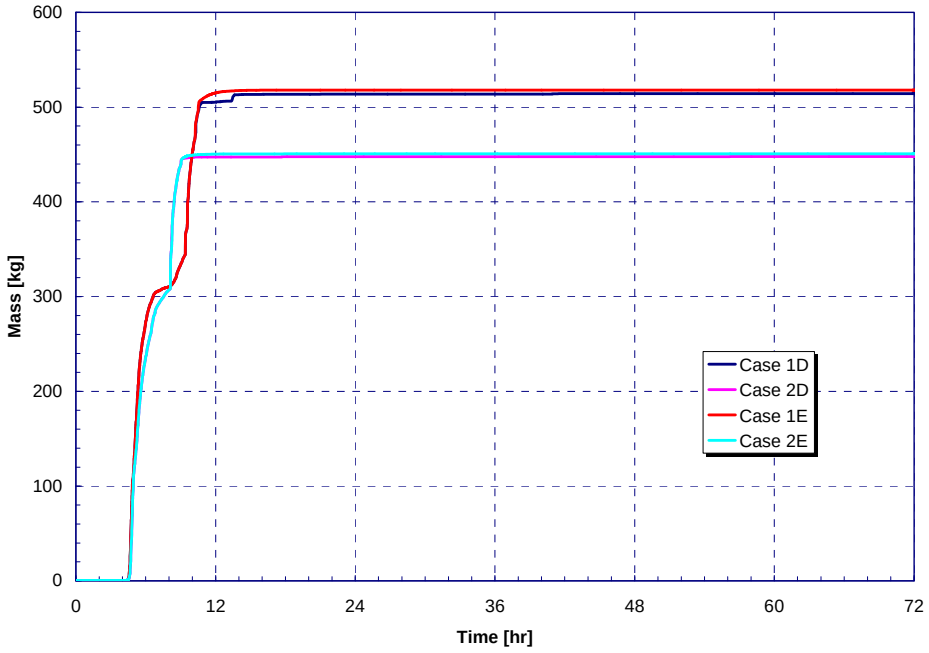

Figure 4-70. Noble Gas Release to Containment for SLOCA with Early Containment Failure.

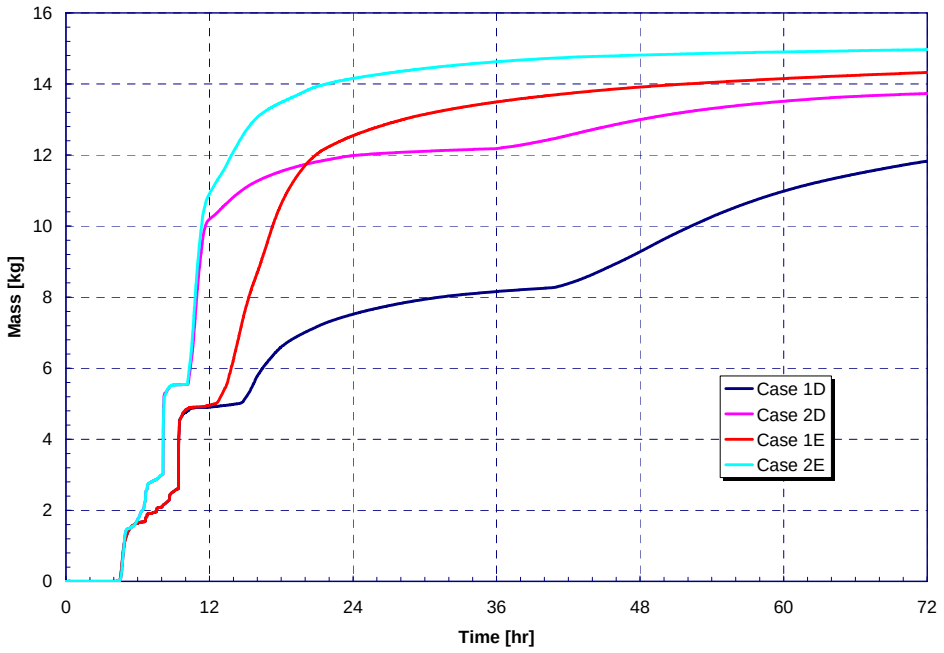

Figure 4-71. Halogen Release to Containment for SLOCA with Early Containment Failure.

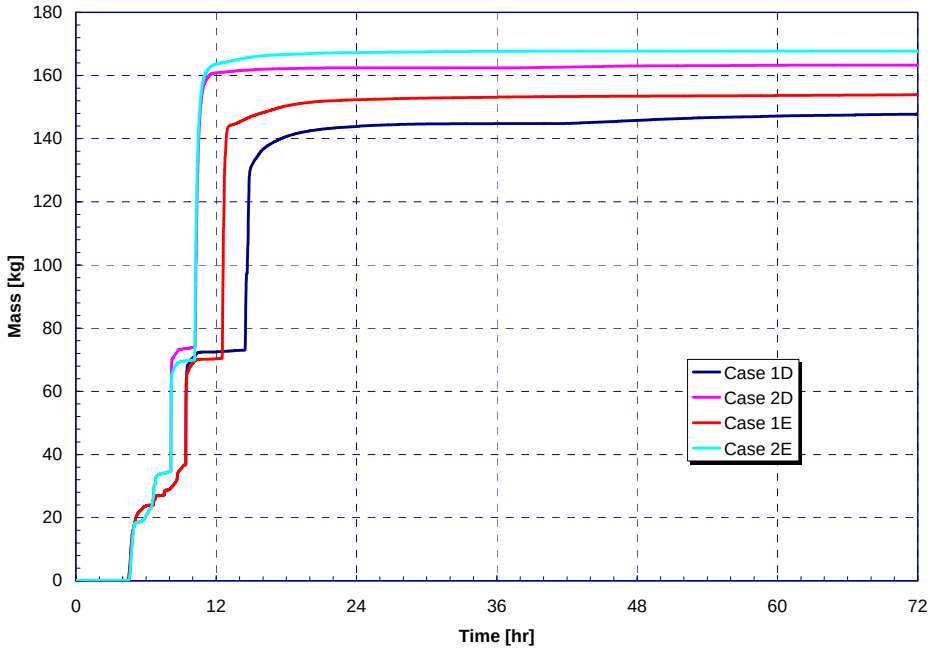

Figure 4-72. Alkali Metal Release to Containment for SLOCA with Early Containment Failure.

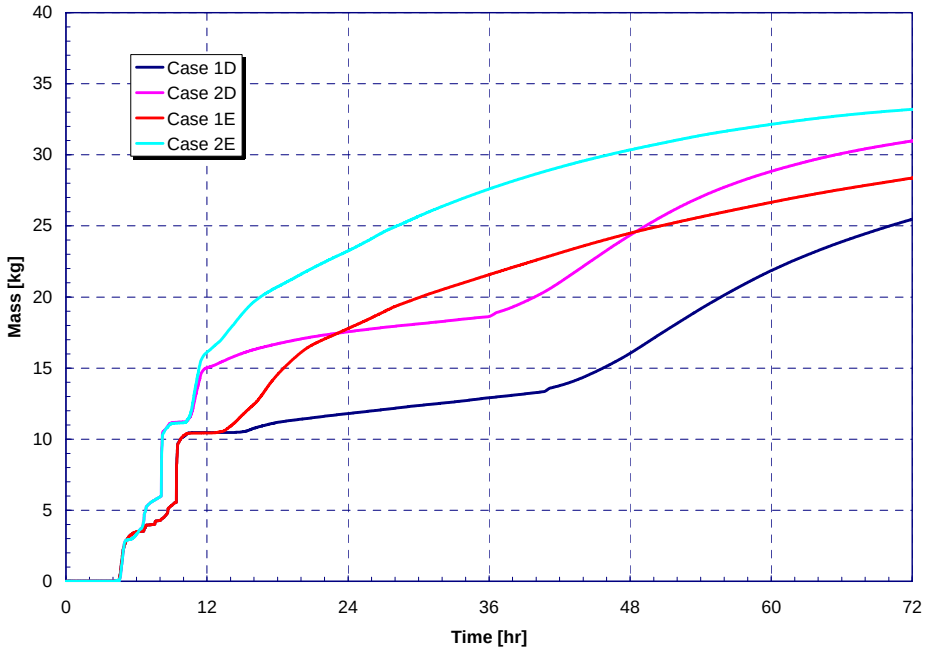

Figure 4-73. Tellurium Group Release to Containment for SLOCA with Early Containment Failure.

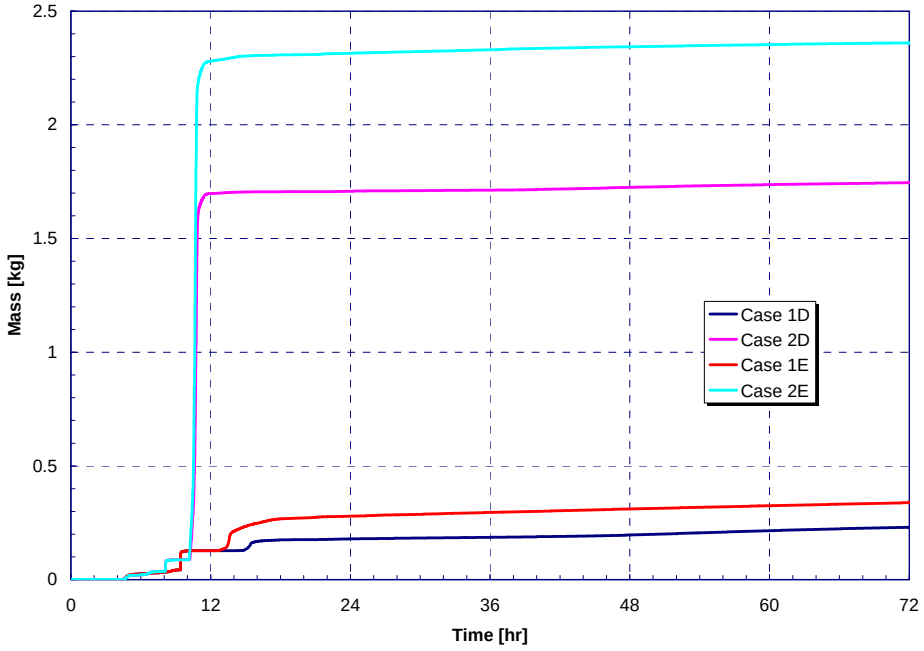

Figure 4-74. Barium, Strontium Group Release to Containment for SLOCA with Early Containment Failure.

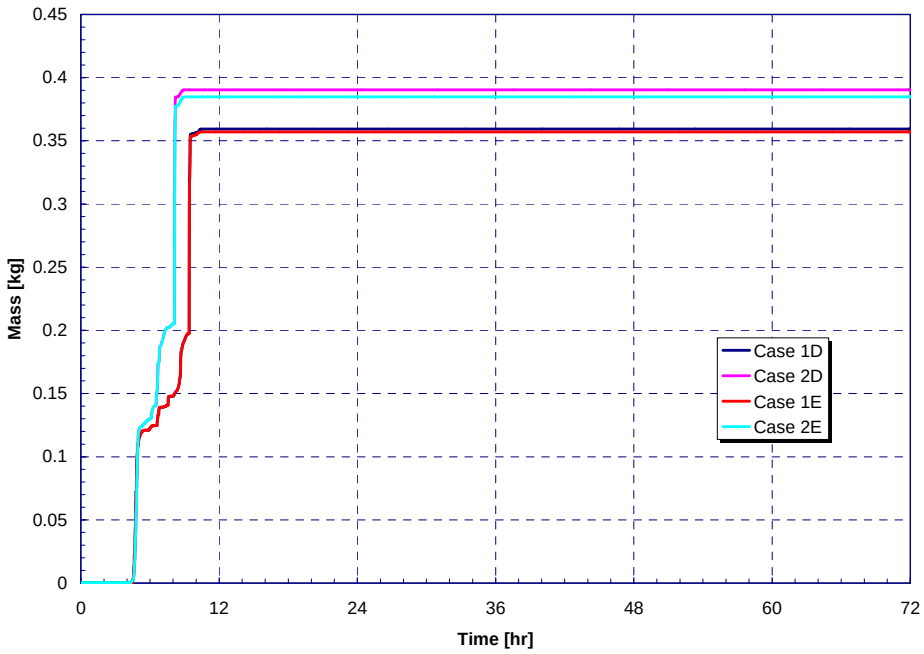

Figure 4-75. Noble Metal (Ru) Release to Containment for SLOCA with Early Containment Failure.

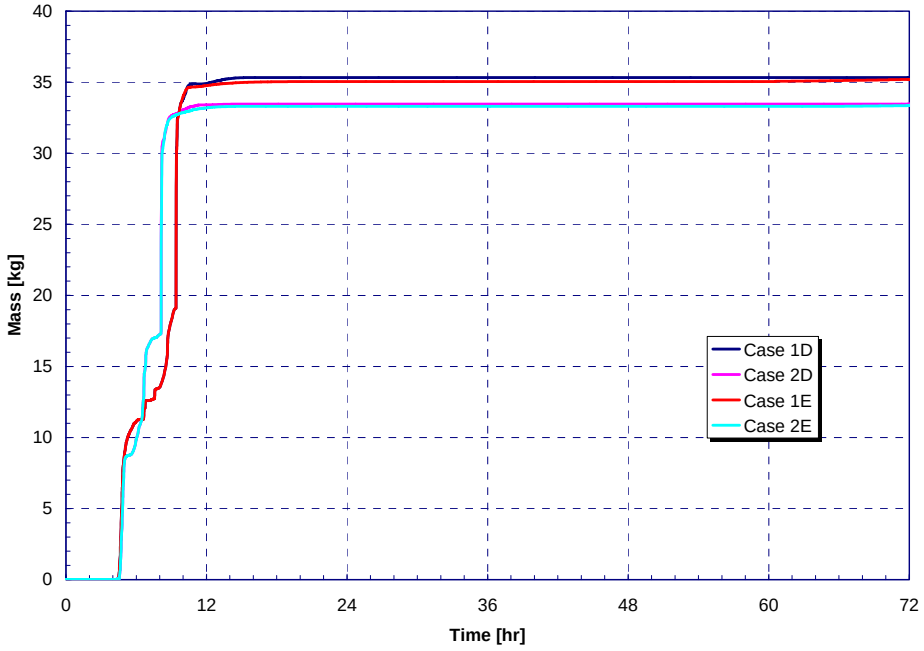

Figure 4-76. Noble Metal (Mo) Release to Containment for SLOCA with Early Containment Failure.

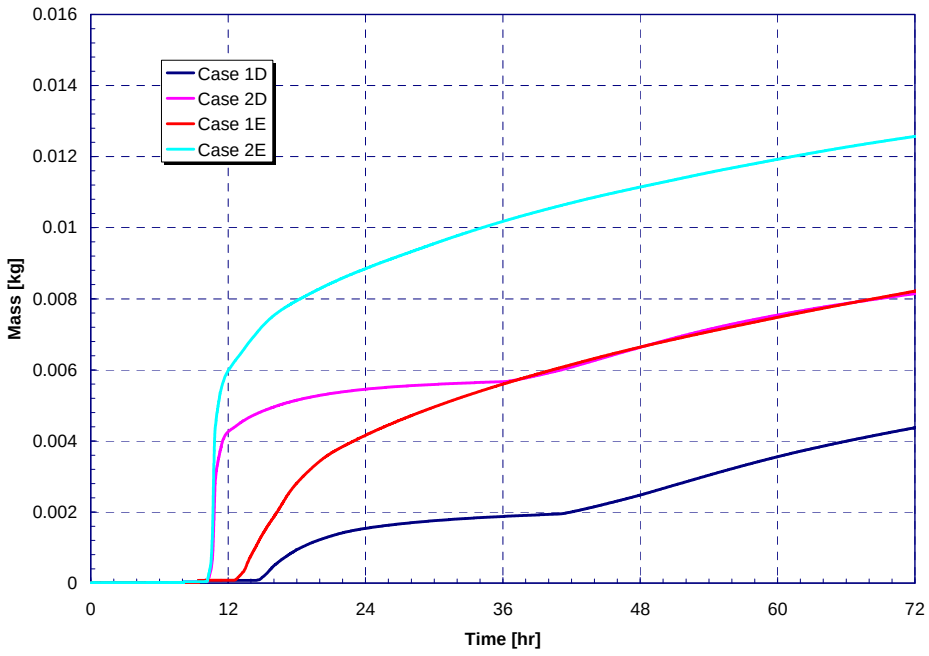

Figure 4-77. Lanthanide Release to Containment for SLOCA with Early Containment Failure.

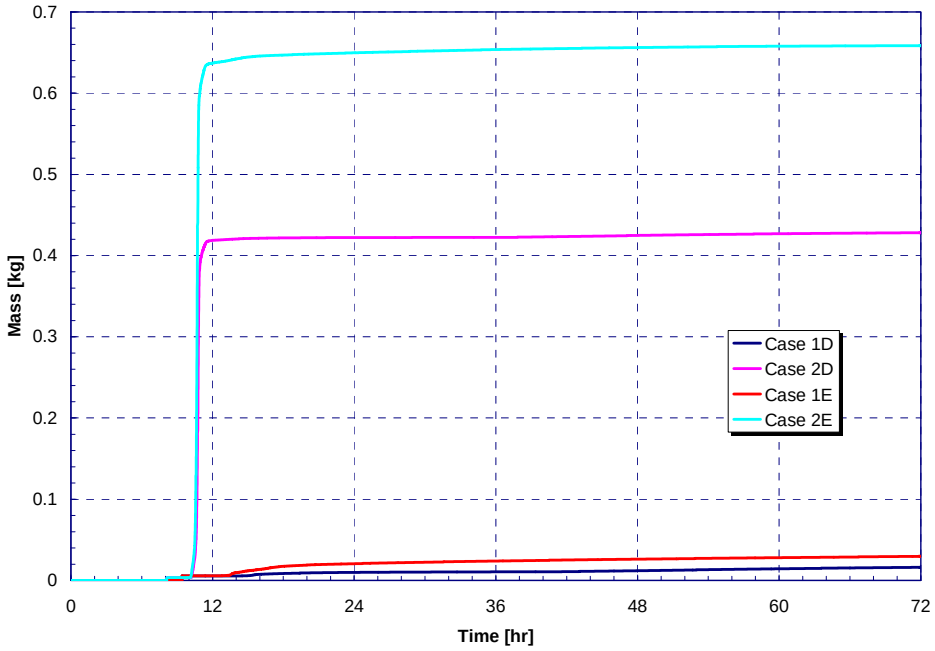

Figure 4-78. Cerium Group Release to Containment for SLOCA with Early Containment Failure.

Table 4-29. Release Timing for SLOCA with Early Containment Failure.

Timing (hr)	NUREG-1465	Case 1E	Case 2E
Onset of Release	~0	2.7	3.0
Coolant Release Duration		1.3	1.1
Gap Release Duration	0.5	0.4	0.5
In-Vessel Release Duration	1.3	5.0	3.6
Ex-Vessel Release Duration	2.0	8.2	3.3
Late I-Vessel Release Duration	10.0	0.6	0.8

Table 4-30. Gap Release Fractions for SLOCA with Early Containment Failure.

	NUREG-1465	Case 1E	Case 2E
Noble Gases	0.05	3.0108E-03	1.1906E-02
Halogens	0.05	1.5600E-03	7.7405E-03
Alkali Metals	0.05	2.1424E-03	5.0886E-03
Te Group	0	2.5722E-03	7.1874E-03

Table 4-31. In-Vessel Release Fractions for SLOCA with Early Containment Failure.

	NUREG-1465	Case 1E	Case 2E
Noble Gases	0.95	6.6191E-1	6.1998E-1
Halogens	0.35	1.0715E-1	1.1019E-1
Alkali Metals	0.25	1.2411E-1	1.1872E-1
Te Group	0.05	1.1072E-1	1.1484E-1
Ba, Sr Group	0.02	1.9545E-4	1.9474E-4
Ru Group	0.0025	5.5710E-4	5.1220E-4
Mo Group	0.0025	5.0938E-2	5.1429E-2
Lanthanides	0.0002	1.3714E-8	1.3261E-8
Ce Group	0.0005	1.3423E-8	1.4460E-8

Table 4-32. Ex-Vessel Release Fractions for SLOCA with Early Containment Failure.

	NUREG-1465	Case 1E	Case 2E
Noble Gases	0	2.8540E-1	2.5526E-1
Halogens	0.25	2.1169E-1	1.7543E-1
Alkali Metals	0.35	2.8005E-1	3.4458E-1
Te Group	0.25	7.6452E-2	8.0051E-2
Ba, Sr Group	0.1	8.3928E-4	1.1575E-2
Ru Group	0.0025	7.346E-12	4.491E-11
Mo Group	0.0025	1.956E-12	1.371E-11
Lanthanides	0.005	3.8075E-6	8.4761E-6
Ce Group	0.005	1.1357E-5	2.8605E-4

Table 4-33. Late In-Vessel Release Fractions for SLOCA with Early Containment Failure.

	NUREG-1465	Case 1E	Case 2E
Noble Gases	0	3.7589E-2	3.3786E-2
Halogens	0.1	9.1629E-2	9.5460E-2
Alkali Metals	0.1	1.0423E-1	1.0844E-1
Te Group	0.005	9.5728E-2	1.0087E-1
Ba, Sr Group	0	1.4801E-4	1.6130E-4
Ru Group	0	4.3923E-4	4.3700E-4
Mo Group	0	4.0104E-2	4.3344E-2
Lanthanides	0	1.0372E-8	1.1334E-8
Ce Group	0	9.8649E-9	1.1372E-8

4.6 Sensitivity of SLOCA Results to Break Size, Break Location, and Failure of ECCS (40% MOX Core)

Four calculations were performed to examine the sensitivity of the SLOCA source term results to potential deviations from the baseline 40% MOX Core (i.e., Case 2D) accident progression assumptions, as identified in the plant-specific PRAs. The first calculation, identified as Case 2Q in Table 3-1, examines sensitivity to break size. The baseline SLOCA case assumed a break size equivalent to a 1-in.- diameter hole in the cold leg piping; Case 2Q increased that break size to a 2-in. diameter-equivalent. The second sensitivity, Case 2R, is identical to Case 2Q except that ECCS is assumed to fail to start. That is, Case 2R represents a departure from the baseline SLOCA case in terms of break size (2 in. vs. 1 in.) and ECCS operation (failure to realign vs. failure to start). The final two sensitivity calculations examine the sensitivity of results to break location. Case 2U assumes a break in the hot leg with failure to start ECCS; all other assumptions are identical to the baseline case (Case 2D). Case 2V is identical to the baseline case, except that the break is assumed to occur in the hot leg.

The timing of key events for the four SLOCA sensitivity cases is provided in Table 4-34.

Table 4-34. Key Event Timing for SLOCA Sensitivities.

Event	Case 2Q [hr]	Case 2R [hr]	Case 2U [hr]	Case 2V [hr]
Small LOCA	0.0	0.0	0.0	0.0
Reactor trip	0.02	0.02	0.07	0.08
ECCS starts	0.02	n/a	n/a	0.09
Containment spray signal	0.02	0.02	0.37	0.14
FWST Empty	0.50	0.57	0.92	0.65
ECCS fails	0.50	0.02	0.07	0.65
Containment sprays fail	0.50	0.57	0.92	0.65
RCS pumps fail on high void	0.51	0.07	0.30	0.88
Vessel swollen water level at TAF	0.92	0.47	2.2	2.9
Start of fuel cladding failures	1.4	0.84	3.4	4.4
Accumulators injection starts	1.5	1.0	5.9	7.0
First hydrogen burn in containment	1.7	1.1	4.3	5.2
Containment design pressure	2.1	1.4	4.6	5.5
Start of core support plate failures	2.4	1.4	4.2	5.2
Debris relocation to lower head	3.3	2.7	5.0	6.6
Accumulators empty	4.7	5.6	9.4	12.9
Vessel failure	6.2	5.8	10.1	12.8
Containment failure	29.1	31.3	37.1	36.2
Calculation terminated[17]	168.	130.	145.	168.

[17] Cases 2R and 2U terminated early due to failures in the CAV at very low rates of core-concrete interaction.

Key accident signatures for the four SLOCA sensitivities are compared to the baseline SLOCA case in Figures 4-79 through 4-83. As one would expect, early accident progression is faster in the cases with the larger assumed break size. Figure 4-79 shows the more rapid depressurization of Cases 2Q and 2R, both of which assume a 2-in. break. The corresponding accelerated drop in core water level for these cases is shown in Figure 4-80. These same figures show a slightly slower accident progression for the cases with a hot leg break (Cases 2U and 2V) after the core is uncovered. This is because the coolant loss from the RCS after core uncovery is entirely steam due to the break elevation, whereas the cold leg breaks continue to model a "liquid drain" during the time period during accumulator injection and ECCS operation. This slows the progression of the hot leg break accidents (relative to equivalent cold leg break accidents) until after vessel failure. Except for these timing effects, the accident progressions for the four sensitivity cases are quite similar to the baseline case.

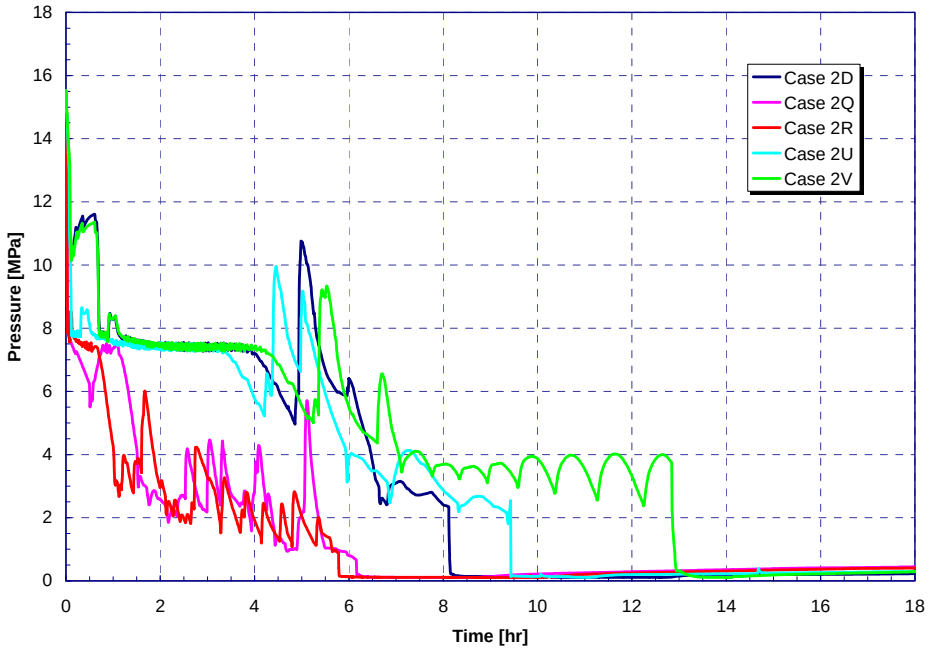

Figure 4-79. RCS Pressure for SLOCA Sensitivities.

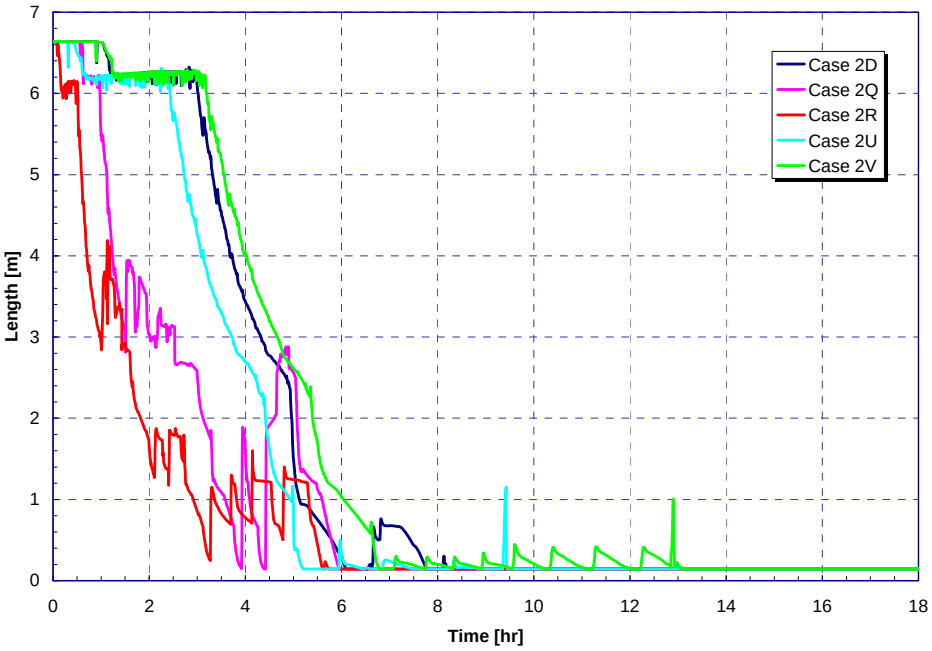

Figure 4-80. Vessel Swollen Water Level for SLOCA Sensitivities.

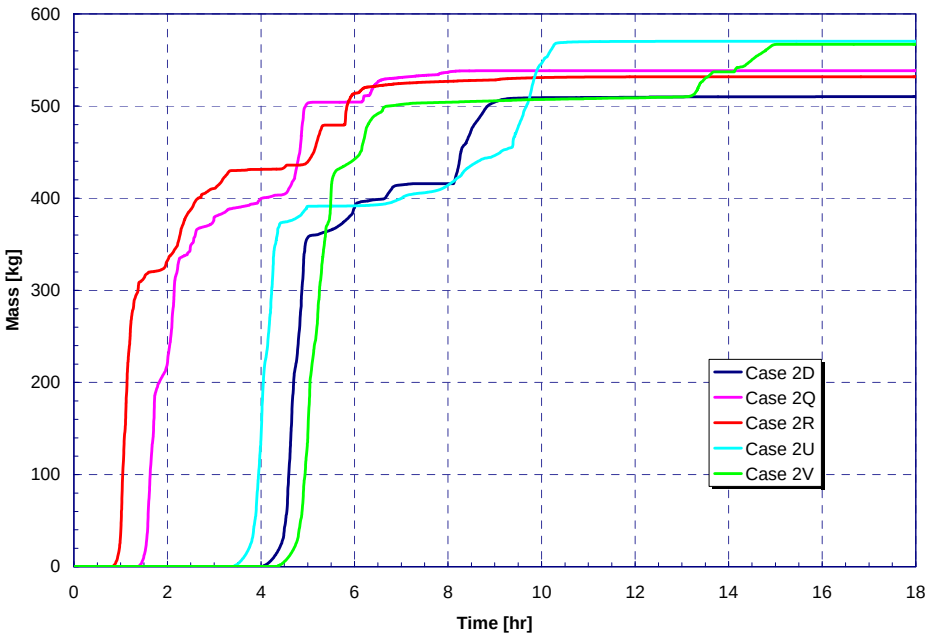

Figure 4-81. In-Vessel Hydrogen Production for SLOCA Sensitivities.

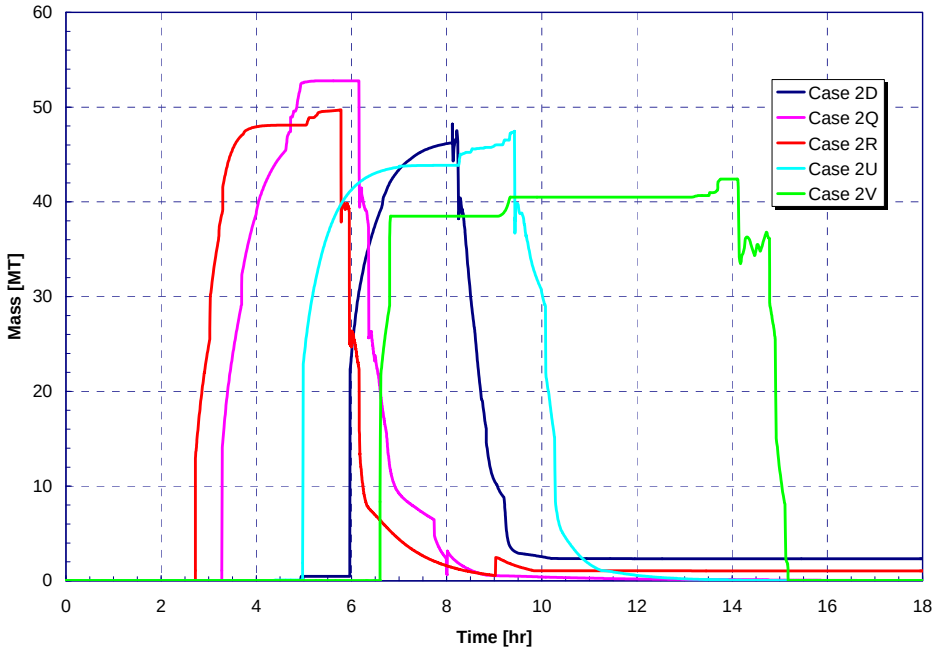

Figure 4-82. Uranium Dioxide Mass on the Vessel Lower Head for SLOCA Sensitivities.

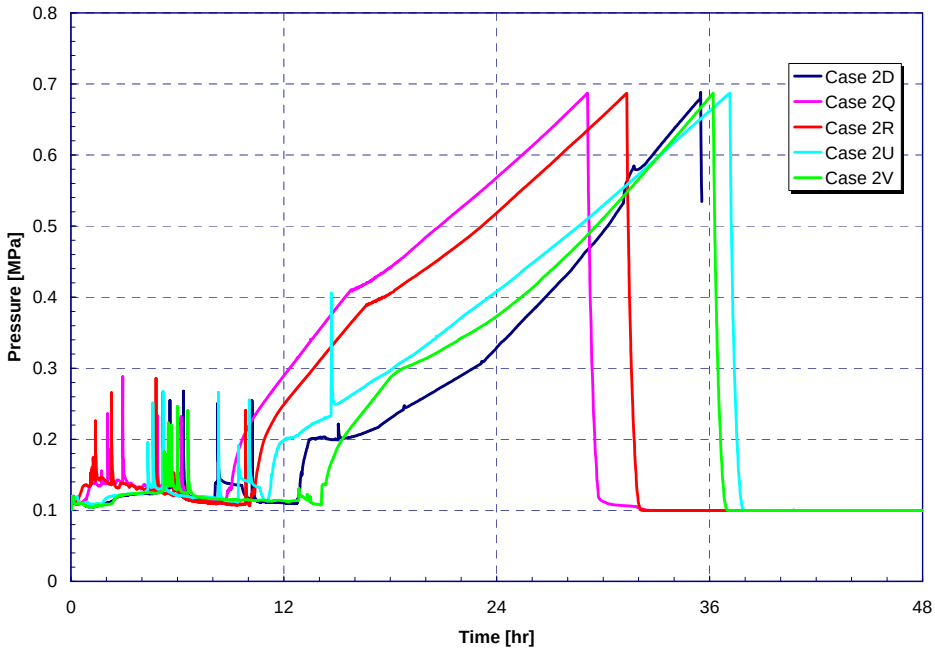

Figure 4-83. Containment Pressure Response for SLOCA Sensitivities.

The fission product release results for the SLOCA sensitivity cases are compared to the 40% MOX SLOCA baseline case in Figures 4-84 through 4-92. These figures summarize the total fission product mass released to containment. Durations of each of the NUREG-1465 release phases are presented in Table 4-35. In addition, the magnitudes of release to containment for each of the NUREG-1465 radionuclide groups are tabulated Tables 4-36 through 4-39 for all release phases. In contrast to Figures 4-84 through 4-92, the results in the tables present the releases to containment as a fraction of the initial core inventory rather than absolute mass. This enables direct comparison with NUREG-1465 results. In addition, the tabulated values present only the results for the four sensitivity cases (2Q, 2R, 2U, and 2V); the tabulated results for the baseline case (2D) were included in Section 4.4.

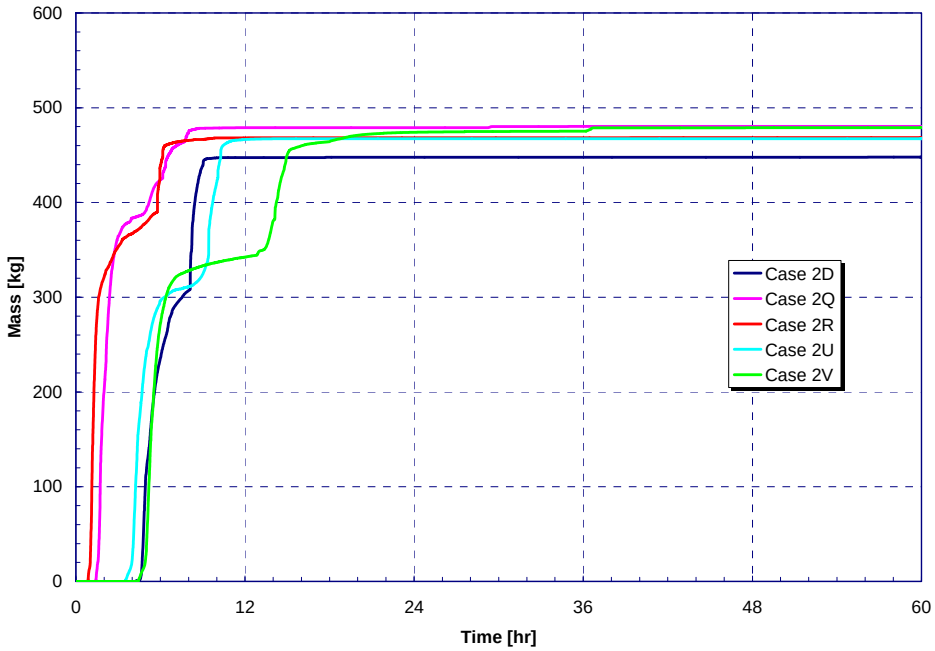

Figure 4-84. Noble Gas Release to Containment for SLOCA Sensitivities.

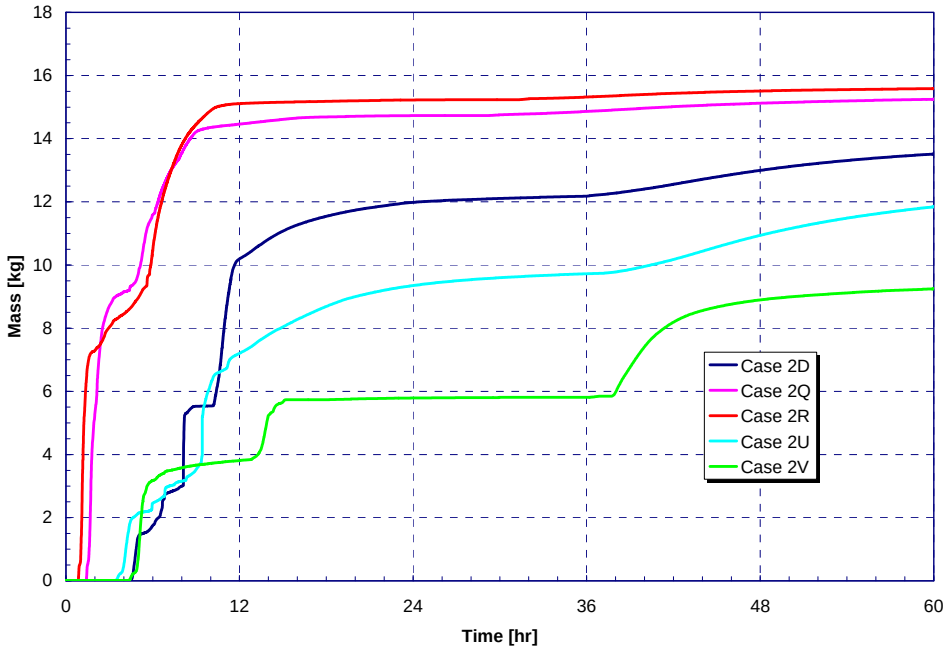

Figure 4-85. Halogen Release to Containment for SLOCA Sensitivities.

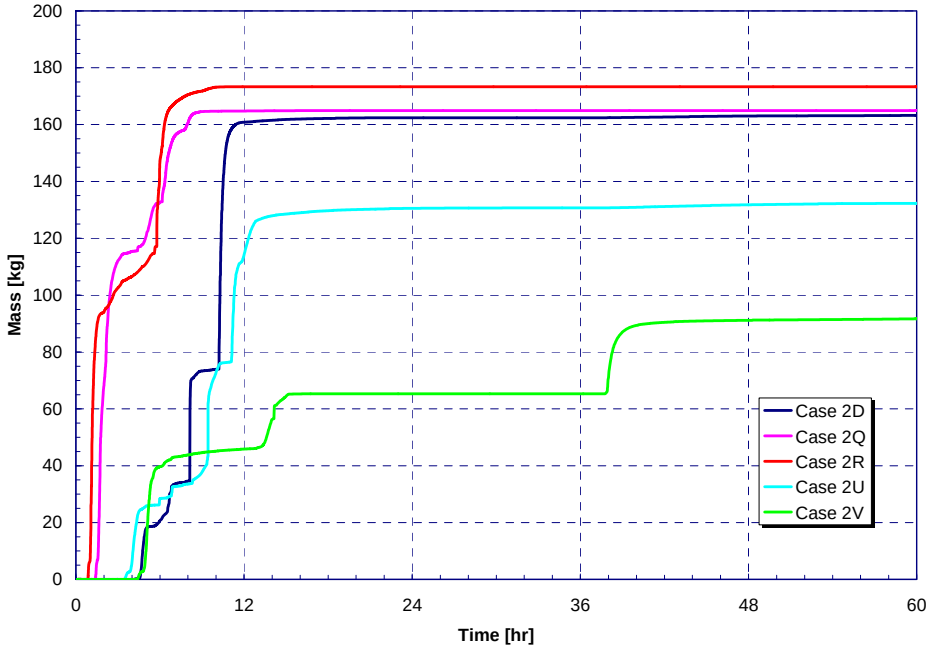

Figure 4-86. Alkali Metal Release to Containment for SLOCA Sensitivities.

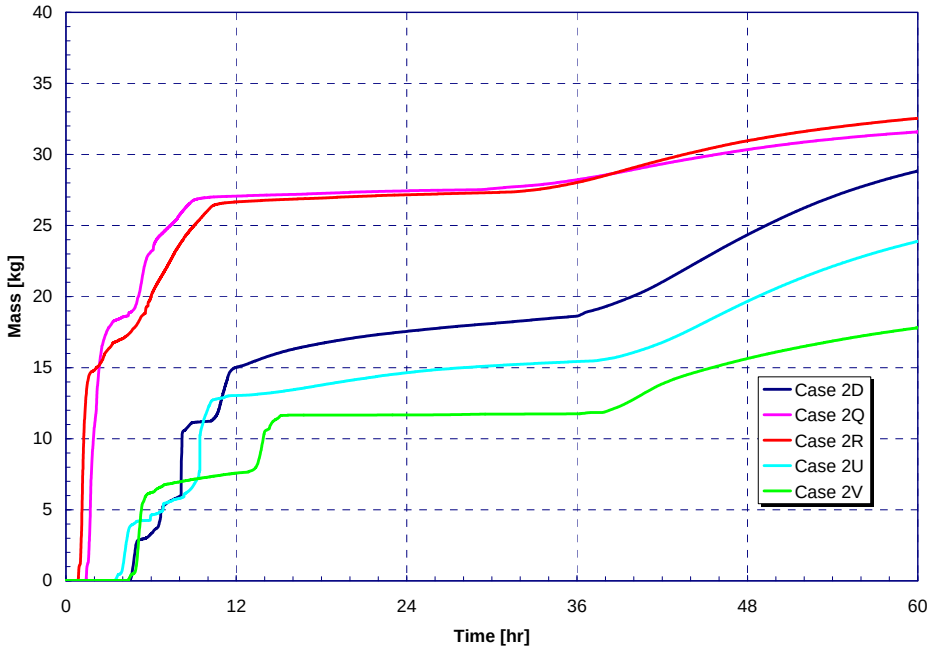

Figure 4-87. Tellurium Group Release to Containment for SLOCA Sensitivities.

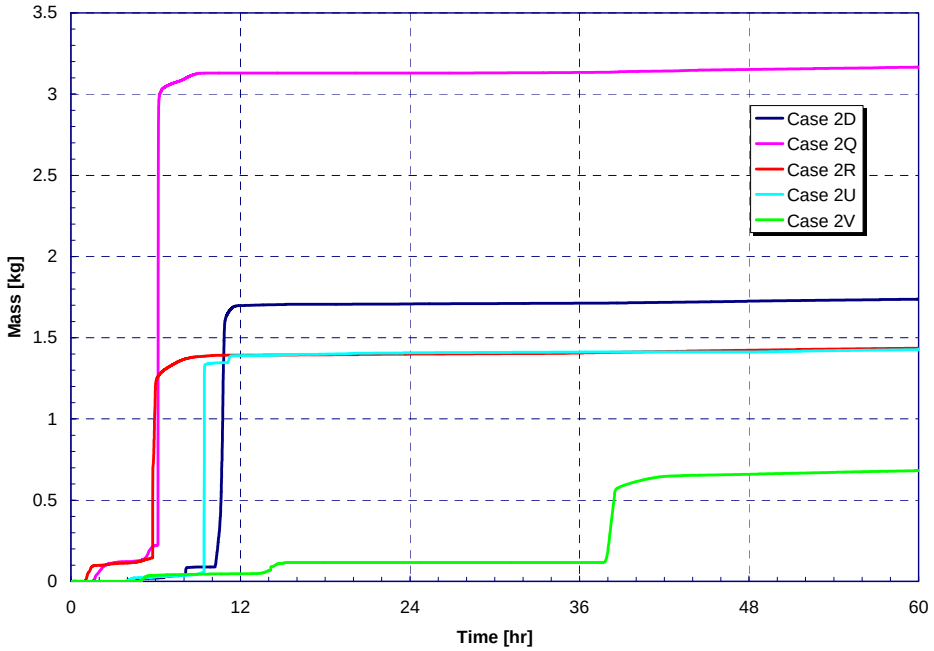

Figure 4-88. Barium, Strontium Group Release to Containment for SLOCA Sensitivities.

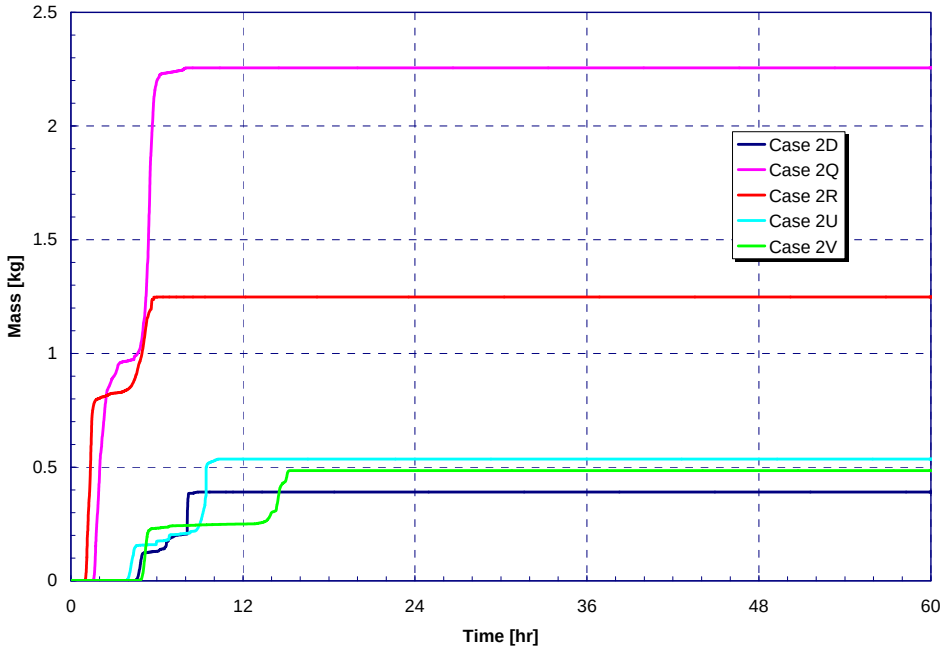

Figure 4-89. Noble Metal (Ru) Release to Containment for SLOCA Sensitivities.

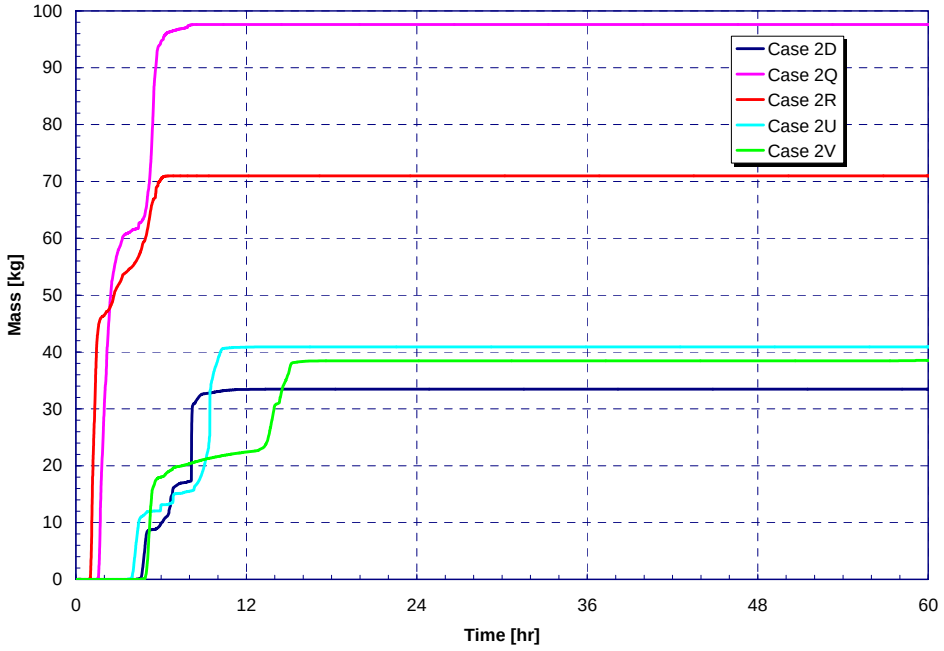

Figure 4-90. Noble Metal (Mo) Release to Containment for SLOCA Sensitivities.

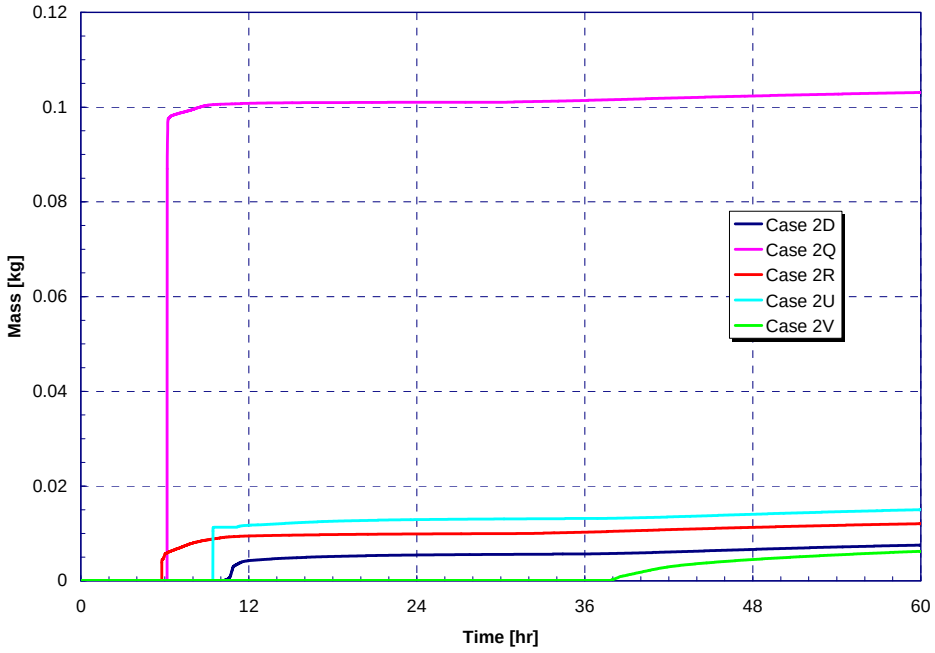

Figure 4-91. Lanthanide Release to Containment for SLOCA Sensitivities.

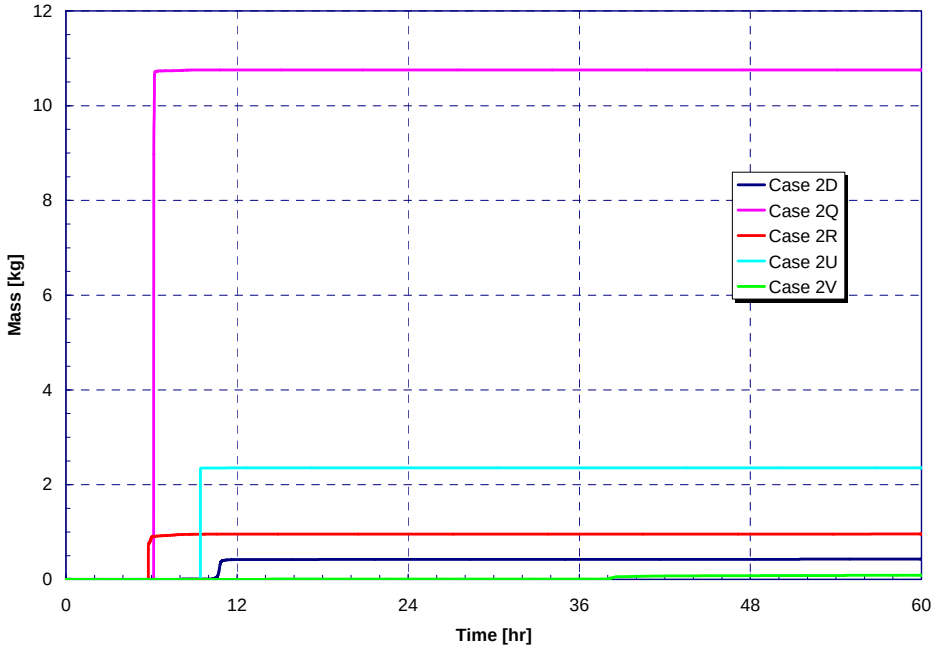

Figure 4-92. Cerium Group Release to Containment for SLOCA Sensitivities.

Table 4-35. Release Timing for SLOCA Sensitivities.

Timing (hr)	NUREG-1465	Case 2Q	Case 2R	Case 2U	Case 2V
Onset of Release	~0	0.9	0.5	2.2	2.9
Coolant Release Duration		0.5	0.4	1.2	1.5
Gap Release Duration	0.5	0.2	0.2	0.4	0.4
In-Vessel Release Duration	1.3	4.6	4.8	5.6	8.0
Ex-Vessel Release Duration	2.0	2.5	2.7	30.8	28.4
Late I-Vessel Release Duration	10.0	1.7	0.5	0.9	2.2

Table 4-36. Gap Release Fractions for SLOCA Sensitivities.

	NUREG-1465	Case 2Q	Case 2R	Case 2U	Case 2V
Noble Gases	0.05	4.3848E-02	3.5545E-02	2.4898E-02	2.9068E-02
Halogens	0.05	2.6063E-02	2.3237E-02	9.7983E-03	1.0541E-02
Alkali Metals	0.05	2.6577E-02	2.3695E-02	9.5572E-03	1.0102E-02
Te Group	0	2.6860E-02	2.4147E-02	9.8600E-03	1.0459E-02

Table 4-37. In-Vessel Release Fractions for SLOCA Sensitivities.

	NUREG-1465	Case 2Q	Case 2R	Case 2U	Case 2V
Noble Gases	0.95	8.2786E-1	7.6335E-1	6.8103E-1	6.7621E-1
Halogens	0.35	4.2203E-1	3.4978E-1	1.4278E-1	1.3720E-1
Alkali Metals	0.25	4.4794E-1	3.9499E-1	1.4509E-1	1.5434E-1
Te Group	0.05	4.3919E-1	3.6268E-1	1.4538E-1	1.4259E-1
Ba, Sr Group	0.02	1.1795E-3	7.6309E-4	3.0967E-4	2.4965E-4
Ru Group	0.0025	5.4022E-3	3.0210E-3	9.1564E-4	6.1181E-4
Mo Group	0.0025	2.7150E-1	2.6039E-1	7.2307E-2	6.4731E-2
Lanthanides	0.0002	1.0282E-7	9.1480E-8	2.2213E-8	1.7057E-8
Ce Group	0.0005	1.0107E-7	9.0351E-8	2.2399E-8	1.8235E-8

Table 4-38. Ex-Vessel Release Fractions for SLOCA Sensitivities.

	NUREG-1465	Case 2Q	Case 2R	Case 2U	Case 2V
Noble Gases	0	7.7519E-2	1.4700E-1	1.6768E-1	7.4805E-2
Halogens	0.25	7.8335E-2	1.5946E-1	9.8149E-2	8.2146E-2
Alkali Metals	0.35	1.0467E-1	1.8614E-1	2.1314E-1	1.0539E-1
Te Group	0.25	4.9765E-2	8.7671E-2	6.1113E-2	3.2462E-2
Ba, Sr Group	0.1	1.5292E-2	6.4849E-3	6.9389E-3	2.8657E-3
Ru Group	0.0025	1.500E-08	2.173E-10	1.913E-10	1.032E-11
Mo Group	0.0025	1.138E-09	3.526E-11	8.826E-10	2.056E-12
Lanthanides	0.005	1.5647E-4	1.2962E-5	2.0903E-5	3.9464E-6
Ce Group	0.005	4.8688E-3	4.2929E-4	1.0655E-3	3.1470E-5

Table 4-39. Late In-Vessel Release Fractions for SLOCA Sensitivities.

	NUREG-1465	Case 2Q	Case 2R	Case 2U	Case 2V
Noble Gases	0	2.5188E-2	8.2806E-3	8.1782E-2	1.4826E-1
Halogens	0.1	1.3140E-2	1.0065E-2	9.4771E-2	6.9535E-2
Alkali Metals	0.1	7.2946E-3	6.6355E-3	9.5955E-2	5.0561E-2
Te Group	0.005	1.3026E-2	8.6732E-3	9.6342E-2	7.7814E-2
Ba, Sr Group	0	1.4597E-5	7.7494E-6	1.4892E-4	2.2080E-4
Ru Group	0	9.1238E-5	2.3595E-5	3.9031E-4	5.0293E-4
Mo Group	0	6.5833E-3	4.6954E-3	4.3422E-2	4.1193E-2
Lanthanides	0	1.0609E-9	8.877E-10	8.2922E-9	1.7388E-8
Ce Group	0	1.5174E-8	7.2978E-9	3.4469E-9	1.6141E-8

4.7 LLOCA with ECCS Failure and Late Containment Failure

This section presents results for LLOCAs with failure of the ECCS; a MELCOR calculation was performed for both an LEU and 40% MOX core (Cases 1G and 2G, respectively). This accident sequence begins as a complete guillotine break of the RCS cold leg recirculation piping. The passive accumulators discharge into the RCS to initially cool the core. However, all other RCS safety injection systems are assumed to fail. As described in the plant-specific PRAs, the containment sprays are assumed to work until water is drained from the FWST; realignment of containment sprays to recirculation mode is assumed to occur, and the sprays operate for another 2 hr. Key events for the two LLOCA cases are summarized in Table 4-40.

Table 4-40. Key Event Timing for LLOCA.

Event	Case 1G [hr]	Case 2G [hr]
DEGB in Cold Leg Pipe (LLOCA)	0.0	0.0
Reactor trip	~0	~0
ECCS fails to start	~0	~0
Containment spray signal	~0	~0
Vessel swollen water level at TAF	~0	~0
RCS pumps fail on high void	0.001	0.001
Containment design pressure	0.001	0.001
Accumulators injection starts	0.002	0.002
Accumulators empty	0.013	0.013
Start of fuel cladding failures	0.14	0.13
FWST Empty	0.56	0.56
First support plate failure	0.57	0.57
Debris relocation to lower head	0.80	0.77
Containment sprays fail	2.6	2.6
Vessel failure	2.6	2.7
First hydrogen burn in containment	2.6	0.65
Containment failure	53.9	44.3
Calculation terminated[18]	103.	168.

[18] Case 1G terminated early due to failures in the CAV at very low rates of core-concrete interaction.

Figures 4-93 through 4-98 show comparisons of the calculated responses for the two LLOCAs. The short-term and long-term RCS pressure responses are shown in Figures 4-93 and 4-94, respectively. Upon the start of the LLOCA, the RCS pressure drops to containment pressure extremely rapidly. The reactor trips on a high containment pressure signal almost instantly. It is assumed that the RCS pumps fail on high void conditions at 1.9 seconds. The accumulators begin to discharge by 7.8 seconds and finish discharging by 45 seconds. Other than the accumulator water, there was no water injection into the RCS. Consequently, the vessel water level dropped quickly (Figure 4-95) and the fuel heatups began at 0.04 to 0.05 hr (Figure 4-96), respectively. By approximately 8 minutes, the fuel had heated to >1173 K and gap fission product releases began. Zirconium-steam reactions ensue, which creates hydrogen (Figure 4-97).

In response to the RCS blowdown, the containment pressurizes very quickly to approximately the design pressure (see Figure 4-98). The containment sprays are successfully activated and the contents of the FWST are sprayed into the containment by approximately 0.56 hr. The containment sprays are successfully realigned to recirculation mode. The containment sprays continue to run for 2 hr. After vessel failure at 2.6 and 2.7 hr, debris from the vessel relocates into the containment cavity and starts ablating the concrete.

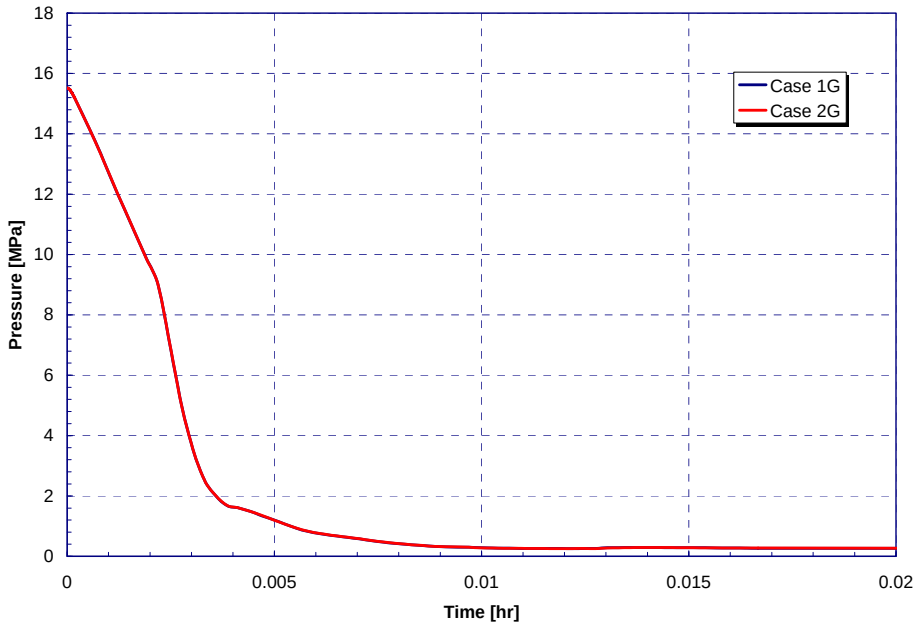

Figure 4-93. Short-Term RCS Pressure Response for LLOCA.

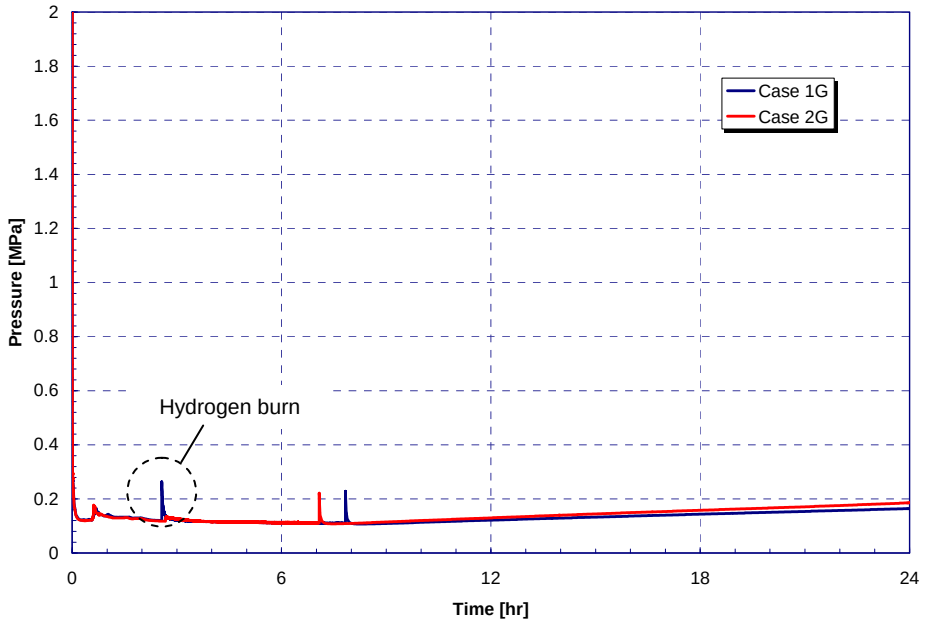

Figure 4-94. Long-Term RCS Pressure Response for LLOCA.

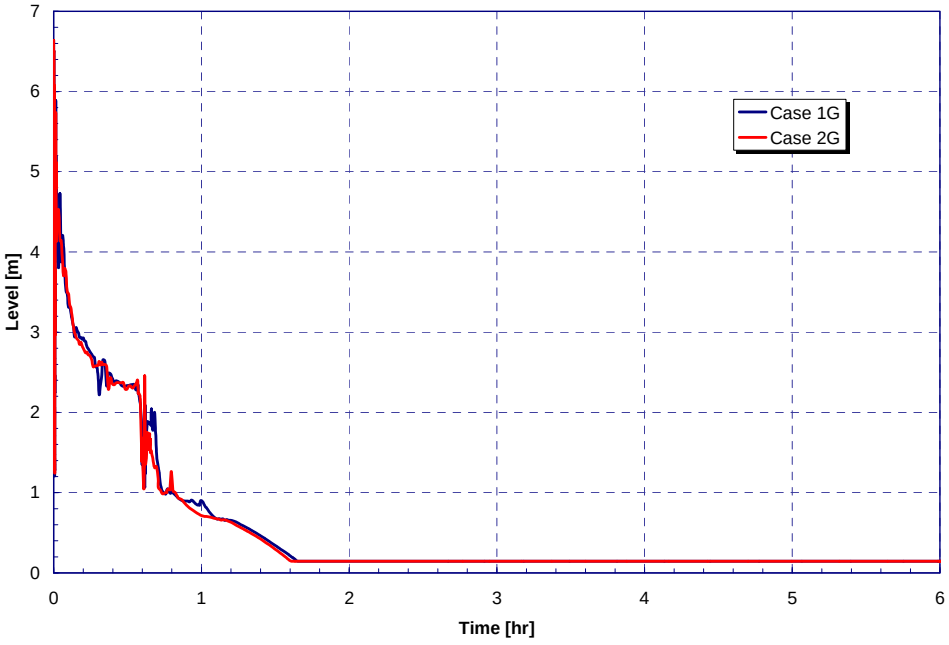

Figure 4-95. Vessel Level Response for LLOCA.

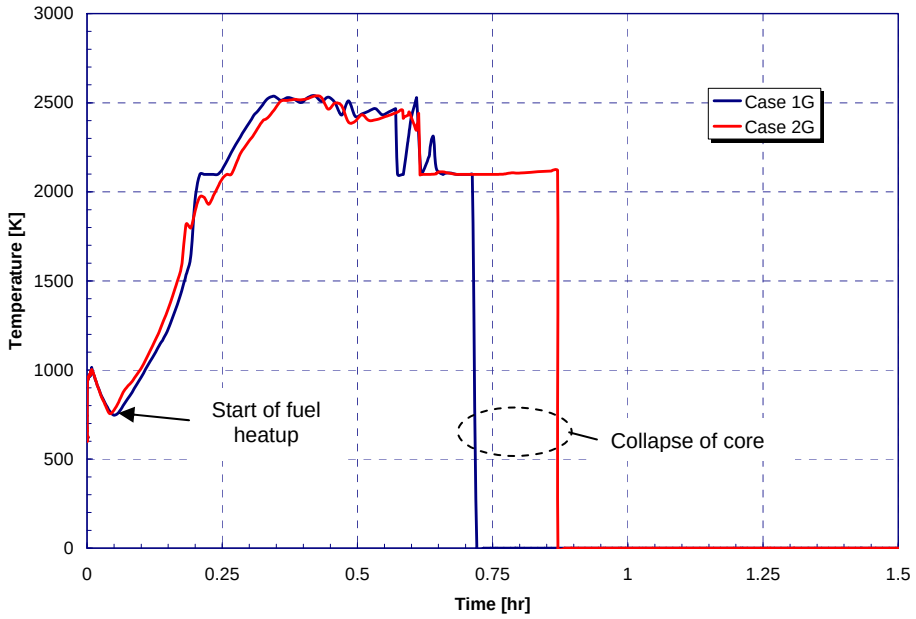

Figure 4-96. Peak Cladding Temperature Response for LLOCA.

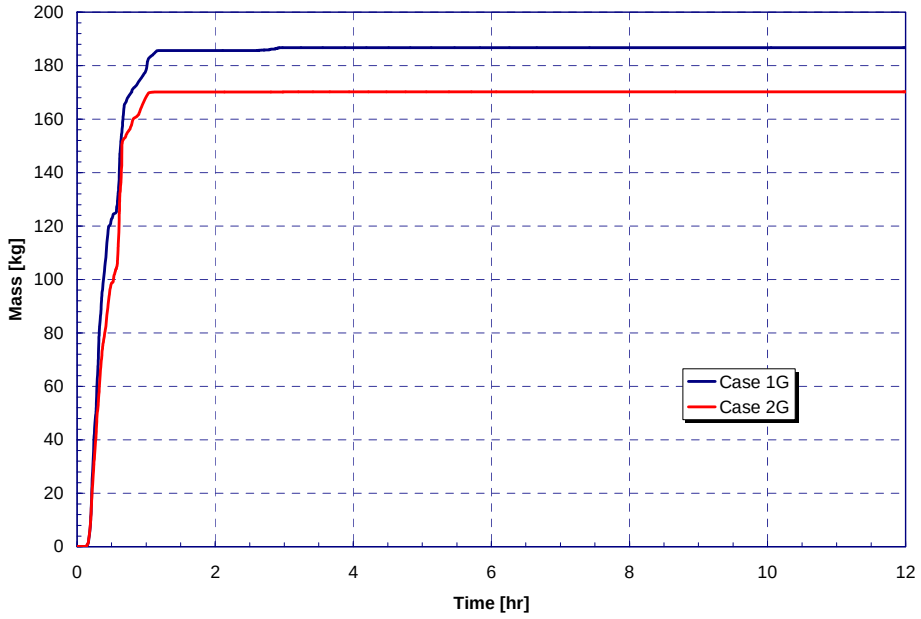

Figure 4-97. In-Vessel Hydrogen Production for LLOCA.

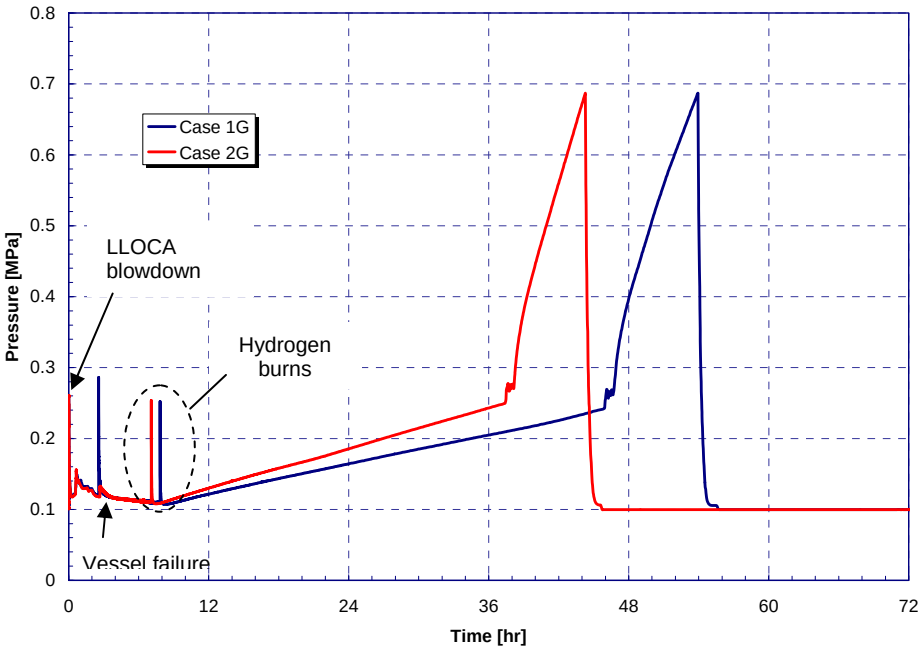

Figure 4-98. Containment Pressure Response for LLOCA.

The fission product release results are shown in Figures 4-99 through 4-107 for the nine NUREG-1465 radionuclide groups. These figures summarize the total fission product mass released to containment. Durations of each of the NUREG-1465 release phases are presented in Table 4-41. In addition, the magnitudes of release to containment for each of the NUREG-1465 radionuclide groups are tabulated in Tables 4-42 through 4-45 for all release phases. In contrast to Figures 4-99 through 4-107, the results in the tables present the releases to containment as a fraction of the initial core inventory rather than absolute mass. This enables direct comparison with NUREG-1465 results.

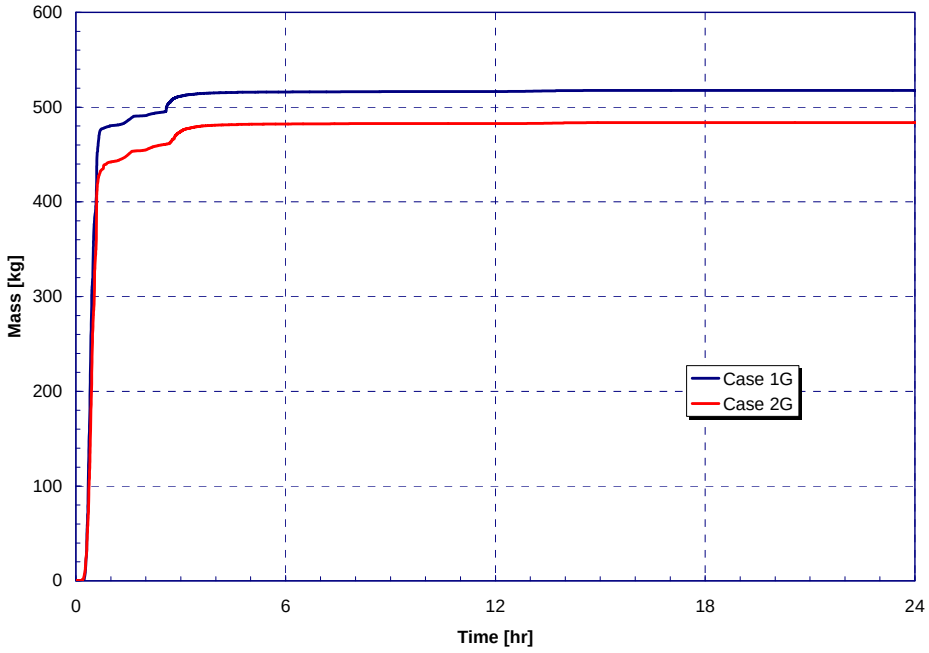

Figure 4-99. Noble Gas Release to Containment for LLOCA.

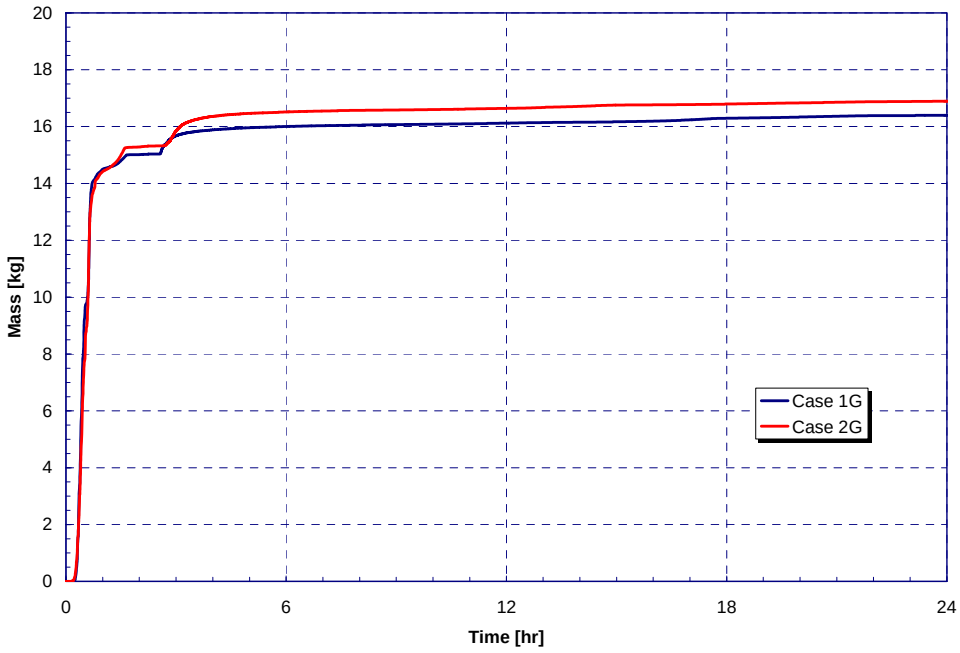

Figure 4-100. Halogen Release to Containment for LLOCA.

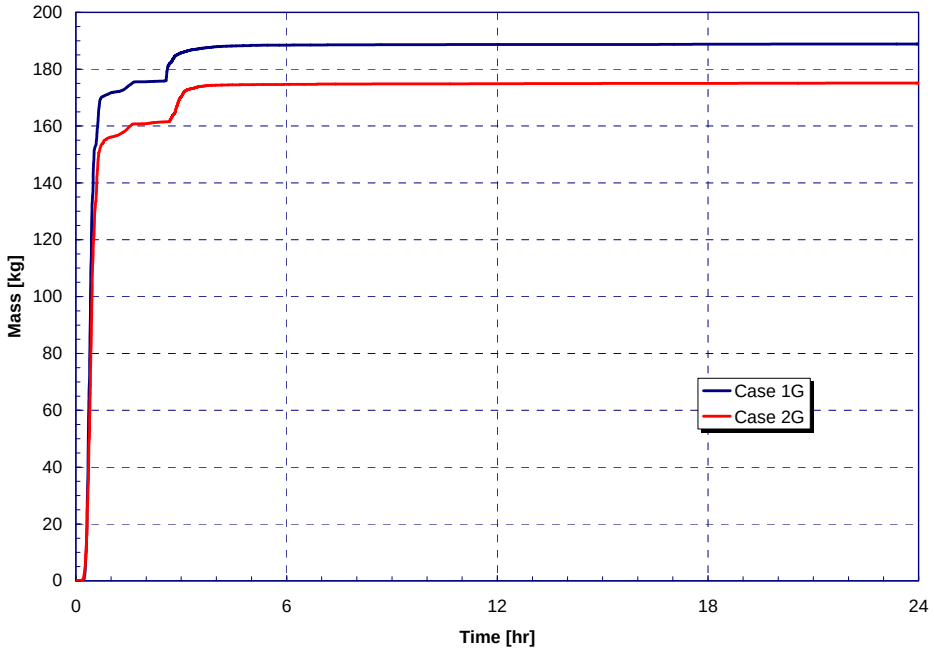

Figure 4-101. Alkali Metal Release to Containment for LLOCA.

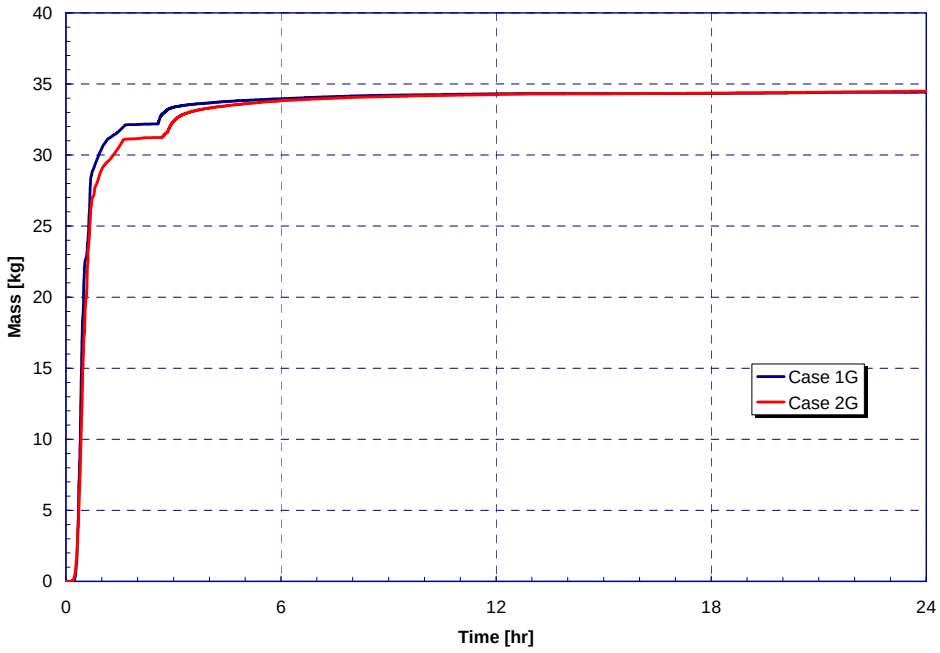

Figure 4-102. Tellurium Group Release to Containment for LLOCA.

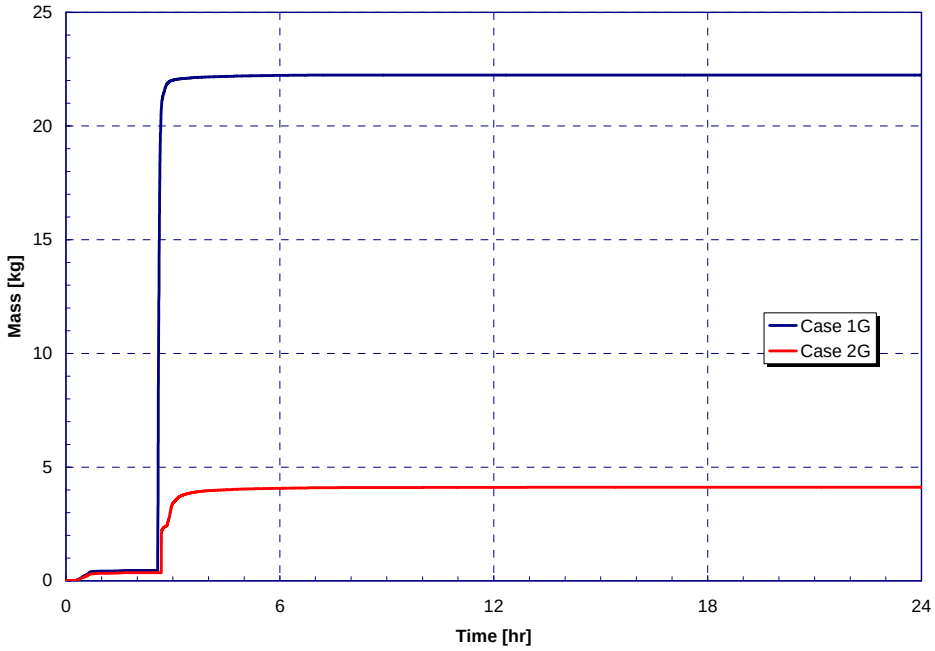

Figure 4-103. Barium, Strontium Group Release to Containment for LLOCA.

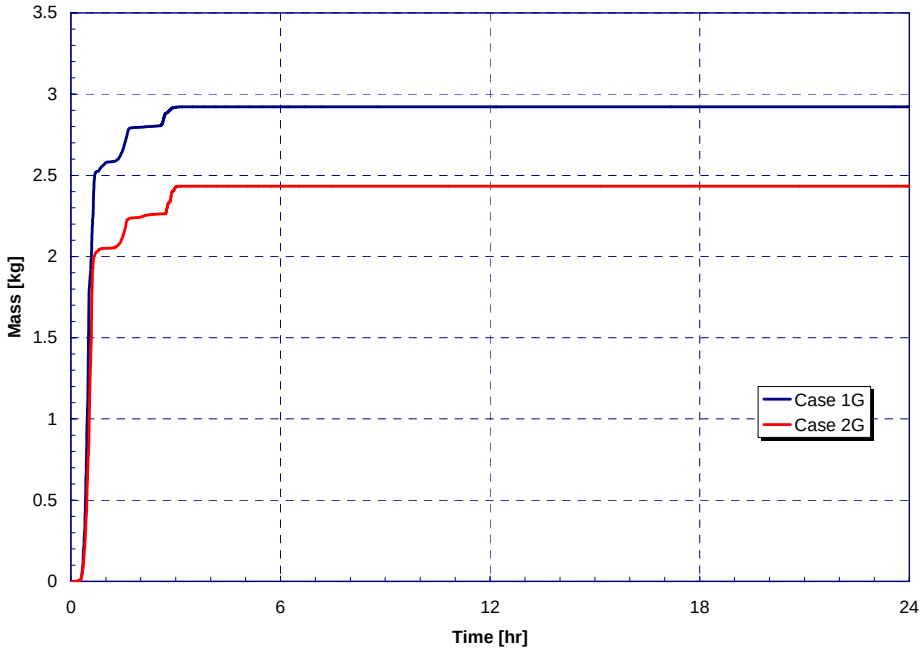

Figure 4-104. Noble Metal (Ru) Release to Containment for LLOCA.

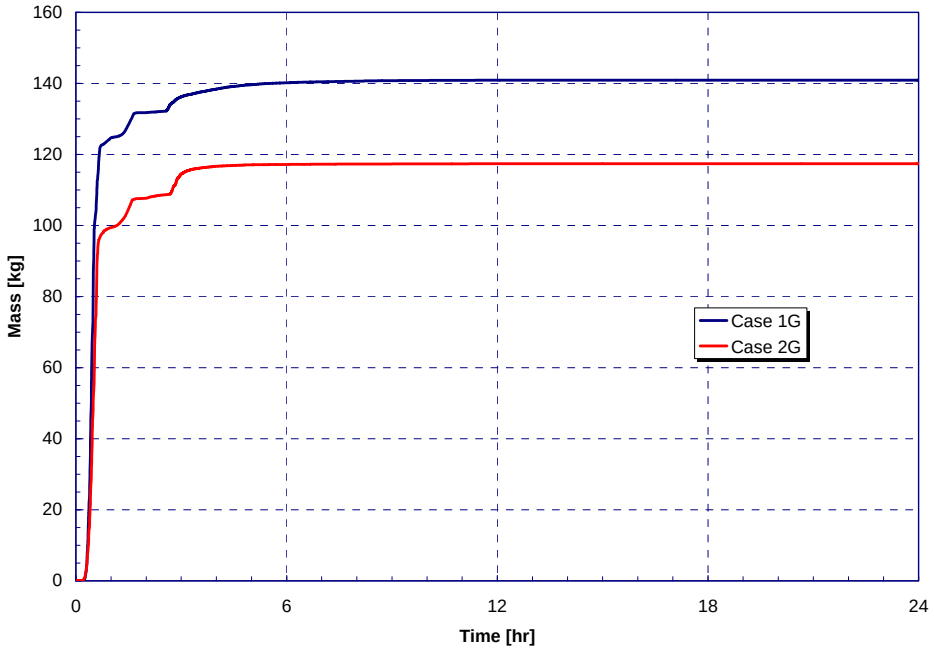

Figure 4-105. Noble Metal (Mo) Release to Containment for LLOCA.

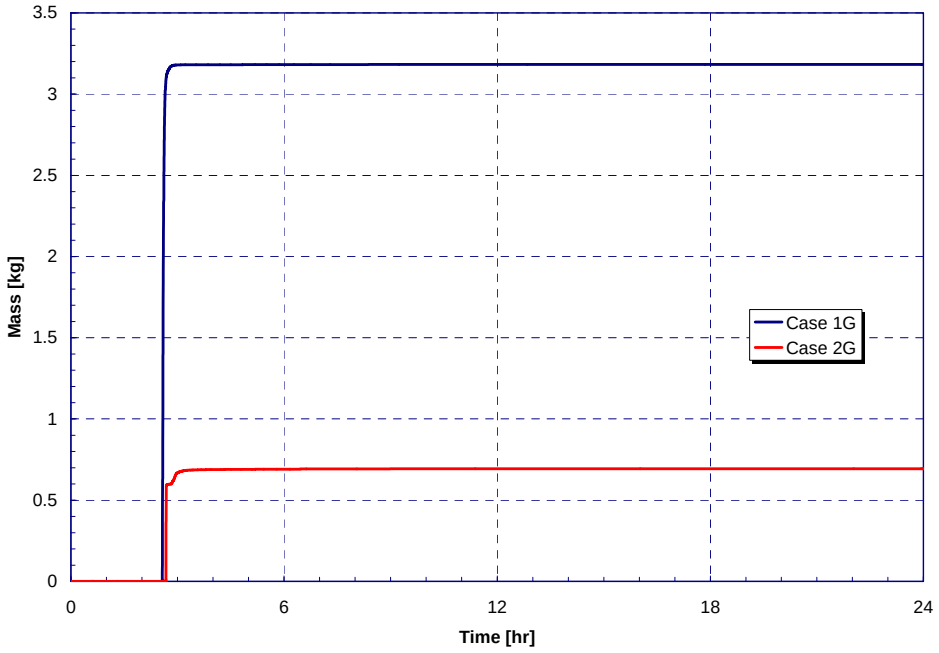

Figure 4-106. Lanthanide Release to Containment for LLOCA.

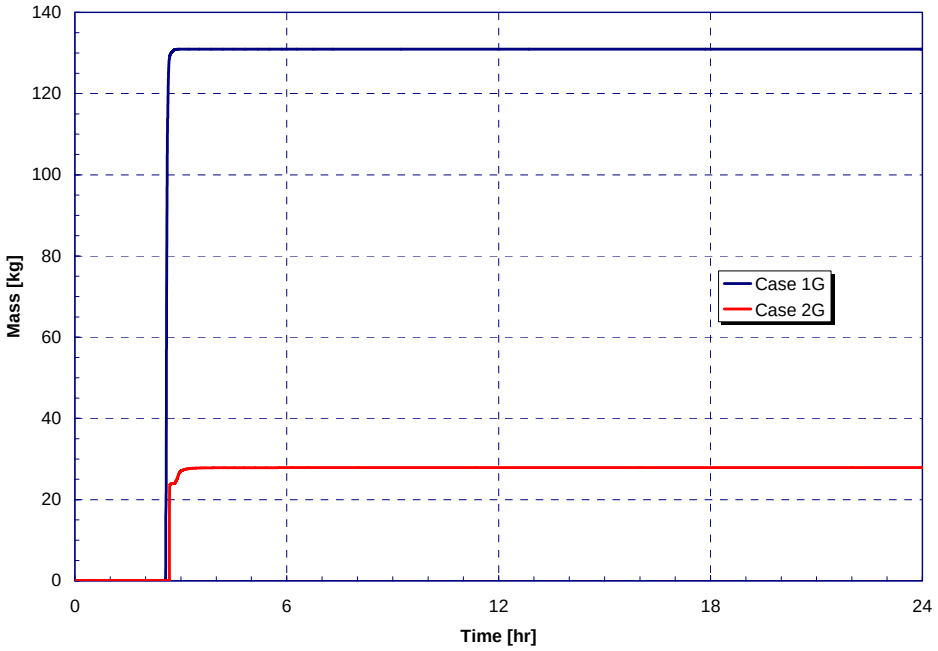

Figure 4-107. Cerium Group Release to Containment for LLOCA.

Table 4-41. Release Timing for LLOCA.

Timing (hr)	NUREG-1465	Case 1G	Case 2G
Onset of Release	~0	0.0	0.0
Coolant Release Duration		0.1	0.1
Gap Release Duration	0.5	0.1	0.1
In-Vessel Release Duration	1.3	2.3	2.4
Ex-Vessel Release Duration	2.0	1.1	0.9
Late I-Vessel Release Duration	10.0	75.8	61.1

Table 4-42. Gap Release Fractions for LLOCA.

	NUREG-1465	Case 1G	Case 2G
Noble Gases	0.05	3.5282E-02	4.6502E-02
Halogens	0.05	1.8911E-02	2.9917E-02
Alkali Metals	0.05	2.7612E-02	3.6063E-02
Te Group	0	2.7164E-02	3.5974E-02

Table 4-43. In-Vessel Release Fractions for LLOCA.

	NUREG-1465	Case 1G	Case 2G
Noble Gases	0.95	9.2099E-1	9.0019E-1
Halogens	0.35	6.0942E-1	5.5966E-1
Alkali Metals	0.25	5.8091E-1	5.4316E-1
Te Group	0.05	6.3073E-1	5.8887E-1
Ba, Sr Group	0.02	2.0909E-3	1.8947E-3
Ru Group	0.0025	7.7994E-3	5.6098E-3
Mo Group	0.0025	3.5389E-1	3.1143E-1
Lanthanides	0.0002	1.3143E-7	1.0608E-7
Ce Group	0.0005	1.2752E-7	9.4894E-8

Table 4-44. Ex-Vessel Release Fractions for LLOCA.

	NUREG-1465	Case 1G	Case 2G
Noble Gases	0	1.9684E-2	1.5317E-2
Halogens	0.25	3.0608E-2	2.9165E-2
Alkali Metals	0.35	3.0370E-2	3.4734E-2
Te Group	0.25	2.3244E-2	2.8194E-2
Ba, Sr Group	0.1	9.9397E-2	1.8544E-2
Ru Group	0.0025	1.0660E-6	2.8049E-7
Mo Group	0.0025	8.3703E-8	2.1540E-8
Lanthanides	0.005	4.5600E-3	1.0735E-3
Ce Group	0.005	8.8182E-2	1.2578E-2

Table 4-45. Late In-Vessel Release Fractions for LLOCA.

	NUREG-1465	Case 1G	Case 2G
Noble Gases	0	2.3919E-2	3.1879E-2
Halogens	0.1	2.9717E-2	3.4603E-2
Alkali Metals	0.1	1.4353E-2	1.4501E-2
Te Group	0.005	2.9408E-2	3.2874E-2
Ba, Sr Group	0	1.273E-14	2.6696E-5
Ru Group	0	3.2136E-4	4.1638E-4
Mo Group	0	2.3611E-2	2.5638E-2
Lanthanides	0	7.143E-14	1.560E-14
Ce Group	0	6.712E-14	2.847E-18

4.8 Sensitivity of LLOCA Results to Break Size and Break Location

Four calculations were performed to examine the sensitivity of the LLOCA source term results to potential deviations from the baseline 40% MOX Core (i.e., Case 2G) accident progression assumptions. In particular, the effect of limiting break size such that the break was in the transitional break size range (i.e., 6-in. to 10-in. diameter-equivalent MLOCAs) was examined. The first calculation, identified as Case 2I in Table 3-1, assumes a 6-in. diameter-equivalent break, whereas the baseline DEGB was approximately 28-in. diameter-equivalent. The second sensitivity, Case 2J, is identical to Case 2I except that the break is assumed to occur in the hot leg. The final two sensitivity calculations assume a slightly larger transitional break, with Cases 2K and 2L examining 10-in. diameter-equivalent breaks in the cold leg and hot leg, respectively.

The timing of key events for the four MLOCA sensitivity cases is provided in Table 4-46.

Table 4-46. Key Event Timing for LLOCA Sensitivities (MLOCAs).

Event	Case 2I [hr]	Case 2J [hr]	Case 2K [hr]	Case 2L [hr]
MLOCA	0.0	0.0	0.0	0.0
Containment spray signal	0.002	0.002	0.001	0.001
ECCS fails to start	0.002	0.002	0.001	0.001
Reactor trip	0.002	0.002	0.001	0.001
RCS pumps fail on high void	0.015	0.020	0.004	0.006
Vessel swollen water level at TAF	0.027	0.029	0.015	0.016
Accumulators injection starts	0.094	0.10	0.036	0.034
Accumulators empty	0.13	0.17	0.050	0.056
FWST Empty	0.56	0.56	0.56	0.56
Containment sprays fail	0.56	0.56	0.56	0.56
Start of fuel cladding failures	0.57	0.63	0.38	0.56
First hydrogen burn in containment	0.79	0.86	3.4	1.0
First core support plate failure	1.2	1.3	0.91	1.1
Debris relocation to lower head	1.4	1.6	1.4	1.6
Vessel failure	3.0	2.7	3.4	3.9
Containment design pressure	6.9	6.6	8.0	3.9
Containment failure	51.7	39.2	49.2	44.7
Calculation terminated[19]	168.	168.	141.	168.

Key accident signatures for the four LLOCA sensitivities are compared to the baseline LLOCA case in Figures 4-108 through 4-112. As with the SLOCA sensitivities, early accident progression is faster in the cases with the larger assumed break size. Figure 4-108 shows the more rapid depressurization of Cases 2G in the first 30 minutes, with less rapid pressure drop from the 10-in. diameter-equivalent cases (2K and 2L) and even slower pressure drops for the 6-in.- diameter cases (2I and 2J). The corresponding delays in the dropping core water level for these cases are shown in Figure 4-109. The most significant difference between the different cases is the amount of cladding oxidation that occurs before fuel rod failure and collapse; this is

[19] Case 2K terminated early due to failures in the CAV at very low rates of core-concrete interaction.

evident in the in-vessel hydrogen production signature (Figure 4-110). Except for the oxidation and timing effects, the accident progressions for the four sensitivity cases are quite similar to the baseline case.

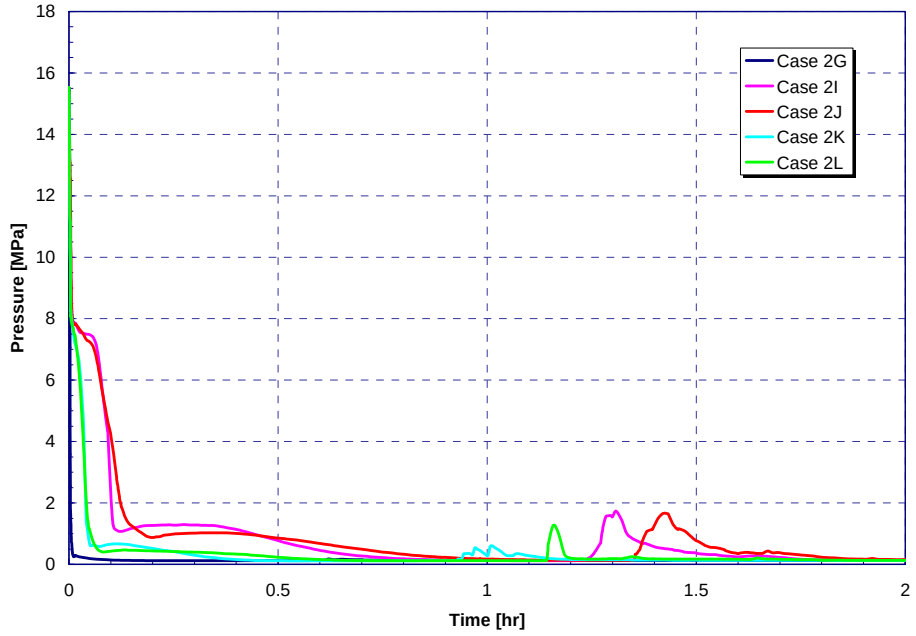

Figure 4-108. RCS Pressure for LLOCA Sensitivities (MLOCA).

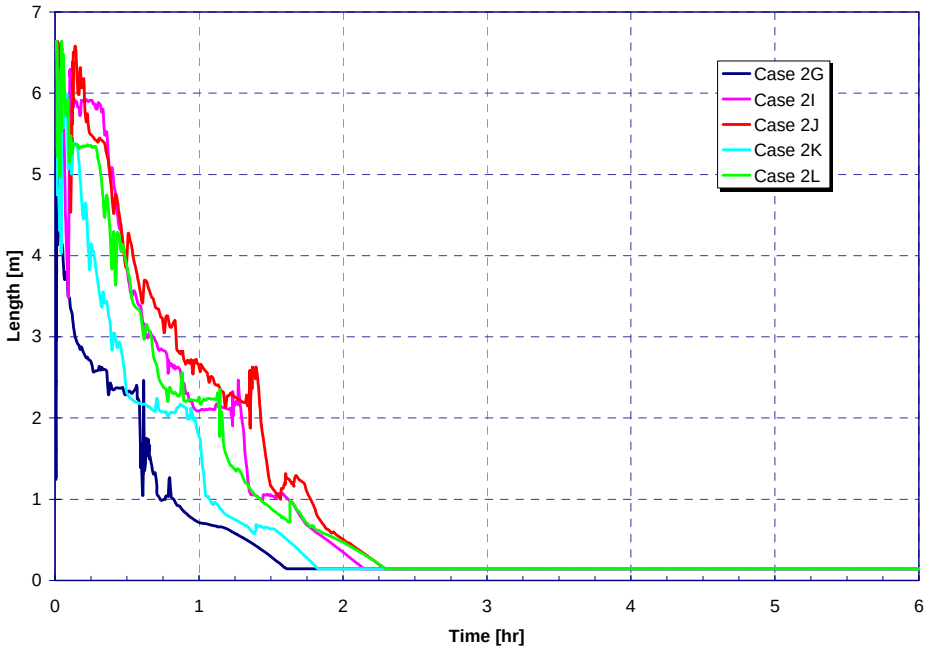

Figure 4-109. Vessel Swollen Water Level for LLOCA Sensitivities (MLOCA).

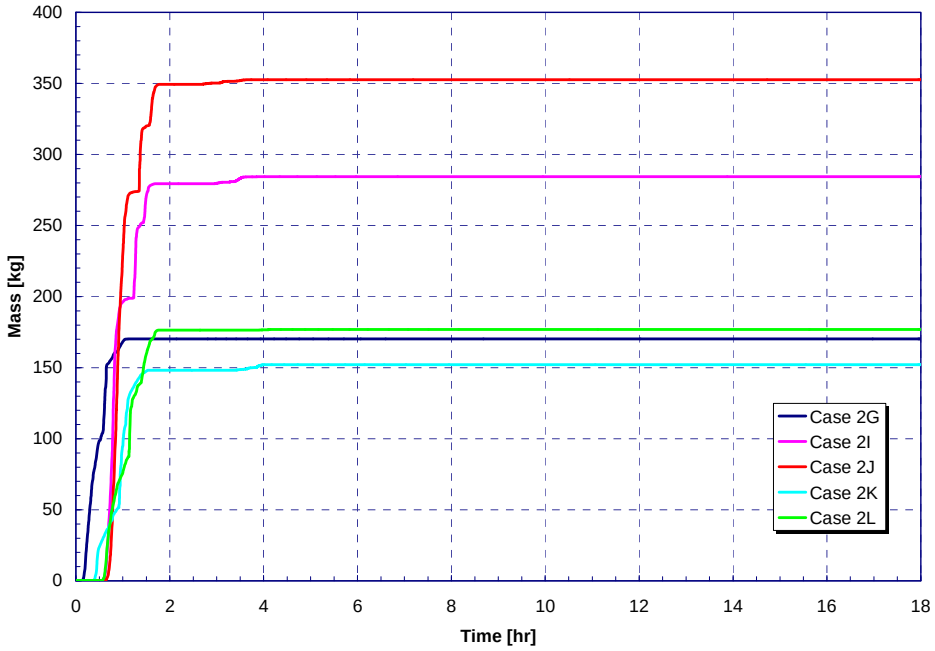

Figure 4-110. In-Vessel Hydrogen Production for LLOCA Sensitivities (MLOCA).

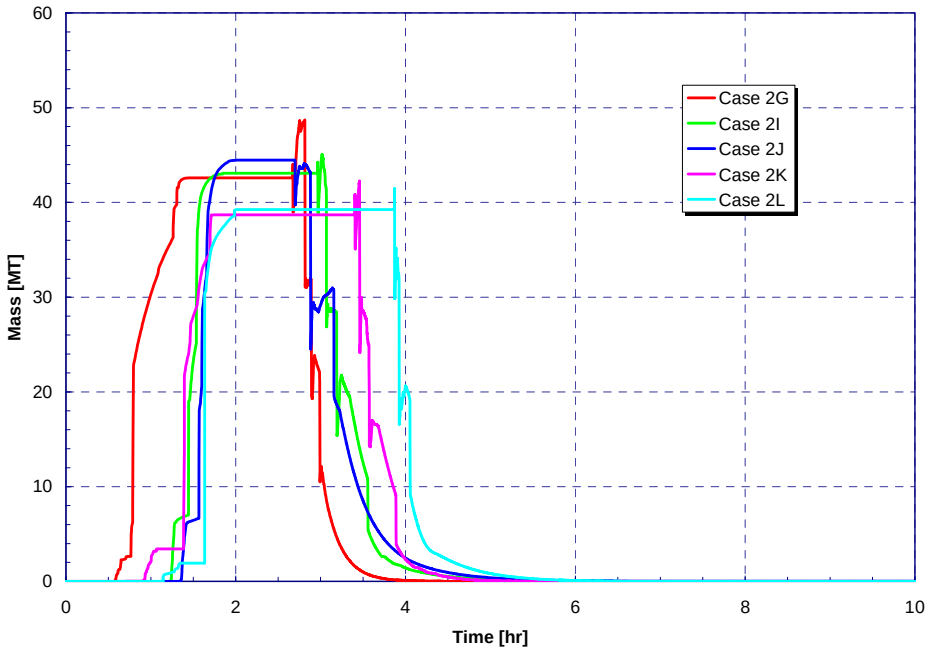

Figure 4-111. Uranium Dioxide Mass on the Vessel Lower Head for LLOCA Sensitivities (MLOCA).

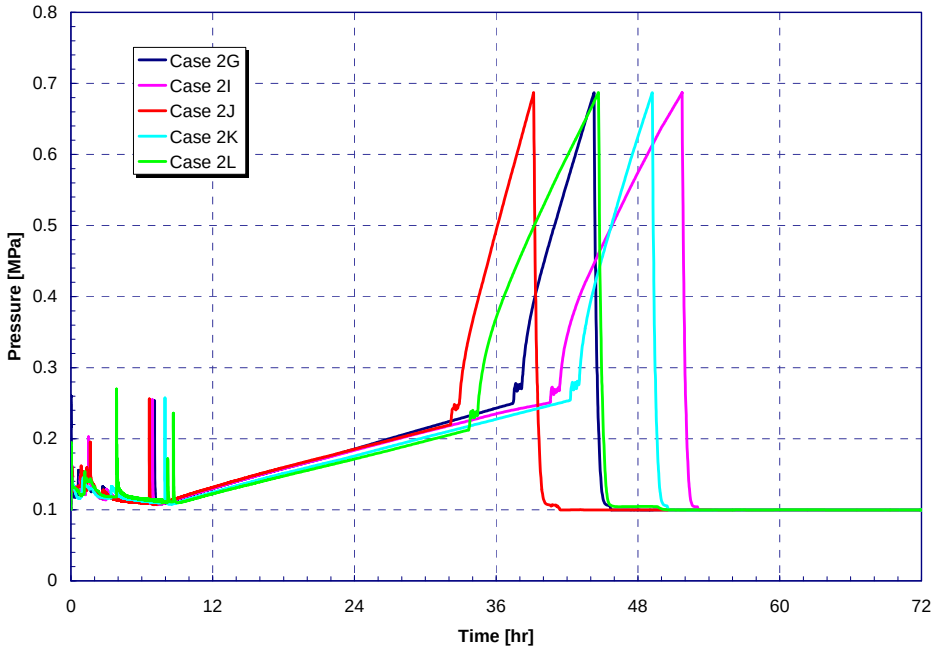

Figure 4-112. Containment Pressure Response for LLOCA Sensitivities (MLOCA).

The fission product release results are shown in Figures 4-113 through 4-121 for the nine NUREG-1465 radionuclide groups. These figures summarize the total fission product mass released to containment. Durations of each of the NUREG-1465 release phases are presented in Table 4-47. In addition, the magnitudes of release to containment for each of the NUREG-1465 radionuclide groups are tabulated in Tables 4-48 through 4-51 for all release phases. In contrast to Figures 4-113 through 4-121, the results in the tables present the releases to containment as a fraction of the initial core inventory rather than absolute mass. This enables direct comparison with NUREG-1465 results.

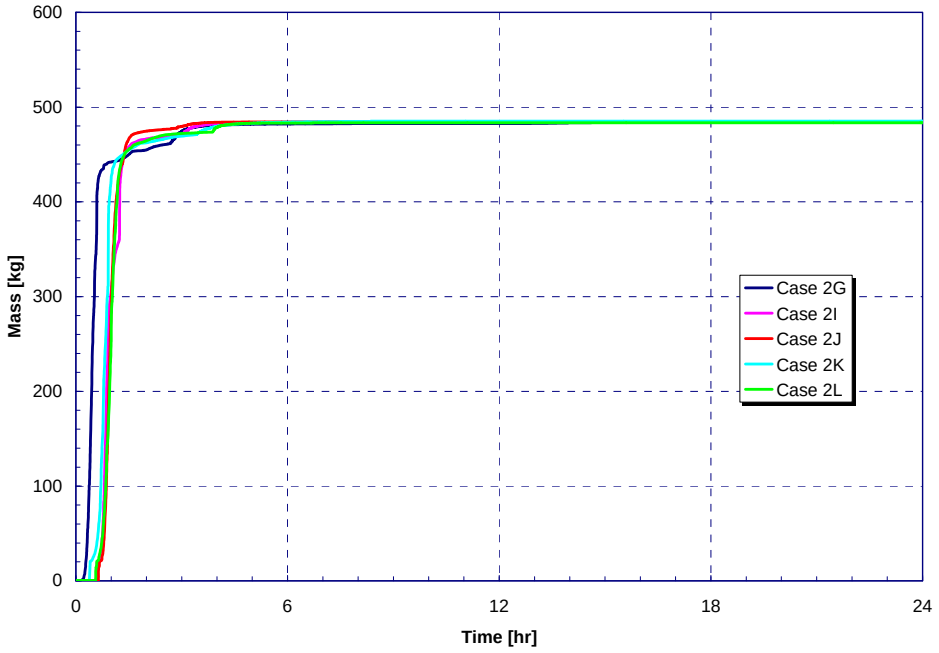

Figure 4-113. Noble Gas Release to Containment for LLOCA Sensitivities (MLOCA).

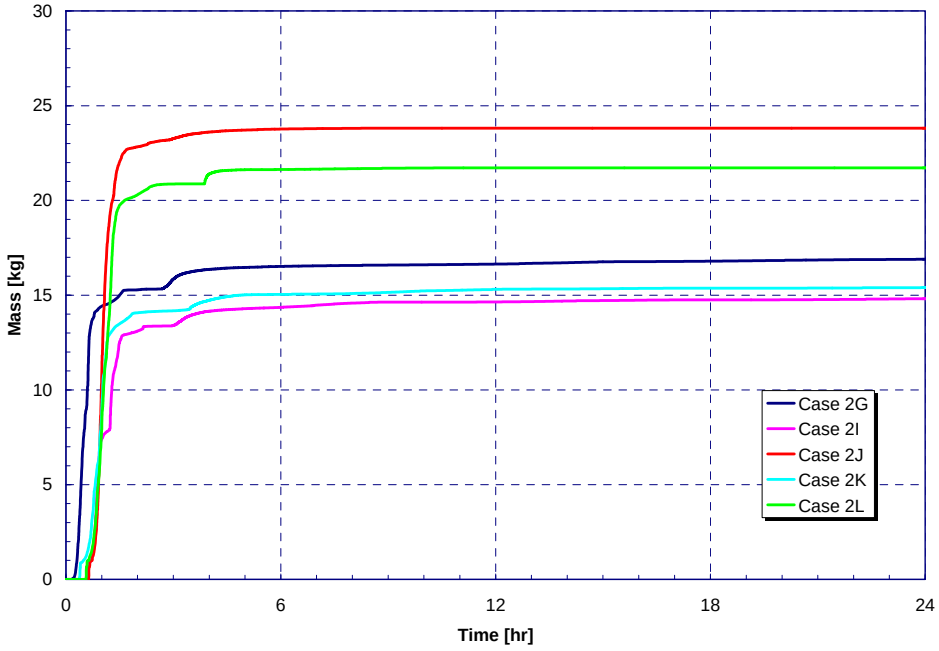

Figure 4-114. Halogen Release to Containment for LLOCA Sensitivities (MLOCA).

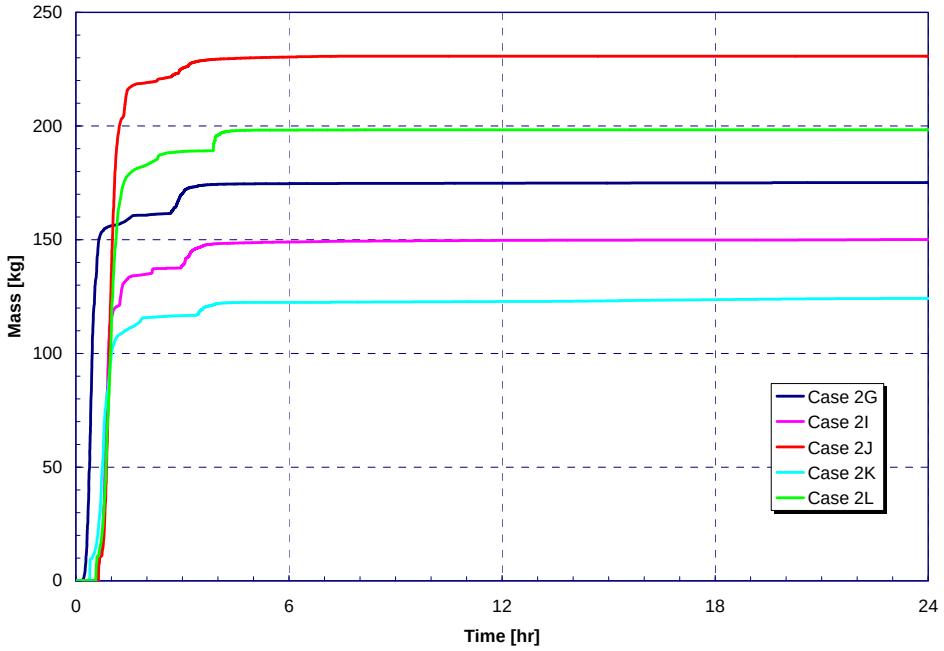

Figure 4-115. Alkali Metal Release to Containment for LLOCA Sensitivities (MLOCA).

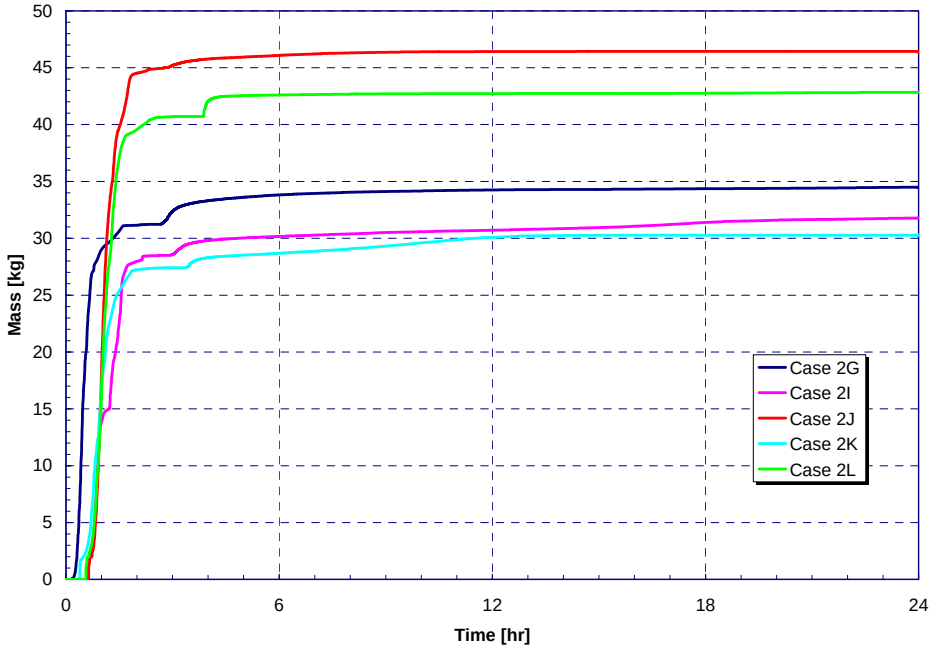

Figure 4-116. Tellurium Group Release to Containment for LLOCA Sensitivities (MLOCA).

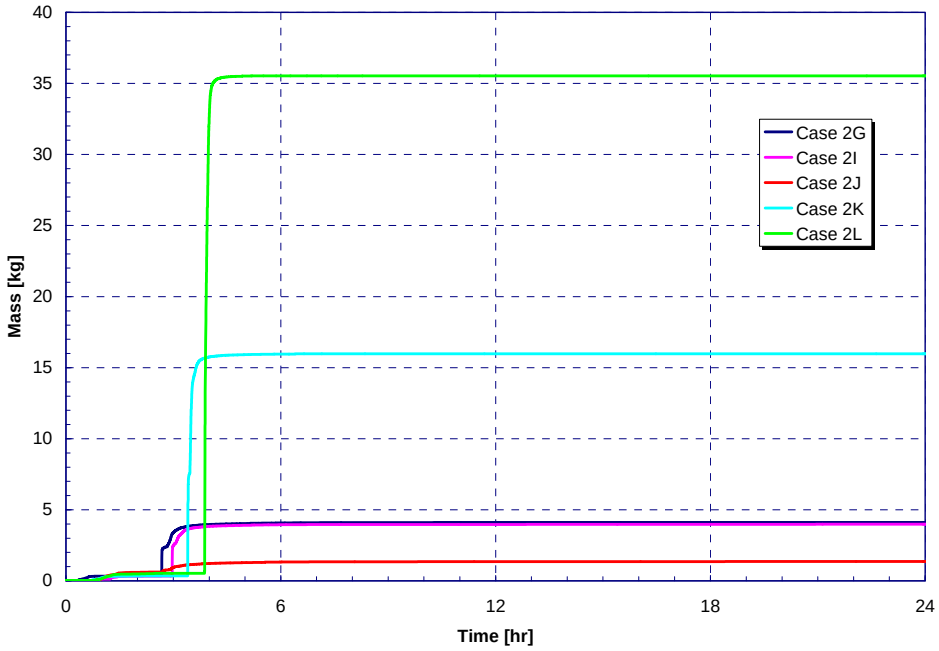

Figure 4-117. Barium, Strontium Group Release to Containment for LLOCA Sensitivities (MLOCA).

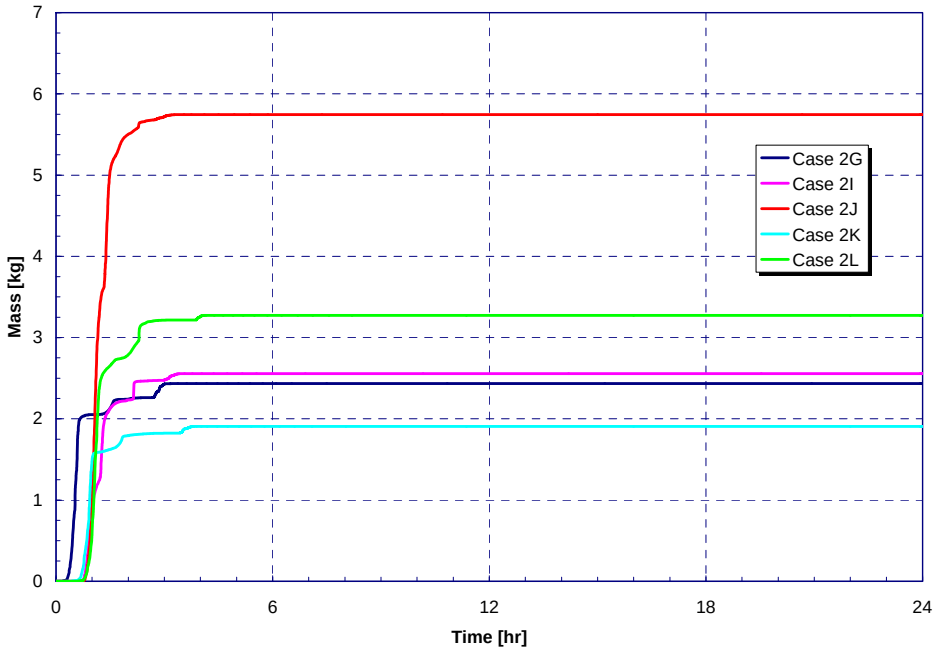

Figure 4-118. Noble Metal (Ru) Release to Containment for LLOCA Sensitivities (MLOCA).

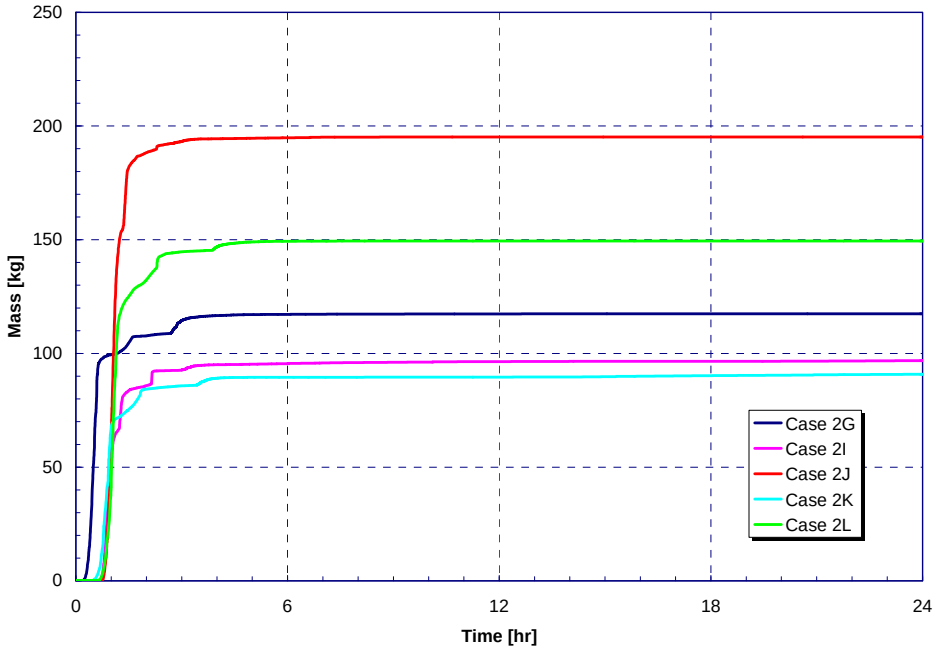

Figure 4-119. Noble Metal (Mo) Release to Containment for LLOCA Sensitivities (MLOCA).

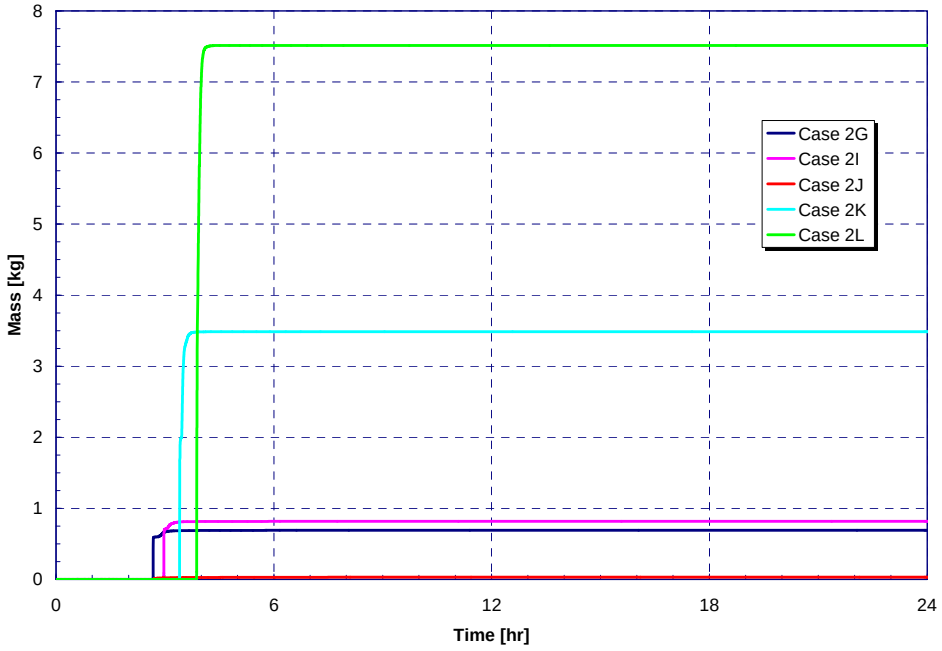

Figure 4-120. Lanthanide Release to Containment for LLOCA Sensitivities (MLOCA).

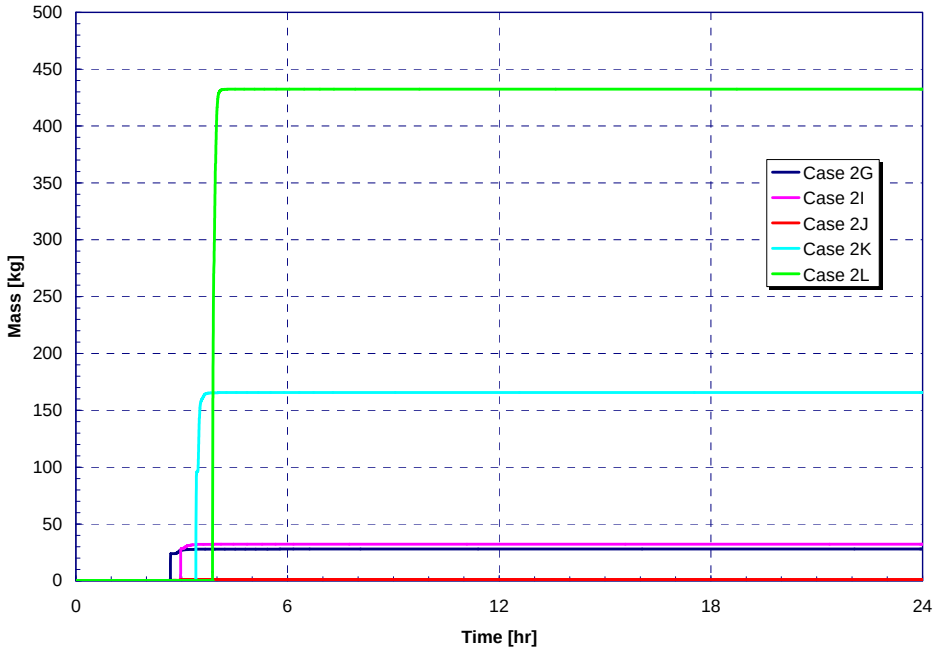

Figure 4-121. Cerium Group Release to Containment for LLOCA Sensitivities (MLOCA).

Table 4-47. Release Timing for LLOCA Sensitivities (MLOCAs).

Timing (hr)	NUREG-1465	Case 2I	Case 2J	Case 2K	Case 2L
Onset of Release	~0	0.027	0.029	0.015	0.016
Coolant Release Duration		0.5	0.6	0.4	0.5
Gap Release Duration	0.5	0.1	0.1	0.1	0.1
In-Vessel Release Duration	1.3	2.3	2.0	2.9	3.2
Ex-Vessel Release Duration	2.0	0.9	1.6	0.9	0.4
Late I-Vessel Release Duration	10.0	20.6	4.2	36.4	1.1

Table 4-48. Gap Release Fractions for LLOCA Sensitivities (MLOCAs).

	NUREG-1465	Case 2I	Case 2J	Case 2K	Case 2L
Noble Gases	0.05	4.6105E-02	5.4080E-02	4.7432E-02	5.3654E-02
Halogens	0.05	3.4181E-02	4.5732E-02	3.6480E-02	4.5610E-02
Alkali Metals	0.05	3.5571E-02	4.8032E-02	3.7664E-02	4.7584E-02
Te Group	0	3.5875E-02	4.8104E-02	3.7704E-02	4.7502E-02

Table 4-49. In-Vessel Release Fractions for LLOCA Sensitivities (MLOCAs).

	NUREG-1465	Case 2I	Case 2J	Case 2K	Case 2L
Noble Gases	0.95	9.1658E-1	9.2299E-1	9.1770E-1	9.1654E-1
Halogens	0.35	4.8027E-1	8.4488E-1	5.1074E-1	7.5705E-1
Alkali Metals	0.25	4.5559E-1	7.4353E-1	3.7951E-1	6.2797E-1
Te Group	0.05	5.3412E-1	8.5089E-1	5.1067E-1	7.6655E-1
Ba, Sr Group	0.02	1.7672E-3	3.2892E-3	1.8403E-3	2.7731E-3
Ru Group	0.0025	6.0329E-3	1.3854E-2	4.4468E-3	7.8473E-3
Mo Group	0.0025	2.6457E-1	5.4947E-1	2.4571E-1	4.1517E-1
Lanthanides	0.0002	9.8669E-8	2.5126E-7	8.8857E-8	1.6532E-7
Ce Group	0.0005	9.4379E-8	2.2609E-7	8.3536E-8	1.4716E-7

Table 4-50. Ex-Vessel Release Fractions for LLOCA Sensitivities (MLOCAs).

	NUREG-1465	Case 2I	Case 2J	Case 2K	Case 2L
Noble Gases	0	1.3811E-2	1.1403E-2	5.5064E-3	8.9605E-3
Halogens	0.25	2.1540E-2	1.7715E-2	1.4484E-2	2.4540E-2
Alkali Metals	0.35	3.2601E-2	2.4699E-2	1.5616E-2	2.6711E-2
Te Group	0.25	2.1233E-2	1.4870E-2	1.6670E-2	3.2481E-2
Ba, Sr Group	0.1	1.8334E-2	3.2331E-3	8.2072E-2	1.8441E-1
Ru Group	0.0025	7.1365E-7	4.2072E-8	2.3428E-6	2.7779E-6
Mo Group	0.0025	4.8856E-8	3.3247E-9	1.4129E-7	2.1877E-7
Lanthanides	0.005	1.2729E-3	4.4193E-5	5.4541E-3	1.1747E-2
Ce Group	0.005	1.4542E-2	4.5219E-4	7.4992E-2	1.9586E-1

Table 4-51. Late In-Vessel Release Fractions for LLOCA Sensitivities (MLOCAs).

	NUREG-1465	Case 2I	Case 2J	Case 2K	Case 2L
Noble Gases	0	1.5672E-2	3.9826E-3	2.6044E-2	1.0175E-2
Halogens	0.1	2.3266E-2	1.9224E-3	2.7148E-2	1.4542E-3
Alkali Metals	0.1	1.0652E-2	6.2142E-3	1.4229E-2	4.5457E-3
Te Group	0.005	2.6485E-2	2.8908E-3	3.3395E-2	1.7872E-3
Ba, Sr Group	0	0.000E+0	2.1047E-5	5.26E-10	1.64E-13
Ru Group	0	2.0319E-4	1.5716E-4	2.0396E-4	1.3281E-4
Mo Group	0	1.2104E-2	7.7862E-3	1.7443E-2	1.0446E-2
Lanthanides	0	0.00E+00	2.34E-13	3.93E-18	0.00E+00
Ce Group	0	0.00E+00	2.71E-13	3.66E-18	1.72E-17

4.9 Tabulated Results for All Cases

For ease of comparison, this section provides tabulated results that compare all MELCOR calculations. First is a simplified calculation matrix that provides an easy cross-reference between the "case numbers" and the accident sequences that those cases represent. Tables 4-52 through 4-66 provide a table for each of the NUREG-1465 release phase timing and magnitude parameters. While detailed results for the LEU cases are only presented for selected sequences, the following tables contain comparisons between results for LEU cores and 40% MOX cores for each accident sequence simulated.

Table 4-52. Calculation Matrix.

Accident Sequence	LEU Case	40% MOX Case
SBO, RCP Seal Fails, 3 hr AFW, Late Containment Failure	1A	2A
SBO, RCP Seal Fails, 3 hr AFW, Early Containment Failure	1B	2B
SBO, RCP Seal Fails, no AFW, Late Containment Failure	1S	2S
SBO, RCP Seal Fails, 3 hr AFW, SORV, Late Containment Failure	1T	2T
SBO, No Seal Failure, No AFW, Late Containment Failure	1P	2P
1-in. SLOCA in Cold Leg, ECCS Recirc Failure, Late Containment Failure	1D	2D
1-in. SLOCA in Cold Leg, ECCS Recirc Failure, Early Containment Failure	1E	2E
1-in. SLOCA in Cold Leg, no ECCS, Late Containment Failure	1U	2U
1-in. SLOCA in Hot Let, ECCS Recirc Failure, Late Containment Failure	1V	2V
2-in. SLOCA in Cold Leg, ECCS Recirc Failure, Late Containment Failure	1Q	2Q
2-in. SLOCA in Cold Leg, no ECCS, Late Containment Failure	1R	2R
27.5-in. LLOCA in Cold Leg, no ECCS, Late Containment Failure	1G	2G
6-in. MLOCA in Cold Leg, no ECCS, Late Containment Failure	1I	2I
6-in. MLOCA in Hot Leg, no ECCS, Late Containment Failure	1J	2J
10-in. MLOCA in Cold Leg, no ECCS, Late Containment Failure	1K	2K
10-in. MLOCA in Hot Leg, no ECCS, Late Containment Failure	1L	2L

Table 4-53. Onset of Release of Radionuclides.

Case	LEU Core (hr)	40% MOX Core (hr)
A	6.5167	6.6167
B	6.5167	6.6167
S	2.1195	2.2927
T	6.5540	6.5836
P	2.2342	2.3935
D	2.7333	3.0000
E	2.7333	3.0000
U	2.1942	2.2292
V	2.8344	2.8626
Q	0.9555	0.9169
R	0.4730	0.4704
G	0.0000	0.0000
I	0.0265	0.0268
J	0.0292	0.0285
K	0.0156	0.0153
L	0.0160	0.0161

Table 4-54. Duration of Coolant Release.

Case	LEU Core (hr)	40% MOX Core (hr)
A	1.4667	1.4833
B	1.4667	1.4833
S	0.8525	0.9157
T	1.4286	1.5160
P	0.8553	0.9416
D	1.2833	1.0500
E	1.2833	1.0500
U	1.2166	1.2012
V	1.5023	1.4998
Q	0.4170	0.4774
R	0.3585	0.3708
G	0.1417	0.1267
I	0.5182	0.5423
J	0.5655	0.6026
K	0.3433	0.3621
L	0.4874	0.5425

Table 4-55. Duration of Gap Release.

Case	LEU Core (min)	40% MOX Core (min)
A	39.0000	40.0000
B	39.0000	40.0000
S	34.4293	35.2490
T	37.5442	40.0217
P	26.6348	29.1481
D	25.7510	27.5000
E	25.7510	27.5000
U	24.6042	24.1762
V	27.5495	26.7596
Q	9.6504	10.5931
R	10.6107	10.0301
G	5.5000	6.4000
I	6.0652	6.1014
J	6.8199	6.8852
K	5.2191	5.6053
L	6.2925	5.9845

Table 4-56. Duration of Early In-Vessel Release.

Case	LEU Core (hr)	40% MOX Core (hr)
A	9.2333	7.9000
B	2.4333	2.6833
S	4.7400	7.9787
T	9.2646	8.3573
P	10.2376	9.1055
D	4.9542	3.6083
E	4.9542	3.6083
U	3.2360	5.5922
V	5.3390	8.0322
Q	4.3880	4.5861
R	3.8941	4.7719
G	2.3333	2.4333
I	2.4308	2.2947
J	3.0282	1.9514
K	3.1569	2.9320
L	2.2592	3.2097

Table 4-57. Duration of Ex-Vessel Release.

Case	LEU Core (hr)	40% MOX Core (hr)
A	6.6000	85.1333
B	17.1667	16.8167
S	24.7141	24.6255
T	13.8271	87.3094
P	12.0291	8.6738
D	38.2333	3.2167
E	8.2250	3.2500
U	3.5159	30.8412
V	29.4986	28.3595
Q	2.3084	2.5261
R	2.8108	2.7031
G	1.1000	0.8867
I	1.0888	0.8659
J	0.7938	1.5582
K	0.3768	0.9123
L	1.1909	0.4028

Table 4-58. Duration of Late In-Vessel Release.

Case	LEU Core (hr)	40% MOX Core (hr)
A	0.6333	
B	18.2667	25.2833
S	76.7808	124.2922
T	104.5271	118.7760
P	55.3625	54.1405
D	0.8667	0.5500
E	0.6333	0.8000
U	0.9599	0.8579
V	0.8485	2.2094
Q	0.5536	1.7432
R	0.0559	0.4782
G	75.7667	61.1334
I	45.3901	20.6011
J	0.8468	4.1528
K	57.5973	36.3971
L	60.4659	1.0513

Table 4-59. Gap Release Fractions for an LEU Core.

Case	Noble Gases	Halogens	Alkali Metals	Te Group
1A	1.3876E-02	2.7343E-03	9.4631E-04	8.5784E-04
1B	1.3876E-02	2.7343E-03	9.4631E-04	8.5784E-04
1S	1.6991E-02	3.1554E-03	3.3847E-03	3.3528E-03
1T	1.3392E-02	2.5897E-03	8.1673E-04	7.3745E-04
1P	1.3692E-02	1.9797E-03	5.2658E-04	4.4922E-04
1D	2.5050E-02	9.0961E-03	9.4596E-03	9.2456E-03
1E	2.5050E-02	9.0961E-03	9.4596E-03	9.2456E-03
1U	2.3837E-02	8.6630E-03	8.9746E-03	8.7550E-03
1V	2.7852E-02	9.3627E-03	9.8010E-03	9.4101E-03
1Q	3.9505E-02	2.3444E-02	2.5084E-02	2.4202E-02
1R	3.3672E-02	2.1414E-02	2.3070E-02	2.2178E-02
1G	4.3580E-02	3.5352E-02	3.6898E-02	3.6344E-02
1I	4.3268E-02	3.2447E-02	3.3894E-02	3.3610E-02
1J	4.6535E-02	4.0503E-02	4.2278E-02	4.1860E-02
1K	4.2497E-02	3.3963E-02	3.4988E-02	3.4725E-02
1L	5.1557E-02	4.4636E-02	4.7026E-02	4.6115E-02

Table 4-60. Gap Release Fractions for a 40% MOX Core.

Case	Noble Gases	Halogens	Alkali Metals	Te Group
2A	1.2111E-02	5.4231E-03	1.9500E-03	2.6400E-03
2B	1.2111E-02	5.4231E-03	1.9500E-03	2.6400E-03
2S	2.0838E-02	4.0278E-03	3.7525E-03	3.9471E-03
2T	1.6758E-02	3.5018E-03	9.9706E-04	1.0479E-03
2P	1.6214E-02	3.4645E-03	6.8973E-04	6.6604E-04
2D	1.1906E-02	7.7405E-03	5.0886E-03	7.1874E-03
2E	1.1906E-02	7.7405E-03	5.0886E-03	7.1874E-03
2U	2.4898E-02	9.7983E-03	9.5572E-03	9.8600E-03
2V	2.9068E-02	1.0541E-02	1.0102E-02	1.0459E-02
2Q	4.3848E-02	2.6063E-02	2.6577E-02	2.6860E-02
2R	3.5545E-02	2.3237E-02	2.3695E-02	2.4147E-02
2G	4.6502E-02	2.9917E-02	3.6063E-02	3.5974E-02
2I	4.6105E-02	3.4181E-02	3.5571E-02	3.5875E-02
2J	5.4080E-02	4.5732E-02	4.8032E-02	4.8104E-02
2K	4.7432E-02	3.6480E-02	3.7664E-02	3.7704E-02
2L	5.3654E-02	4.5610E-02	4.7584E-02	4.7502E-02

Table 4-61. Early In-Vessel Release Fractions for an LEU Core.

Case	Noble Gases	Halogens	Alkali Metals	Te Group	Ba/Sr Group
1A	8.9250E-1	7.6602E-1	6.4304E-1	6.6098E-1	2.0000E-3
1B	3.8433E-1	7.0103E-2	3.2979E-2	3.7101E-2	1.5909E-4
1S	8.1263E-1	5.7966E-1	4.2937E-1	4.4602E-1	2.3528E-3
1T	9.2710E-1	6.0363E-1	4.4512E-1	5.7558E-1	1.5176E-3
1P	9.1162E-1	6.6602E-1	5.3128E-1	5.6296E-1	1.6397E-3
1D	6.3987E-1	9.9629E-2	1.1679E-1	1.0405E-1	1.9545E-4
1E	6.3987E-1	9.9612E-2	1.1679E-1	1.0405E-1	1.9545E-4
1U	6.7799E-1	1.1391E-1	1.2474E-1	1.1327E-1	2.3279E-4
1V	5.8686E-1	1.0655E-1	1.2551E-1	1.0922E-1	2.0197E-4
1Q	7.5003E-1	3.0930E-1	3.6827E-1	3.3263E-1	8.6364E-4
1R	8.9117E-1	4.0677E-1	4.3584E-1	4.2192E-1	1.4928E-3
1G	9.1269E-1	5.9298E-1	5.7162E-1	6.2155E-1	2.0909E-3
1I	9.1179E-1	5.3317E-1	4.9298E-1	5.3637E-1	2.0848E-3
1J	9.2939E-1	8.2895E-1	7.6271E-1	8.3515E-1	2.9437E-3
1K	9.1988E-1	4.7903E-1	3.4622E-1	4.8401E-1	1.8266E-3
1L	9.2317E-1	7.1872E-1	6.2124E-1	6.9024E-1	2.9375E-3

Case	Ru Group	Mo Group	Lanthanides	Ce Group
1A	9.7493E-3	4.6113E-1	1.8571E-7	1.8121E-7
1B	1.5320E-4	1.3941E-2	3.8571E-9	3.7584E-9
1S	1.3569E-2	4.0085E-1	2.2358E-7	2.2350E-7
1T	5.1271E-3	2.8659E-1	1.1161E-7	1.1145E-7
1P	7.7798E-3	4.0350E-1	1.5068E-7	1.5066E-7
1D	5.5710E-4	5.0938E-2	1.3714E-8	1.3423E-8
1E	5.5710E-4	5.0938E-2	1.3714E-8	1.3423E-8
1U	7.9348E-4	5.8472E-2	1.6048E-8	1.6078E-8
1V	5.7869E-4	5.2619E-2	1.3782E-8	1.3802E-8
1Q	4.0437E-3	2.0426E-1	7.4536E-8	7.4542E-8
1R	8.0133E-3	3.1508E-1	1.3484E-7	1.3490E-7
1G	7.7994E-3	3.5389E-1	1.3143E-7	1.2752E-7
1I	8.1660E-3	3.2633E-1	1.2484E-7	1.2466E-7
1J	1.3205E-2	5.5559E-1	2.4264E-7	2.4132E-7
1K	5.8646E-3	2.5659E-1	1.0397E-7	1.0347E-7
1L	1.0160E-2	4.3966E-1	1.8878E-7	1.8837E-7

Table 4-62. Early In-Vessel Release Fractions for a 40% MOX Core.

Case	Noble Gases	Halogens	Alkali Metals	Te Group	Ba/Sr Group
2A	9.0820E-1	7.8462E-1	6.4893E-1	6.7000E-1	1.9474E-3
2B	4.4078E-1	8.8846E-2	3.6429E-2	4.3600E-2	2.0000E-4
2S	9.1074E-1	7.7297E-1	5.1116E-1	5.3541E-1	1.8800E-3
2T	8.9966E-1	6.0545E-1	4.6321E-1	5.4992E-1	1.8768E-3
2P	9.3412E-1	7.6128E-1	5.7060E-1	6.0131E-1	2.5970E-3
2D	6.1998E-1	1.1016E-1	1.1872E-1	1.1480E-1	1.9474E-4
2E	6.1998E-1	1.1019E-1	1.1872E-1	1.1484E-1	1.9474E-4
2U	6.8103E-1	1.4278E-1	1.4509E-1	1.4538E-1	3.0967E-4
2V	6.7621E-1	1.3720E-1	1.5434E-1	1.4259E-1	2.4965E-4
2Q	8.2786E-1	4.2203E-1	4.4794E-1	4.3919E-1	1.1795E-3
2R	7.6335E-1	3.4978E-1	3.9499E-1	3.6268E-1	7.6309E-4
2G	9.0019E-1	5.5966E-1	5.4316E-1	5.8887E-1	1.8947E-3
2I	9.1658E-1	4.8027E-1	4.5559E-1	5.3412E-1	1.7672E-3
2J	9.2299E-1	8.4488E-1	7.4353E-1	8.5089E-1	3.2892E-3
2K	9.1770E-1	5.1074E-1	3.7951E-1	5.1067E-1	1.8403E-3
2L	9.1654E-1	7.5705E-1	6.2797E-1	7.6655E-1	2.7731E-3

Case	Ru Group	Mo Group	Lanthanides	Ce Group
2A	7.0732E-3	4.2000E-1	1.5133E-7	1.4460E-7
2B	1.6585E-4	1.5714E-2	4.6802E-9	4.4736E-9
2S	7.6366E-3	4.0733E-1	1.6837E-7	1.6092E-7
2T	7.8806E-3	3.4375E-1	1.4431E-7	1.4260E-7
2P	1.2309E-2	5.0420E-1	2.3109E-7	2.2069E-7
2D	5.1220E-4	5.1429E-2	1.3261E-8	1.4460E-8
2E	5.1220E-4	5.1429E-2	1.3261E-8	1.4460E-8
2U	9.1564E-4	7.2307E-2	2.2213E-8	2.2399E-8
2V	6.1181E-4	6.4731E-2	1.7057E-8	1.8235E-8
2Q	5.4022E-3	2.7150E-1	1.0282E-7	1.0107E-7
2R	3.0210E-3	2.6039E-1	9.1480E-8	9.0351E-8
2G	5.6098E-3	3.1143E-1	1.0608E-7	9.4894E-8
2I	6.0329E-3	2.6457E-1	9.8669E-8	9.4379E-8
2J	1.3854E-2	5.4947E-1	2.5126E-7	2.2609E-7
2K	4.4468E-3	2.4571E-1	8.8857E-8	8.3536E-8
2L	7.8473E-3	4.1517E-1	1.6532E-7	1.4716E-7

Table 4-63. Ex-Vessel Release Fractions for an LEU Core.

Case	Noble Gases	Halogens	Alkali Metals	Te Group	Ba/Sr Group
1A	8.1925E-2	6.7990E-2	1.0217E-1	2.6451E-2	2.3524E-2
1B	2.7965E-1	2.1178E-1	2.7352E-1	8.5661E-2	1.0853E-3
1S	1.4747E-1	9.8701E-2	1.4053E-1	6.8043E-2	2.2812E-4
1T	5.1187E-2	5.9921E-2	6.1588E-2	2.2777E-2	3.0276E-2
1P	6.8122E-2	5.7456E-2	7.2260E-2	2.1561E-2	1.5538E-2
1D	2.7498E-1	1.6887E-1	2.6649E-1	9.4534E-2	5.2318E-4
1E	2.8540E-1	2.1169E-1	2.8005E-1	7.6452E-2	8.3928E-4
1U	2.5735E-1	1.8799E-1	2.5216E-1	5.7717E-2	7.3861E-3
1V	3.2372E-1	2.2021E-1	3.2764E-1	7.0983E-2	3.7427E-3
1Q	1.9078E-1	1.4805E-1	1.8739E-1	7.0299E-2	5.7700E-3
1R	6.0409E-2	6.8549E-2	6.1589E-2	3.5793E-2	7.5456E-3
1G	1.9684E-2	3.0608E-2	3.0370E-2	2.3244E-2	9.9397E-2
1I	2.2896E-2	3.5789E-2	2.9502E-2	2.9219E-2	2.2097E-2
1J	1.4664E-2	2.9053E-2	2.7267E-2	2.6379E-2	2.4315E-1
1K	1.6535E-2	2.9734E-2	2.8692E-2	2.7176E-2	2.9617E-1
1L	1.3328E-2	2.4617E-2	2.0204E-2	1.7948E-2	1.8909E-1

Case	Ru Group	Mo Group	Lanthanides	Ce Group
1A	2.0946E-9	2.318E-10	1.1916E-4	4.9592E-3
1B	1.449E-11	9.148E-12	3.3601E-6	1.2695E-5
1S	0.0000E+0	6.4418E-9	3.4426E-6	6.6594E-6
1T	1.4816E-9	1.7216E-10	1.1098E-4	5.3921E-3
1P	1.5783E-9	1.8808E-10	7.7870E-5	3.1215E-3
1D	5.3402E-12	1.5953E-9	3.4900E-6	7.9901E-6
1E	7.3459E-12	1.9563E-12	3.8075E-6	1.1357E-5
1U	2.3866E-11	5.6486E-12	5.4057E-6	1.3819E-4
1V	6.8845E-12	2.2773E-12	3.7722E-6	5.5949E-5
1Q	1.6648E-8	1.0886E-9	4.1881E-5	9.9855E-4
1R	2.2656E-8	1.3066E-9	9.9688E-5	1.7301E-3
1G	1.0660E-6	8.3703E-8	4.5600E-3	8.8182E-2
1I	5.9718E-7	4.3947E-8	1.0243E-3	1.2167E-2
1J	3.7044E-6	2.4867E-7	1.6573E-2	2.7914E-1
1K	5.5658E-6	3.2412E-7	2.3200E-2	3.4839E-1
1L	2.2283E-6	1.3118E-7	1.0490E-2	1.8233E-1

Table 4-64. Ex-Vessel Release Fractions for a 40% MOX Core.

Case	Noble Gases	Halogens	Alkali Metals	Te Group	Ba/Sr Group
2A	3.9130E-2	5.8845E-2	7.2377E-2	5.8582E-2	1.7224E-3
2B	7.3003E-2	8.5667E-2	1.0715E-1	4.0369E-2	1.4321E-4
2S	3.7696E-2	4.6742E-2	6.0875E-2	3.1775E-2	1.2746E-2
2T	2.7171E-2	3.8505E-2	3.5126E-2	5.0247E-2	4.9414E-4
2P	3.4747E-2	3.2927E-2	4.1672E-2	1.9328E-2	1.6973E-3
2D	2.4983E-1	1.4720E-1	3.3477E-1	5.7292E-2	8.4958E-3
2E	2.5526E-1	1.7543E-1	3.4458E-1	8.0051E-2	1.1575E-2
2U	1.6768E-1	9.8149E-2	2.1314E-1	6.1113E-2	6.9389E-3
2V	7.4805E-2	8.2146E-2	1.0539E-1	3.2462E-2	2.8657E-3
2Q	7.7519E-2	7.8335E-2	1.0467E-1	4.9765E-2	1.5292E-2
2R	1.4700E-1	1.5946E-1	1.8614E-1	8.7671E-2	6.4849E-3
2G	1.5317E-2	2.9165E-2	3.4734E-2	2.8194E-2	1.8544E-2
2I	1.3811E-2	2.1540E-2	3.2601E-2	2.1233E-2	1.8334E-2
2J	1.1403E-2	1.7715E-2	2.4699E-2	1.4870E-2	3.2331E-3
2K	5.5064E-3	1.4484E-2	1.5616E-2	1.6670E-2	8.2072E-2
2L	8.9605E-3	2.4540E-2	2.6711E-2	3.2481E-2	1.8441E-1

Case	Ru Group	Mo Group	Lanthanides	Ce Group
2A	4.333E-11	1.505E-08	7.8937E-6	1.6611E-4
2B	3.673E-11	3.369E-11	3.3783E-6	5.5393E-6
2S	1.448E-09	1.294E-09	6.7982E-5	2.8622E-3
2T	3.048E-10	3.055E-08	7.0169E-6	4.5174E-5
2P	1.342E-08	9.449E-10	4.2619E-5	4.7057E-4
2D	2.294E-11	1.272E-11	5.8528E-6	1.8673E-4
2E	4.491E-11	1.371E-11	8.4761E-6	2.8605E-4
2U	1.913E-10	8.826E-10	2.0903E-5	1.0655E-3
2V	1.032E-11	2.056E-12	3.9464E-6	3.1470E-5
2Q	1.500E-08	1.138E-09	1.5647E-4	4.8688E-3
2R	2.173E-10	3.526E-11	1.2962E-5	4.2929E-4
2G	2.8049E-7	2.1540E-8	1.0735E-3	1.2578E-2
2I	7.1365E-7	4.8856E-8	1.2729E-3	1.4542E-2
2J	4.2072E-8	3.3247E-9	4.4193E-5	4.5219E-4
2K	2.3428E-6	1.4129E-7	5.4541E-3	7.4992E-2
2L	2.7779E-6	2.1877E-7	1.1747E-2	1.9586E-1

Table 4-65. Late In-Vessel Release Fractions for an LEU Core.

Case	Noble Gases	Halogens	Alkali Metals	Te Group	Ba/Sr Group
1A	5.8848E-3	3.229E-3	2.4069E-3	3.3247E-3	1.3645E-9
1B	3.2215E-1	3.8696E-1	6.3424E-2	3.3364E-1	5.4893E-4
1S	1.0637E-2	9.7347E-2	1.8965E-2	1.9245E-1	2.8056E-4
1T	1.0441E-2	1.9087E-1	1.2803E-1	1.9224E-1	2.6265E-4
1P	8.3629E-3	1.0725E-1	1.1012E-2	5.7132E-2	8.1845E-9
1D	4.2756E-2	9.0945E-2	1.0631E-1	9.7179E-2	1.5079E-4
1E	3.7589E-2	9.1629E-2	1.0423E-1	9.5728E-2	1.4801E-4
1U	3.6116E-2	1.1248E-1	1.1558E-1	1.1789E-1	1.9899E-4
1V	4.8083E-2	4.1305E-2	4.4799E-2	4.5931E-2	6.4083E-5
1Q	1.1745E-2	3.7390E-2	3.5594E-2	3.9170E-2	1.1898E-4
1R	4.6384E-3	6.9053E-2	6.1921E-2	7.0441E-2	1.5236E-2
1G	2.3919E-2	2.9717E-2	1.4353E-2	2.9408E-2	1.2727E-14
1I	2.5328E-2	2.4461E-2	1.2548E-2	2.6165E-2	4.5463E-10
1J	4.4639E-3	3.8552E-4	1.7213E-3	1.0707E-3	4.5481E-10
1K	2.4489E-2	3.0576E-2	1.4648E-2	4.3060E-2	4.5458E-10
1L	1.5133E-2	1.6865E-2	1.6333E-2	2.1169E-2	5.9096E-9

Case	Ru Group	Mo Group	Lanthanides	Ce Group
1A	1.7531E-5	3.4439E-3	1.429E-13	1.343E-13
1B	2.2636E-4	2.5306E-2	7.5373E-9	5.6805E-8
1S	2.1366E-4	7.9439E-3	1.7742E-9	1.4767E-12
1T	1.0086E-4	7.6950E-2	1.4247E-11	1.0539E-11
1P	8.6510E-5	5.0788E-3	8.5742E-13	8.0564E-13
1D	4.4749E-4	4.0958E-2	1.0629E-8	9.7490E-9
1E	4.3923E-4	4.0104E-2	1.0372E-8	9.8649E-9
1U	6.4359E-4	5.1454E-2	1.4885E-8	1.4805E-8
1V	1.6239E-4	1.7886E-2	4.8858E-9	2.5945E-9
1Q	7.7105E-4	3.0110E-2	1.2778E-8	1.1409E-8
1R	9.1473E-2	9.7571E-2	1.5320E-6	1.5305E-6
1G	3.2136E-4	2.3611E-2	7.1429E-14	6.7116E-14
1I	2.9296E-4	1.4441E-2	8.5721E-14	6.7121E-14
1J	7.1341E-5	6.2572E-3	3.4286E-17	6.7148E-14
1K	1.7120E-4	1.5401E-2	0.0000E+0	4.4295E-18
1L	1.8296E-4	2.8170E-2	5.7147E-13	5.3696E-13

Table 4-66. Late In-Vessel Release Fractions for a 40% MOX Core.

Case	Noble Gases	Halogens	Alkali Metals	Te Group	Ba/Sr Group
2A	2.5862E-2	4.3894E-2	2.2330E-2	6.3494E-2	1.0338E-4
2B	4.6621E-1	6.8752E-1	1.3765E-1	6.6507E-1	1.0124E-3
2S	1.6216E-2	6.5507E-2	2.0431E-2	1.9367E-1	2.0350E-4
2T	4.3567E-2	2.2671E-1	1.3258E-1	2.6286E-1	8.1510E-4
2P	3.9307E-3	9.1594E-2	1.4831E-2	2.9339E-2	6.9347E-5
2D	2.9003E-2	9.3185E-2	1.0700E-1	9.8135E-2	1.6050E-4
2E	3.3786E-2	9.5460E-2	1.0844E-1	1.0087E-1	1.6130E-4
2U	8.1782E-2	9.4771E-2	9.5955E-2	9.6342E-2	1.4892E-4
2V	1.4826E-1	6.9535E-2	5.0561E-2	7.7814E-2	2.2080E-4
2Q	2.5188E-2	1.3140E-2	7.2946E-3	1.3026E-2	1.4597E-5
2R	8.2806E-3	1.0065E-2	6.6355E-3	8.6732E-3	7.7494E-6
2G	3.1879E-2	3.4603E-2	1.4501E-2	3.2874E-2	2.6696E-5
2I	1.5672E-2	2.3266E-2	1.0652E-2	2.6485E-2	0.0000E+0
2J	3.9826E-3	1.9224E-3	6.2142E-3	2.8908E-3	2.1047E-5
2K	2.6044E-2	2.7148E-2	1.4229E-2	3.3395E-2	5.2636E-10
2L	1.0175E-2	1.4542E-3	4.5457E-3	1.7872E-3	1.6421E-13

Case	Ru Group	Mo Group	Lanthanides	Ce Group
2A	3.4695E-4	2.6619E-2	2.028E-13	5.016E-14
2B	6.9462E-4	8.4576E-2	3.1035E-8	2.9532E-8
2S	1.6936E-4	2.2461E-2	0.0000E+0	0.0000E+0
2T	6.1817E-4	9.9687E-2	3.9018E-9	2.2601E-13
2P	2.5908E-4	1.0864E-2	0.0000E+0	0.0000E+0
2D	4.4506E-4	4.2390E-2	1.1192E-8	1.1078E-8
2E	4.3700E-4	4.3344E-2	1.1334E-8	1.1372E-8
2U	3.9031E-4	4.3422E-2	8.2922E-9	3.4469E-9
2V	5.0293E-4	4.1193E-2	1.7388E-8	1.6141E-8
2Q	9.1238E-5	6.5833E-3	1.0609E-9	1.5174E-8
2R	2.3595E-5	4.6954E-3	8.8768E-10	7.2978E-9
2G	4.1638E-4	2.5638E-2	1.560E-14	2.847E-18
2I	2.0319E-4	1.2104E-2	0.000E+00	0.000E+00
2J	1.5716E-4	7.7862E-3	2.340E-13	2.711E-13
2K	2.0396E-4	1.7443E-2	3.931E-18	3.660E-18
2L	1.3281E-4	1.0446E-2	0.000E+00	1.717E-17

5.0 SUMMARY

As part of an NRC research program to evaluate the impact of using MOX fuel in commercial nuclear power plants, a study was undertaken to evaluate the impact of the usage of MOX fuel on the consequences of postulated severe accidents. A series of 23 severe accident calculations was performed using MELCOR 1.8.5 for a four-loop Westinghouse reactor with an ice condenser containment. The calculations covered five basic accident classes that were identified as the risk- and consequence-dominant accident sequences in plant-specific PRAs for the McGuire and Catawba nuclear plants. These were:

1. Long-term SBO with late containment failure,
2. Long-term SBO with early containment failure,
3. SLOCA with failure to realign ECCS for recirculation and late containment failure,
4. SLOCA with failure to realign ECCS for recirculation and early containment failure, and
5. LLOCA with failure of ECCS and late containment failure.

For each of these five accident categories, separate calculations were performed for traditional LEU core loading and a core loaded with 40% MOX fuel assemblies and 60% LEU fuel assemblies. The EOC fission product inventory and decay heat distribution for the 40% MOX core were determined based on planned administrative limits as described in the Pu disposition plans for the Catawba and McGuire nuclear plants.

In general, the accident progression and source terms for the LEU and 40% MOX cases were similar. This was initially unexpected because the experimental data for fission product releases from MOX fuel may have suggested higher releases than LEU. However, the MELCOR calculations show that at severe accident fuel temperatures, the volatile fission product releases occur at a very high release rate, regardless of the fuel type. Hence, the differences noted in the experimental results at lower temperature were not prototypical of severe accident conditions in the long term and did not greatly impact the integral source term.

Ultimately, the results of these MELCOR simulations will be used to provide a supplement to the NRC's alternative source term described in NUREG-1465. The NUREG-1465 Source Term considers both the timing and the chemical composition of the source term, and it divides releases from degrading reactor fuel into five phases:

- Coolant activity release,
- Gap release,
- In-vessel release,
- Ex-vessel release, and
- Late in-vessel release.

The MOX supplement to the NUREG-1465 Source Term should be a representative source term that could be used for a variety of accident sequences. The plant-specific PRAs for Catawba and McGuire were used to identify important uncertainties in accident progression in the five baseline accident categories described above. Sensitivity calculations were performed to examine the effects of these uncertainties to ensure that the NUREG-1465 style source term

developed was truly *representative* of any of the risk- and consequence-dominant accident sequences. Sensitivities examined included failure of AFW, coincident RCP seal failure with SBO, pressurizer SORV, LOCA break size, and LOCA break location. For each calculation performed, source term timing results are presented in a form based on the NUREG-1465 prescription. That is, timing information is presented in terms of:

- onset of release,
- duration of coolant activity release,
- duration of gap release,
- duration of in-vessel release,
- duration of ex-vessel release, and
- duration of late in-vessel release.

Similarly, source term magnitude results are presented consistent with the NUREG-1465 format. Magnitudes are presented for each of the release phases described above for the NUREG-1465 radionuclide groups. MELCOR results showed variation of noble metal releases between those typical of Ru and those typical of Mo; therefore, results for the noble metals were presented for Ru and Mo separately.

The collection of the source term results for all of the 40% MOX core MELCOR calculations can be used as the basis to develop a representative source term (across all accident types) that will be the MOX supplement to NUREG-1465.

6.0 REFERENCES

1. U.S. Nuclear Regulatory Commission, *Generic Environmental Impact Statement for License Renewal of Nuclear Plants*, Supplement 9, Regarding Catawba Nuclear Station Units 1 and 2, Final Report, NUREG 1437, December 2002.
2. Duke Energy Corporation, *McGuire Nuclear Station, Individual Plant Examination (IPE) Submittal Report*, 1992.
3. Duke Energy Corporation, *Catawba Nuclear Station, IPE Submittal Report*, 1992.
4. Gauntt, R.O., Cole, R.K., et al., *MELCOR Computer Code Manuals, Version 1.8.5*, NUREG/CR-6119. Rev. 2, October 2000.
5. L. Soffer, S.B. Burson, C.M. Ferrell, R.Y. Lee, and J.N. Ridgely, *Accident Source Terms for Light-Water Nuclear Power Plants*, NUREG-1465. U.S. Nuclear Regulatory Commission, February 1995.
6. R.O. Gauntt and K.C. Wagner, *An Uncertainty Analysis of the Hydrogen Source Term for a Station Blackout Accident in Sequoyah Using MELCOR 1.8.5.* Sandia National Laboratories Letter Report to U.S. NRC, October 2002.
7. K.W. Ross, K.C. Wagner, and R.O. Gauntt, *Progress Report on Progress Report on Mixed Oxide (MOX) Versus Low Enrichment Uranium (LEU) Fuel Severe Accident Response*. Sandia National Laboratories Letter Report, December 2003.
8. S.B. Ludwig and J.P. Renier, *Standard and Extended Burnup PWR and BWR Reactor Models for the ORIGEN2 Computer Code*, ORNL/TM 11018. Oak Ridge National Laboratory, Oak Ridge, TN, December 1989 (CCC 0371/17).
9. R.J. Ellis, *System Definition Document: Reactor Data Necessary for Modeling Plutonium disposition in Catawba Nuclear Station Units 1 and 2*, ORNL/TM 1999/255. Oak Ridge National Laboratory, Oak Ridge, TN, 1999.
10. F. Ceccaldi, B. Gleizes, M. Prouve, and P. P. Malgouyres, Rapport de Synthese de l'essai VERCORS RT2, *CEA Note Technique*, DEC/S3C/01 013, March 8, 2001.
11. Y. Pontillon, G. Ducros, M. Gnemmi, P. P. Malgouyres, and P. Prouve, Rapport de Synthese de l'essai VERCORS RT7, *CEA Note Technique*, DEC/S3C/01 002, July 23, 2001.
12. T. Nakamura and R. A. Lorenz, *A Study of Cesium and Krypton Releases Observed in HI and VI Tests Using a Booth Diffusion Model*, Oak Ridge National Laboratory Research Paper, May 1987.
13. R. A. Lorenz and M. F. Osborne, *A Summary of ORNL Fission Product Release Tests with Recommended Release Rates and Diffusion Coefficients*, NUREG/CR-6261, 1995.
14. Duke Energy Corporation, *Probabilistic Risk Assessment Revision 2b, Catawba Nuclear Station*, April 18, 2001.

15. M. Pilch, K. Bergeron, and J. Gregory, *Assessment of the DCH Issue for Plants with Ice Condenser Containments*, NUREG/CR-6427, SAND99-2553. Sandia National Laboratories, Albuquerque, NM, April 2000.

16. S.G. Popov, J.J. Carbajo, V.K. Ivanov, G. L. Yoder, *Thermophysical Properties of MOX and U02 Fuels Including the Effects of Irradiation*, ORNL/TM 2000/351. Oak Ridge National Laboratory, Oak Ridge, TN, November 2000.

DISTRIBUTION

External Distribution:

1 Richard Lee
U.S. Nuclear Regulatory Commission
RES/DSA/FSTB
Mail Stop C3A07M
Washington, DC 20555-0001

1 Jay Lee
U.S. Nuclear Regulatory Commission
NROR/DSER/RSAC
Mail Stop 7 F27
Washington, DC 20555-0001

1 Mr. Michael Salay
U.S. Nuclear Regulatory Commission
RES/DSA/FSTB
Mail Stop C3A07M
Washington, DC 20555-0001

1 Mr. Mark Leonard
Dycoda, LLC
267 Los Lentes Rd. NE
Los Lunas, New Mexico 87031-9390

Internal Distribution:

3	MS0736	Dana Powers	06762
1	MS0748	Nathan Bixler	06762
5	MS0748	Randy Gauntt	06762
1	MS0748	Larry Humphries	06762
1	MS0748	Joonyub Jun	06762
1	MS0748	Don Kalinich	06762
1	MS0748	Jesse Phillips	06762
1	MS0748	K.C. Wagner	06762
1	MS1348	Scott Ashbaugh	04240
1	MS0899	Technical Library	9536 *(1 electronic copy)*


Sandia National Laboratories